A SYSTEM FOR AIDING THE USER ASSIMILATION OF ACQUIRED MOTORSPORT DATA

By

Matthew C. Parker
BEng. (Hons) DIS

A Doctoral Thesis submitted in partial fulfilment of the requirements for the award of Doctor of Philosophy of Loughborough University

2010

Abstract

A racing car is a complex machine, featuring many adjustable components, used to influence the car's performance and tune it to a circuit, the prevailing conditions and the driver's style. A race team must continually monitor the car's performance and a race engineer communicates with the driver to decide how best to optimise the car as well as how to extract most from the driver himself. Analysis of acquired vehicle performance data is an intrinsic part of this process.

This thesis presents an investigation into methods to aid the motorsport user's assimilation of acquired vehicle performance data. The work was directly prompted by personal experience and published opinion. These both find that the full potential of acquired data in motorsport is seldom realised, primarily because of the time available to analyse data with the resources available to a racing team. A complete solution including data management methods and visualisation tools was conceived here as a means of addressing these issues.

This work focuses on part of the overall solution concept; the development of a visualisation application giving the user a detailed and realistic three-dimensional replay of a data set. The vehicle's motion is recreated from acquired data through a kinematic vehicle model driven by measured damper and ride height data. Ground displacement is computed from wheel speed and accelerometer measurements as well as a new optical sensor approach aiming to achieve better accuracy. This implements a two dimensional auto-correlation of doubly exposed ground images, calibrated to distance on the basis of an integrated ride height measurement. Three sensor units are used to allow not only displacement but also heading data to be derived.

The result of the work described in this thesis is the proof of principle of both a display and sensor system, both of which were deemed worthy of further study and development to fully meet the demands of the motorsport application. The visualisation tool presented a new and applicable method of viewing acquired data, whilst the sensor was proven as a new method of deriving vehicle position data, from potentially low cost hardware.

“…racing is life. Anything before or after is just waiting.”

Steve McQueen

For Mum, Dad, Jo and Rach.

Acknowledgements

I must first thank my supervisor Professor Graham Hargrave at the beginning of what will be a long list, for firstly working to give me the opportunity to be able to come back to Loughborough University and research an area of such interest to me. His support throughout the work, particularly with the various hardware and time problems faced, has been invaluable.

I must also thank Roly Vincini of P1 Motorsport and Jeff Allen of Scion Sprays for their support of my work. Roly for giving me the opportunity to work with a professional racing team and Jeff for his sponsorship to purchase the project's test vehicle.

I must also thank Adam Airey of Lola Cars, for assistance with testing of the Kinematic code developed here and Benoît Dupont of Renault-Sport Technologies for supply of the detail which allowed the World Series by Renault car to be modelled. Also Ru Sirimanna needs thanking for lending me a copy of *Data Power*, which proved so difficult to get hold of.

The broad nature of the project has called for the assistance of a broad range of technical staff. I should particularly thank Pete Wileman and Dave Britton for all their assistance in preparing the test vehicle, as well as for their reassuring line of advice and humour.

Steve Hammond and Tim Rowe were both extremely helpful sources of information and advice when wiring the data acquisition system and received much questioning throughout my PhD.

Many other technical staff helped with various aspects of getting the test vehicle running, Jagpal Singh, Keven Smith, Robert Smith, Mick Porter, Dick Price and Bob Ludlum all spring to mind as having helped along the way.

I feel very lucky to have made many great friends during my PhD, many of whom helped with my work along the way and deserve thanks. Ben “Curly” Reid, John “The Job” Rimmer, Ed “The Long” Long, Pete “Pedro” Martin and David “Mysterious” Grimble were always there to lend advice and opinion. Although it seemed a drag at the time (company aside) Heema Unadkat convinced me in to the lab to get the ball rolling on weekend work which would eventually become a feature of my research, which was a good job done. Practical work and testing was only made possible by some of the guys mentioned above as well as Ed Putman, Dan Lloyd and Sian Slawson who helped during preliminary sensor testing. Sarah Mullane and Tanya Le Sage also gave me help and advice on the slightly confusing subjects of GPS and Kalman filters.

The final and biggest work based acknowledgement though has to go to “Little” Matt Harrison and Ian “Small Hands” Jordan. I cannot begin to guess at how many summer evenings and weekend days they both gave up to help me collect the data I needed from the test vehicle.

I would also just like to say thanks to three other friends who stand out as has having helped along the way, Lucy Reid, Sarah Bale and Hannah Townley Smith; because life isn’t just about work.

Last but not least I must thank my family. My two sisters, Joanne and Rachel have always been supportive and on the end of a phone to cheer me up when things have got stressful. I can’t begin to thank my Mum and Dad enough though. They have really gone beyond the call of duty of even a parent, particularly in the last 6 months or so to make sure I could see this through.

Contents

Nomenclature

Acronyms

2D	–	2-Dimensional
3D	–	3-Dimensional
ADC	–	Analogue to Digital Convertor
ANN	–	Artificial Neural Network
API	–	Application User Interface
C/A	–	Coarse Acquisition
CAD	–	Computer Aided Design
CCD	–	Charged Couple Device
CF	–	Compact Flash
CMM	–	Coordinate Measurement Machine
CMOS	–	Complimentary metal-oxide-semiconductor
CoG	–	Centre of Gravity
CSV	–	Comma Separated Variable
DAS	–	Data Acquisition System
DATAS	–	Data Analysis Tools and Simulation
dc	–	Direct Current
DFA	–	Design for Assembly
DGPS	–	Differential Global Positioning System
DLL	–	Dynamic-link library
DPIV	–	Digital Particle Image Velocimetry
ECU	–	Electronic/Engine Control Unit
EGNOS	–	European Geostationary Navigation Overlay Service
F1	–	Formula 1
F3	–	Formula 3
FR 3.5	–	Formula Renault 3.5
FTT	–	Fast Fourier Transform
GEM	–	Grip Evaluation and Measurement
GLU	–	OpenGL® Utility Library

GLUT	–	OpenGL® Utility Toolkit
GP2	–	GP2 Series
GPS	–	Global Positioning System
GUI	–	Graphical User Interface
HIL	–	Hardware in the Loop
hp	–	Horse Power
IDS	–	Imaging Development Systems
IGES	–	Initial Graphics Exchange Specification
INS	–	Inertial Navigation System
LED	–	Light Emitting Diode
LSP	–	Laser Speckle Photography
LVDT	–	Linear Variable Differential Transformer
NASCAR	–	National Association of Stock Car Automobile Racing
NI	–	National Instruments
ODS	–	Optical Displacement Sensor
OOP	–	Object Oriented Programming
OpenGL	–	Open Graphics Library
OTF	–	On the Fly
OTS	–	Off the Shelf
PC	–	Personal Computer
PCMIA	–	Personal Computer Manufacturer Interface Adaptor
PIV	–	Particle Image Velocimetry
QFD	–	Quality Function Deployment
RAM	–	Random Access Memory
RGB	–	Red Green Blue
RH2BP	–	Robin Hood 2B Plus
RST	–	Renault Sport Technologies
RTD	–	Resistant Temperature Device
SAE	–	Society of Automotive Engineers
SDK	–	Software Development Kit
SHARK	–	Suspension Hardpoint and Real-time Kinematics
SNR	–	Signal to Noise Ratio
USB	–	Universal Serial Bus
VB	–	Visual Basic
VC++	–	Visual C++

VIDS	–	Video Indexed Data System
WAAS	–	Wide Area Augmentation System
WRC	–	World Rally Championship
WSbR	–	World Series by Renault

Symbols

Roman Symbols

a, b, c, d	–	Coefficients of kinematics quadratic formulation
a_n	–	Normal acceleration (m.s^{-2})
A	–	Normal acceleration (m.s^{-2})
$A, B, C, D, E, F, G, H, I$	–	Coefficients of kinematics quadratic formulation
E_ψ	–	Orientation/heading angle error (rad)
E_x	–	Lateral coordinate error (m)
E_y	–	Longitudinal coordinate error (m)
f	–	Correvit® signal frequency (Hz)
FL	–	Fixed length
FP	–	Final position
g	–	Correvit® grid constant
i	–	Horizontal pixel location
i	–	Direction along the lateral axis
I_1	–	First image
I_2	–	Second image
IP	–	Initial position
j	–	Vertical pixel location
j	–	Direction along the longitudinal axis
k	–	Gauge factor
k	–	Direction along the vertical axis

K_t	–	Curvature (m)
$KP_{x,y,z}$	–	Known point x, y and z coordinates
L_T	–	Total physical length of potentiometer track (mm)
L_w	–	Distance of pickoff to ground connection (mm)
m	–	Horizontal pixel shift
m	–	Mass (kg)
M	–	Correvit® projection scale
n	–	Vertical pixel shift
$N(ai+bj+ck)$	–	Normal vector to plane
$P(x,y,z)$	–	Point on plane
$P_o(x_o,y_o,z_o)$	–	Origin of plane
r	–	Path radius (m)
R	–	Electrical resistance (Ω)
R	–	Correlation factor
R_t	–	Cornering radius (m)
R_T	–	Total potentiometer trackway resistance (Ω)
R_w	–	Resistance between pickoff and ground (Ω)
s	–	Path distance (m)
S	–	Total lap length (m)
t	–	Time (s)
$UP_{x,y,z}$	–	Unknown point x, y and z coordinates
v	–	Yaw rate sensor vibrational velocity ($m.s^{-1}$)
v	–	Path tangential velocity ($m.s^{-1}$)
v	–	Correvit® sensor velocity ($m.s^{-1}$)
V	–	Potentiometer pickoff voltage (V)
V_s	–	Potentiometer supply voltage (V)
x	–	Lateral coordinate (mm)
x_t	–	Lateral coordinate (m)
$\bar{x}_t$	–	Corrected lateral coordinate (m)
y	–	Longitudinal coordinate (mm)

y_t	–	Longitudinal coordinate (m)
$\bar{y}_t$	–	Corrected longitudinal coordinate (m)
z	–	Vertical coordinate (mm)

Greek Symbols

$\alpha, \beta, \chi, \varepsilon, \phi,$ $\lambda, \mu, \sigma, \xi$	–	Coefficients of kinematics quadratic formulation
ε	–	Strain
ω	–	Yaw rate (rad.s^{-1})
ψ_t	–	Heading angle (rad)
$\bar{\psi}_t$	–	Corrected heading angle (rad)

Suspension Notation

D	–	Damper
FL	–	Front left
FR	–	Front right
I	–	Inboard
LWB	–	Lower wishbone
O	–	Outboard
RL	–	Rear left
RR	–	Rear right
SA	–	Stub axle
TR	–	Track rod
UWB	–	Upper wishbone
WB	–	Wishbone

Chapter 1

Introduction

1.1 Background

Figure 1 - Adam Carroll driving for P1 Motorsport leads the British Formula 3 Race at Donington Park, April 3rd 2004.

Motor racing is a sport arguably testing more individual aspects of its competitor than any other. Whilst the driver reaps the rewards of victory, he represents only one part of a team working towards the same goal. The sport tests the physical conditioning and endurance of the driver, his mental capacity as well as his skill in pushing a car to the limit of its performance envelope. It also tests a racing team's technical ingenuity, their strategic skills, ability to work as a team unit, to communicate with each other and the driver and provide him with the most competitive car possible. A typical race car (Figure 1) is adjustable in its aerodynamic, suspension and powertrain configurations. Within the numerous configurations of the adjustable components lies an optimal setup, which the team and driver must find. The driver's performance itself is not constant also and he must often be coached to extract the most of his potential.

Figure 2 - The P1 Motorsport/Cram Competition team attend to Fairuz Fauzy's World Series by Renault car in the garage during a test session at Magny-Cours. This includes downloading and analysing recorded data, communicating with the driver and making setup changes.

Competition drives development and the quest for a performance advantage and that elusive goal; the optimal setup. A natural area of development in the past has been in the quantification of driver and car performance. The most obvious and perhaps fundamental measure is lap time and this remains today a source of data providing much insight to a racing team. However, the desire to understand what constitutes the generation of a quick lap time leads to the development of a much broader system of quantification; a digital Data Acquisition System (DAS).

The acquisition of performance data by a DAS appears to have been first achieved by Chevrolet Research and Development for US Can-Am racing in the 1970s (Haney, 2001). When it was more routinely used in top level racing during the 1980s, it instantly provided a team with performance measures and information which could help them and the driver answer all that the sport demands of them. Although initially restricted to these higher classes of racing, as with most electronic technologies and particularly in the last 10 years, hardware costs have reduced to the point where data acquisition is prolific through all levels of motorsport (Segers, 2008). Systems continually evolve such that budget systems record an ever increasing amount of data, at higher capture

rates and from a wider range of sensors. This has presented its own issues as the lower level teams have smaller budgets, staff levels and expertise with which to effectively use the vast quantities of data they record (Purnell, 1998).

Personal Computer (PC) hardware, used by a team to analyse the data recorded from a car has also clearly developed in this time frame. Despite this, there appear to have been no large steps forward in the software tools provided to junior level teams to harness this extra analysis capability and help them better understand and utilise their recorded data. As a result, the user can be overwhelmed and much of the data recorded is unused completely during the running of a track session and much of its potential for optimising the team's performance is lost.

The work described in this thesis is borne from personal experience within motor racing, which lead to a concept developed alongside a leading Formula racing team, P1 Motorsport. The work developed describes one strand of a two part concept aiming to provide a junior racing team with software tools which would help them better understand, assimilate, collate and detect trends in their data. The part developed here is for a 3D graphical animation of recorded data which replays the suspension motion of the car, together with the car's position on circuit. This is intended to provide a method of helping the user assimilate data and providing a focal point for driver/team discussions and presents an alternative means to camera based methods of visualising the vehicle performance on track (Moloney *et al*., 1998; Pi Research, 2000).

Two developments are presented in this thesis; one uses real speed and inertial data from a World Series by Renault (WSbR) car racing at one of the highest levels of motorsport and a second more developed version uses data collected from a test vehicle constructed during the PhD, providing better control of the dataset for validation of the developed models and algorithms. Between these two versions lies the development of a optical vehicle displacement sensor array that was developed to answer a need to more accurately approximate the vehicle's trajectory for display. All the data combined gives an indication of the potential of the system to aid the analysis of data ranging from that which could be obtained from the most basic DAS to a system requiring additional and expensive optical sensor hardware.

The remainder of this section is divided into a number of subsections giving the reader some appreciation of motorsport itself, the roles within a racing team and the place of data acquisition and analysis within the sport. It also introduces P1 Motorsport who, whilst not an official technical partner, provided data and an opportunity for involvement with the real application of data acquisition in motorsport. Finally, this chapter broadly summarises the key issues with current motorsport data acquisition and analysis practice, which have been considered as the focus of this research project.

1.2 Introduction to Motorsport

Motorsport is an all encompassing term referring to a varied collection of sports which involve the competitive use of a motorised vehicle. However, this work focuses on circuit racing, whereby a number of cars race against each other to be the first to complete a set number of laps of a circuit or to complete the most laps in a fixed time.

Motor racing has a hierarchy, which although not completely clear in its middle has a definite foundation and pinnacle. The hierarchy applies not only to drivers, but also mechanics and engineers who all aspire to be part of the sport's highest categories, by working through some of a number of lower level classes. The variety of racing taking part on circuits can be illustrated in the selection of photographs in Figure 3 through 5.

Figure 3 – A Rotax Max 125cc Two-stroke kart. Rotax Max is an extremely popular club, national and international kart class.

Figure 4 – A BMW 320i racing in the British Touring Car Championship.

Figure 5 - Heikki Kovalainen driving a McLaren MP4-25 Formula 1 car at Silverstone during practice for the 2009 British Grand Prix. Formula 1 is the global pinnacle of motorsport and the target of almost all drivers when embarking on their junior careers.

Formula One (F1) is globally renowned as the pinnacle of motorsport. It is the highest FIA (Fédération Internationale de l'Automobile) sanctioned series which gives its victor the title of World Champion. Most young drivers starting racing in karts (Figure 3) outside of North America will be targeting F1, whereas North America has its own equivalent series known as Indycar as well as a Stock Car series NASCAR which are highly regarded within the USA in particular and are often a young driver's target there. F1 and indeed Indycar are single-seater categories, for purpose-built racing cars featuring only a single seating position and open wheels. Other categories exist for cars derived from road cars as well as closed wheel sports prototype cars. A driver failing to find a long term drive in F1 can look to the various American series as a good alternative, or a number of other professional racing categories such as the Le Mans series or various Touring Car categories for production based cars (Figure 4). Many drivers will fall short of making a career from racing as one might expect, since the opportunities gradually reduce towards the top of the hierarchy. Whilst there are many branches at each level, for clarity the career from the perspective of a European driver, moving through single-seater racing to F1 is considered in Figure 6.

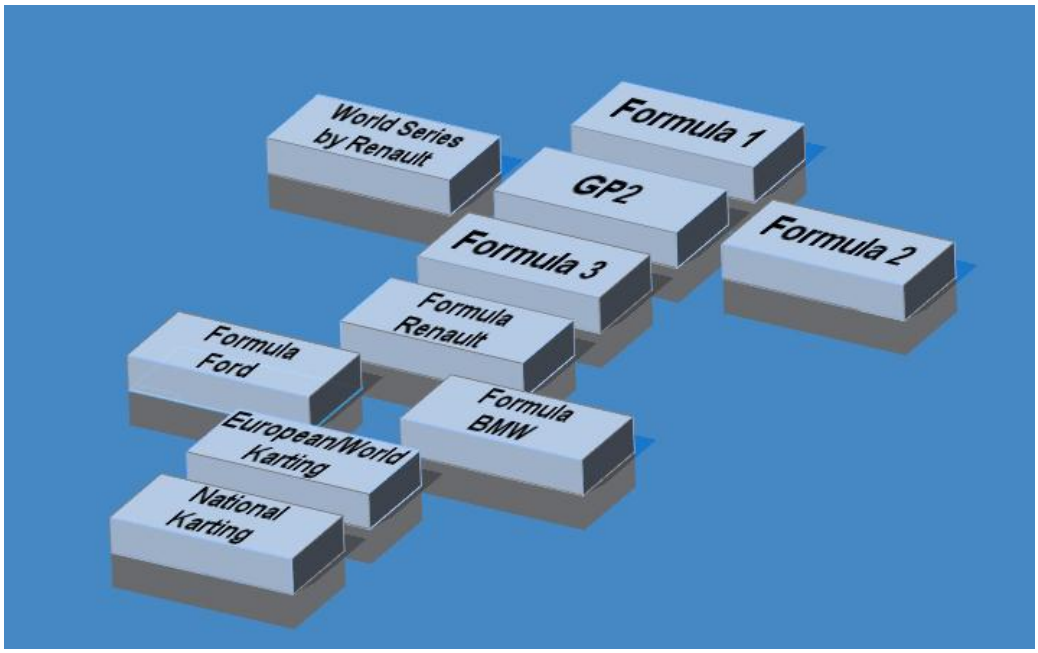

Figure 6 - The stepping stones between karting and F1.

A further complication is that not all racing is professional or part of building a professional career. There are a number of drivers who compete as a hobby in what is known as club racing. These competitors use a range of cars from historic cars to close to current state-of-the-art single-seaters. They are mentioned as data acquisition is also part of this level of racing and, as is explained later, the team size here is perhaps the smallest and most likely least experienced.

1.3 The Use of Data Acquisition in Motorsport

A racing car features many different components which can be adjusted to operate in a range of configurations. These vary from car to car and category to category, but include the car's gear ratios, the stiffness and damping performance curves of the suspension, the geometry of the suspension and particularly in single-seater racing, the aerodynamic balance of the car through

wings and other devices. Each of these is set and carefully documented by a race team to create the car's setup sheet (Figure 7). The complexity of a typical single-seater car is clear from Figure 7 and each of these individual components has an influence on the overall performance of the car and are duly adjusted during test sessions and the practice, qualifying and races involved in a meeting to better suit the car to a track, condition or the driver's driving style.

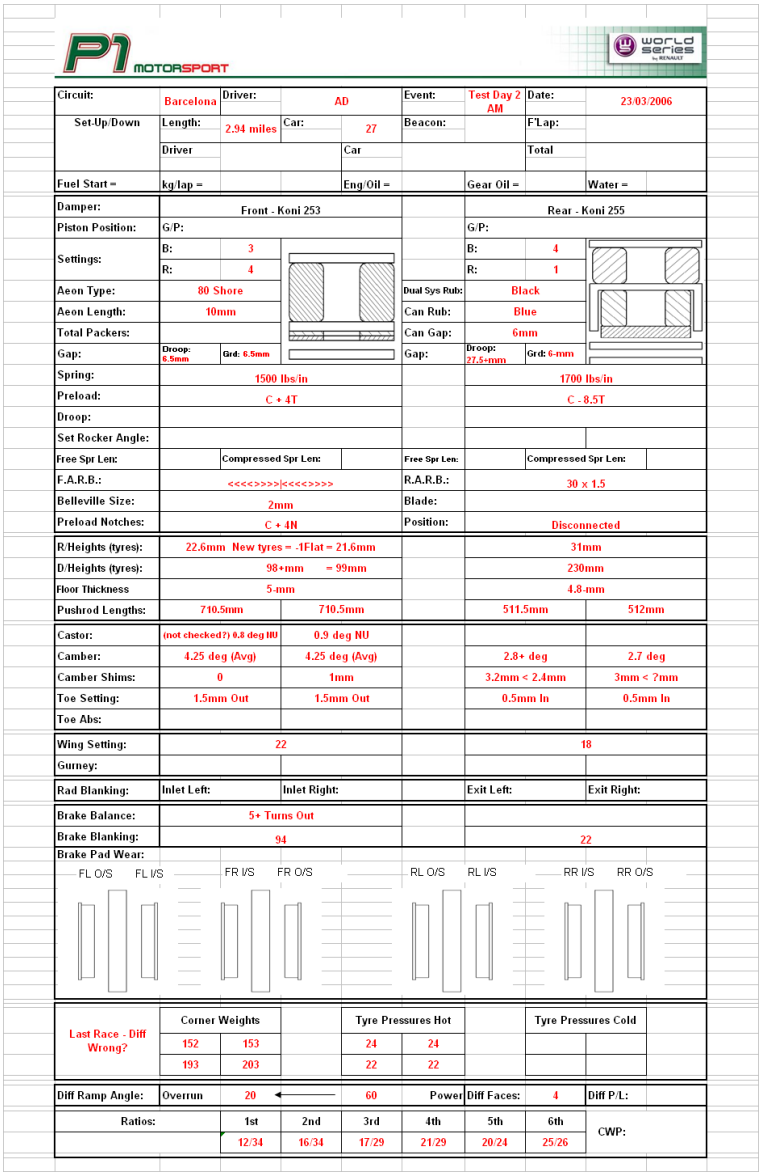

P1 MOTORSPORT — World Series by Renault

Circuit:	Barcelona	Driver:	AD	Event:	Test Day 2 AM	Date:	23/03/2006
Set-Up/Down	Length:	2.94 miles	Car: 27	Beacon:		F'Lap:	
	Driver		Car			Total	
Fuel Start =	kg/lap =		Eng/Oil =		Gear Oil =		Water =

Damper:	Front - Koni 253				Rear - Koni 255		
Piston Position:	G/P:				G/P:		
Settings:	B:	3			B:	4	
	R:	4			R:	1	
Aeon Type:	80 Shore			Dual Sys Rub:	Black		
Aeon Length:	10mm			Can Rub:	Blue		
Total Packers:				Can Gap:	6mm		
Gap:	Droop: 6.5mm	Grd: 6.5mm		Gap:	Droop: 27.5+mm	Grd: 6-mm	
Spring:	1500 lbs/in				1700 lbs/in		
Preload:	C + 4T				C - 8.5T		
Droop:							
Set Rocker Angle:							
Free Spr Len:		Compressed Spr Len:		Free Spr Len:		Compressed Spr Len:	
F.A.R.B.:	<<<<>>>>|<<<<>>>>			R.A.R.B.:	30 x 1.5		
Belleville Size:	2mm			Blade:			
Preload Notches:	C + 4N			Position:	Disconnected		

R/Heights (tyres):	22.6mm New tyres = -1Flat = 21.6mm		31mm	
D/Heights (tyres):	98+mm = 99mm		230mm	
Floor Thickness	5-mm		4.8-mm	
Pushrod Lengths:	710.5mm	710.5mm	511.5mm	512mm
Castor:	(not checked?) 0.8 deg NU	0.9 deg NU		
Camber:	4.25 deg (Avg)	4.25 deg (Avg)	2.8+ deg	2.7 deg
Camber Shims:	0	1mm	3.2mm < 2.4mm	3mm < 7mm
Toe Setting:	1.5mm Out	1.5mm Out	0.5mm In	0.5mm In
Toe Abs:				
Wing Setting:	22		18	
Gurney:				
Rad Blanking:	Inlet Left:	Inlet Right:	Exit Left:	Exit Right:
Brake Balance:	5+ Turns Out			
Brake Blanking:	94		22	

Brake Pad Wear:

Last Race - Diff Wrong?	Corner Weights		Tyre Pressures Hot		Tyre Pressures Cold	
	152	153	24	24		
	193	203	22	22		

Diff Ramp Angle:	Overrun	20	← 60	Power	Diff Faces:	4	Diff P/L:

Ratios:	1st	2nd	3rd	4th	5th	6th	CWP:
	12/34	16/34	17/29	21/29	20/24	25/26	

Figure 7 - A setup sheet for a WSbR car.

A series of team members are involved in the decision making process regarding the adjustment of these parameters. Most notable is the race engineer, who

requires information regarding the performance of the vehicle and the driver before deciding which adjustments to make to the car. This is the role performed by data acquisition and analysis. Since its inception in the highest levels of motorsport, the use of data acquisition has filtered through the sport's lower or junior categories. It is undoubted that is has developed into an intrinsic part of the operation of a racing team. It has gained such widespread use by revolutionising the supply of information to the race engineer. Before it was employed, the race engineer would have to base decisions on the information supplied by the driver as to how the car felt and any of its dials which he could read, the lap time achieved by the car and, perhaps, a subjective appraisal of the car's behaviour, gleaned from watching it on circuit. Data acquisition provides information on a vast number of performance measurements, sampled at high frequencies throughout the running of the car. This information gives an insight into far more aspects of the car and with greater accuracy than was possible before. It also allows the driver's influence on the performance to be assessed and accounted for in making decisions and for direction to be given as to how this can be improved.

1.4 The Motorsport Data Acquisition System

As was described previously, data acquisition provides the tool for taking various performance measurements of the vehicle and storing these measurements. If the system is expanded to include the analysis process, a software application for reconstructing and analysing the data is also included. The flow of information in a total Data Acquisition and Analysis system is therefore from the vehicle component to the end user via the various stages depicted in Figure 8.

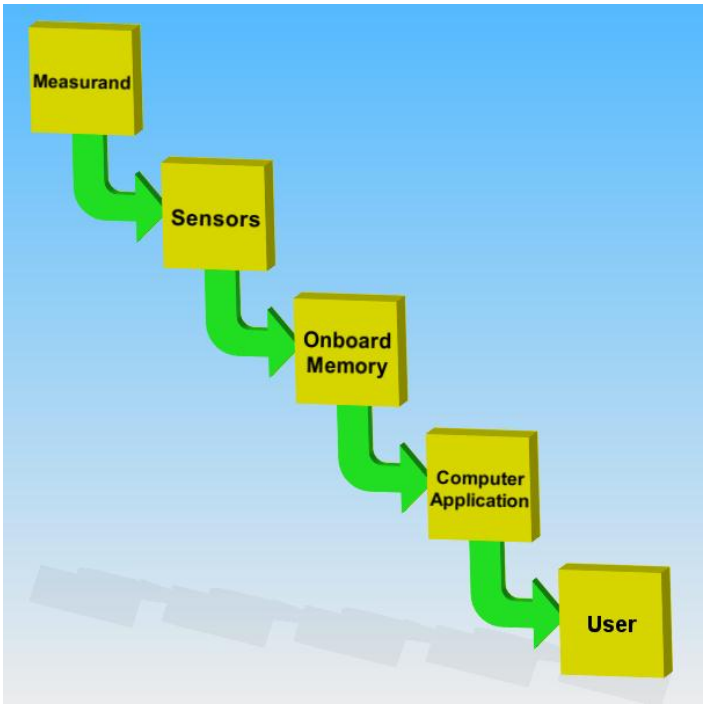

Figure 8 – Flowchart depicting the 'total' motorsport data acquisition and analysis system.

A system consists of several key aspects, which are indicated by the flow of information in Figure 8. The first is a range of sensors, which measure various aspects of the vehicle's performance. Parameters that are measured include speed, suspension displacement (as illustrated by Figure 9), brake pressure, acceleration and steering angle as well as others. The sensors operate on a wide range of principles, which are described in Chapter 2.

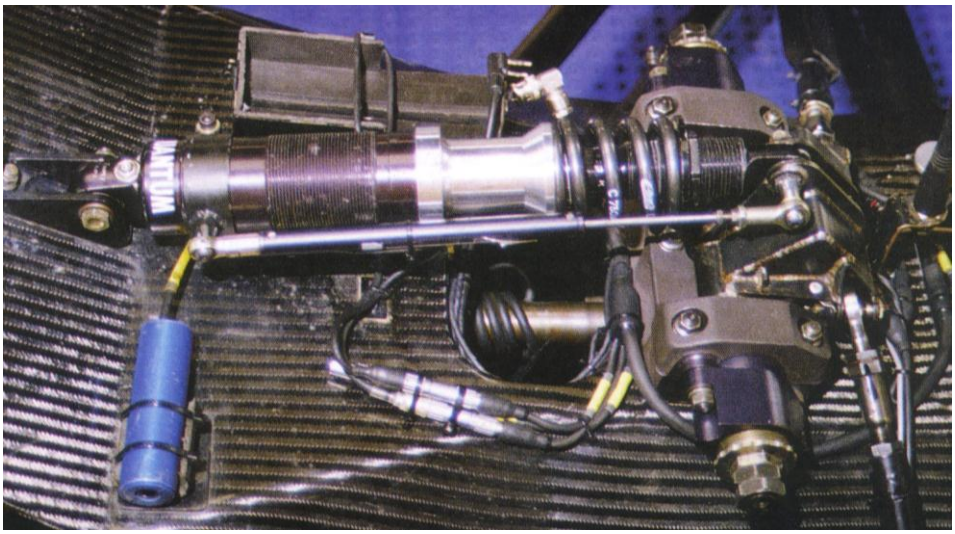

Figure 9 - A linear potentiometer in situ for measurement of the displacement of the single front spring on a Dallara Formula 3 Car (McBeath, 2002).

Another key component in the system, is the unit often referred to as the ‘data logger’ (Figure 10). This commonly contains the onboard memory for storing the sensor’s measurements and an analogue to digital converter, for creating digital words from many of the analogue sensors which are used, such as resistive potentiometers for measurement of suspension displacement. It also contains the circuitry for controlling the system. The sensors are connected to the data logger via a wiring harness, which is generally custom made, to suit the particular measurements of the car (Figure 10).

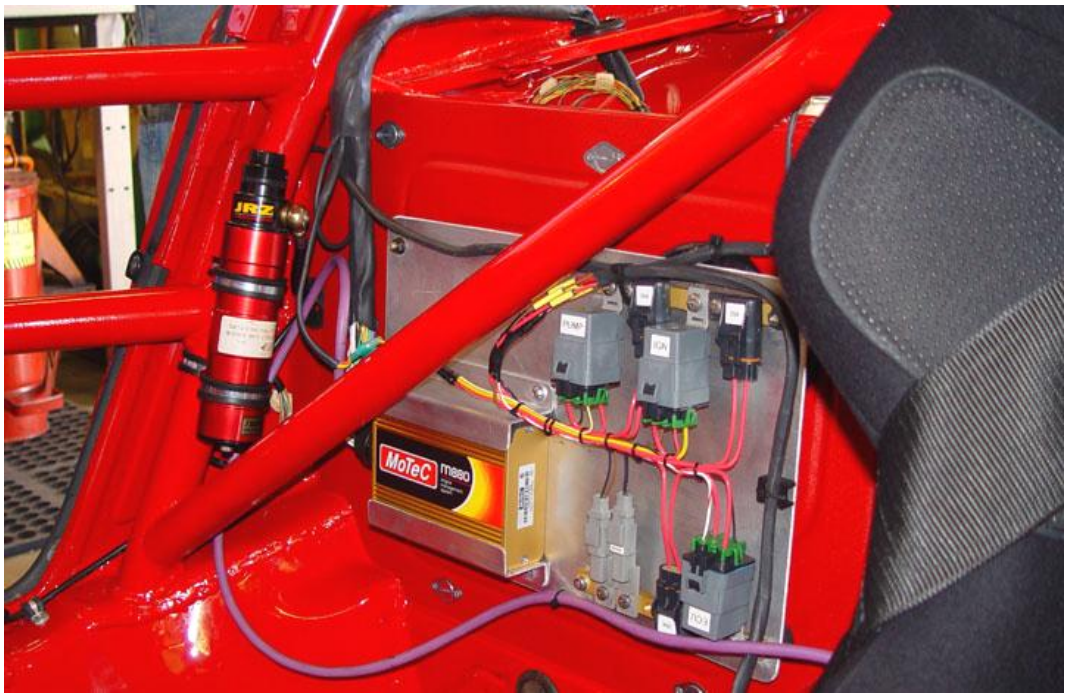

Figure 10 – A MoTeC data logger shown mounted into a race prepared Porsche 911. The wiring loom feeding signals from sensors back to the data logger can also be seen (Patrick Motorsports, 2010).

The final component of the data acquisition and analysis system, and the subject of this research is the software application used to view and analyse the data. Such software, generally also provides an interface and functionality for retrieving the data from the data acquisition system memory. This may include a wired link transfer between the memory on the car and a laptop computer or may be achieved directly, by copying from a removable compact flashcard. The software will therefore:

- Name the data and create key information which can be used for later reference, such as the date, number of laps and the laptimes achieved;
- Provide tools for plotting the data (see Chapter 2), such as against the time at which the data was sampled, the distance covered from a lap marker and so forth.

The general standard of motorsport data analysis software is depicted by the screenshot of a distance plot analysis window shown in Figure 11. A fuller discussion is provided in Chapter 2 but briefly the car's distance around a lap is shown along the X-Axis and various channel values plotted against the Y-Axis.

The user is typically presented with a numeric display of the channel values at the position of a cursor or cross hair, which they can move along the graphs. Various other tools are provided for zooming data, finding maximum values and so on.

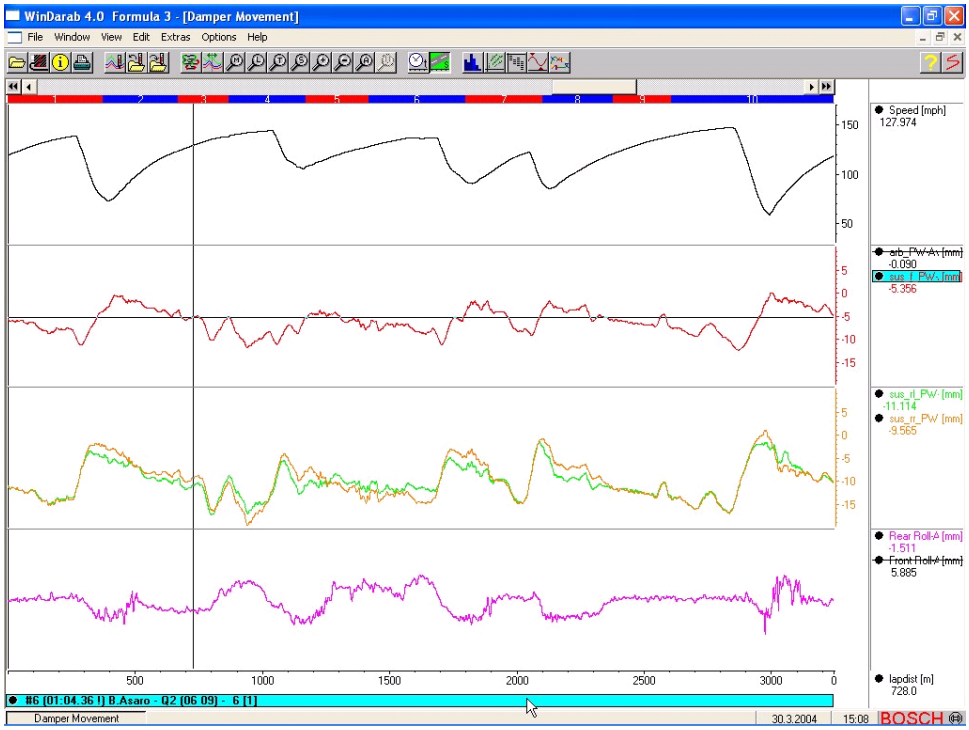

Figure 11 - A distance plot analysis window from the Bosch Motorsport WinDARAB application. This is indicative of the level of functionality of current commercial software.

1.5 Team Personnel Using Acquired Data in Motorsport

There is a distinct range in the number of team personnel who are involved in the use of acquired data during a race meeting, through various different levels of racing. The driver's requirements of the data and the four main roles amongst other team members are explained below although each of these is not involved at some levels of the sport and indeed in some teams roles are shared by a single member:

Chief Race Engineer

Typically the Chief Race Engineer will only be present at the highest levels of the sport, notably F1and GP2. His role is to oversee the running of all the team's cars by liaising with the race engineers and drivers of the team in debriefs. Part of this role will involve understanding the data acquired from the team's cars on circuit.

Race Engineer

The race engineer (shown in Figure 12) is responsible for working directly with their driver(s) to adjust the setup of the car and optimise its performance for the given circuit, conditions and event type. They are also likely, at least in part, to perform some of the role of a driver coach by instructing the driver on how he/she can improve their performance. Many sources of information are used by the race engineer, including driver comments on the performance or 'balance' of the car, lap time and lap sector analysis, published speed trap data as well as the focus of this study, acquired data. In some of the higher categories of racing, the race engineer will only perform the role of analyst and decision maker with regard to data, whilst a junior or data engineer will be responsible for collection of the data, operation of the analysis software and often some of the analysis to provide answers to the race engineer.

Junior Engineer/Data Engineer

Where a junior or data engineer (shown in Figure 12) is employed, they will generally be responsible for collecting the acquired data from the car and operating the analysis software employed to provide the race engineer with filtered information he requires. His role may also be expanded to include other duties such as various calculations and other analysis of lap time data and so on to provide the race engineer with further gleaned information. A final aspect of their role in many categories is to monitor the operation of the car itself. A number of engine parameters are recorded and an increasing number of categories also employ 'fly by wire' control systems for clutch, gear and throttle operations, which feature no direct mechanical link between the driver and control. All of these have sensors included in the control loop which are recorded

through an outing and must be carefully monitored to ensure correct operation of the car.

Driver Coach

The driver coach is not always present in a team. The role involves helping the driver to improve their own performance exclusively from a driving technique point of view. This will include observing the car on circuit, analysing lap time and lap sector data and using the acquired data primarily to monitor the driver controls and their relationship to the behaviour of the car. Where the driver coach is not present, the race engineer will perform this role typically.

Driver

The driver himself must be able to understand and appreciate much of the data in order to improve his own performance. This will most commonly involve having to relate traces of speed back to his own performance on the circuit, relating to braking and throttling points as well as driving lines. Also he must understand the behaviour and dynamic balance of the car and be able to relate this back to his own throttle, steering and brake inputs.

Figure 12 - The author (left) working as a data engineer for P1 Motorsport, alongside the team's two drivers and the race engineer (second from right). A debrief session is pictured, with acquired data being analysed.

1.6 Current Trends in Motor Racing

For several years there has been a widespread drive through essentially all levels of motorsport to cut costs. This has been manifested in a number of ways but most notable to this study is a large cut in the time teams are allowed to test under a series' rules. This has been enforced in essentially all levels of the sport, including F1 (Kowalczyk, 2002; Wright, 2001; Formula One Administration, 2010).

With this reduction in testing, there is now a greater emphasis on using the available time to best effect. Experience has shown in practice this has sometimes lead to poorly informed decisions as proper discussion and analysis is overlooked in favour of sending the car back onto the circuit as quickly as possible.

1.7 P1 Motorsport

P1 Motorsport is a professional racing team based near the Snetterton racing circuit in Norfolk, 20 miles south west of Norwich. It is owned and was founded by Roly Vincini, an extremely experienced race engineer, who previously worked as a mechanic in the Brabham F1 team in the early to mid 1980s and later as a workshop manager at Lotus F1. The team has always concentrated on single-seater racing and has won championships at both a national and international level.

Figure 13 - The P1 Motorsport Team before the 2008 World Series by Renault Championship.

This team has provided the author with the opportunity to work in a racing environment which ultimately lead to the concept of this research. Through the time researching this PhD, the link with the team and Roly Vincini has been kept, partly through two further seasons of competition and has also been used to provide insight and the use of data acquired from a modern single-seater.

The involvement with the team earned the following key results, illustrating the team's position as one of the best junior racing teams in the UK:

2002 – British Formula 3 (part season) – Scholarship Champion – Adam Carroll

2003 – British Formula 3 – Scholarship Champion – Ernesto Viso

2004 – British Formula 3 – Overall Championship runner up – Adam Carroll

2006 – World Series by Renault as part of Comtec – Champion – Alx Danielsson

2007 – World Series by Renault as Cram Competition

2008 – World Series by Renault (preseason testing) – Champion – Giedo Van der Garde

1.8 The Problem Posed by Current Data Acquisition Practice

Experience has told that in junior levels of motorsport the amount of data provided by a typical modern system can overwhelm the user. This is most applicable in the lower levels of the sport.

If the stages of the motorsport hierarchy detailed in Figure 6 are considered with the exception of the top level F1, there are undoubtedly cases where the staff available to analyse data and draw conclusions from it will be extremely stretched. This problem increases in regularity amongst teams typically towards the lower levels where sometimes the presence of separate data engineers becomes rarer and where a race engineer can even have to run more than one car and perform all the data related duties.

Through a survey of data analysis software and an exhaustive review of research, it is apparent that there has been little development of motorsport data

analysis tools. Some tools have undoubtedly been introduced, including the use of basic expert systems for highlighting key areas of interest. There have also been some graphical tools for helping the user assimilate the data to the car itself, although these have appeared only basic and appear to fall short of being particularly useful to all but the most inexperienced user.

This suggests two opportunities for development; one for the development of a software package to provide a new level of data assimilation and second for the advancement of expert system design currently employed in motor racing data analysis.

1.9 Research Objectives

The key objective of the research presented within this thesis is to create an application representative of a commercial software solution which could prove the concept of a system for assimilating vehicle suspension and ground displacement recorded from a racing car. This has involved a number of key smaller objectives:

- To develop a system for calculating vehicle suspension motion from measured spring compression;
- To develop a system for graphical display of a vehicle in real time at a rate of 50fps;
- To develop a code to approximate vehicle trajectory from recorded lateral acceleration and speed data, in a similar vein to current commercial approaches;
- To develop an optical sensor system for approximating vehicle ground trajectory;
- To prepare a vehicle which can be instrumented with a data acquisition system and used to test the optical system and software;
- To obtain results which allow a subjective appraisal of the potential of the visualisation software application for aiding the analysis of racecar data;

- To obtain results which allow quantitative analysis of the optical sensor system's trajectory reconstruction in comparison to the current common method based on acceleration and speed data.

1.10 Contribution to Knowledge

The research presented in this thesis made the following contributions to knowledge:

- The research identifies and formulates an outline concept for developing motorsport data analysis tools to include functionality not reported in the literature. This will aid the user's understanding and the speed which they could assimilate a set of recorded data;
- An application incorporating a data display technique not previously commercially released for motorsport applications, nor reported in the literature is developed. This approach is designed to meet the rigours of the application to racing, particularly with its speed of operation;
- The principle of a new 3D vehicle displacement sensor design is proven, using image capture and analysis routines not previously used to measure vehicle displacement. This is found to offer the potential for attaining high displacement accuracy;
- The work develops a vehicle trajectory plotting algorithm not previously implemented, using 3 displacement measures from known points of the vehicle to attain heading information. It is hypothesised that, with suitable refinement and combined with the potential accuracy of the displacement data it processes, this approach can arguably provide an alternative trajectory mapping method to Global Positioning System (GPS)-Inertial Navigation Systems (systems combining satellite derived position data with that recorded from inertial based sensors), the use of which at the race circuit is practically limited.

1.11 Thesis Overview

This thesis is divided into nine chapters, including this introductory chapter, which has aimed to give the reader some background of motorsport, the use of data acquisition and analysis and some of the current and future issues with the practice. P1 Motorsport, who were strongly involved in shaping parts of this work and in providing data are also introduced to the reader. Finally, the objectives of the research documented by this thesis are also given as a pretext to the content of the other chapters.

Chapter 2 presents a survey of current data acquisition and analysis techniques, considering software tools as well as typical sensors used in motor racing. It also provides a brief overview of other tools associated with performance analysis in motorsport, including expert systems which are considered the largest area of focus for further work as well as vehicle or lap simulation software.

Chapter 3 gives a brief outline of the preliminary concept to answer the issues which were identified and described previously in Chapter 2.

Chapter 4 is the first of several chapters to present extensive detail on key aspects of the final software solution. The chapter presents work contributing towards the preliminary version of the display application developed. This was tested with data from a World Series by Renault car and details of how the car was graphically modelled and the display created are given. Also presented is the development of a trajectory approximation routine based on accelerometer and wheel speed data. This is typical of a commercially available motorsport data analysis package and indicates the potential of the display system using data created from the most basic commercially available DASs.

Chapter 5 details a test vehicle, which was in effect this work's equivalent of an experimental rig. The detail includes its procurement, preparation and fitting with a data acquisition system to provide test data representative of a real racing car.

It also details the measurement of the car which was necessary, both for graphical and kinematic modelling.

Chapter 6 documents the development of an optical vehicle displacement sensor array, which aimed to improve the ground displacement trajectory approximation of the car around a circuit. This includes sections describing the specification of components, the design and layout of the sensors, the analysis of images collected and the reconstruction of the trajectory from the results collected.

Having been taken through the test vehicle and optical sensor development, the reader is then introduced in Chapter 7 to the development of the final version of the display application. This version was based on data collected from the project test vehicle and features suspension kinematic motion. The calculation of this motion from the measured data, as well as a description of the vehicle trajectory reconstruction is presented to the reader.

Chapter 8 presents results from both versions of the display software, in the form of screenshots, to give some visual impression of the recreation produced. A more traditional data presentation is then given to the results derived from the optical displacement system. Data is presented for tests of the sensor to measure vehicle velocity and also to recreate the trajectory around a simple circular course and a more complex circuit.

Chapter 9 draws conclusions from the work and gives suggestions for further work.

Chapter 2

Current Motorsport Data Acquisition and Analysis Software and Techniques

2.1 The Uses of Acquired Data in Motorsport

The purpose of analysing acquired vehicle data in motorsport is to improve the performance of the driver, car and the way in which the two complement each other. Each of these three target areas are described below, where it is clear there is much similarity but also a number of differences between the approaches employed for each.

2.1.1 Driver Coaching

Data acquisition is used to assess the performance of the driver using a range of tools. However, it is commonly achieved using speed measurement provided by a typical system (see section 2.2.1), plotted against the distance around the lap (also calculated from the speed sensor). This provides a characteristic trace of the vehicle speed across an entire lap which can be compared with another lap of data, to gauge losses or gains in the driver's technique between runs or indeed between two different drivers (Haney and Braun, 1995). Typically this display will also be combined with a 'math channel' (see section 2.4.1 and Figure 14) which compares the elapsed time of displayed laps relative to some datum lap and can be used as a strong visual reference as to where one lap gains or loses to another (Parker, 2004a)

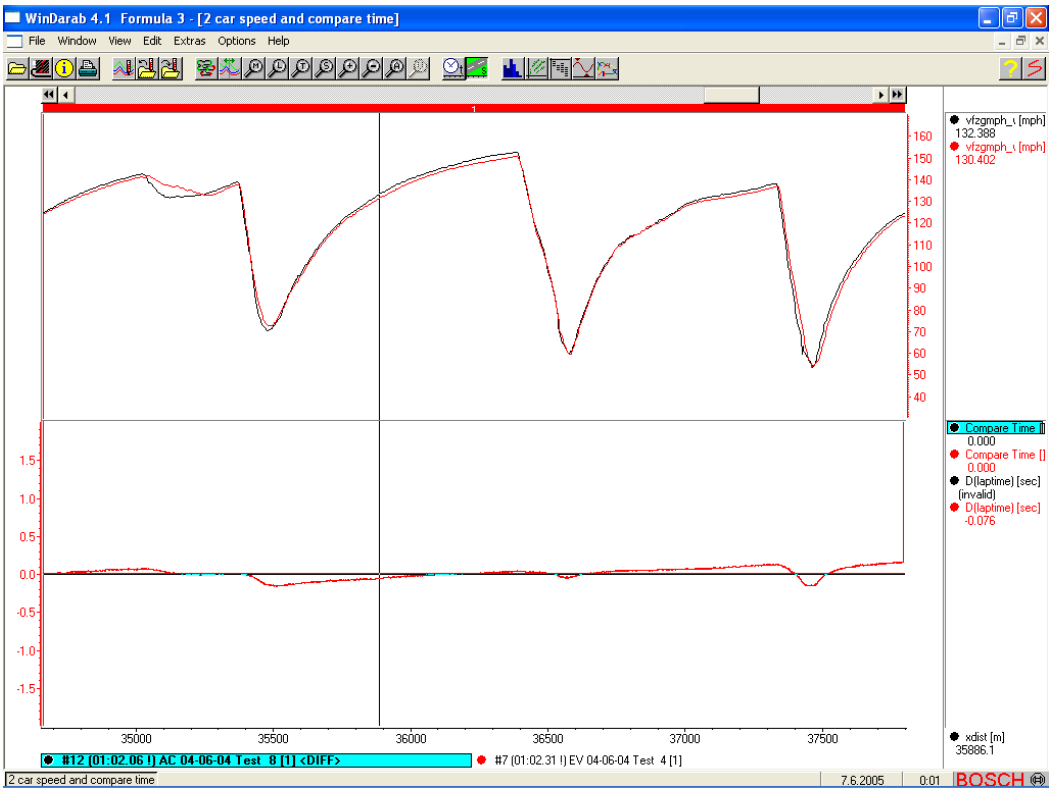

Figure 14 - Screenshot from Bosch WinDARAB showing a typical analysis window for assessing driver performance, including traces of Speed and Compared Elapsed Time against Distance

Upon identifying an area of interest in the data, additional channels will then be overlaid on the plot, in order to determine the particular aspect of the driver's performance which led to the gain or loss. For this purpose, traces of throttle angle, steering and brake pressure are amongst the most revealing measures of driver technique.

Other plotting tools, featured within current commercial software, are also used in assessing the driver performance. These include circuit maps with data labels, to give a graphic illustration of the data and tabular split reports showing the calculated times for a driver over a range of segments of a lap, which gives an indication of consistency and allows a theoretical lap to be calculated from the best set of split times. These tools are described in more detail in section 2.4.

2.1.2 Vehicle Setup Development

Another key use of the acquired data is in making informed decisions about the car setup development. This refers to a series of adjustments which can be made to the car to better suit it to a particular track and the prevailing conditions. It is the role of the race engineer to decide where these adjustable parameters are set and he uses the acquired data to aid this decision. The stopwatch is perhaps the ultimate measure of a vehicle's setup, but data acquisition provides insight into the entire lap, leading to more informed and reasoned decisions. For example an improvement in laptime could be because of an improvement in the driver's performance, although there could be indications in the data that the vehicle setup, however, was detrimental. There is then a requirement for somewhat subjective analysis to separate these two contributions and act accordingly.

Once again, various channels are plotted, usually against distance to form the basis of decisions on vehicle setup. Channels such as suspension displacement, measured by a linear potentiometer or Linear Variable Differential Transformer, can be used to infer the vehicle's ride height, which will allow the vehicle's aerodynamics to function optimally when at some specific clearance, for example. Other plotting functions, such as histograms can also be considered, to assess the time spent at various throttle levels across a lap, although this can be influenced by driver performance (these are once again considered in greater depth in section 2.4.1).

2.1.3 The Crossover between Driver and Setup Development

Consideration of sections 2.1.1 and 2.1.2 should have made it clear that there is a considerable crossover between assessing vehicle and driver performance from acquired data. There is a need for a subjective analysis of the data in order to decide upon events caused by the vehicle setup and those caused by the performance of the driver. This subjective analysis can require considerable time, which is not available in the course of a test session, where time on circuit

must be maximised owing to ever increasing restrictions on testing from series organisers as a way of cutting costs (Kowalczyk, 2002; Wright, 2001; Formula One Administration, 2010). Further to this, subjective analysis can potentially be of poor quality because of this time restriction and is not entirely repeatable (Martin and Law, 2002).

A key aspect of both vehicle and driver development was identified as the communication between the driver and engineer. To aid this, they should both have a full understanding of the vehicle's behaviour, to assist in working through a wide range of potential roots of a given problem (Strout, 1998; Haney, 2000).

2.2 Current Sensor Technology

The following section details key aspects of current vehicle sensor technology. The measurands considered are ones collected from racing cars, whilst many of the sensor principles are likewise. This should give the reader an appreciation of the vast quantity and range of data which can be collected from a racing car and the scale of the requirement for handling all of this data. In some instances additional sensor technologies are described, mainly from the road car industry but which would also provide potential for measurement in racing applications. All of this information is considered in determining the sensor set used to instrument the test vehicle described in Chapter 5.

2.2.1 Speed and Vehicle Displacement Measurement

Speed is one of the most fundamental measures of racing car performance, after laptime and acceleration. It is the goal of the race engineer to optimise car and driver performance to maximise speed at all points of the circuit. It also forms the basis of the distance measurement used as the horizontal axis in the most common plotting method of channel value against distance (Parker, 2004b; Templeman, 2008). Speed measurement could be made from a number of

different sensor technologies. By the nature of their measurement these sensing principles provide displacement or distance data also. Technologies such as the Hall Effect sensor could also be applied to measuring the engine speed from the rotation of the crankshaft.

- ***Wheel Rotation*** – Both Hall Effect and magnetic proximity pickups can be utilised to measure the rotation of a wheel, from a ferrous trigger plate, which caused them to produce a voltage pulse (Barnes *et al*, 2000; Ramsay, 1996; Templeman, 2008). These pulses can be counted (Ramsay, 1996) or used to start and stop the timing of a clock (Hammond, 2005);
- ***Differential/Dynamic Air Pressure of Airflow*** – A pitot static tube is a sensing device used to measure fluid velocities and applied in racing to measure relative air velocity for aerodynamic development. It actually senses stagnation pressure, from a tapping in the direction of the flow at its nose and static pressure by a tapping(s) perpendicular to the direction of flow (Ramsay, 1996). By Bernoulli's law, subtraction of the static pressure from the stagnation pressure gives the dynamic pressure which will yield air velocity with a knowledge of the air density (Munson, Young and Okiishi, 1998);
- ***Doppler Phase Shift Sensor*** – This sensor used microwaves emitted from the underside of the car (Ditchi *et al*, 2002), which are reflected to a receiver. The Doppler phase shift, associated with scattering of the waves from obstacles, can be used to fit both the forward velocity and height of the sensor from the ground. The sensor could therefore also be used to measure ride height. Such sensors are manufactured by a range of companies including the DICKEY-john Corporation and GMH Engineering (DICKEY-john, 2010; GMH Engineering, 2010).
- ***Optical Speed Sensors*** – Sensors such as the Correvit® manufactured by Corrsys-Datron used photoelectric detector to produce a signal output from a focussed image of the ground, which was modulated through a grating. This modulation of light intensity produces a sinusoidal output from the photo detector, the frequency of which is proportional to the velocity of the image across the grating. These are typically used to

measure slip angles as described by the Corrsys-Datron technical paper (Corrsys-Datron, 2009a);

- ***Global Positioning System (GPS)*** – GPS uses a receiving device which decodes messages transmitted from satellites orbiting the earth. The system determines the difference between transmission time (contained in the signal) and the receival time from each satellite. Multiplication by the speed of light at which the transmissions are sent gives the distance between the receiver and the satellite. Three satellites would allow for a trilateration of the receiver position, but the difference between the satellites' synchronised atomic clocks and the receiver clock needs to be corrected, adding a fourth unknown to the positioning solution. For this reason a fourth satellite is required to form 4 equations (u-blox, 2007).

  GPS accuracy data does not seem to be completely in agreement, but when using the standard absolute and differential forms of GPS it appears the positional accuracy can be expected to be 2-3m and 1-2m respectively (Segers, 2008), There are additional corrections which can be applied in order to improve accuracy which are described in more detail in section 2.7.3.2.

A wide range of techniques for measuring speed have been presented. The measurement of the dynamic air pressure to infer forward speed relative to the air is specific to aerodynamic development however.

Of the other ground speed measurement techniques, the Hall Effect sensor offers the best robustness and accuracy relative to cost. The Doppler and Optical techniques provide a higher level of accuracy, but are expensive and it would appear that Doppler techniques may struggle with smooth track surfaces. Meanwhile GPS offers the potential for very accurate displacement measurements in an absolute frame of reference and has been seen to emerge as an alternative method of speed and displacement measurement to the Hall Effect wheel speed sensor. However, as is described more fully in section 2.7, there are a number of additional measures required to make a standard receiver produce accurate results, which does hinder the application of the technique, particularly to the application of vehicle trajectory mapping (McBeath, 2008).

2.2.2 Linear Displacement

The measurement of linear displacement has a number of applications in motorsport, providing data relating to driver inputs such as the throttle application and gear position as well as allowing for measurement of the vehicle's suspension deflection. It is measured using the following sensor types:

- ***Resistive Linear Potentiometers*** – The linear potentiometer is a variable voltage divider, where the division ratio is set by the movement of a sliding wiper, which contacts a conductive track. One end of the sensor is attached to the system being measured and moves the wiper, whilst the other is attached to a fixed point. The track is supplied with a voltage and the wiper, with an electrical connection picks off a proportion of this as a signal voltage. Since the resistance experienced by the signal is linearly proportional to the length of the sensor track it flows through, the signal voltage can be calibrated against the slider position with a linear calibration (Ramsay, 1996; AllAboutCircuits.com, 2000).
- ***Linear Variable Differential Transformer*** – This sensor is outwardly similar to the linear potentiometer. However, it is a non-contact device, which moves a magnet between a series of primary and secondary coils. This induces a voltage in the secondary coils, whose magnitude and phase can be used to determine the amount and direction of displacement (Ramsay, 1996).

The two methods of linear displacement measurement provide a sensor of very similar dimensions and measuring the parameter in a broadly similar way. However, where the higher cost of the LVDT can be justified, it is used in favour for its non-contact operation, making it less susceptible to noise over time. LVDTs also tend to be limited in their measurement range because of the practical limit of the core and windings employed (Ramsay, 1996). Throughout most junior categories, linear potentiometers are prevalent.

2.2.3 Rotary Displacement

Rotary displacement measurement is made by a ***Rotary Resistive Potentiometer***. It operates on essentially the same principle as the linear version, but with a curved track and the wiper attached by a shaft which is rotated rather than pushed by the measured system (Ramsay, 1996). The sensor can also measure linear motion where fitting of a linear potentiometer is not practical, by a wire connection to the measured system (Segers, 2008).

2.2.4 Strain

Strain is the deformation of an object under the action of an applied load, due to its internal resistive forces (stress) (Segers, 2008). It is a phenomenon which can be measured and used to determine the force acting on a component and which can offer a significant amount of information to the race engineer. For example the strain recorded in a single seater's pushrods can be used to infer the total effective weight of the car as the basis for evaluation of aerodynamic performance. Similarly, the wheel reaction forces during cornering can be assessed by considering each wheel's pushrod individually. A metallic foil strain gauge is used to measure strain, whose electrical resistance changes in proportion to the amount by which it is deformed (Gough and Huggett, 1998). It is bonded to a component's surface such that it experiences the same deformation as the substrate. The relationship between the strain and the electrical resistance of the gauge (Equation 1) can be seen to be linear.

$$\frac{\partial R}{R} = k\varepsilon \qquad \text{Equation 1}$$

Where, R is the original resistance of the strain gauge, ∂R is the change in resistance, due to the strain ε and k is a constant of proportionality, termed the gauge factor.

Strain gauges are used in a Wheatstone bridge circuit, to produce a voltage proportional to their deformation and amplify their effective signal, which is small (Ramsay, 1996).

They are used routinely in high level categories and at times in lower more junior categories, particularly during testing where they are less likely to be physically damaged.

2.2.5 Acceleration

The ability of the car to maximise longitudinal and lateral accelerations has been used as one definition of a race car (Milliken and Milliken, 1995a), so is a fundamental measure of car and driver performance, typically forming the Traction Circle (Milliken and Milliken, 1995b). The lateral acceleration measurement also forms part of the track mapping procedures within all commercial software (see section 2.4.1). It is such an integral part of a data acquisition system that, in some cases it is even integrated within the data logger unit itself (Performance Trends, 2005; Pi Research, 2005; MoTeC, 2002).

Accelerometers, used to measure acceleration, feature a small mass which is suspended within a housing. The housing is mounted to the vehicle/component and the acceleration experienced is sensed by the movement of the suspended mass relative to the housing due to the applied forces that deform its supports (Ramsay, 1996). Measurement is in absolute terms, with no need for a reference frame, owing to the derivation directly from Newton's second law (Westbrook and Turner, 1994). The movement is translated to an output voltage using three different principles:

- ***Piezoelectric Principle*** – The supports are made from a piezoelectric material, which produce a potential difference in proportion to their deformation and hence the force and therefore acceleration acting on them (Segers, 2008).
- ***Piezoresistive Principle*** – The supports are formed from a piezoresistive material, which changes its electrical resistance in proportion to an applied deformation (Westbrook and Turner, 1994).

This complements the resistance change occurring in most materials from a reduction in cross sectional area under a deformation. These are used in a Wheatstone bridge circuit, to produce a voltage proportional to the deformation and amplify the effective signal. They can also be produced in a thick-film form, which provides potential for easy integration with circuit boards (Westbrook and Turner, 1994).

- ***Capacitive Principle*** – In this type, the mass makes one plate of a capacitive device (the other being attached to the housing). Under movement of the supports, from applied force, the capacitive coupling is varied as this mass moves closer to the static plate (Westbrook and Turner, 1994). The change in capacitance can be converted to a voltage signal, using signal conditioning circuitry.

It is not clear from the packaged acceleration transducers available on the racing market precisely which of these principles is used. However, the use of accelerometers is routine in all categories of racing. All the data analysis applications reviewed in this chapter offer a means of inferring vehicle trajectory through a routine utilising a measurement of lateral acceleration.

2.2.6 Pressure

Measurement of pressure on racing cars is widespread, allowing for monitoring of fuel, oil, coolant, crankcase, hydraulic system and inlet manifold pressures for example. It is also often used as a measure of driver brake input. Pressure transducers use a flexible diaphragm which is exposed to the applied pressure to be measured on one side and a reference pressure on the other (Westbrook and Turner, 1994). A difference in pressure on either side results in the flexing of the diaphragm which is then converted to an output voltage signal using strain gauges bonded to its surface or by transmission through a volume of oil to a separate gauge (Ottake *et al*, 1998). The three strain gauge principles described previously can be used (Yokomori and Suzuki, 2003) although a piezoresistive type is most commonly applied to automotive and racing applications, bonded to a silicon based chip (Segers, 2008).

The reference pressure can be either a vacuum, causing the measured pressure to be absolute pressure, or atmospheric pressure meaning the pressure is gauge. Sensors are also available for differential pressure measurement, exposing each side of the diaphragm to the user's choice of pressure (Segers, 2008).

The number of pressures recorded increases through the categories of racing, but teams at all levels will be prepared for monitoring at least an oil and fuel pressure signal and in most cases a brake pressure signal also for evaluating driver performance.

2.2.7 Temperature

As one might expect and as on a road car, various temperatures are monitored by several different types of contact temperature sensor to ensure the correct operation of various systems, including the measurement of oil, water and air temperatures (Segers, 2008). The three types of contact sensor generally found in racing are:

- ***Thermocouple*** sensors feature two wires of different metals joined in two locations to form a circuit that allows a measurable voltage to be generated by the Seebeck effect when the two junctions are at different temperatures, owing to the difference in the effect on the two metals (Ramsay, 1996). The voltage produced by each type of thermocouple can be related back to the temperature difference between the two junctions. If the temperature of one junction, kept as the reference, is known the other at the point of measurement can be determined. This requires either a thermistor or diode with known characteristics to monitor the reference junction. Thermocouples can sense temperature over a large range (Segers, 2008).
- A ***thermistor*** generally comprises two glass or epoxy encapsulated metal oxides and experiences a change in resistance with temperature. Their output is not linear, but can be conditioned as such and they can either increase or decrease in resistance with temperature. Their high resistance change makes their output sensitive but narrow (Segers, 2008);

- ***Resistive Temperature Devices*** (RTD) again work on the basis of a temperature controlled change of electrical resistance, but a wire coil or thin film of pure metal is used, such as platinum or nickel (Segers, 2008). They combine a similar sensitivity to the thermistor with a range comparable to the thermocouple.

Non-contact temperature measurement has also increased in use in recent years and is typically applied to measurement of the brakes and tyre temperatures. This kind of measurement is not generally used in junior racing and where it is, it is often limited to testing because of the vulnerability of the sensors (particularly in the case of tyre temperature). ***Infrared temperature sensors*** measure radiation emitted from a surface with one of two types of detector. An issue with their use is different surfaces emit differing amounts of radiation, so the surface characteristic must be known.

The measurement of brake temperature helps ensure correct functioning and use of the brake system. The tyre temperature data will provide an insight to the driver's use of the tyres and how effectively the chassis configuration of the car allows the tyres to perform at their optimal temperature.

Again the principles applied to temperature measurement in racing can be varied in the case of contact measurement, but all categories of racing will utilise some temperature measurement for monitoring engine operation. In higher categories additional temperature measurements may be made of other systems on the car and non-contact techniques will tend to be applied here to tyre and brake temperature also.

2.2.8 Yaw Rate

Angular Rate Sensors, more commonly called Yaw Rate Sensors, determine the rate of rotation of the vehicle to which they are mounted by measurement of Coriolis force, arising through the so called Coriolis Effect. This force is experienced by a body subject to both rotation and translation, being proportional to the rate of rotation, ω and the velocity of translation v of the body (Meriam

and Kraig, 1998). A sensing element of known mass is used as the body subject to this force; the rotation being a result of the vehicle's vibration and the translation being introduced by excitation of the sensing element, causing it to vibrate at a known velocity.

In racing the yaw rate of the vehicle is used to assess various aspects of the vehicle's handling. For example, the measure of attitude velocity, derived from yaw rate, speed and lateral acceleration measurements, gives an indication of the handling behaviour of the vehicle, suggesting either an oversteer or understeer condition (Pi Research, 1997).

There are several configurations of sensing element (Yukawa *et al.*, 1998), but a typical arrangement of a tuning fork element is considered here and illustrated by Figure 15. Generally piezoelectric ceramics are used to vibrate the tuning fork normal to the forward direction of the car. During straight ahead motion, no acceleration from the Coriolis Effect is detected, however, during cornering, the top of the tuning fork vibrates out of plane due to the tendency of the tips to follow their path, whilst the base of the fork rotates. This subjects the tuning fork to the Coriolis force normal to the plane of vibration, which can be sensed as the difference between the readings from accelerometers located on the tuning fork and on its base, which does not vibrate. Also the use of a set of accelerometers on each side of the fork allows the direction of rotation to be determined. The rate of rotation or the yaw rate is proportional to the force experienced and therefore, with knowledge of the sensing element mass and the vibration velocity, this can be determined from the measured acceleration (Yukawa *et al.*, 1998; Schatz, 2003).

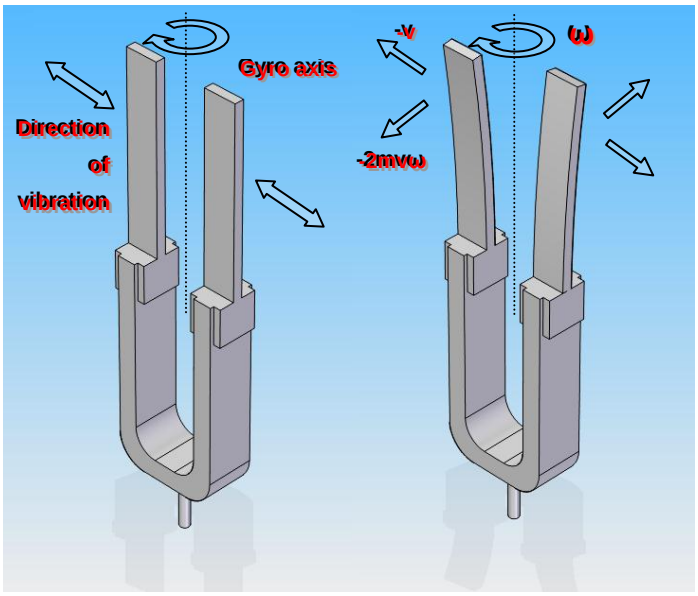

Figure 15 - The operating principle of a Tuning Fork based angular rate sensor where v is the velocity of the sensing element from vibration, m is the mass of the sensing element and ω is the yaw rate of rotational speed (adapted from Yukawa *et al*, 1998).

Yaw rate will tend to only be measured in the higher levels of racing, due to sensor cost. However, it is a parameter which is potentially inferred by the displacement sensor system developed in this research and detailed in Chapter 6.

2.2.9 Ride Height

Ride height, or this distance between the ground plane and the floor of the car is an important parameter for ensuring the effective operation of the car's aerodynamic 'package' and for ensuring the rubbing or 'bottoming' of the underside of the car on the ground is minimised (Milliken, Milliken and Best, 1995). Two forms of sensor are commonly applied to making this measurement:

- ***Optical Triangulation Sensors*** are regarded as the most commonly employed method of measuring distances of 10m or less (Laser Components, 2003). A beam of light is emitted from a Light Emitting Diode (LED) or a Laser, which reflects from the surface being measured to (Accuity, 2005; Segers, 2008). The reflected light is focussed onto a Charged Couple Device (CCD) type camera sensing element, which is

located adjacent to the light source. By calculating the position of the sensed spot of reflected light on the CCD element, it is possible to determine the height of the sensor from the ground trigonometrically, as the angle at which the light was emitted is known;

- ***Ultrasound Distance Sensors*** are not common in racing but have previously been successfully developed for the control of semi-active suspensions (Sugasawa *et al* 1985). An emitted ultrasonic wave was reflected and sensed by a receiver. The distance of the sensor above the ground was determined from the time taken for the wave to reflect and the acoustic velocity in air (which is dependent on temperature and air density, but which could also be measured).

Ride height is not commonly measured outside of the higher levels of racing, but is a measurement that many teams in junior categories would consider during testing. This is mainly because of the importance of ride height to the aerodynamic function of a single seater car.

Ride height measurement is also of significance to the vehicle displacement sensor system developed in this work and described in Chapter 6.

2.2.10 Aerodynamic Force

Although a quantification of the aerodynamic forces acting on the vehicle can be derived in a number of ways (e.g. from measuring strain or the deflection of springs of a known rate) it can be measured more directly using surface pressure sensors or tappings. A number of such sensors were described by the Pi Research Aerodynamic Application note (Pi Research, 1998a). There is a range of such sensors, which can generally be interfaced through a manifold so as to be referenced to a common pressure (Pi Research, 1998a). These ultimately operate on the same pressure measurement principles described in section 2.2.6.

This arrangement for measuring aerodynamic force is unlikely to be used in junior racing. A more probable approach would be the use of strain gauges to measure

the wheel reaction loads to the combined effect of the car's weight and the aerodynamic downforce. Post processing of this data would allow an inference of the aerodynamic load generated.

2.2.11 Lateral Wheel Load

A race engineer will always be trying to maximise the lateral wheel load generated by the car. It is a direct quantification of the cornering capability of the car and the driver's use of the grip available to him. Two sensor configurations were found which measured this quantity. Aside from its importance to the race engineer, it also influences tyre modelling as identified in the SAE paper discussing the Halliday Technology Grip Evaluation and Measurement (GEM) device (Halliday and Grider, 1998), since previously the majority of tyre force data was collected from a moment measurement machine (Milliken and Milliken, 1995c), which is steady state in nature. The developed sensors provide the ability to measure dynamic tyre forces. The two systems were:

- The ***Grip Evaluation and Measurement (GEM)*** device measures the reactive axial force between the axle and the upright allowing the engineer to infer the lateral force at the tyre contact patch (Halliday, 1997). It featured an arrangement which allowed the reaction force between the stub axle and wheel upright, during cornering, to be sensed by a strain gauge which was attached between the upright and an additional carrier, which held the wheel bearing. The levels of camber typically run on a racing car (4º or less) mean the axial force between the bearing carrier and upright was within 0.25% of the lateral force developed in the contact patch.
- The ***RoaDyn® Device*** - The RoaDyn® (Road Dynamometer) system was manufactured by Kistler. Under the action of a cornering force, the device sensed the reaction force between the rim of the wheel (where the force is first realised) and the wheel hub, by a set of strain gauges sandwiching a plate, which is contacted by an adaptor from the wheel rim (Kistler Instruments, 2003). Each of these produced a charge proportional to the deformation experienced under the action of an applied force and were

'picked-off' the sensor by electrodes and subsequently converted to a voltage signal using a charge amplifier.

These sensors are expensive and personal knowledge and experience suggests that they are not commonly used. The GEM device also requires modification to the upright (Halliday, 1997).

2.2.12 Torque Measurement

A number of sensors have also been developed to measure the torque acting on shafts, including optical techniques (Ramsay, 1996). The type most commonly applied to motor racing, owing primarily to the packaging constraints (Bitar *et al,* 2000), works on a magnetorestrictive principle, owing to the magnetoelasticity of the shaft material (Wallin *et al*, 2002*).* This is a principle, whereby the application of a mechanical stress causes a change in the material's magnetic permeability. A sensor would typically feature primary and secondary windings around the shaft; when the sensor is excited, a voltage is induced in the secondary windings, in proportion to the torque acting on the shaft, which will have modified the magnetic coupling. Applications include in-vehicle engine dynamometry, differential tuning and aerodynamic drag estimation (Bitar *et al*, 2000).

Torque is again a parameter seldom measured outside of the top levels of racing, but it is identified here for completeness.

2.3 Sensor Processing Methods

There follows a brief overview of two techniques of combining data streams to improve the individual outputs or indeed produce a new quantity, not directly measured. These approaches are not investigated in this research as they represent studies in the own right, but background information is included for completeness.

The first is ***Sensor Fusion*** a general term given to a range of techniques, presented and defined for completeness, whilst the second ***Kalman Filters*** are essentially a specific application of sensor fusion. A top level consideration was given to the use of a Kalman filter for application to vehicle trajectory reconstruction as the technique was implemented in commercially available hardware and was in use in other research areas within the field of Sports Technology at Loughborough University. For reasons defined in Chapter 3 this work sought to improve a direct measurement of vehicle trajectory, but one which could be introduced into a Kalman filter algorithm as is recommended in Chapter 9 as further work.

2.3.1 Sensor Fusion

Sensor fusion is a technique whereby sensor information from different physical sensors is merged (Persson *et al*, 2001). This is both to improve the output of a physical sensor, allowing a cheaper sensor to be used for example and using sensor fusion to 'restore signal quality' or to produce a new type of sensor which has no physical counterpart. This technique has similarities with the math channels in analysis software (see section 2.4).

2.3.2 Kalman Filters

The Kalman filter is an estimator of the instantaneous state of a dynamic system Its estimation is made using measurements which are linearly related to the state itself and which the approach assumes is affected by white noise within the sensor system and environment (Grewal and Andrews, 2001). As estimators, Kalman filters can be used as a means of predicting or inferring measurements which cannot be made or which it is not desirable to make. At the same time they provide a method of deriving useful information from noisy measurements.

The state is a collection of variables which represent the system in question at any given time, their variation is equal to a constant matrix multiplied by the state vector (made up of all state variables), which defines the system as a linear dynamic one.

The filter operates in two phases, predicting the state vector and then updating it based on some measured data. The prediction is derived from measured data, such as that from an inertial navigation system (INS) and is combined with a physical model. The correction will be derived from a comparison of a physical measurement, such as a GPS position measurement, against a prediction and is multiplied by the Kalman gain. This gain is optimally derived by an error minimisation method and uses a record of the uncertainness in each measurement which influences their effect on the correction (Grewal *et al.*, 2007). The combination of the two data streams via the Kalman filter produces a better state estimate than one obtained by using either in isolation (Grewal and Andrews, 2001).

Kalman filtering techniques were first applied to the navigation of a plane by combining an INS and airborne radar system (Grewal *et al.*, 2007) and they have likewise been applied to the navigation or trajectory measurement of racing cars as described in more detail in section 2.7.3.3.

2.4 Current Commercial Data Analysis Tools

Seventeen applications from fifteen different manufacturers provided an insight into the tools available to the current user of data analysis software. The features of the applications are summarised in Table 1, before being discussed further.

Table 1 - Table summarising the features of the surveyed range of data analysis software.

Application	2D Datarecording Analyzer	AiM Sports Race Studio 2	Astratech Racing Analysis	Bosch Motorsport WinDARAB	Competition Data Systems Track Master 2000	Corsa Instruments WinCorsa	EFI Technology Analysis	Magnetti Marelli Wintax	McLaren Electronic Systems Atlas	Performance Trends Datamite Analyzer	MoTeC Interpreter	Pi Research ToolBox	Pi Research Analysis Version 6	Pi Research Club Expert	Race Technology Data Analysis Software	Stack DataPro	William C. Mitchell Debrief3
Manufacturer																	
Feature																	
Channel vs. Distance Plots	■	■	■	■	■	■	■	■	■	■	■	■	■	■	■	■	■
Channel vs. Time Plots	■	■	■	■	■	■	■	■	■	■	■	■	■	■	■	■	■
Tabular Split Sector time Reports	■	■	■	■	■	?	■	■	■	■	■	■	■	■	■	■	■
Tabular Outing Channel Reports	■	■	■	■	■	?	■	■	■	■	■	■	■	■	■	■	■
Mapping	■	■	■	■	■	■	■	■	■	■	■	■	■	■	■	■	■
Map Based Graphical Reports	■	■	■	■	■	?	■	■	■	■	■	■	■	■	■	■	■
Map Shaded Circuit Reports						?					■						■
X-Y Plots	■	■			■	■	■	■	■	■	■	■	■	■	■	■	■
FFTs	■	■	■			?	■	■	■	?		■	■		?	?	■
Histogram	■	■	■	■	■	■	■	■	■	■	■	■	■	■	■	■	■
3D Contour Plots							?	■									
Driver Activity Map																	■
Math Channels	■	■		■	■	?	■	■	■		■	■	■		■	■	■
Statistical Tools																	■
Predefined Math Channel Analyses					■												■
Event Based Sorting	■											■	■				
Online Setup Sheets										■				■			
Database Storage System, to Search Data on Various Criteria		■															
Driver control Animation			■		■	?				■			■		■		
Vehicle Animation	?				■	?							■				■
Link With Recorded Video	■											■	■		■	■	
DLL Support									■			■					
Link To Suspension Kinematics Software										■							

■ Denotes Feature Present
Denotes Feature Not Present
? Denotes Unclear From Evidence Available

2.4.1 Standard Analysis Software Tools

The standard analysis tools were generally featured in all, or the majority of the commercial applications which were tested. Amongst them are the analysis tools which personal experience had dictated were the most commonly used at the race circuit, such as distance plots and split lap time tabular reports.

2.4.1.1 Distance Plots

The distance plot is perhaps the most widely used data plotting tool (Parker, 2004a; McBeath, 2002; Haney and Braun, 1995). It became popular for showing

trends in data channels over a long period and for conveniently referencing the data to a point on track, which is repeatable and allows for comparison of multiple laps, since there are very few different lines taken (Mitchell, 1998). Generally a lap of data is considered as it links to the official circuit and team timing, as well as being sensible for comparison, by containing a single instance of each corner.

A trained race engineer will often use a plot of vehicle speed against distance to form a visual reference alongside other plotted data, as various features of the circuit become recognisable, having a signature shape of speed trace associated with them. A typical distance plot window, from Bosch Motorsport WinDARAB was illustrated in Figure 14.

The distance measurement itself is generally computed from the wheel speed sensor (see section 2.2.1). This introduces several inaccuracies with the method since the speed measurement is not always accurate because of slip under braking/acceleration (Mitchell, 1998) and tyre wear, tyre squash under aerodynamic and cornering loads and growth from with speed, due to tendency of the tread to follow a tangential path to its rotation. All these factors contribute to making the the tyre rolling radius variable (Dixon, 1996; Blundell and Harty, 2004).

There are several strategies for mitigating these effects, such as from using GPS technology for calculating speed (Race Technology, 2005) and using multiple wheel speed sensors to provide two measurements of distance since it is rare to lock both front wheels (Pi Research, 1998b).

2.4.1.2 Time Plots

Plots of channel value against time were the second predefined Cartesian plot available in all applications surveyed. They are commonly not used as frequently as the distance plot, since the lap time is effectively a moving reference, based on the driver's performance and the circuit conditions more than physical and reasonably static distance reference (Parker 2004a, b and c).

2.4.1.3 X-Y Plots

All software applications also provided the flexibility to plot a scatter or X-Y plot of any two channels. A typical example of their application is for generating the traction circle, commonly referred to as the 'g-g' diagram. This plot provides a visual impression of how close the driver operates to the overall grip limit of the vehicle (Milliken and Milliken, 1995b).

2.4.1.4 Fast Fourier Transforms

A Fast Fourier Transform (FFT) algorithm is coded within the majority of the analysis applications. This allows a trace to be decomposed to a series of sinusoidal waves of varying frequency, amplitude and phase (Croft *et al*, 1996). A plot of power spectrum (component's amplitude squared) against frequency can be plotted and used as the basis of filtering techniques by illustrating the characteristic frequencies of the system (AiM Sports, 2003). For example, the suspension displacement can be analysed in this way, allowing a visual impression of the limit of gross motion of the sprung mass of the vehicle.

2.4.1.5 Histograms

Histograms are generally configured in the commercially available software to allow a channel to be divided into a number of bands and the time spent within those bands to be plotted as a bar (see Figure 16). This can give a good impression of the time spent at different throttle angles during an outing, for example, which can be used to asses how well both the driver and car performed. It can also be used to display the time that the engine spent operating in various speed bands and assess how well the car's gear ratios were selected.

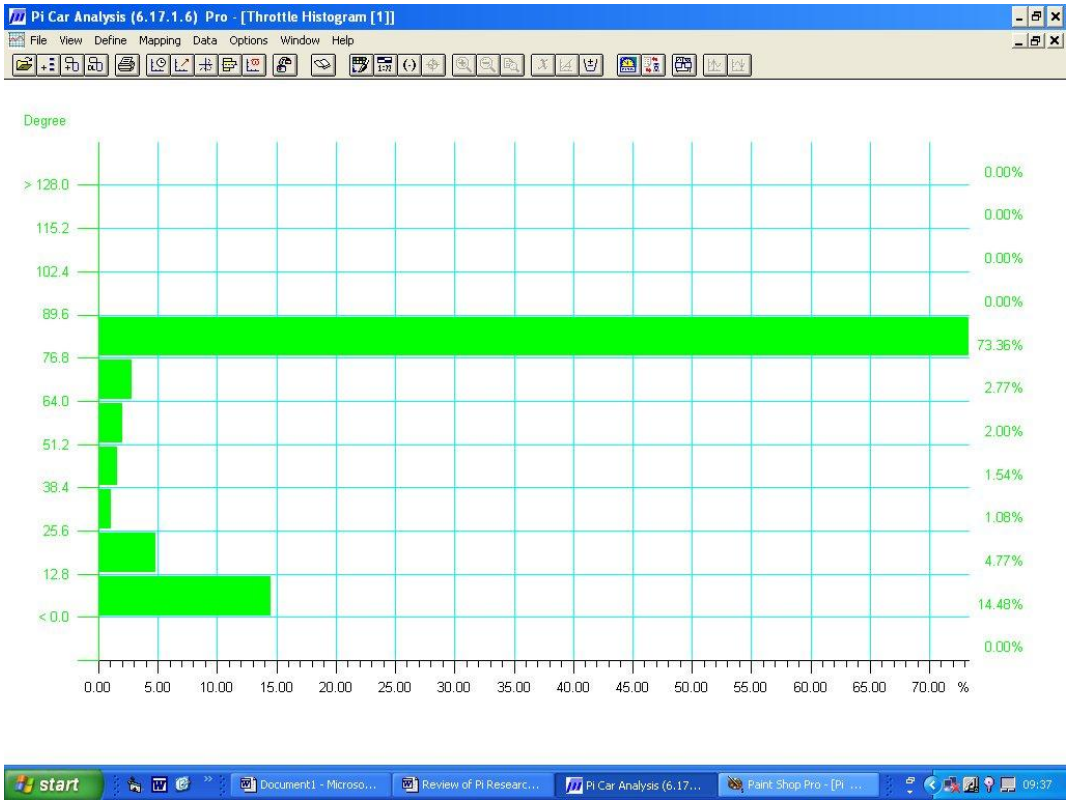

Figure 16 - Screenshot of a typical Histogram plot showing the time spent at various throttle angles throughout the course of an outing.

2.4.1.6 Track Maps

The ability to generate a map of the vehicle's racing line or trajectory is a standard feature of all analysis applications. All packages appeared to offer the ability to reconstruct this from accelerometer and wheel speed data in a method described in more detail in Chapter 4, whilst others could use GPS data to produce a trajectory (Pi Research, 2004a).

The use of GPS in junior racing is not commonplace, but it does offer potential to achieve positional accuracies of 0.02m when combined with an inertial system in a Kalman filter (Oxford Technical Solutions, 2009). Aside from its cost, there are some practical reasons why its use is not particularly prevalent, which are more appropriately presented to the reader in detail in Chapter 6.

The common method of using lateral acceleration and forward speed data is based on simplifying the car to a point kinematic problem and applying the formula of uniform circular motion in Equation 2:

$$a_n = v^2/r \Rightarrow r = v^2/a_n \qquad \text{Equation 2}$$

Where r is the path radius, a_n is the normal acceleration and v is the particle tangential velocity (Meriam and Kraig, 1998). This enables the cornering radius of the vehicle to be inferred from the measured speed and acceleration data and forms the basis of a piecewise reconstruction.

A more detailed description of the full application, derived from the methodology presented in Casanova *et al*'s paper (2001) is given in Chapter 4 where the method is applied to position a vehicle model in a graphical visualisation application.

2.4.1.7 Tabular Outing Report

The tabular outing report shows values of a user defined selection of channels for each lap of an outing in a data file. The values can be selected on the basis of a number of criteria, such as minimum, maximum and average for a lap. The tool is typically used for monitoring engine parameters to ensure temperatures and such like do not exceed limits, but could also be used to derive information about performance, such as the peak lateral acceleration during an outing for example.

2.4.1.8 Split Time Tabular Lap Report

Split time tabular reports are based upon the circuit map generated from onboard data, described previously. Once generated, the user can overlay a series of 'soft' lap beacons onto the map (Pi Research, 1998b). These are effectively virtual timing beacons, which the software uses to divide the complete lap time into segments. The report displays each sector time for an entire run. It generally also highlights the best instance of each sector and adds them together to create a theoretical ideal lap. Further, the best 'rolling' lap is also calculated,

which is made of the best series of consecutive splits. This is a slightly more realistic time, since it is actually achieved as a complete lap but simply timed from a different location. This then avoids the slightly unrealistic connotations of the ideal lap where sectors are picked from across the entire run despite not necessarily being physical plausible as a complete lap because of physical changes in vehicle weight and grip levels. The driver's theoretical and rolling laps, compared to his actual achieved, as well as the spread of best sector times, can indicate how well the driver utilised the tyres (whose performance peaks at a certain lap) and how consistent he was.

2.4.1.9 Graphical Lap Reports

The maps of the racing line described previously can be used as the basis of a display which can vary slightly between systems. Generally the plot simply shows data labels for user defined sections of the track, which display values of certain channels, and can usually be configured to provide maximum, minimum, average and such like measures or plot channel values as bands of colour (see Figure 17). The Mitchell Software Debrief3 (Mitchell, 2005a) overlaid lateral acceleration, steering and throttle channels as bar charts on the inside, outside and middle of a track map. These channels represent the three key driver inputs and the approcach by which they were combined and illustrated was unique to Mitchell Software's package, allowing all three to be displayed on a single track map.

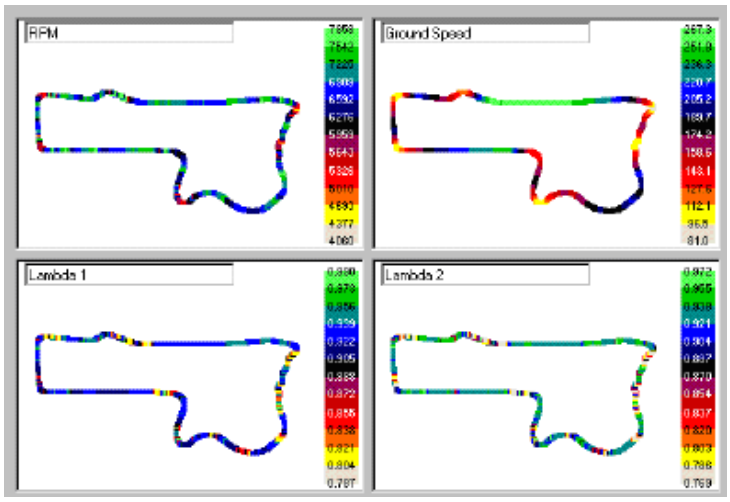

Figure 17 - A graphical lap report form MoTeC Interpreter, showing bands of different colour, representing different value of various channels (one channel per sub-window; MoTeC, 2002).

2.4.1.10 Math Channels

Math channels were another feature found to be standard across the range of commercial software. They allow for the definition of a mathematical expression, which can combine various recorded data channels with physical constants and mathematical operators. The functions are calculated for various data points and plotted along with recorded data. This allows the recorded data to be converted to more objective measures of the vehicle and driver performance, but may clearly introduce inaccuracy, dependent on the simplicity of the formulations used.

2.4.2 Advanced Analysis Software Tools

A series of tools featured in different applications which represented a development and move away from the standard analysis tools common to most or all applications. These covered a diverse range of needs, including data filtering/sorting, graphic display and data organisation.

2.4.2.1 Car and Driver Control Animation

A number of systems showed the use of simplistic animations of driver controls and car attitude to help convey a visual impression of the recorded data. Typically the data would be highlighted with a cross hair, which would move through the file at a speed to recreate real time. Graphic illustrations of the steering wheel, driver controls and the car attitude would be updated to give a visual impression of the data, as illustrated by Figure 18. A stand alone package, called Linpotsim (Harris, 2006) provided a separate tool for animating suspension data as a moving 3D plane.

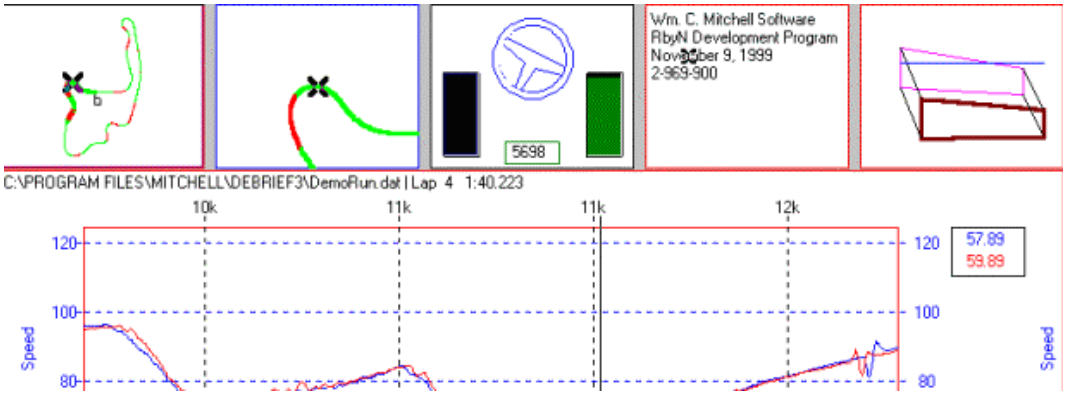

Figure 18 – Screenshot illustrating the driver controls and car attitude graphics from Mitchell Software Debrief3 (Mitchell, 2005b).

Pi Research had also previously developed a data presentation system where numeric data was displayed upon a static graphic of a car, and updated in real-time (Figure 19; Pi Research, 1998b). The user could define the channels displayed in a number of boxes to position them near to their source. This represents early attempts at trying to aid the user in assimilating the data to the vehicle.

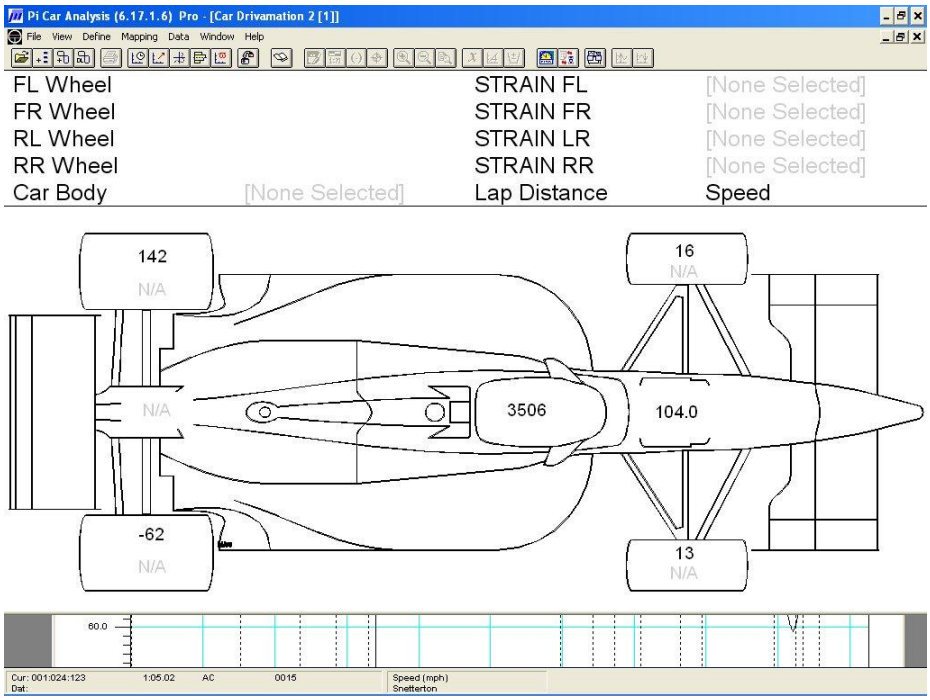

Figure 19 - Screenshot of the display tool in Pi Research Analysis Version 6, for displaying numeric data on a graphic of a racing car, helping the user assimilate it to the system by which it was generated.

2.4.2.2 Bosch 3D Animation

Although actually a simulation/lap time prediction package, Bosch Motorsport LapSim (Bosch Motorsport, 2004a and b) featured a wire frame model of a racing car for animating predicted data, but could also animate recorded data files loaded into the software. The system was developed and released at the same time as the previous work conducted on this project (Parker, 2004 a, b and c). The model was limited in that there was no way of defining suspension geometry changes, sensor locations and so forth and the visual impression was limited as there was no sense of the car being located on circuit. It did, however, indicate other commercial work towards part of the aim of this project (the visualisation of vehicle performance data), but, as with the other graphic animations, discussed in section 2.4.2.1, left substantial room for development.

2.4.2.3 Online Setup Sheets

Pi Research Club Expert (Pi Research, 2004b) provided an online setup sheet for documenting fixed and user defined parameters of the car, to accompany recorded data, as seen in Figure 20. The setup has clearly been designed to be intuitive and quick to use, by locating the various parameters on a diagram of a racing car.

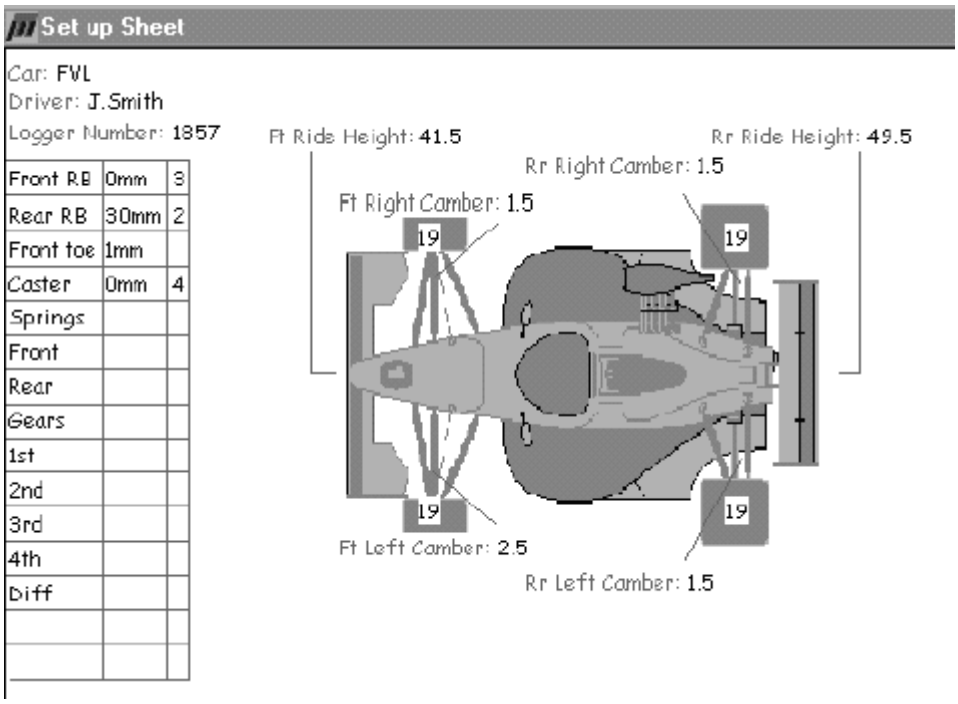

Figure 20 - The "Setup Sheet" utility within Pi Research Club Expert Analysis. This allows the user to enter information regarding the performance settings of the car and quickly assimilate these to the vehicle itself (Pi Research, 2004b).

2.4.2.4 Triggers/Events

Pi Research produced the first commercial application to feature a method for performing automatic analysis. This was featured in Analysis Version 6 and the more recent, Formula 1 standard Toolbox application (Pi Research 1998b and 2004a). Pi Research strongly advocate this technology, stating that it represents Toolbox's 'foundation' and that future developments will focus on 'event based technology' (Pi Research, 2004a). 2D Datarecording also incorporated a similar technique (2D Datarecording, 2004).

In its earliest form, the technology allowed for a simple form of expert system to be implemented. The user could specify predefined values of channels, which when met, would trigger an 'event'. An 'event' could represent the occurrence of low fuel pressure or use of excessively high engine speed, for example.

The events within the data file were highlighted on standard plots, such as channel value vs. distance to draw the user's attention to these potential areas of interest. There were also tabular reporting methods, which could provide a log of the occurrences of these events or a report detailing the occurrence together with the values of other channels. However, there was no real attempt to use the events to measure the performance of the car; i.e. by measuring the total time during which certain events occurred in a lap. Finally the position of the events around the circuit could be displayed on a map of the racing line to help the user locate and assimilate them with a position on circuit.

The system was later developed to allow for more flexibility in the definition of events, providing the user with a scripting facility similar to a generic programming language, which is likely to extend the functionality and the usability of the system.

Work in this vein, on Expert Systems, by Martin and Law (2002) and Vaduri and Law (2000) are discussed in section 2.7 along with a similar technique described by Replogle (1994) and indicate some research interest in automatic analysis of motorsport data.

2.4.2.5 Dynamic Linked Libraries

A development of Pi Research Toolbox, which was not implemented elsewhere, was the ability to execute Dynamic Linked Libraries (DLLs) from within the software. These are scripted by the user and accept input from Toolbox, in the form of channel values and return a computed value. They would typically be used to perform a calculation which could not be performed by a simple math function statement. The user guide sees this as offering potential for incorporating kinematic models of the vehicle for example (Pi Research, 2004a). However, these could still only provide numeric values of the vehicle kinematic

behaviour, rather than a visual impression with which to assimilate the recorded data. No evidence in the form of literature or from experience has indicated this has been realised.

2.4.2.6 Video Integration

A recent growth area of the data acquisition and analysis market has been in the use of video based data logging, predominantly, in the form of video based systems, which require no analysis software. Such systems record a limited amount of numeric data over a video recording of an outing (Drivedata, 2004; Competition Data Systems, 2005b).

However, these were preceded by the Video Indexed Data System (VIDS), developed by Pi Research. The system consists of a small camera which is mounted to the car, attached to the data acquisition wiring harness and records to a Personal Computer Manufacturer Interface Adaptor (PCMIA) card. The camera receives a beacon pulse which can later be used to synchronise it with the measured data using the same beacon signal (Pi Research 2000, 2004a), allowing display in both Analysis Version 6 and Toolbox alongside measured data. Once again, a cursor indicates the location in the measured data file, whilst the video plays.

This provides the user with a visual reference to the data, helping them better assimilate it to the actual car on circuit. The system was also described in an article featured in Racecar Engineering magazine (Bunkhall, 2001), where it was identified that its primary objective or greatest use was for correlating driver feedback and data; it is often difficult to understand precisely the driver's feeling and much of the skill of race engineering is identified as being able to relate engineering principles to the feel of the driver. The race engineer interviewed in the article identified that it was not always easy to identify terms such as 'nervous' in the recorded data, but the visualisation provided from the onboard camera allowed the engineer to gain some understanding of the driver's point of view (Bunkhall, 2001).

Another application, suggested by Bunkhall (2001) is for filming components, to compare alongside measured data relating to their loading. He indicated that this may have application to the understanding of tyre behaviour, for example. This was also advocated in a paper written by Moloney *et al*. (1998) describing the use of high speed imaging from static track side cameras, to provide performance measures and understanding in drag and oval racing applications in the USA.

2.5 Kinematics and Simulation Tools

Previous work identified the concept of a visual animated display of the race car depicting its suspension motion (Parker 2004a, b and c), tools for calculating vehicle suspension motion and for simulating whole vehicle displacement are briefly reviewed.

2.5.1 Suspension Analysis Software

Five suspension analysis applications were considered for the visual description of the vehicle's kinematic and dynamic movement which they provided. However, it was found that only a single example could currently interface with the data provided by a data acquisition system.

2.5.1.1 Two-Dimensional Kinematic Analysis Software

A wide range of 2D suspension kinematic packages were found to be available, which generally gave an indication of the wheel, body and suspension link positions during a wheel input. The input generally had to follow a prescribed, user-defined motion, as an overall displacement was usually divided into steps (Mitchell, 2004), however Performance Trends' *Suspension Analyzer* application (Performance Trends, 2002) could accept suspension displacement files from their data analysis application, so recorded track data could be inputted. The results of this system were typical of the various applications reviewed and could

be analysed as raw figures, plotted on graphs or animated through a line drawing of the vehicle's suspension (Performance Trends, 2002), similar to Figure 21.

The applications produced very similar, close scale measures of suspension performance, but did not offer a substantial insight into the behaviour of the car, most notably as only a single end of the car could be viewed graphically. The standard range of measures included Camber gain, Caster gain, Roll Centre Height, Roll Centre Lateral Location and several others (Performance Trends, 2002; Mitchell, 2004). Generally these measures are of more interest to the suspension design engineer, who is aiming at certain levels of such parameters, through making small adjustments to the suspension geometry. From personal experience, the race engineer is primarily concerned with the global measures of car performance, such as lap time, as well as vehicle level measures, such as roll and pitch angles.

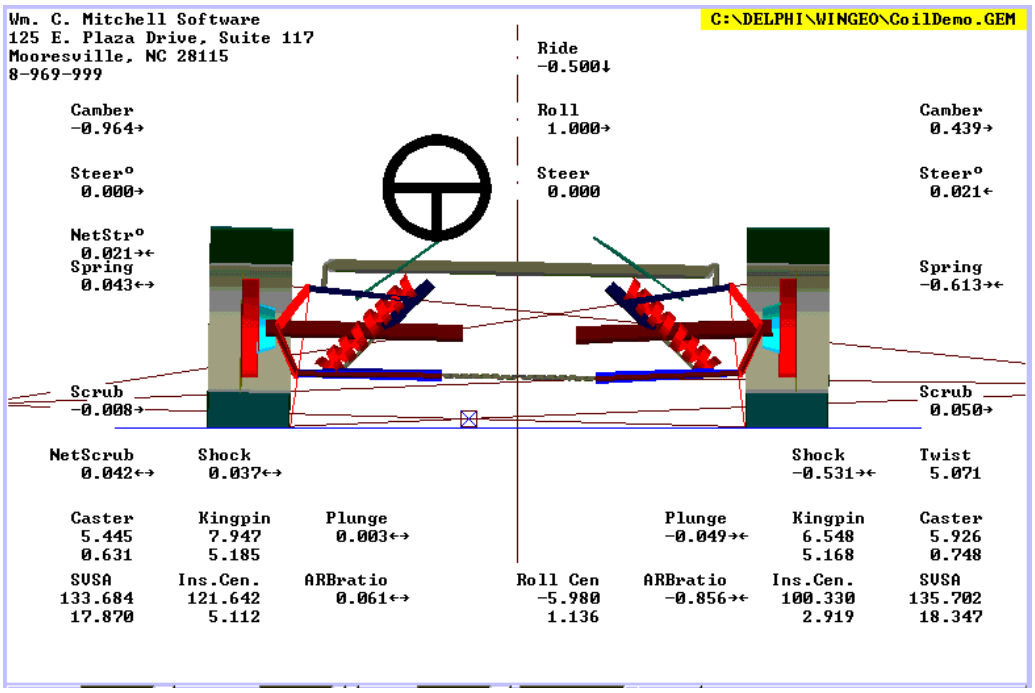

Figure 21 - The graphic display provided by Mitchell Software WinGeo3 Suspension Geometry package (Mitchell, 2004).

2.5.1.2 Three-Dimensional Kinematic and Multi-body Dynamics Software

Several 3D packages were available for the analysis of suspension kinematics and whole vehicle dynamics. These included packages that could incorporate a force based compliant deflection, representing motion deriving from the suspension bushes and links. Two key solution approaches were evident and are considered in more detail in section 7.2.

Various tests could be performed in these packages, such as prescribed displacements as well as virtual vehicle dynamics simulator tests (MSC Software, 2003). These packages provided a similar data output to the 2D packages described in section 2.5.1.1, but the graphical representation of the results can be seen to be far more refined in Figure 22. The presentation of a entire vehicle suspension viewpoint also greatly aided the visualisation of the computed results.

Compliance was also incorporated in applications, but only recommended when it had a significant effect upon the vehicle (Clarke, 2005). This was mainly due to the fact that the solution of the compliance could encounter high frequency variation in the integration stage, and hence required a very small time step, which would greatly slow the solution procedure (MSC Software, 2003).

Figure 22 - Screenshot from ADAMS/Car showing the simulated deflection of the control arm or a suspension system.

2.5.2 Vehicle Dynamics Simulation Software

Six vehicle dynamics packages were considered, as they could calculate a number of vehicle parameters, including position and vehicle attitude, based on complex vehicle dynamics models. Some systems also provided a 3D animated display of their results, such as CARSIM (Mechanical Simulation Corporation, 2004a) and ADAMS/Car (MSC Software, 2003; Hegazy *et al,* 2000).

A number of sources, mainly comprising technical magazine articles, software manuals and promotional sales literature highlighted the salient aspects of the vehicle dynamics simulators. In most cases the user was provided with a graphical interface, similar to Figure 23. Here they would input the details of a number the aspects of the vehicle, including:

- Vehicle mass and dimensions including centre of gravity location, wheel base, track widths and so forth;

- Aerodynamic data, generally in the form of lift and drag coefficients for the front and rear of the vehicle;
- Drive-train characteristics, such as the engine's torque curve as a function of engine speed and throttle position, the gear and differential ratios and the differential control characteristics;
- Suspension kinematics, generally in the form of performance curves, defining various suspension measures, such as camber and toe angle for the suspension's travel;
- Suspension compliance;
- Tyre characteristics, usually in the form of coefficients of various tyre models such as the brush model or widely used Pacejka model (Pacejka, 2002).

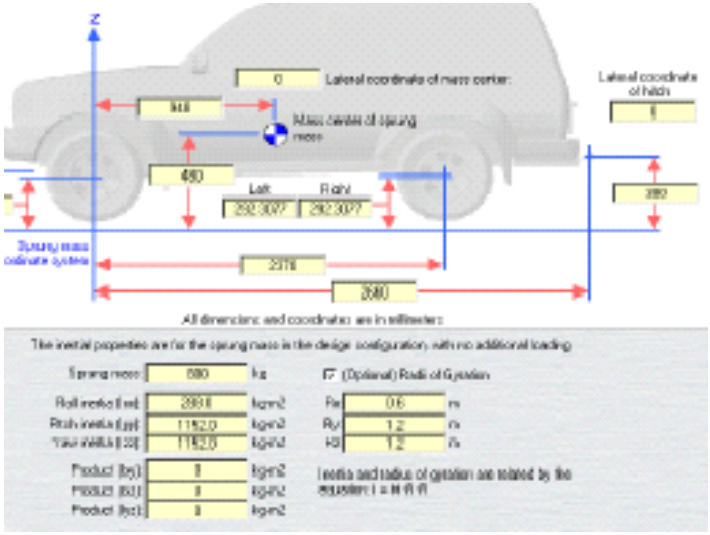

Figure 23 - The user interface for defining the vehicle's mass and dimension properties in Mechanical Simulation Corporation's CarSim (Mechanical Simulation Corporation, 2004a).

There were several features which differed between applications. The most notable were the inclusion of animated results (see Figure 24), as well as the potential for incorporating Hardware-In-the-Loop (HIL) control of CarSim, to test vehicle dynamics controllers (Mechanical Simulation Corporation, 2004b). The interface for HIL control had raised the possibility of introducing acquired data to the software and using its solver and display functionality, to present the acquired data. However it became clear that the system was only designed to be a virtual test bed for such controllers and there was no provision to allow this.

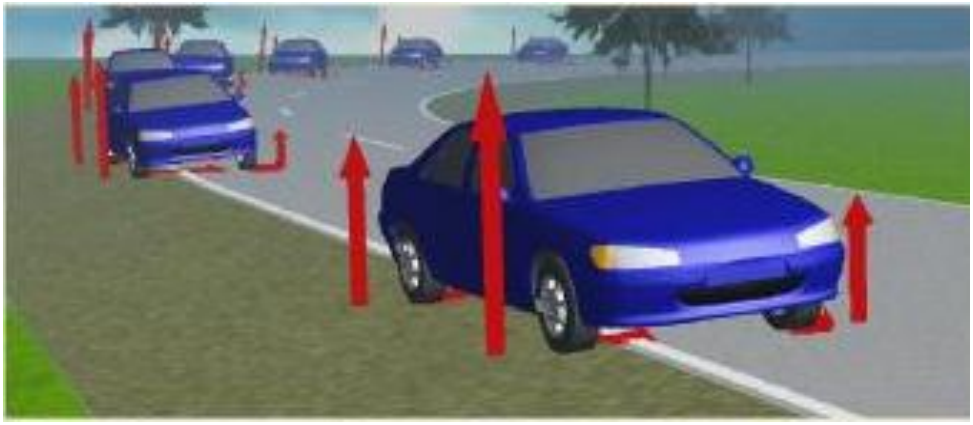

Figure 24 - Screenshot from CarSim animation, showing the simulated motion of a vehicle (utilising ghost images of the car's of the car's previous positions) and tyre force vectors (Mechanical Simulation Corporation, 2004a).

The Randle vehicle handling model varied from the majority of the other packages, in that it provided the user with 'vehicle level' metrics regarding handling (Randle, 2004). It was aimed at providing the user with an understanding of the ingredients which make the car behave the way it does, without overwhelming with very close scale suspension performance measures, such as camber, castor and toe angles. In this sense, it was concerned not with 'how each vehicle system performs its task but what it actually does'. The model was driven by a number of stiffness and damping matrices, which defined the relationship between the various major masses of the vehicle. This allowed for very rapid changes in the model configuration, whilst neglecting the intricacies of the suspension's actual behaviour.

It was suggested that the Randle model could interface with acquired data (Howard, 2002) run in real time and infer 'important data' which is otherwise hard to measure. This, however, would still only provide the vehicle level impression of the data, without the apparent needed level of detail, as discussed previously.

2.5.3 Laptime Simulation Software

Lap simulation software marks only a slight progression from the Vehicle Dynamics Simulation software. The core of these applications is still a vehicle dynamics model, but they are also concerned with how that vehicle circulates a

given circuit and the ultimate lap time that a setup is capable of attaining. Once again, these were reviewed because of the kinematics and dynamics models which underlie them and the potential for using these models to process recorded data, infer missing parameters and drive an animated display

Four applications were researched and tested, where possible, and highlighted both common and unique features. The most important are described here.

As with the vehicle dynamics simulation applications, the software applications featured an underlying detailed mathematical model and required definitions of vehicle parameters and track profile (Pi Research, 2001). The complexity of the parameters required varied between applications. At the most basic level, these included suspension motion ratios, mass, wheel base, track, tyre, aerodynamic, engine and gear train dimensions and/or characteristics. However, this was greatly expanded upon by the likes of DATAS RaceSim, for example, where over 1600 parameters defined the vehicle (Murphy, 2000; DATAS, 2005). Full topological maps of the circuit could be introduced to Pi Sim using the Line application (Pi Research, 2001), whereas RaceSim required manual manipulation of the vertical height of a circuit map generated from recorded data (see section 2.4; Murphy, 2003).

Pi Sim, produced channels of virtual data, which could be analysed against one another or against a real lap of data, using Analysis Version 6 (see section 2.4).

Perhaps the ultimate aim of these applications however, was in producing a broad measure of the attainable lap time for a given setup, since the user may not be keen on analysing predicted data against actual measurements. This would allow the user to investigate the effects of vehicle setup changes.

RaceSim, produced by Data Analysis Tools and Simulation (DATAS) featured the facility for adjusting the track conditions of the model to better match simulated data with recorded data of the same vehicle configuration. The tyre grip factor is adjusted to control the overall lap time, corner camber is adjusted to match simulated and measured minimum cornering speeds, whilst the wind or ‘drag’ controls the ultimate top speed of the vehicle. If the wind was continually

manipulated however, without any consideration as to whether the model is accurate, results could surely never be relied upon. This 'fiddle factor' is criticised in Clarke (2004) by the creator of a model validation procedure, Richard Dorling, since the fundamental issue of whether the model of the vehicle is accurate is not answered, rather the weather and track conditions are simply adjusted to yield the correct results (Clarke, 2004).

Bosch Motorsport LapSim was described as both a lap simulation and 'vehicle identification' tool (Bosch Motorsport, 2004b). By combining simulated and measured results, the application aimed to determine vehicle parameters such as the aerodynamics and tyre characteristics. For example, the 'drag factor' assigned to the vehicle could be adjusted to yield the best correlation between measured and simulated speed traces and the vehicle's lift coefficients were adjusted to arrive at the best match between simulated and recorded ride heights (which are controlled by the downforce generated by the vehicle). Likewise, the steering angle data was used to determine the Pacejka tyre model coefficients (van Rutten, 2003a and b). This was a particularly notable aspect, since obtaining accurate tyre property data was documented as being particularly difficult (Dixon, 1996), (Wallentowitz *et al.*, 1999). Once the vehicle parameters were defined, the application could then function as all others, and be used to predict the affect of various setup changes on laptime.

Another notable feature of Bosch LapSim was a graphical wireframe model of the car, to display simulated results. It is also possible, by introducing recorded data to the application (as is standard practice for the 'vehicle identification' process) to 'play' this data through the model (see Figure 25).

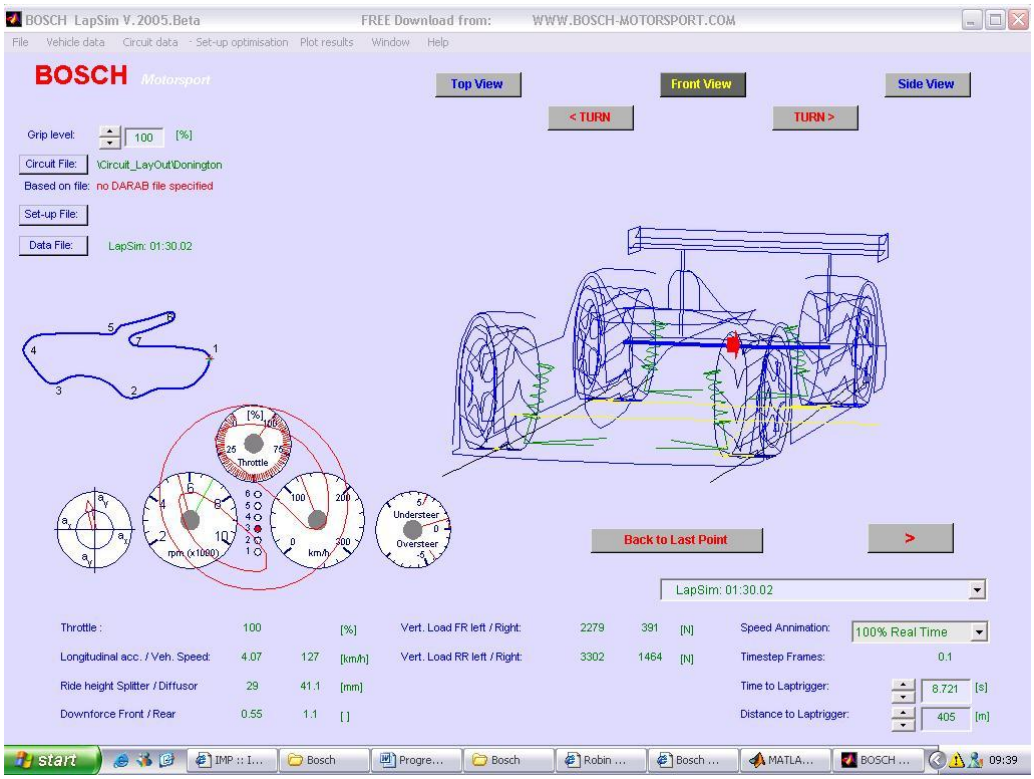

Figure 25 - The wire frame 3-Dimensional model of the racing car, used to display data to the user in Bosch LapSim.

The accuracy of the model was dependent upon the data which is supplied to it. Its highest level of accuracy was attained when it is supplied with suspension displacement, speed and yaw rate data. However, it still did not afford the user a particularly good visualisation of the vehicle. The wireframe nature made this difficult but was compounded by there not being any real impression of the vehicle's position on track or its travel. It was also apparent that there was no consideration of system compliance and tyre deflection.

2.6 Expert Systems and Neural Networks

Expert systems and neural networks represented two tools which were used to perform autonomous analysis. Background to both is detailed here, owing to

their potential for helping the user analyse data by identifying certain combinations of events and patterns in data, which are the analysis strategies most commonly employed in the analysis of motor racing data (McBeath, 2002)

2.6.1 Expert Systems

Expert systems have already been briefly mentioned as part of discussion about the “events” based analysis approach employed by Pi Research (Pi Research, 2004a), but they are given a fuller consideration here.

An *Expert System* is essentially a computer system which emulates the decision-making ability of a human expert (Giarratano and Riley, 1998). A complete system consists of two key parts, a knowledge base, which encapsulates the expert’s knowledge and an inference engine, which reasons about a problem, using that knowledge. They usually also feature heuristic search routines, which represent an expert strategy or rule of thumb for using the expert knowledge to solve a problem (in essence a shortcut to a solution; Jackson, 1999).

Systems are formed from various different approaches. For example, rule based systems are a simple form, providing a series of ‘If-Then’ statements, to work to a solution for a given problem. Other, more complex systems, are based around associative networks, such as trees, giving a hierarchical structure to the information and linking parts which are directly associated with one another (Jackson, 1999).

Neural Networks, described in the following section, can also be incorporated within an Expert System to perform tasks such as pattern recognition and data mining (Oatley and Ewart, 2003).

There are many different classifications of Expert System task, from interpretation, prediction and diagnosis to debugging and control of systems, which has lead to an application in a wide range of fields, including medicine, engineering and business (Giarratano and Riley, 1998).

2.6.2 Neural Networks for Pattern Recognition

Artificial Neural Networks (ANNs) are computer based networks, replicating some of the functionality of the human brain. They have emerged as a means of recognising patterns in recent years (Bishop, 1995); a task that the human brain is very good at (Anderson, 1995) and is performed extensively in current motorsport data analysis.

Typically an ANN will feature various interconnected units. Each connection has a weighting associated with it, which multiplies its input. A function within the unit then produces a result, which causes the unit to 'fire' under certain conditions and not under others; this relates to the signal it sends along its output connections to subsequent units (typically either the value of the unit's function or 0 respectively; Anderson, 1995). This cascade effect results in the output unit(s) receiving a number of inputs which are summed and form the basis of network decision. Often the weightings of each connection are adaptive, allowing the system to evolve as it is presented more input data. An ANN is typically viewed as a network diagram, such as that shown in Figure 26, but is processed and considered as a set of underlying mathematical functions (Bishop, 1995).

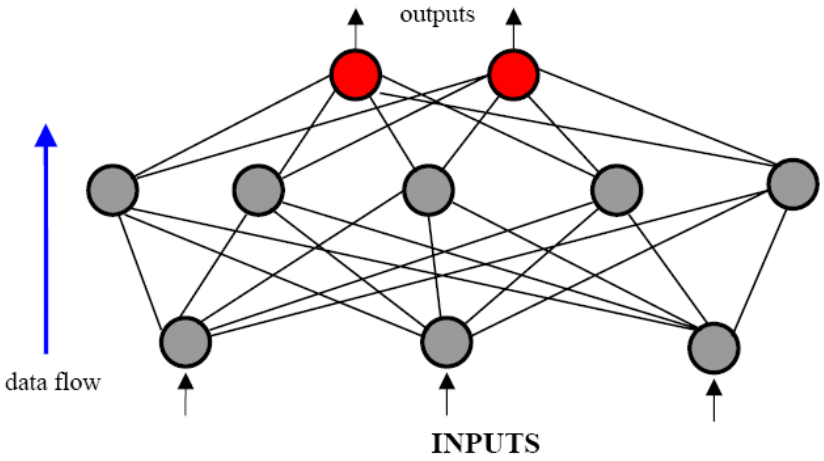

Figure 26 - A typical Feed Forward Neural Network (Kerr, 2005).

2.7 Development of Motorsport Data Analysis Techniques

In a discussion of the then current use of computers in the operation of a racing team Purnell (1998) identified some areas for development in motorsport data analysis software and the use of computers within a team in general:

- There was a need for a 'data culture' within motor racing, which would help the driver and race engineer understand the race car better, in order to both optimise their performance. As part of this ideal, measurement of every aspect of the car's behaviour was laid down as being necessary;
- Most race engineering work was based on intuition and few race engineers are actually trained. The level of data needed for a full understanding may be overwhelming;
- The great technical insight provided by acquired data was not integrated and presented in a way which was easy to comprehend when the 'pressure's on at the race circuit'. There was a need for a presentation of data in a form which allowed the engineers to quickly and effectively 'relate events to the track position and the driver's actions';
- There is a broad need to integrate every aspect of racing team operation within computer software, to ensure the most accurate and efficient job is carried out. This extended to tracking vehicle setup, inventory and car development.

The survey of literature in the area of motorsport data analysis, together with enquiries at many universities with a direct interest in motorsport, indicated that there was very little research activity and published work in this area. The most probable reason for this is that much of the work is likely to be conducted by or in collaboration with teams themselves. Such proprietary information would not be released, owing to the highly competitive nature of motor racing.

The remainder of this section however presents information on the limited research available and apparent commercial development in the area of data handling. It also considers visualisation of data to aid user assimilation, a tool which is observed to be prolific in other areas such as the vehicle simulation software, described previously. Finally trajectory reconstruction is considered and more detail in given on the background to sensors and measurement techniques that can provide this information. This could be considered a vital part of a data visualisation tool and also a key step towards Purnell's ideal of measuring and understanding every aspect of the car's performance (Purnell, 1998).

2.7.1 Expert Systems

The most significant area of research and development with regard to motorsport data acquisition was in the development of so called 'Expert Systems' for automatic analysis of data. The main motivation for these systems is that they can assist the user with the large volumes of data, which are presented to them, performing routine analysis, which would otherwise not be completed during the test (Martin and Law, 2002). It was identified by Replogle (1994) in his discussion of an Expert System that the user is overwhelmed by data and they do not tend to perform the analysis which results in the most significant gains. Tests do not tend to be driven directly by the findings from acquired data (Martin and Law, 2002), except at the highest levels, where there are many personnel (Wright, 1997) and the most detailed analysis is carried out post session (Vaduri and Law, 2000). This fact was highlighted in all of the sources considered in this section. The fact that track time is also so expensive and limited by many championship rules further fuels the need to maximise its use. A secondary motivation was that the Expert System can potentially deliver much more repeatable analysis than a human; usually analysis is performed as subjective appraisal of data trends. Also the short time available for this analysis could endanger the accuracy of the conclusions drawn by a human and the quality in general is entirely dependent on their experience (Martin and Law, 2002).

2.7.1.1 Logic Based Expert Systems

It was identified in section 2.4.2.4 that Pi Research had already implemented a limited form of expert system, which could highlight the occurrence of certain combinations of channel value occurring within a data file (Pi Research, 1998b and 2004a). However, Replogle (1994) detailed work on a more sophisticated system, which aimed to detect the characteristic trends in certain data channels which relate to handling events.

Replogle's system was based around analytical decision models (Replogle, 1994). These models were founded on vehicle dynamics theory and when supplied with recorded data, they presented output in such a way to the team that it is 'relevant to setup and development decisions'. Replogle (1994) identified that if the full potential of the acquired vehicle data was to be realised, systems had to be able to assist the user in making rapid decisions. He also identified that the ability of a system to discern aspects of the car's behaviour, which the driver could not detect, should also be exploited (Wright, 1999).

Replogle's system was designed to detect the precise nature and severity of oversteer and understeer events, and to distinguish real but non-typical data, such as where a driver made a sharp manoeuvre to avoid debris. Replogle aimed to achieve this by developing a metric, whose value would indicate the balance of the car; the tendency of its handling away from a neutral condition, towards the front sliding (understeer) or the rear sliding (oversteer).

Replogle first developed metrics based on the ratio of steering input to lateral acceleration and the 'excess steering angle' (the difference between the measured steering angle and the steering angle required to maintain the vehicle in a zero slip angle condition). He finally developed the 'Stability Index', which was calculated as the difference between first time derivatives of front and rear slip angles with respect to the lateral acceleration. This would indicate a change in the vehicle's yaw rate (rotational rate about its vertical axis) proportional to the cornering force being generated by the vehicle. This value would be maximised by a neutral handling car generating a high lateral acceleration. A rapid change in the yaw rate, indicative of a handling imbalance, would sharply

increase/reduce its value. This method could distinguish oversteer and understeer, but was slightly flawed by the expense associated with measuring slip angles, typically with a non-contact speed measurement method in two dimensions (see section 2.2.1; Replogle, 1994).

2.7.1.2 Fuzzy Logic Based Expert Systems

A recently active research interest at Clemson University, North Carolina, USA was in the use of Fuzzy Logic based Expert Systems for performing automatic analysis of acquired data. This research, however, halted in 2004 (Law, 2004).

Vaduri and Law (2000) presented the first published work in the area. They aimed to develop an 'expert system' to increase the quality and speed of data analysis. It was specifically focussed on the detection of oversteer and understeer in data. A set of computer based algorithms resulted, which searched the data, considered several channels and performed various mathematical operations to provide results. These were arrived at quickly and automatically and pinpointed areas of interest in an easy to understand format (Vaduri and Law, 2000).

Their algorithms were mainly based upon human observations of various signals during the actual events, which could provide a specific characteristic for the algorithm to identify. For example, the lateral acceleration trace during oversteer was seen to produce a 'rough' characteristic since the car loses and regains grip during this event, causing a variation in acceleration. Also the driver's steering correction input was studied, and it was concluded that the time duration of corrections (typically around 0.3 seconds) leads to a frequency of approximately 3.5Hz in such an event. Further, the magnitude of the corrections was about 0.3 to 0.4 times the total steering angle (Vaduri and Law, 2000). This basis represented the encapsulation of experts' knowledge within computer software.

Martin and Law (2002) presented later work, which developed that of Vaduri and Law (2000) to making judgements about the driver and chassis performance. The aims of the earlier work remained strong and as part of the process various measures were taken, such as the speed with which the driver changes gear,

whether the driver applied the throttle soon enough after exiting a corner and how assertively he applied the throttle, for example.

The analysis process of Vaduri and Law (2000) and Martin and Law (2002) utilised the concept of Fuzzy Logic, the control methodology which allows imprecise/noisy/incomplete or ambiguous inputs to be processed by a system to produce a definite conclusion or output (Kaehler, 2004). This effectively replicates a human's perception and analysis, but in a repeatable way, trading off 'precision and significance' (The MathWorks, Inc., 1996).

Fuzzy Inference was combined with conventional logic by Martin and Law (2002), to allow processing of the typical noisy signals received on a racing car. This is significant as there are considerable sources of noise and vibration on a racing car. In contrast Replogle (1994) advocated the preciseness of data as input to the models he used. This is a difficult requirement to meet on a racing car.

Martin and Law (2002) also indicated a benefit of their form of post-processing in that some data analysis could not be performed visually, in the subjective fashion often employed. A particularly strong example was the ability to distinguish some percentage/fraction of a signal's peak value. This means that human analysis is sometimes not particularly repeatable.

2.7.2 Visualisation

The capture and visualisation of dynamic events is an important area of science which was realised as far back as 1878 when English photographer Eadweard Muybridge first achieved a series of twelve synchronised photographs capturing the gallop of a horse, famously entitled *The Horse in Motion* (Pain, 2008).

The advantages of video recordings to assist data analysis is clear in the proliferation of small camera recording systems for race car applications in recent years, such as the Pi Research VIDS, Drivedata and Competition Data Systems approaches (Pi Research, 2000; Drivedata, 2004; Competition Data Systems, 2005b). These however all feature a relatively low speed small camera and are

generally aimed at providing a driver's view from the cockpit of the car. In 1998, Moloney *et al*. published a technical paper advocating the use of fixed trackside high speed cameras for aiding the user in understanding the data recorded from a data acquisition system onboard a racing car. They also recommended the use of motion analysis software for being able to track points through a film, performing analysis from the images not possible with the acquired data alone.

Although not published, television coverage of the World Rally Championship (WRC) and F1 has recently included overlaid segments of video showing two cars negotiating the same section of track, taken from a fixed location camera. The producers have evidently seen the benefit of illustrating the differences between drivers to the audience by using this approach.

The use of captured footage or images for visualisation has the obvious advantage of being a direct impression of the event itself, rather than relying on any reconstruction. However, the hardware required, the limitations on capture rate and the restriction to only the camera's point of view present the potential for visualisation via computer graphics to be of benefit to understanding recorded data.

It is clear that visualisation based on computer graphics is already employed as a means of presenting data and offering a certain level of insight not afforded by more standard graph based data presentation methods. There are various applications utilising graphical displays, but examples include the visualisation of vehicle dynamics simulations presented earlier (Figure 24 and Figure 25) and of crash scene reconstructions, (Fay and Scott, 1999).

A particularly noteworthy area of development is in the 3D visual reconstruction of flight data. A sample of several applications were found to be available, all of which advocated benefits which could be expected to carry over to a similar technique's application to motorsport acquired data. In their paper focussing on the *Flight Animator* application Bolduc and Jackson (1999) describe the benefit of 3D animations of recorded data as an effective way of presenting data to a range of users, representing engineers to pilots. As described by Teledyne (2010), the animated reconstruction has the ability to allow the assimilation of large volumes

of data more effectively than graphed or tabulated methods. Data can be presented in an intuitive manner that can more easily be grasped by the user. Corporate literature for two other animation tools, *FlightViz* and *CEFA Flight Data Animation* identify the animation reconstruction as a communication tool (SimAuthor, 2010; CEFA, 2010). This is specifically identified by SimAuthor (2010) in the application of pilot training and the communication between instructor and trainee pilot; this is precisely the same scenario encountered between race engineer and driver in motor racing.

2.7.3 Trajectory Reconstruction

Whilst sections 2.7.1 and 2.7.2 described primarily software based developments, it is worth expanding the detail of the area of vehicle trajectory reconstruction, which has developed primarily through hardware advances.

It is interesting to consider motor racing data analysis texts through 1994 to 2008, a period where GPS has grown from a purely military technology to a consumer one and where it has found application in motor racing (Segers, 2008). In Fey's *Data Power* (1993), considered the seminal text on motorsport data acquisition for many years (Vaduri and Law, 2000), there is no coverage given to the use of trajectory plotting method. At the time, an approximation based on lateral acceleration and wheel speed data was the only method of calculation available and this was perhaps deemed too inaccurate for anything more than the creation of a track impression for reference. By 2008 the books of Segers and Templeman were discussing the reconstruction of GPS data to form a vehicle trajectory; although it was not agreed to what level the results could be used for comparison. However, it is clear that the development of GPS technology for racing has opened the real possibility of being able to accurately analyse driver racing lines.

2.7.3.1 Lateral Acceleration and Wheel speed

The most established and universal method of estimating vehicle trajectory is a planar trajectory mapping algorithm using data recorded with a standard

accelerometer and wheel speed sensor, described in more detail by Casanova *et al*. (2001). A kinematic model of the car is considered, simplified to the form of Equation 2 whereby the cornering radius of the vehicle can be determined from its forward velocity and lateral acceleration. The method works from the start of the lap forwards, in a stepwise fashion, at each point determining the car's cornering radius and change of heading from the previous calculation point. From this, the distance covered on the current cornering radius can be found, or indeed the distance measured by the wheel speed sensor(s) can be used. The distance increment and heading angle allow longitudinal and lateral components of the car's movement to be approximated and the coordinates at that time point to be determined.

The majority of Casanova *et al's* paper considers compensating for errors arising in this approach. A number of sources are likely, including errors from the acceleration integration incorporated in the stepwise approach, errors due calibration and the zero level of the accelerometer, track inclination and also tyre deformation invalidating the calibrated tyre circumference for wheel speed measurement. The result is that the circuit trajectory is shown to be discontinuous and two algorithms are proposed to correct for the errors. However, Casanova *et al* (2001) conclude that the distortion of the resulting circuits indicates there are still errors present which need addressing. Whilst the circuit lengths calculated can be closely matched to the nominal length of the circuits used, the actual trajectory shapes can vary greatly; sometimes in the order of tens of metres.

2.7.3.2 Global Positioning System

In 2008 the books of Segers and Templeman both discuss the use of GPS technology and the potential for comparison of racing lines. The views of the two authors are slightly conflicting, perhaps reflecting the levels of the sport to which the books were aimed. Segers, who appears to cover technology applicable to a high level of International racing, advocates the use of GPS signals, fused with accelerometer measurements to provide comparable track maps, but in describing a method for surveying the track edge with GPS alone indicates inaccuracies of raw GPS data. Templeman meanwhile, rules out the comparison

of racing lines with GPS data, citing an accuracy of a “few” metres as insufficient for meaningful comparisons and the survey standard methods and corrections, which would potentially make comparisons acceptable, as being too expensive for junior racing. Perhaps the most worthy endorsement, or lack of, comes from an interview with Mike Wroe, Head of Electronics at the Force India F1 team at the end of the 2008 racing season, who believed the accuracy of current GPS systems, including the use of Kalman filters described later, was insufficient for comparison of driver lines (McBeath, 2008). He also highlighted difficulties of accurate use at a circuit, with buildings, grandstands and so forth causing reception issues and there being a range of other radio transmissions occurring at a typical meeting causing interference.

Accuracy and its improvement are the clear issues with the use of GPS, with its ability to position a moving vehicle in an absolute coordinate frame making it otherwise very suitable to the application of trajectory reconstruction. In the United States Department of Defense Global Positioning System Standard Positioning Service Performance Standard (2008) a 95% positional accuracy of 7.8m is quoted with a 99.94% positional accuracy of 30m. Further to this, it is reported that “well designed” GPS receivers can achieve 3m horizontal accuracy. An accuracy of 3m is undoubtedly insufficient to compare driver trajectories, as identified by Templeman (2008); however there are several key methods for trying to improve the accuracy of GPS measurements.

All methods aimed at improving the accuracy of data recorded from a GPS receiver ultimately incur extra cost as one might expect, and some present practicality issues, requiring a lengthy initialisation. Where possible, some achievable accuracies are quoted for inertial and GPS navigation systems manufactured by Oxford Technical Solutions, which give a good indication of the achievable accuracies from a commercial system. However, it should be noted that these systems use inertial measurements as well as part of a Kalman filter technique to achieve these positional accuracies, a technique described in more detail in section 2.7.3.3.

Normal operation of a GPS receiver, code phase matching, involves using the Coarse/Acquisition (C/A) pseudorandom code received from the satellite and

shifting an internally generated copy over this, the shift required being equal to the transmission time. The alignment of modern receivers is typically accurate to approximately 10 - 20ns (1 – 2% of the pulse width), with the wave propagating at the speed of light this equates to approximately 3 - 6m in the distance between the receiver and satellite typically (Trimble, 2008).

A technique applied to GPS for surveying is to use the GPS satellite's carrier signal to measure the distance between satellite and receiver. Carrier phase measurements can be made to improve the accuracy, since the carrier wave at a frequency of 1575.42MHz has an approximate wavelength of 20cm (United States Department of Defense, 2008). This is much shorter than the distance between the C/A code bits and presents the potential for achieving an accuracy of 3-4mm (Trimble, 2008). The method effectively counts the number of carrier cycles between the receiver and satellite, but experiences problems associated with the fact that every cycle of the carrier is identical, whereas the C/A is deliberately variable in its nature to aid alignment. The key issue with this approach is the ambiguity of the signal which leads to an integer bias to the calculated phase measurement. There are various techniques available for determining this bias in order to correct, which are described by Yang *et al*. (2002). It would appear that the most reliable method is to hold the receiver stationary for a period of time allowing movement of the satellite to yield a range of data with a fixed global location for solution. This approach is employed commercially by Oxford Technical Solutions on their racecar based system which can achieve an optimal accuracy of 0.02m, using differential corrections also, but requires a 15 minute initialisation period (Oxford Technical Solutions, 2002). Another key issue is that if the lock with a satellite is lost, the phase biases must be determined once more (How *et al*., 2002), presenting obvious issues when the accurate initialisation can take as long as reported. Alternative faster methods of bias calculation have been developed and are reported in papers such as How *et al*. (2002). The phase bias calculation techniques are not given an exhaustive consideration as Grewal *et al*. (2007) report that no system is fully robust and without its limitations and it would appear that the racing commercial application of GPS technology ultimately relies on the lengthy initialisation sequence with stationary receivers (Oxford Technical Solutions, 2002). There is also

considerable extra cost involved in implementing some of the phase bias solutions (How *et al*., 2002).

Sources of error affecting GPS signals can include atmospheric (ionospheric and tropospheric) delays, multipath effects caused by reflection from solid entities such as buildings, receiver clock and orbital position errors as well as a receiver seeing a low number of satellites or a tightly grouped selection of satellites (Grewal *et al.*, 2007). One increasingly common way to reduce these errors is to use Differential GPS (DGPS), which can be applied to either code-phase or carrier-phase based GPS.

DGPS works by using a second static receiver in relatively close proximity to the area of operation of the moving receiver. The errors experienced by the static receiver will be essentially the same as those experienced by the moving one; subtraction of the static receiver's position estimate from the moving one will provide some error correction. If the static receiver is at a known point, such as an established survey point or a professionally surveyed location the corrected data can be related to an absolute global frame, otherwise the coordinates are in a local grid, originating at the static receiver. This method applied to a code phase measured estimate can achieve 0.4m accuracy in a commercially available system (Oxford Technical Solutions, 2009) but is typically around 1m. It does suffer the problem however, that the further the moving receiver is from the stationary one, the less accurate and relevant the corrections are as various atmospheric effects and so forth vary (Grewal *et al.*, 2007).

An extension of DGPS is the augmentation system such as the Wide Area Augmentation System (WAAS) in the USA. These are essentially networks of receivers which monitor the GPS satellite constellation and measure errors based on their calculated location. In the case of the WAAS, corrections are transmitted to two geostationary satellites which in turn transmit these back to consumers' GPS receivers on the ground, to improve their signal. The European equivalent of this system is termed European Geostationary Navigation Overlay Service, EGNOS (European Space Agency, 2004) whilst Europe is also covered by proprietary DGPS network called Omnistar, which sells its service via a subscription method (Oxford Technical Solutions, 2002, Omnistar, 2010). It is

claimed that EGNOS improves GPS accuracy to 1-2m (European Space Agency, 2004) and the use of Omnistar is required to achieve the Oxford Technical Solutions RT3042/RT4042 navigation system optimal accuracy of 10cm at additional cost to the user (Oxford Technical Solutions, 2009).

Techniques using the Doppler phase shift caused by the relative motion of GPS satellites and the receiver were highlighted in several papers (How *et al.*, 2002; Zhang *et al*., 2006; Chalko, 2007 and 2009). Doppler phase shift based GPS would definitely appear to be an emerging approach to velocity measurement from GPS but it was not given exhaustive consideration as it was still dependent on four or more GPS receivers for accurate results (Zhang *et al.*, 2006) and appeared to have a positional accuracy of 0.05m (Chalko *et al.*, 2007 and 2009). It did achieve the aim proposed by How *et al*. (2002) of improving the accuracy of GPS without having to rely on the phase ambiguity solution routines of carrier phase GPS and the associated time delays and costs. However, it still did not meet the accuracy of optical position sensors described in section 2.7.3.5.

2.7.3.3 Inertial and Global Positioning System Kalman Filter Techniques

Another approach to trajectory approximation is to combine both accelerometer and GPS data together. The description of GPS mapping techniques by Segers (2008) indicates this as being the only realistic way of obtaining a usable trajectory estimate from GPS in racing.

Rezaei and Sengputa studied the use of Kalman filters to improve accuracy of GPS measurements for accurate lane discrimination as part of collision avoidance systems (2005 and 2007). In their development of a vehicle dynamics model to replace the commonly used point kinematic model, they tabulate the accuracy achieved by other systems using this more traditional approach (2007). Of these, the use of carrier phase GPS yields the most accurate systems with a 0.02m positional accuracy with a code-phase system achieving approximately 1m positional accuracy. Their motivation for developing the vehicle model in the filter was the already identified higher cost of implementing carrier phase GPS.

Doogue and Walsh (1998) describe the attempts of the Dartmouth Formula Racing Team to develop a track mapping system for use on a Formula SAE car (equivalent to the UK's Formula Student). Their approach utilised integration of accelerometer data in 1 second intervals, with accompanying GPS logging at 1Hz. The two streams of data were combined every second using a Kalman filter which compared the estimated state vector of the car, from the accelerometer data, with the measured one from the GPS, updating the initial conditions for the integration of the next time period. Doogue and Walsh report a final positional standard deviation of 5 feet (1.524m) which is still very high when trying to compare precise driving lines.

Oxford Technical Solutions were previously mentioned in the description of GPS technology as a company producing an extensive range of INS/GPS navigation systems for the automotive sector, some of which have been targeted at racing (Oxford Technical Solutions, 2009). The commercial application of such systems is therefore clear, but as also reported, the maximum accuracy of these systems are again 0.02m when using carrier-phase techniques using both the civilian and military satellite transmissions. Further to this, the description of one system used at a race track highlighted the impracticalities of using the carrier-phase GPS measurements because of the time required for the initialisation procedure. As a result 1m accuracy was the realistic figure achievable at the circuit (Oxford Technical Solutions, 2002).

2.7.3.4 Doppler Shift Speed Sensors

The use of a radiation emitter and receiver fixed to a moving car and aimed at the ground to determine the Doppler frequency of reflected waves in order to infer the vehicle's speed has been reported as the subject of a number of research papers (Corbrion *et al.*, 2001; Ditchi *et al*., 2002; Kleinhempel *et al.*, 1992; Kleinhempel, 1993). It was also used as a method of verification in work on other velocity sensors such as by Kim and Slaughter (2008).

The sensors are mounted to the underside of the vehicle and emit either an ultrasonic or microwave signal onto the ground at an inclined angle (Imou *et al.*, 2001). This means the incident wave experiences a relative motion of the

ground, and when it strikes suitable obstacles it is reflected diffusely. The reflected signals can be received and via signal analysis, compared with the transmitted signal in order to determine a Doppler frequency shift from the relative motion, an established means of determining velocity (Ditchi *et al.*, 2002).

Despite this work and the availability of commercial Doppler speed sensors their use in racing was not reported in any book making up part of the exhaustive review of current motorsport data acquisition texts. A full reasoning for their lack of use has not been found, but it would seem that there reliance on ground obstacles for correct operation seems to present a potential reason.

The lack of reflecting obstacles within the footprint of the emitted wave causes a low or no return of signal for processing, as identified by Imou *et al*. (2001) and Ditchi *et al*. (2002) and has prompted various attempts at methods to increase the chance of signal reflection, primarily by using a broad beam (Ditchi *et al*., 2002; Corbrion *et al.*, 2001) but also with the analysis procedures applied (Kleinhempel, 1993).

Various sources indicate issues with the use of Doppler sensors on smooth surfaces, Kim and Slaughter (2008) and Imou *et al.* (2001) both report lowest accuracies of ultrasonic Doppler sensors on tarmac surfaces in the studies related to the velocity measurement of farm machinery. Although these speeds are low in comparison to that of a race car it still suggests that the smooth surface of a race track may cause inaccuracies to the sensor which has prevented their use. Sensors were also reported to suffer further errors in the case of wet surfaces (Kleinhempel, 1993; Ditchi *et al*., 2002) and therefore the reliability of the sensor as a dependable solution for a racing team seems limited.

Vibration affecting the phase of the returned signal and the assumption that the air is stationary are both mentioned by Imou *et al*. (2001). The vibration levels on a racing car would be high and the air between the car and ground is accelerated by shaped floors on many racing cars to lower the aerodynamic pressure on the underside of the car, potentially representing further inaccuracies to the application of Doppler sensors to racing.

2.7.3.5 Optical Velocity/Displacement Sensors

Optical velocity sensors are available, manufactured by the company Corrsys-Datron, now part of the Kistler group. Lucas has also developed a similar sensor technology (Sakai *et al*., 1992 and 1995). The Corrsys-Datron sensors operate on the so called Correvit® principle, whereby a ground image is focussed through a lens, prismatic grating and second lens onto a photoelectric detector (see Figure 27; Corrsys-Datron, 2004). Movement of the ground image across the grid of the optical grating, i.e. from the sensor mounted to a car body moving across the ground, causes a modulation of the image falling onto the photoelectric detector and hence its output signal (see Figure 27). The periods of this signal represent a distance and the frequency therefore a speed which Corrsys-Datron links through Equation 3:

$$f = (M / g) \times v \qquad \text{Equation 3}$$

Where f is the signal frequency, M is the projection scale of the optics, g is the grid constant and v is the speed of the sensor movement relative to the ground.

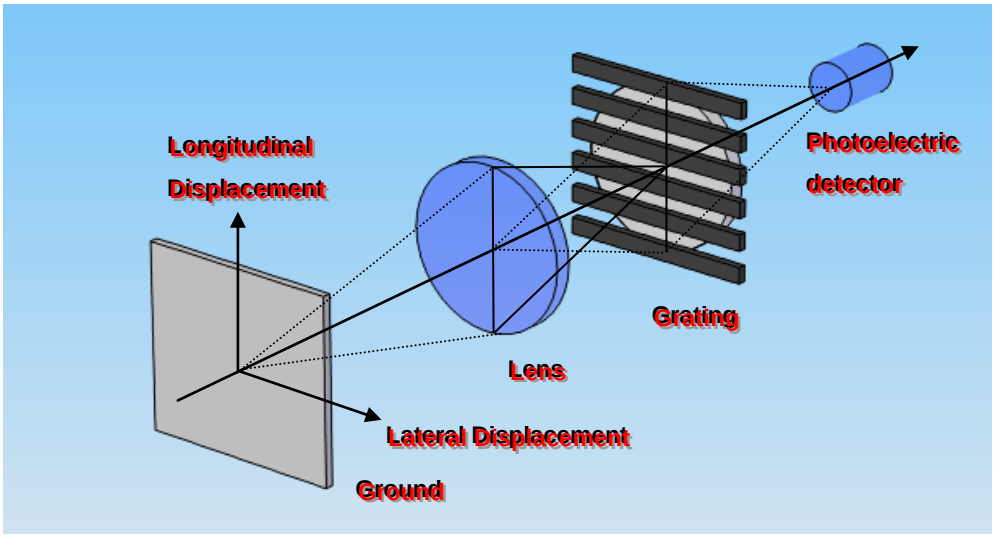

Figure 27 - The Corrsys-Datron Correvit® measurement system (Adapted from Corrsys-Datron, 2004).

A number of versions of the Corrsys-Datron sensors have been produced, with updated lighting technologies and design features for specific applications. Table 2 summarises the applications and accuracies of some of these.

Table 2 - Applications and accuracies of a range of Corrsys-Datron Correvit ® sensors (Corrsys-Datron, 2009 a, b, c, d, e and 2010).

Sensor Model	Application	Accuracy
LF-II P	Single axis, road cars	2.08mm
SF-II P	Dual axis, road cars	2.08mm
S-350 Racing	Dual axis, racing	2.47mm
S-HR	Dual axis, road cars	2.66mm
L-350 Aqua	Single axis, road cars, wet testing	1.47mm

Whilst the accuracy of this type of sensor is high, so too is the cost with the SF-II P currently costing £17,065 per sensor before logging equipment is considered. This immediately prohibits the use of these sensors from junior racing categories.

Two methods of determining velocity from recorded ground images were identified for application to agricultural machinery. One of these captured a single row of pixels, performing a cross correlation between successive images to determine displacement (Stone and Kranzler, 1992). The single row of pixels however limited the measurement to purely longitudinal velocity and errors associated with the vehicle turning were suffered. A second more recent method captured a 640 x 480 8bit image and applied a neural network pattern recognition algorithm to determine the displacement between two images at a series of 200 points across the frame (Kim and Slaughter, 2008). This method would accelerate analysis in comparison to a full image correlation but already produced errors of 2.0mm at a low velocity of 1.36ms^{-1} (Kim and Slaughter, 2008).

Both of the image based methods described report no consideration of height and it is assumed this was considered constant. Also the techniques simply

imaged the ground with a rolling capture sequence, in the case of Stone and Kranzler (1992) using an additional constant light source. The 1ms exposure used by Kim and Slaughter (2008) would not freeze the ground image at the speeds encountered by a racing car.

2.8 Closing Remarks

This chapter has presented the reader with a considerable amount of information regarding the uses of data acquisition and analysis in motorsport, the range of sensors and the tools available to analyse the acquired data. The reader should now have some appreciation of the scale of data collected and the lack of development in the tools supplied with a typical commercial system for analysis.

Additional computer based tools are considered which were largely not directly involved with the analysis of motorsport data but are worth the reader being aware of before they embark upon the work section of this thesis. These included kinematic and simulation packages as well as a brief introduction to expert systems and neural networks for pattern recognition. These utilised various techniques which exhibited potential for addressing areas of the project concept defined in the next chapter.

The final section of the chapter looked at the most recent development of motorsport data acquisition and analysis practice, based on the survey of software and literature presented previously. In doing so, the reader was asked to consider applications outside of racing at times, but which involved a similar use of data acquisition, such as the training of pilots. The section had three broad sub-sections following from the introduction, which considered methods for automated analysis, methods for data visualisation and technologies for vehicle trajectory reconstruction, which involved a more detailed consideration of a number of sensors and techniques, most notably GPS which has been more widely used in racing in recent years.

Chapter 3 pulls together all the detail presented here to define the concept of this research project, to answer the shortcomings of current motorsport data analysis practice and help the user realise the full potential of acquired data.

Chapter 3

Research Concept

3.1 Introduction

This chapter aims to draw together the background to motorsport presented in Chapter 1 with the overview of sensor technology, current issues within motorsport regarding the analysis of data and perceived directions of development presented in Chapter 2. This is complemented by personal experience of 5 years working as a data engineer in motor racing and also the opinions of P1 Motorsport, who were introduced as a successful junior racing team in Chapter 1.

With the problems affecting current motorsport data analysis defined, the concept of a software solution to help answer these problems is identified. The chapter concludes with two sections describing refinement of the two key aspects to this solution.

3.2 Problem Definition

There are several key issues with current data acquisition and analysis practice in motorsport which were made apparent in a number of sources discussing analysis tools and race engineering. When considered alongside the current level of development of motorsport data analysis software, there appeared to be a definite need and opportunity for the development of software tools to help address these issues.

A number of sources identified the vast amounts of data which are recorded by a current motorsport data acquisition system and the need to develop tools to assist the user in analysing this data (Vaduri and Law, 2001; Replogle, 1994). In his paper presented at the SAE Motorsports Conference Purnell (1998) described his perceived need for the motorsport industry to evolve into a data culture which would collate the vast range of vehicle performance data measured from race cars. This not only referred to data recorded from an onboard DAS, but also to

other sources of data such as tyre force data, damper force curves and engine performance characteristics. It was identified that all of these data sources could provide insight and could help guide a team towards a better performing car and driver. However, without software which could assist in the collation, a race team was overwhelmed by the data available and as a result it was seldom used to its full potential. Instead most adjustments and such like were based on driver feedback, a cursory glance at recorded data and a large part of the race engineer's intuition. He concluded, in the 'heat of the moment' little of the data recorded from a racecar is used.

Aside from the analysis tools available to the motorsport data acquisition user, the issues of utilising the data are exacerbated as testing time has become increasingly restricted. Martin and Law (2002) identified the high costs of track rental in their paper describing the development of an expert system for automated data analysis as a restriction on the time for testing and data analysis available to a team. For junior teams in particular, costs have become an increasing issue. Published data unfortunately cannot be sourced and the statement is made based on the experience and personal communications with experienced professionals from motor racing, in particular Roly Vincini of P1 Motorsport. It can be surmised that a general shift in public interest away from the junior categories of racing has reduced corporate sponsorship in general, whilst tobacco advertising restrictions in particular have largely removed what was a massive source of racing sponsorship, reducing the budgets available for running a team. Roly Vincini estimated that a 2004 season budget for British Formula 3 was roughly half the amount supplied by the Phillip Morris International tobacco to sponsor a team he worked for in 1989 under the Marlboro brand.

Through the duration of this research, sanctioning body enforced restrictions on testing have steadily increased. At the time of writing, it is reasonable to consider that the most recent racing season (2009) is the most restricted to date in terms of the testing time available. This is primarily to reduce costs and ensure the number of race entrants is maintained. It has been fuelled by the previously mentioned downturn in corporate sponsorship in junior categories, but also partly by the global economic downturn, which began in 2008. It extends to all levels of the sport, with Formula 1 (where it also tries to reduce the spiralling development

costs) currently banned from testing outside of race meetings during the 2009 racing season (Formula One Administration, 2010).

As acquisition hardware has improved and become cheaper to manufacture, the categories of racing utilising data acquisition has increased. It is now used in almost all categories of racing (McBeath, 2002; Templeman, 2008). However Chapter 1, which introduced the structure of current teams, indicates how small a junior team can be. Personal experience says a data engineer in such categories can often be stretched to much more than simply analysing acquired data, as the short testing time is maximised. An all too common occurrence was the full post-test analysis which revealed insight which would have steered an entire branch of the testing program and which with sufficient time and personnel could arguably have been found during the test session itself. Tools which could help prevent this wasted time would offer a definite competitive advantage to a race team.

In summary, the restrictions on funding and track time and the quantities of data recorded present the opportunity for developing tools to:

- Assist the user in understanding recorded data more quickly;
- Accelerate the analysis of recorded data;
- Collate data and determine new performance trends from large data sets which would ultimately be difficult by a human operator alone.

The potential software and hardware development opportunities that were perceived at the project outset are described in more detail in the following section.

3.3 Potential Development Areas

Section 2.4 presented a review of all commercially available motorsport data analysis applications for which full or demonstration versions of software or product documentation could be obtained. It is clear from a consideration of section 2.4 and particularly Table 1 that there are a basic set of analysis tools

prevalent across all commercially available motorsport data analysis packages. These are mainly what can be termed standard plotting methods, which could typically be found in applications such as Microsoft Excel. Whilst these standard plotting tools obviously have their role to play in analysing data, mainly by giving a visual impression of a trend in a parameter's value over a period of time or distance for example. However, whilst these methods allow for holistic consideration of a data set, they do little to bridge the abstract gap between the measurements they represent and the vehicle itself.

These standard plotting methods also have their place as a useful means of considering a series of data sets. They can provide insight into differences in driver or vehicle performance by the overlaying and comparison of a series of two or more pieces of data. However, they are limited as a means of answering the need identified in section 3.2 for a tool to fully coordinate and collate the vast quantities of data collected by a race team as they rely on the user's control to extract relevant points of interest, which directly conflicts with the need to accelerate the analysis of data.

If Table 1 of section 2.4 is considered again, two key areas of development of analysis tools can also be identified amongst the additional tools, both of which make some effort towards answering the key issues raised in the previous section. The first category are tools for helping organise data and bringing to the user's attention areas of interest. The second category are are tools designed to aid the user's assimilation of data, such as animations of vehicle attitude and plots of channel value on a circuit map.

However, in terms of display tools, most of the efforts are basic and either still leave a level of abstraction between the data and the vehicle or simplify their display such that their ability to aid user assimilation of the data is limited. A good example of this is the display tool from Bosch LapSim, which in fact attempts to display simulated data. This is the most complete use of a graphical vehicle model to display suspension displacement data, but is constructed from plotted lines which are limited in their impression of the vehicle. It also gives no impression of the vehicle's displacement across the circuit. Another example of an alternative plotting method is William C Mitchell's driver input animations.

However, these are massively simplified and therefore are again limited in their ability to help the user assimilate data.

Meanwhile, data assimilation appeared to be well practiced in other areas, with there being a number of applications available for recreating recorded flight data for pilot training (Bolduc and Jackson, 1999; Teledyne, 2010; SimAuthor, 2010; CEFA, 2010).

A widespread area of development in display terms was in the proliferation of small camera systems for recording onboard video. There were systems available such as the Competition Data Systems (2005b) which displayed the video as a standalone stream with numeric data overlaid, whilst there were also examples, such as Pi Research Toolbox which synchronised the video with a cursor displaying on acquired data. The potential of recorded video for providing insight into vehicle dynamics was discussed by Moloney *et al.* (1998) and is clearly one of the most obvious ways of aiding the user's assimilation of acquired data. However, there were still several key issues with the approach. Firstly, small cameras would be limited in their frame rate below the capture rates of a DAS which in turn would limit their ability to depict high frequency phenomena, such as suspension behaviour, which Fey (1993) recommends should be sampled at a frequency of at least 200Hz but ideally 1000Hz. Clearly they also only provide a single viewpoint per camera and only allow for viewpoints fixed relative to the car, which restricts their analysis potential.

Tools for organising and analysing data were also essentially basic, with events based sorting being the primary tool employed for identifying and bringing to the user's attention certain areas of interest indicated by the occurrence of a specific signal level on combinations of data channels. Aim Sports did offer a database function allowing searching of previously recorded data based on user-defined criteria, whilst two applications provided a system for storing vehicle setup information (Aim Sports, 2003). However, there was no obvious attempt at a single application linking all of these information sources together and all of them still depended largely on the user's control and analysis of the areas of interest they highlighted.

There was no published research specifically targeting motorsport acquired data display, but there was indication of the development of data sorting methods from published material, both in the commercial and academic sectors. At the time of writing his paper calling for racing to become a more data orientated industry, Purnell was part of Pi Research, one of the world leading manufacturers of motorsport DASs and software. At that time the company distributed its well known and regarded Version 6 analysis application, which included events-based data sorting. This was since superseded by Toolbox which developed this basic form of expert system to the extent that Pi Research regard events as the software's 'foundation' (Pi Research, 2004a).

The issue of the user becoming overwhelmed with data had also been partly addressed within academia by the work of Vaduri and Law (2000) and Martin and Law (2002), whilst Replogle (1994) represented industry-based research in a similar area. These three pieces of work had developed expert systems for accelerating the data analysis process.

Replogle's work aimed to analyse acquired data by processing through a "decision model", a system incorporating prior understanding of vehicle dynamics. This processed data through a series of equations to provide an output highlighting the vehicle behaviour. Experimentation with various algorithms based on vehicle dynamics theory is described, culminating in the formation of a so called stability index, described in more detail in section 2.7.1.1, as a direct metric of car performance. This metric is envisaged as allowing quick evaluation of the car and steering test sessions without full consideration of the vast and growing quantities of data produced by a racing data acquisition system.

Section 2.7.1.2 introduced Vaduri and Law (2000) and their application of more complex approaches to data analysis, which involved developing an expert system, employing an approach of filtering signals such as steering and lateral acceleration which give characteristic indicators of handling imbalances to approximate the signal which could be expected from a balanced car. Comparison of a less filtered signal with the theoretical signal via a fuzzy logic routine based on vehicle dynamics theory then determined the occurrence of a handling imbalance. Consideration of other data channels, such as throttle

application was subsequently considered to confirm the event, based on certain identified patterns of driver reaction to such a handling imbalance. Martin and Law (2002) develop the approach of Vaduri and Law (2000) by also identifying metrics of driver and vehicle performance using similar methods. The metrics they use are established indicators of good performance driving technique such as the assertiveness of brake and throttle applications made by the driver, and were sourced from the seminal motorsport data acquisition text *Data Power* (Fey, 1993).

Despite of these clear advances in the approaches of commercially available software, the events system and much of the research essentially replicated human analysis of single sets of data and primarily alerted the user to the occurrence of an event (Pi Research, 2004a). In a similar vein, Vaduri and Law (2000) and Martin and Law (2002) use their algorithms as event highlighters also. There was clearly progress from the Replogle (1994) towards pulling sources of data together into metrics used themselves as a means of quantifying the vehicle performance, although it describes the very basic beginnings of such an approach.

One feature clearly lacking from research was for a system to learn and evolve. Some background research on the subject of Expert Systems suggested that a systems software package's performance could evolve by measuring the success of decisions made and so forth (Jackson, 1999). Another clear potential area for development seems to be in the use of Artificial Neural Networks (ANNs) for signal pattern recognition as discussed in a personal communication with Buddy Fey (Fey, 2005) and was described for other applications by Oatley and Ewart (2003).

The broad aims of this research essentially fall out of the overview of current commercial applications and the research that has been undertaken commercially and in academia. The idea of a software application which would strive to meet the visions of Purnell (1998) and support a data culture within racing, introducing some new concepts but also combining and developing some existing approaches was forged. This would involve providing tools to help the user collate various sources of data, understand the data more fully and to

extract answers from it more quickly, such that it is used more effectively during a test session and a greater performance advantage can be derived from it.

3.4 Concept Generation

The potential areas for development of motorsport data analysis software put forward in the previous section led to the generation of a concept of a complete all encompassing suite of data analysis tools. This suite would assist the user in dealing with the vast range of data channels from a current DAS and other vehicle performance measures which are taken or known by a racing team, such as aerodynamic performance characteristics, dynamic suspension test rig data, vehicle setup data and many other others.

The concept could be considered as having two distinct parts; the tools to help the visualisation of recorded data and the tools to assist the user in organising and processing the large amounts of data.

3.4.1 Data Visualisation Tool

A potential answer to the issues of data assimilation via the use of a vehicle animation had already been investigated during previous work by the author at undergraduate level (Parker, 2004 a, b and c) and showed potential for improving the visual illustration of data. Visualisation techniques were presented as a means of assimilating flight data by a number of software houses (Bolduc and Jackson, 1999; Teledyne, 2010; SimAuthor, 2010; CEFA, 2010). There had also been other obvious attempts towards this end, with Bosch Motorsport producing the best example (section 2.4.2.2). However, there was no distinct attempt in any motorsport data analysis software to provide a complete graphical representation of the car, viewable from all angles and traversing a trajectory across the ground.

The previous work had produced a fixed location model viewed in the Solid Edge CAD package and controlled by a Visual Basic application passing model constraints based on recorded damper displacement values at each frame to animate the vehicle's suspension motion. It fell short of achieving level of illustration desired and the further work of Parker (2004a) proposed developing a fuller and more representative stand alone application to assess the concept. As part of the broad aim of this research, it was intended to answer this recommendation.

Conceptual sketches shown below illustrate the conceived display output, depicting a number of different perceived ways in which data could be presented and areas of interest highlighted. Figure 28 illustrates the split screen display envisaged of the application, with separate windows depicting data plotted against distance, a close scale view of an event of interest and a wide angle view of the car traversing the circuit. Figure 29 shows a side view of the car during a brake locking event, whilst Figure 30 shows a wide angle view of the comparison of two laps of data, showing two driver's lines around the same corner.

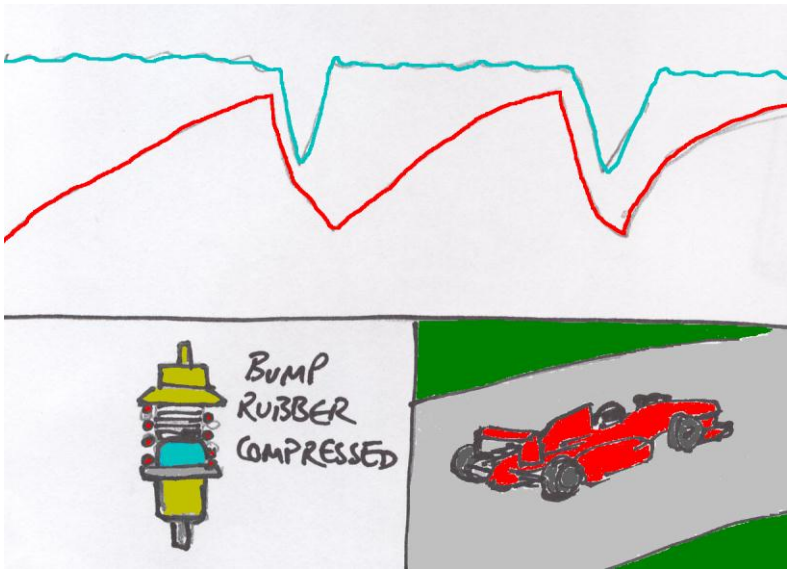

Figure 28 - Conceptual sketch of the data visualisation tool depicting split screen data display.

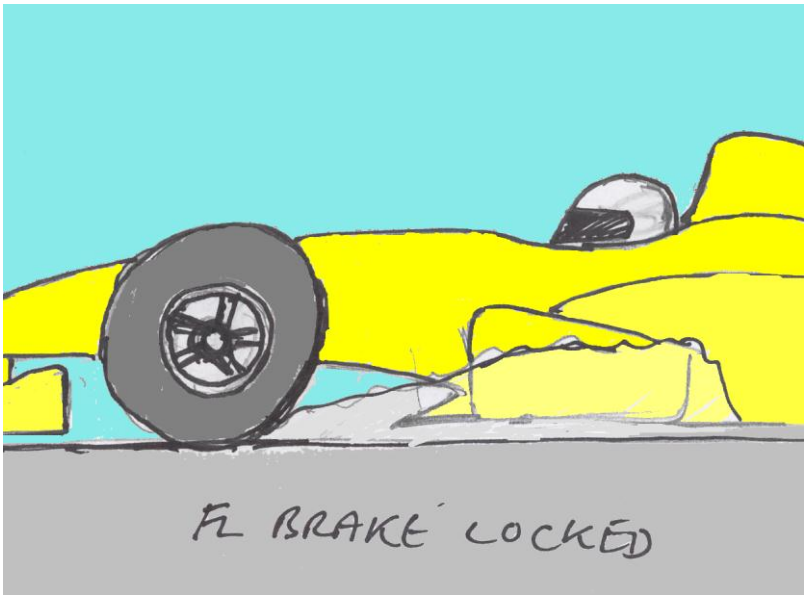

Figure 29 – Conceptual sketch showing a car side view and visually indicating the locking of a brake into a corner.

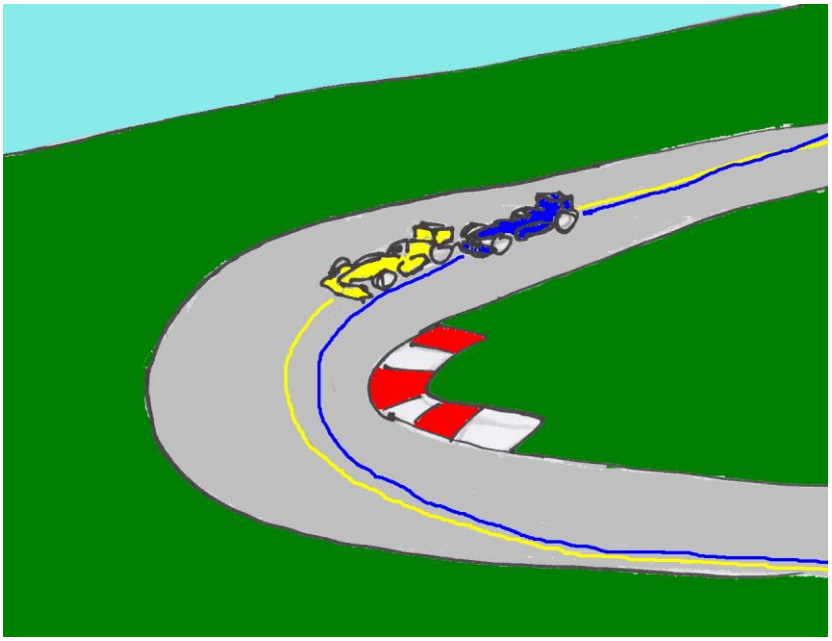

Figure 30 – Conceptual sketch showing a wide angle view illustrating the comparison of two driver's approaches to the same corner, with the different lines indicated on the track.

This graphical model itself would be driven by an underlying kinematic mathematical model. Measured suspension sensor readings from the DAS

would be fed to the kinematic model to induce the same suspension motions in the animations as those which created the actual potentiometer readings. The finer detail of this approach is discussed in more detail in section Chapter 7.

The display method was intended to give a level of data visualisation which reduced the abstraction between recorded data and the vehicle, but as described in more detail in section Chapter 7, would keep computational demands to a minimum to make the demonstration software as viable as possible for actual use at a circuit.

By using solid graphics drawn in a full 3D environment, the user would be able to interact with a model which would better assimilate data in comparison to a line drawn or schematic model and would allow viewing from multiple angles and at high capture rates unlike the use of small vehicle mounted cameras. If the graphics could be processed sufficiently fast that the software could be used in the restricted time available at the circuit, the software would achieve its goal of representing a useful tool for aiding the understanding of and focussing the discussion between both the driver and race engineer, which was indentified as an important need by Haney (2000) and Strout (1998).

By way of illustration, the following mock screen shot in Figure 31, constructed prior to final coding using the Solid Edge CAD package and photo editing software illustrates the impression that was envisaged of the fully developed application.

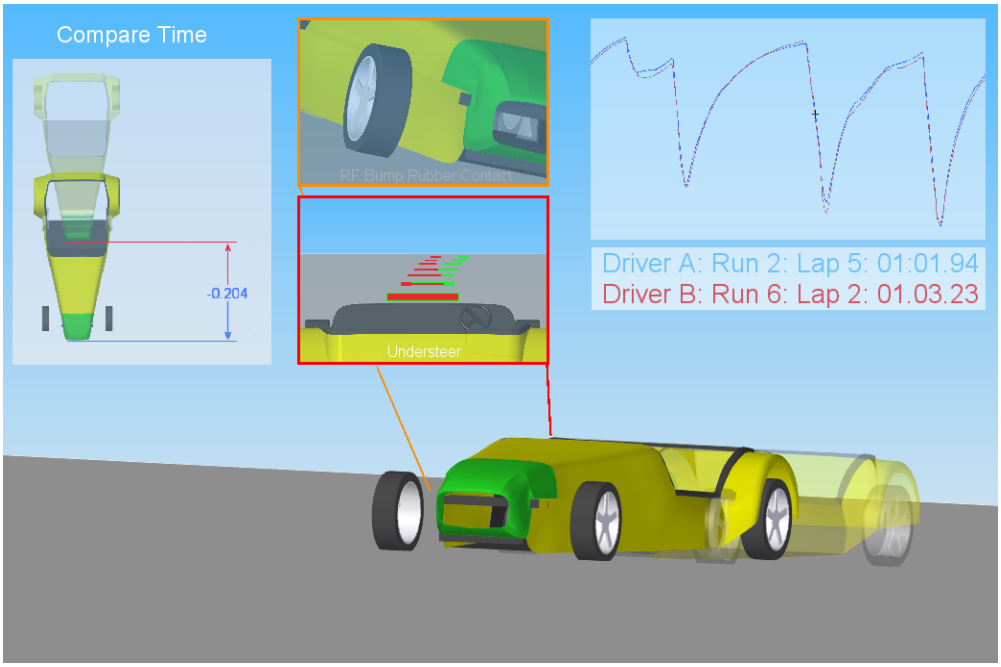

Figure 31 - Mock screenshot of the fully developed version of the data display software showing multiple views of points of interest alongside graphed data.

3.4.2 Expert System for Data Organisation and Analysis

The issue of the user becoming overwhelmed with data had been partly addressed by several applications as well as some published research, as described previously. However, there was no single robust system which could combine the vast range of data streams which a racing team must deal with and all the systems tended to highlight areas of interest in single data files, rather than utilising the previously recorded data and providing actual results to the user. Therefore although they accelerated the analysis process, they still only removed some of the work of the data analyst.

The ultimate development of an expert system could perhaps be considered as an application which could remove the need for the user to even analyse the data and simply provide its own appraisal and opinion of a car's performance. There was also a significant need identified by Purnell (1998) for utilising the other wide ranging sources of information collected or available to a racing team so the

combination of data mining functionality within such a system would also be useful.

Therefore the broad aim of the expert system concept which was intended to be developed here would be to produce a system which could dramatically reduce the user's involvement in the analysis process, whist also providing a mechanism for easily incorporating previously recorded and other forms of data within the analysis. It was intended that some involvement would initially be required and that the system could be trained, with the use of technologies such as Artificial Neural Networks (ANN) to:

- Identify patterns in data linked with certain positive and negative events;
- Encapsulate the operational practices of an race engineer with an appraisal of the success of different practices controlling future replication;
- Combine data from a DAS with other sources of data, such as engine performance, aerodynamic performance and damper characteristic data in drawing conclusions about the success of the vehicle and driver performance and possible developments;
- Analyse data autonomously and calculate metrics of the car and driver performance, based on theoretical measures used by work such as Martin and Law's expert system (2002). The system could ultimately provide a conclusion of the overall success of the car and suggest methods of improvement without the need for the user to sift through large amounts of data.

Pattern recognition was also briefly referred to previously. Much of the analysis of motor racing data centres on the human operator's identification of distinct patterns amongst a series of data channels which indicate the occurrence of some event of interest. The potential for the use of ANNs as an analysis method which is suited to pattern recognition and can also be trained and evolve to improve its analysis, meant that they were envisaged to be included in the expert system.

In the same section, Expert Systems were discussed in a more general light and the concept of their knowledge base was introduced. This would be accessed by

their inference engine in order to make decisions based on data supplied to them. It would be this part of the system which would encapsulate the user's knowledge and potentially contain an ANN based approach in part, evolving to recognise patterns and control how decisions are made and advice given, based on previous results. It is here also that other information would be collated; setup data, vehicle dynamics theory and analysis of previous results would all be combined with decisions made using a heuristic routine based on a race engineer's knowledge to draw a final conclusion.

The work of Replogle (1994), Vaduri and Law (2000) and Martin and Law (2002) used various metrics for assessing vehicle performance and it was envisaged that metric based analysis would be a large part of the expert systems analysis engine. Although not presented for the sake of brevity, a number of other metrics were identified which represented the driver's performance and the dynamic performance of the car. An ultimate aim would be to encapsulate all the metrics into two overall performance factors of the car and driver, which would allow each to be targeted as the requirement for most development and to allow progress to be easily measured.

This approach to appraising a vehicle and driver's performance would represent a change in the standard methods of analysing race data, offering a more quantitative appraisal to the standard qualitative identification of various patterns associated with aspects of the car's performance that do not necessarily determine a clear basis on which to draw a conclusion. This attempt at trying to apply quantitative metrics to analysis has other well known applications within engineering, such as design appraisal using Quality Function Deployment (QFD) and Design for Assembly (DFA) techniques to appraise the design of a product for its ease of manufacture (Boothroyd *et al*, 1994).

A final aspect of the system would be its ability to assess the race engineer's performance, by identifying changes made to the car and their effect on performance. Successful decisions could trigger the storing of the methods by which data were looked at, certain channel levels which existed before and after the change and so forth, to guide the system to make similar choices autonomously at a later date. Potentially the user would also be required to

assess their own performance as a means of developing the system. As a whole, these approaches would ensure that knowledge was retained by a team when staff moved teams.

3.4.3 Vehicle Trajectory Reconstruction

A key aspect of the data assimilation process would be the positioning of the vehicle model in a 3D environment to create the visual impression of the vehicle motion. In order that this be a useful visual aid to the users and similarly not be misleading in any way, this needed to be extremely accurate. The review of vehicle trajectory reconstruction positioning methods in the previous chapter has lead to the following key conclusions:

- The use of a basic accelerometer and speed based approximation of the trajectory was insufficiently accurate for trajectory comparison;
- Inertial and GPS navigation systems could potentially provide sufficient accuracy for line comparison, but with a large additional cost to the user and with some impractical additional time requirements involved in their use. The realistic accuracy where these systems were applied would be of the order of 1m and therefore insufficient for trajectory comparison;
- Doppler shift speed sensors were not used in racing seemingly for the difficulties they suffer with smooth tarmac surfaces;
- Optical ground speed sensors, could potentially achieve high positional accuracy of the order of 2mm, allowing for accurate trajectory comparison. However the cost of these sensors ruled them out of use in junior racing.

Optical sensing of vehicle displacement seems to provide a potential area for investigation. Cost was arguably the key issue restricting these sensor's wider use in racing and this research therefore aimed to test the principles of an alternative optical method which could potentially achieve high accuracy and be manufactured more economically. This measurement of vehicle displacement would add a useful data stream for optimising the effectiveness of the display

tools and could also give the accurate basis for further performance metrics to complement the expert system.

3.5 Scope of Research

The scope of this PhD has changed somewhat throughout its duration. Much of this was due to the aim of producing a commercially representative demonstration application at the completion of the work. However, it became apparent that the vast range of areas which required covering in order to achieve this and some of the approaches which would be necessary, such as the use of an actual test vehicle to collect real data made this unfeasible, particularly for both parts of the software described in section 3.4. Instead, solely the visualisation aspect of the application would be researched here, with an Expert System for organisation and analysis being left as further work.

The development of the visualisation aspect also includes the development of a system for vehicle trajectory reconstruction and placement; an optical sensor system which inherently provides vehicle speed and displacement measurement.

This work aimed to prove the principle of these concepts, with a target application to junior racing categories, which could be considered as all categories below F3 in Figure 6, but could also include smaller WSbR and GP2 teams as well. Since this was the case, the software would also be considered for its ability to convey data with only current sensor streams, as its target application covers teams with minimal funding. The use of the standard inertial based point kinematic trajectory reconstruction described earlier would also be used.

Chapter 4

Development of 3D Data Display Software Preliminary Version

4.1 Introduction

The concept of an animated model of the vehicle recreating data recorded from a car which was introduced earlier had previously also been hypothesised and investigated in work leading to this research (Parker, 2004a). This work aimed to develop this concept to a more representative application which would indicate if the idea had potential for further development. This would involve the creating a bespoke application for display of the car around a lap of recorded data.

It was decided at the outset that code was to be written entirely in Microsoft Visual C++ ® which was an industry standard language and was regarded as allowing for the extremely flexible program development and fast execution times (Young, 1998). For rapid display of graphics, OpenGL graphics libraries were used.

The concept put forward in Chapter 3 was of a car model moving to recreate the vehicle ground displacement and suspension deflection. However, the initial application, described here, simply animated only the car's position around its lap trajectory. This would simplify the problem as the underlying suspension kinematics could be ignored at this stage and would allow the focus to be on implementing the graphics routines in this first instance.

Different methods of calculating the car's trajectory were considered, but it was decided that to be most illustrative of the potential of such a visualisation application, the most common method of vehicle trajectory approximation would be implemented. This was introduced in section 2.7.3.1 whereby the car is treated as a particle and a point kinematic analysis is performed around a lap, using lateral acceleration and wheel speed channels as a basis. This is not at all accurate, as was described previously, but is considered as it represents a way the software would potentially be used in the lowest categories of racing. Also it would suggest whether a pure suggestion of the car's heading change, acceleration and so forth was enough to help aid the user's assimilation of the data recorded.

By the time that the work on this aspect of the work was the beginning, the author was working with P1 Motorsport as a data/junior engineer alongside PhD research. This was initially as part of the Comtec team during the 2006 season, their first in World Series by Renault (WSbR) Formula Renault 3.5 (FR 3.5). This link gave the opportunity to use data from a competitive single seater racing car fighting at the front of an International Championship. For modelling purposes technical literature and advice from Renault-Sport who provide the technical support for the series were available.

This chapter begins by introducing the World Series by Renault and the FR 3.5 car, the Dallara T05 before describing the DAS used and the creation of a graphical model. Methods of approximating vehicle trajectories and the actual one employed are then introduced before an appraisal of the results is discussed.

4.2 The World Series by Renault

The World Series by Renault (WSbR) is a group of three race series which tour Europe as promotional package for Renault road car sales, but is a name commonly given to the Formula Renault 3.5 category (FR 3.5), the premier category of the package (see Figure 32). It is a single seater category which allows a single specification of car, albeit one that can be adjusted in certain ways to optimise its performance.

Figure 32 - A Comtec World Series by Renault FR3.5 Dallara T05, driven by Celso Míguez at Le Mans, France during the 2006 season.

FR 3.5 is regarded as being a direct step to F1, being only slightly below the level of GP2. Like GP2 it is designed to train drivers, by giving them a taste of a lightweight car, with a high power output (in the region of 450 hp), with a number of car features similar to those they could expect in F1, such as electronic fly-by-wire clutch, throttle and gear controls. In recent years, Champions have gone on to enjoy success, both in F1 and GP2, including Heikki Kovalainen and Robert Kubica, who both have won Grand Prix in F1.

The opportunity to work and be able to use data from such a regarded category was incredibly beneficial to this research.

4.3 FR3.5 Dallara T05

The WSbR FR 3.5 category uses a single specification car, which helps to limit costs and make racing closer. The car is a standard single seater configuration of a carbon fibre monocoque chassis or tub mated to an engine and gearbox which are used as stressed components of the chassis. The monocoque, denoted the T05, indicating its first year of service as 2005, is now obsolete but as is common with single specification categories, was in service for a three year cycle. The car was designed by Dallara in Italy, arguably the world leading manufacturer of racing cars.

The suspension configuration is typical at the rear, being of double wishbone, pushrod configuration with a standard “T” shaped anti-roll bar. The front suspension is of a configuration becoming less widely used, with a single front suspension unit connected to both corners, which are again of double wishbone pushrod type. Anti-roll is provided by a spring system either side of the inboard shuttle bar to which the pushrods mount. This allows a small amount of lateral movement of the pushrod inboard mounting point under lateral loads. Both front and rear suspensions feature coil over spring dampers.

The engine used in the car was derived from a 3.5l Renault/Nissan V6 engine and was naturally aspirated, producing approaching 500hp when running on E85 gasoline ethanol mix, but more typically 430hp on standard gasoline. The gearbox used is a six speed sequential unit, manufactured by Ricardo. Its selector arm is actuated by a hydraulic system which is switched by steering wheel mounted electronic paddles. Throttle and clutch control are also via fly-by-wire methods (Renault Sport Technologies, 2006).

4.3.1 Dallara T05's Data Acquisition System

The Dallara T05 used a Magneti-Marelli data logger which was integrated with the car's ECU (Engine/Electronic Control Unit). The system was arguably of a lower level than that used in Formula 3 as a means of reducing costs, being designed for a fairly basic range of sensors, although there was the facility for expansion with an additional interfacing unit.

The sensors required for use in the trajectory reconstruction were all championship prescribed, being two Hall Effect wheel speed sensors and a dual axis accelerometer.

4.4 Modelling the Dallara T05

As part of the preliminary application, the Dallara was modelled using Solid Edge® from a set of measurements and technical drawings sourced from Renault Sport Technologies (RST). The model was created using the Solid Edge CAD package before being converted to the 3D Studio Max® .3ds file format for loading by a .3ds model loader and used with the OpenGL graphics routines utilised for display. The following subsections detail each of these stages in more detail.

4.4.1 Modelling using Solid Edge®

Although not moved in this preliminary version of the 3D display application, the suspension of the Dallara T05 was nonetheless accurately modelled using suspension joint data supplied by RST in the manual which accompanied the T05 (Renault Sport Technologies, 2006). Due to the adjustability of the suspension system of the car, this set of measurements represented only a single example of numerous configurations. The data used was not from a car set to this configuration, but for illustrating the trajectory positioning of the software and

since the suspension movement was not to be included it was deemed acceptable.

The bodywork of the car was modelled using technical drawings supplied by Benoît Dupont of RST (Dallara, 2004). The bodywork was not intended to be completely accurate but the floor is correctly positioned with the measurement set and the body shape created gives a good visual impression of the car.

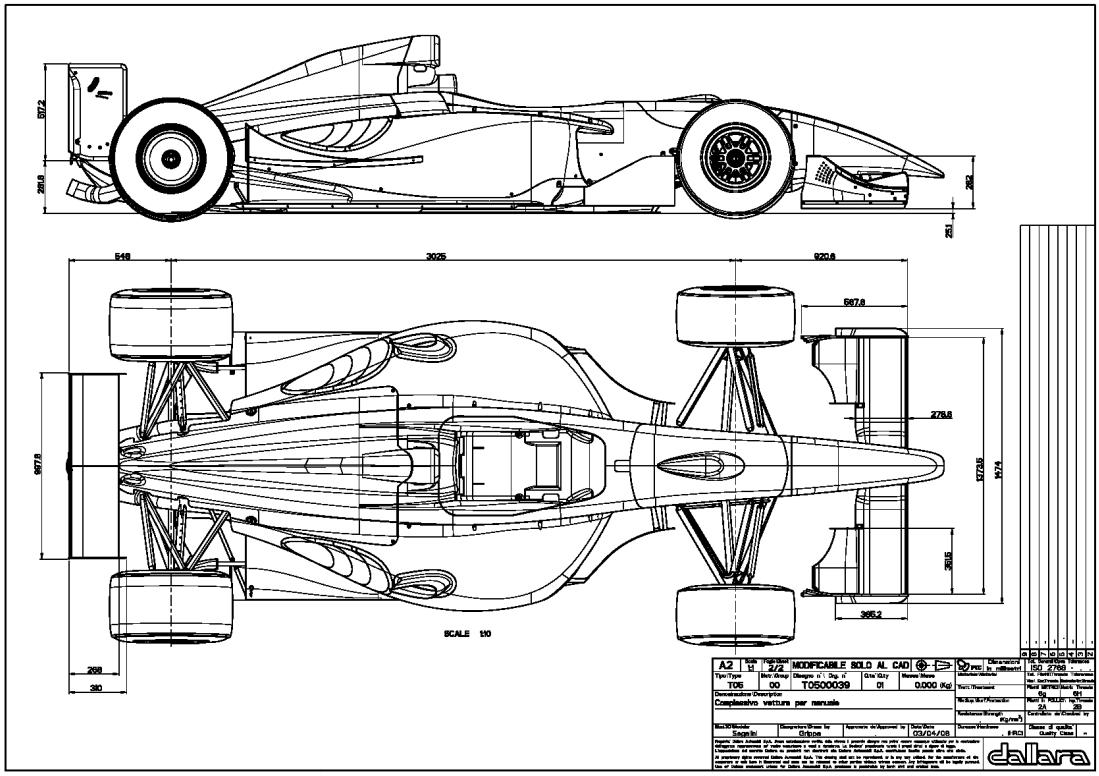

Figure 33 - The technical drawings of the Dallara T05 used for modelling its bodywork (Dallara, 2004).

The following screenshots (Figure 34) illustrate the visual impression of the car achieved, showing the component parts assembled in Solid Edge®.

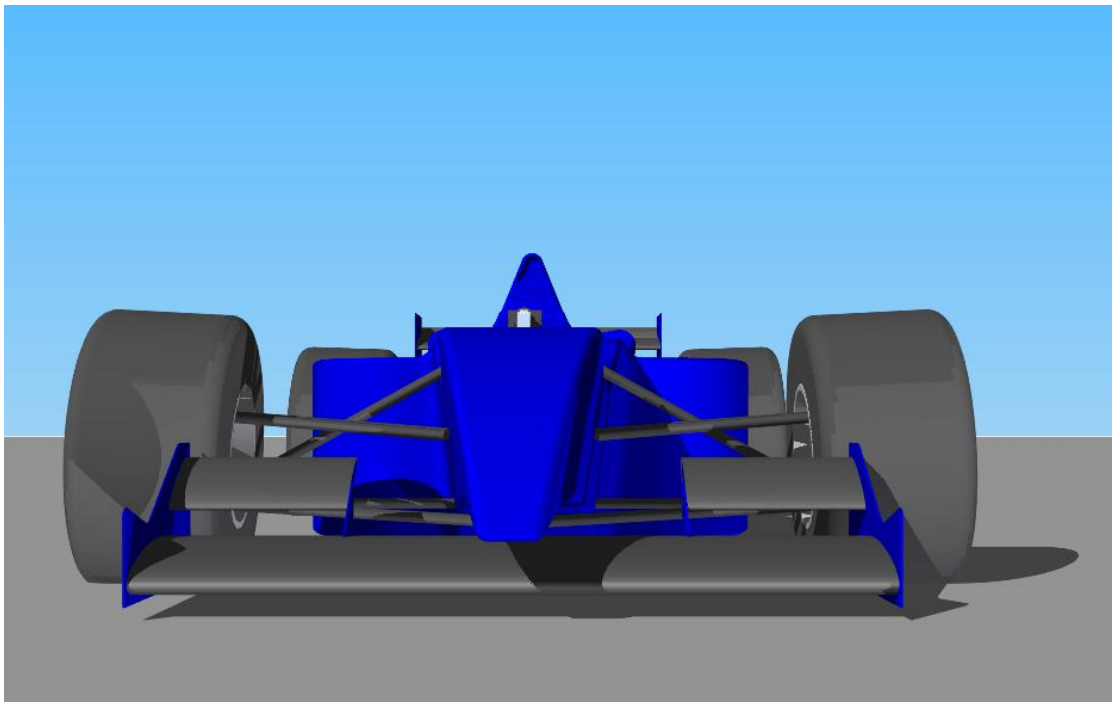

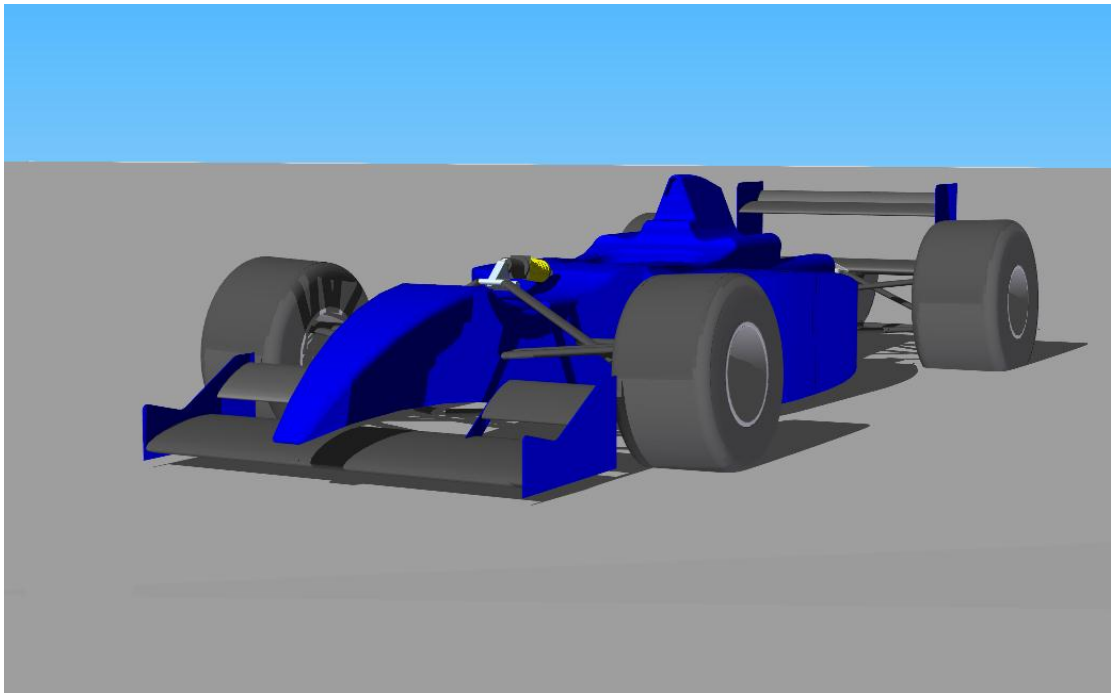

Figure 34 a – Various views of the assembled model of the Dallara TO5 in Solid Edge®.

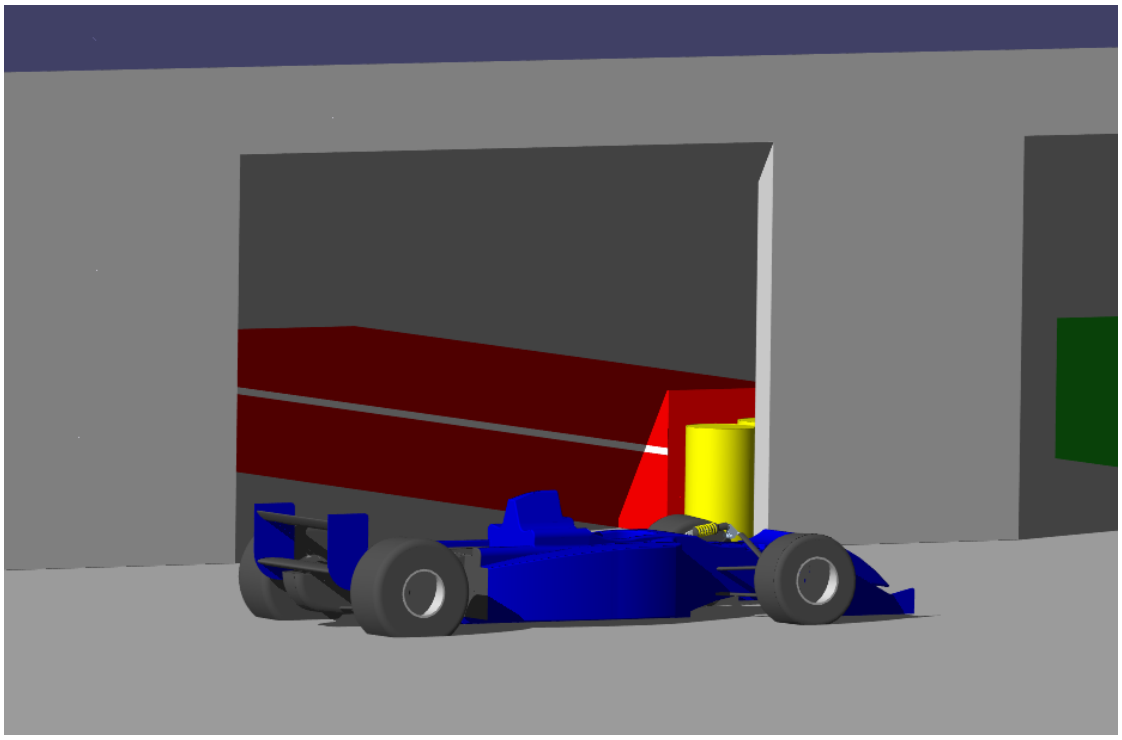

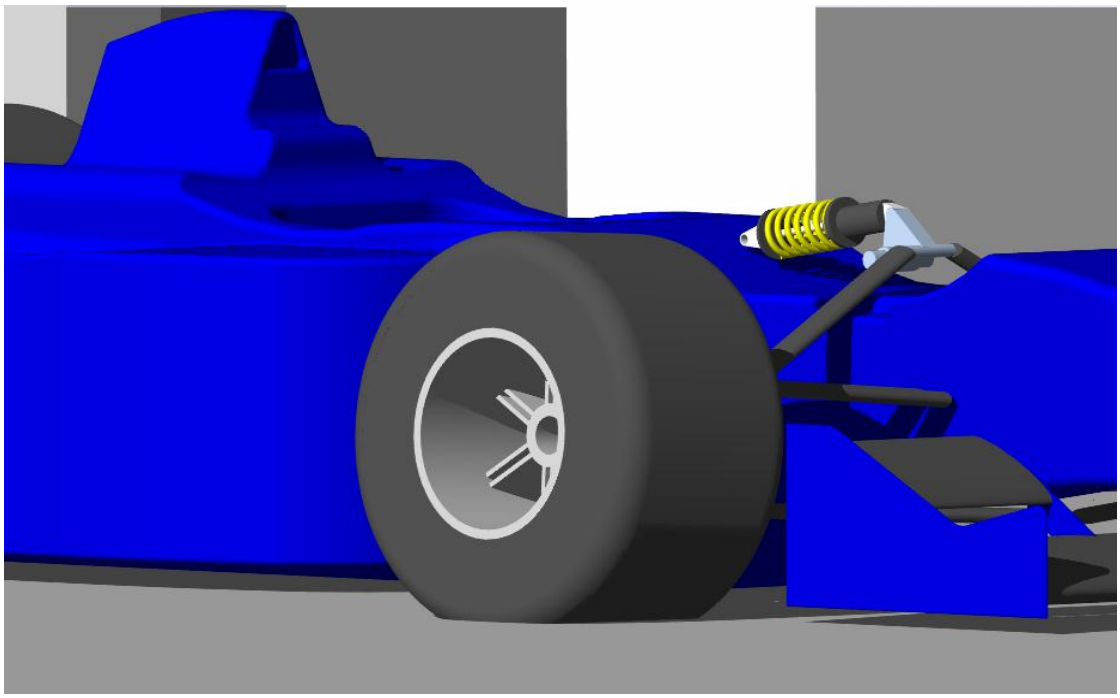

Figure 34 b – Various views of the assembled model of the Dallara TO5 in Solid Edge®.

4.4.2 Conversion to .3ds File Format

In order for the modelled components to be introduced into the C++ visualisation application, they were to be converted to the .3ds file format, a popular format amongst the computer games programming fraternity which had widespread support (Shreiner *et al.*, 2008). It is a binary format which helps achieve faster read times than text based formats and stores model surface information as a mesh of vertices which are used by a loader to reconstruct a set of triangles. Conversion was slightly cumbersome as models required exporting from Solid Edge® as IGES files (a popular CAD export format) and importing in 3D Studio Max before they could be exported in the .3ds format for use with the visualisation application.

4.5 Point Kinematic Inertial Trajectory Algorithm

The requirement to position the vehicle model in 3D space on a model terrain was introduced previously as a requirement to reduce the level of abstraction between the data and car as far as possible. In order to test the potential of the display application for use with the most basic of acquired data, which was already collected across junior levels of racing, a trajectory reconstruction algorithm based on the universal point kinematic approach described in section 2.7.3.1 was developed.

The method was adopted by all motorsport data analysis packages, treating the car as a particle and performing a kinematic analysis of its lateral and longitudinal displacement around a lap.

Casanova *et al*. (2001) gave a good overview of the mathematics underlying the approach which helped steer the development of the algorithm. A basic equation of a point body subject to a circular motion is:

$$A = v^2 / R_t \qquad \text{Equation 4}$$

Where A is centripetal acceleration (m.s^{-2}), v is tangential velocity (m.s^{-1}) and R_t is cornering radius (m).

If the measured speed from a race car is assumed to be the tangential velocity and the measured lateral acceleration of the CoG is the normal acceleration, the cornering radius of the car at a given instant can be calculated by rearranging Equation 4 to give:

$$R_t = v^2 / A \qquad \text{Equation 5}$$

If the plan view of the vehicle trajectory adapted from Casanova *et al.* (2001) is considered (Figure 35), three differential equations can be formed which govern the coordinates and heading of the car.

Firstly, if the path distance covered by the car is denoted s then:

$$ds = R_t d\psi_t \qquad \text{Equation 6}$$

Where ψ_t is the heading angle of the car (initially equal to 0). Equation 6 can be rearranged to:

$$d\psi_t = \frac{1}{R_t} ds = k_t ds \qquad \text{Equation 7}$$

Where k_t is the inverse of the radius R_t, termed the curvature.

The increment of the lateral and longitudinal coordinates can be expressed in the form of Equation 8 and Equation 9.

$$dx_t = \cos(\psi_t)ds$$ Equation 8

$$dy_t = \sin(\psi_t)ds$$ Equation 9

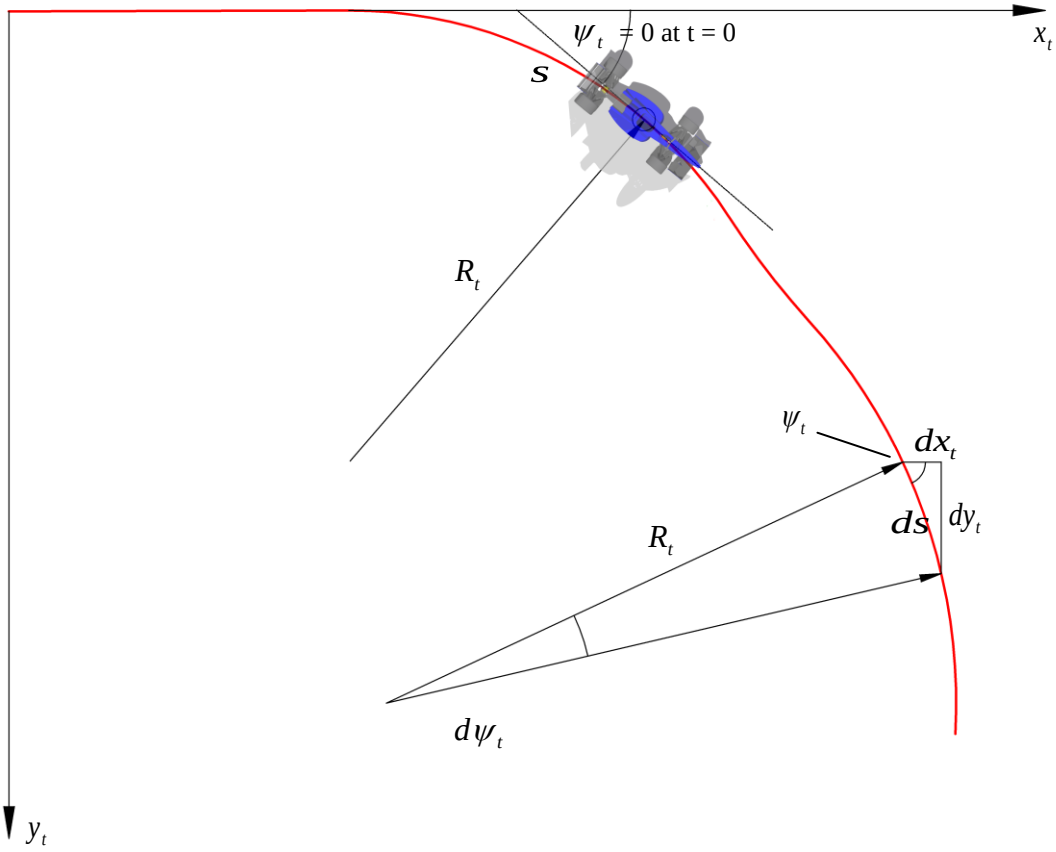

Figure 35 - Plan view of the trajectory followed by the race car (adapted from Casanova *et al.*, 2001)

A substitution for ds is made using Equation 10 in Equation 7, Equation 8 and Equation 9 to express in terms of time, allowing the formation of three integrals (Equation 11, Equation 12 and Equation 13).

$$ds = vdt$$ Equation 10

$$\psi_t(t) = \int_0^t k_t(t)v(t)dt$$ Equation 11

$$x_t(t) = \int_0^t \cos[\psi_t(t)]v(t)dt \qquad \text{Equation 12}$$

$$y_t(t) = \int_0^t \sin[\psi_t(t)]v(t)dt \qquad \text{Equation 13}$$

Where x_t and y_t (m) are the longitudinal and lateral coordinates respectively.

Equation 10 is also integrated, giving distance as a function of elapsed time:

$$s(t) = \int_0^t v(t)dt \qquad \text{Equation 14}$$

The trajectory is then reconstructed by calculation of the heading angle at each time step dt from the lateral acceleration and vehicle speed. This yields the lateral and longitudinal coordinates for that time.

The algorithm was tested with data recorded from the Donington Park circuit, producing the trajectory illustrated in Figure 36. It is apparent that the trajectory does not join however, which is a consequence of a range of potential error sources:

- A constant lateral acceleration offset caused by incorrect zeroing or mounting of the accelerometer;
- A time proportional error caused by integration drift;
- A scaling error caused by accelerometer and wheel speed calibration errors, tyre growth and slip;
- A scaling error caused by body roll, causing gravitational acceleration to contribute to the measured acceleration.

Errors can also arise from the vehicle sliding, as the lateral acceleration measurement axis is no longer perpendicular to the heading of the car (Doogue and Walsh, 1998).

A final source of error, not reported by Casanova *et al*. will arise from the gradient around a circuit. The approach described above effectively draws the path followed by the car to length on a 2-Dimensional (2D) plane, rather than projecting it on to the plane. Therefore the trajectory could not join on this basis, even in the absence of any other sources of error. This is an issue which is increased with the level of altitude variation around the circuit and will be a definite factor in the reconstruction of the Donington Park trajectory, known for its elevation change

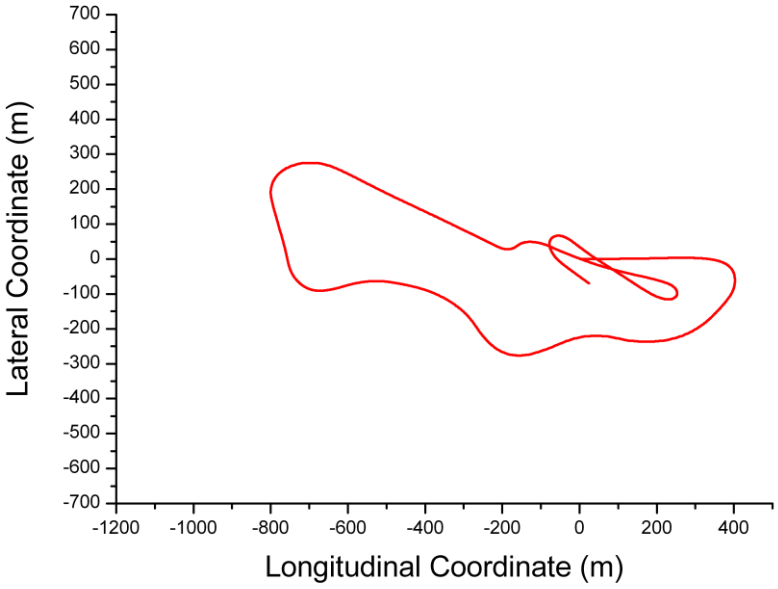

Figure 36 – The inertial trajectory computed before correction.

A method proposed by Casanova *et al.* (2001) corrects the curvature by applying a correction to each of the three error types, offset, time proportional and scaling error, correcting only the acceleration data. This method is not used here, but instead an orientation and stretching correction algorithm, which was shown by Casanova to produce better results, was applied.

This method effectively looked empirically at the errors present in the trajectory results after the first reconstruction pass (see Figure 36). It is clear from these

results that an orientation and coordinate error exist. The start finish errors can be expressed as:

$$E_{\psi} = \psi_t(T) - 2\pi \qquad \text{Equation 15}$$

Where E_{ψ} is the orientation or heading angle error and T is the total lap time.

The coordinate errors can be expressed as:

$$E_x = x_t(T) \qquad \text{Equation 16}$$

$$E_y = y_t(T) \qquad \text{Equation 17}$$

Where E_x is the longitudinal coordinate error and E_y is the lateral coordinate error.

The corrections are applied uniformly by their application being on a per unit distance basis, as shown in the following equations:

$$\overline{\psi}_t(t) = \int_0^t \left[k_t(t) - \frac{E_{\psi}}{S} \right] V(t)dt \qquad \text{Equation 18}$$

$$\overline{x}_t(t) = \int_0^t \left\{ \cos\left[\overline{\psi}_t(t)\right] - \frac{E_x}{S} \right\} V(t)dt \qquad \text{Equation 19}$$

$$\overline{y}_t(t) = \int_0^t \left\{ \sin\left[\overline{\psi}_t(t)\right] - \frac{E_y}{S} \right\} V(t)dt \qquad \text{Equation 20}$$

Where, $\overline{\psi}_t$, $\overline{x}_t$ and $\overline{y}_t$ are the corrected heading angle, longitudinal and lateral coordinates. S is the total lap length, i.e. s integrated over the whole lap.
The heading change applied independently can be seen to match the heading angle of the start and end of the circuit as shown in

Figure 37, whilst the effects of adding the coordinate stretch correction also is illustrated by Figure 38.

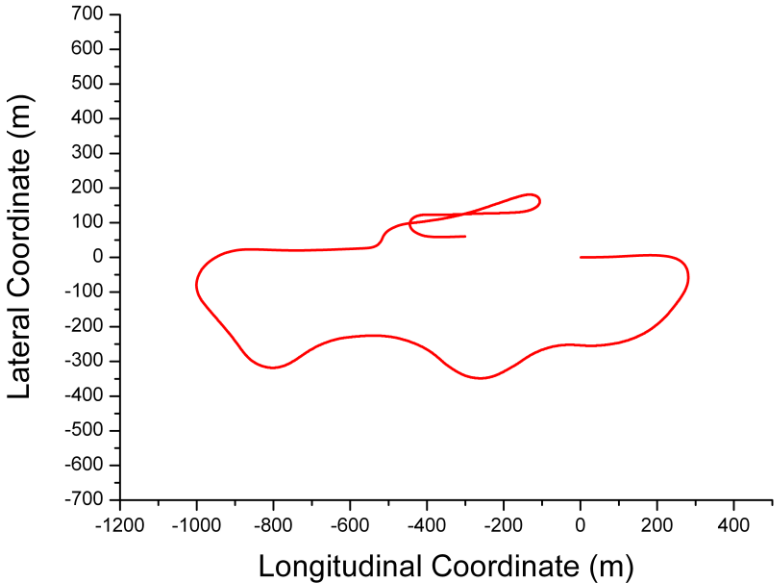

Figure 37 - Trajectory with the heading angle correction only applied.

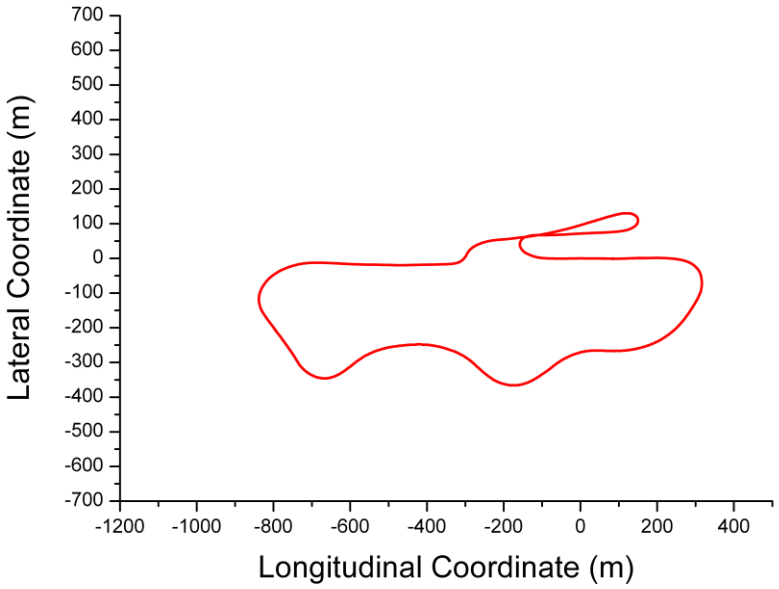

Figure 38 – Trajectory with heading angle and coordinate stretching correction applied.

If the aerial view of the Donington Park track in Figure 39 is considered, it can be seen that the inertial kinematic trajectory algorithm has succeeded in defining all the corners and given a good visual impression of their curvatures relative to one another. This is generally sufficient for the technique's application to producing a circuit for referencing data. However, there is a number of features of the circuit trajectory which give a clear indication that the method is not sufficiently accurate for comparison of driver's lines. Corner names are given to aid reference and these areas of interest are labelled on Figure 39 as:

1. The heading between the start/finish straight and the straight between the Melbourne Hairpin and Goddard's are clearly not parallel as the calculated trajectory in Figure 38 suggests;
2. The Esses appear slightly above the start finish straight in the orientation of the aerial view, yet Figure 38 would suggest they are slightly below;
3. Clearly there is a noticeable separation of the entry and exit straights of the Melbourne hairpin, but the trajectory calculated in Figure 38 shows the two straights overlapping.

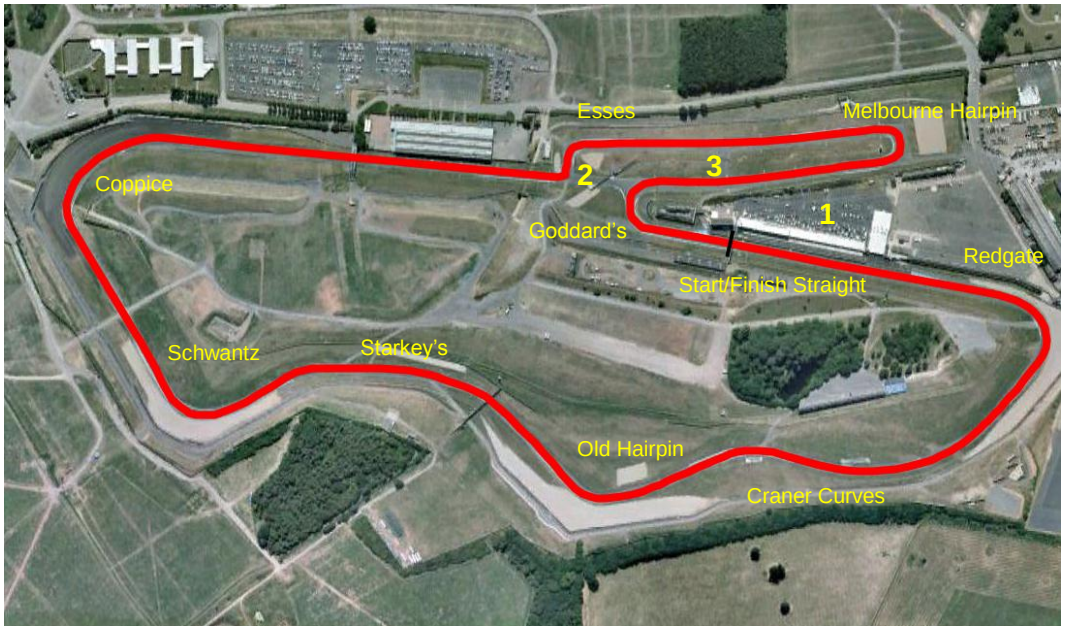

Figure 39 – Aerial view of the Donington Park circuit (google Maps, 2010a).

4.6 Animating the Vehicle Model

This section details the actual programming of the preliminary display application which was created to test the use of the approach employed for its potential to achieve the final level of the visualisation application detailed in Chapter 7.

4.6.1 Tasks to be performed by the Display Application

The preliminary visualisation application was intended to test the concept devised for the final version which was the ultimate deliverable of this research. This final version of the software would animate suspension movement and replicate the car's position on circuit. The preliminary version, however, would be used to achieve the following:

- To test the graphics rendering approach to be employed;
- To test the potential of vehicle trajectory placement for aiding user assimilation.

With these two key points considered, the application would therefore need to:

- Load modelled vehicle components;
- Determine the vehicle's trajectory from lateral acceleration and speed data;
- Draw the vehicle components to screen;
- Move the vehicle components around the defined trajectory, performing necessary transformations to give the visual impression of the vehicle turning.

4.6.2 OpenGL® Background

OpenGL (Open Graphics Library) is a graphics Application User Interface (API), used for writing applications which can draw 2D or 3D graphics to screen. It is essentially a software interface to graphics hardware (Shreiner *et al*., 2008). It is titled “Open” as when produced by Silicon Graphics Inc. in 1992 its specification was made freely available which makes it widely supported and flexible (Martz, 2006). The OpenGL® Utility Library (commonly referred to as GLU) is packaged with OpenGL® as standard, to provide higher level drawing functionality from the OpenGL primitive functions. The OpenGL Utility Toolbox (GLUT) was also used. This is a library of utilities which handles operations between the graphics application and the host operating system, such as defining windows and monitoring control inputs from keyboards and such like. OpenGL® itself does not carry the functionality to perform these tasks on its own, since it is designed to be completely device independent (Shreiner *et al*., 2008).

Together these were used to control the visualisation application which would perform the operations detailed in section 4.6.1. They were regarded as tools usable by beginners but which provided sufficient functionality and efficiency for use in commercial level applications (Martz, 2006), so together with their popularity and support were ideally suited to the application conceived here.

OpenGL® restricts the user to constructing a graphical model from points, lines and polygons. The use of polygons for representing a surface is well illustrated by the 3D Studio Max view of the chassis model geometry used in this section of the work (Figure 40), which was handled by the same approach. The different views show the number of vertices making up the model and how, despite of the primitive nature of the construction, a smooth model can result.

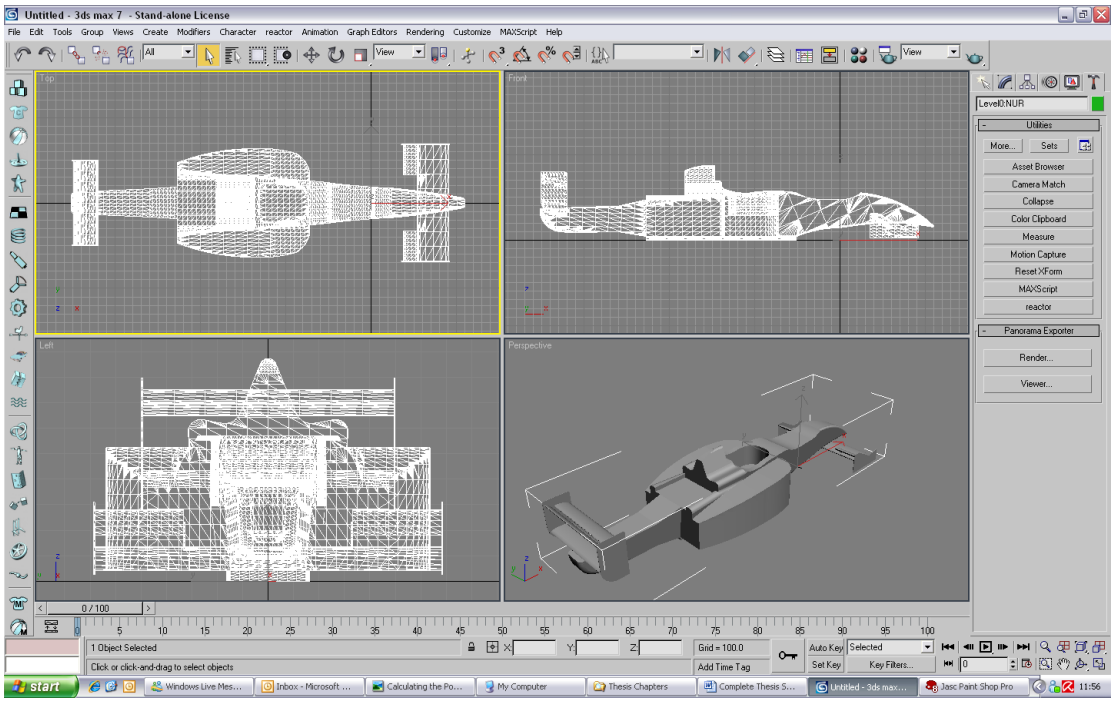

Figure 40 - A screenshot of the Dallara T05 chassis model viewed in 3D Studio Max, illustrating its polygonal construction.

Model data is processed through the transformation pipeline to provide the final window coordinates of the data to be drawn to screen. The transformation pipeline exploits the operation of OpenGL® as a state machine, with the use of transformation matrix stacks to provide a convenient way for manipulating large hierarchical models, consisting of many parts. The transformation pipeline and these aspects of its operation are described in more detail in the following section.

4.6.3 The OpenGL® Transformation Pipeline

The OpenGL® Transformation Pipeline is the series of transformations applied to a set of model or object coordinates, which together apply a translation associated with a physical movement and one associated with the location chosen to view the model from. A further series of transformations apply perspective to the view and determine which parts will be visible on the screen

before the final transformed data is drawn. The diagram adapted from Shreiner *et al*.'s text (2008) in Figure 41 illustrates the various stages of the pipeline.

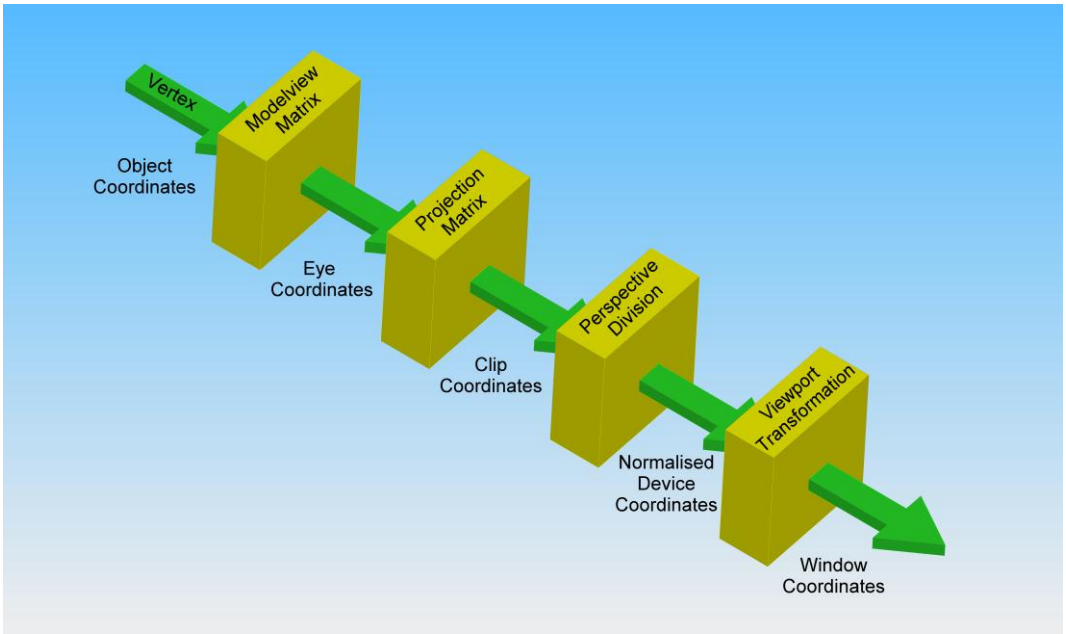

Figure 41 - The OpenGL® Transformation Pipeline adapted from Shreiner *et al.* (2008)

Below is a more detailed overview of some of the key stages of the pipeline and of the key methods which are used by OpenGL® to optimise its operation. This includes its operation under a state machine computing model and the matrix and transformation methods and conventions used.

4.6.3.1 OpenGL® Operation as a State Machine

A state machine is a common computing model, which is essentially a machine or system that remains in the same state until told to change. OpenGL® is a finite state machine as it has a predefined number of states, a state being the configuration of the system at a given time (Shreiner *et al.*, 2008).

State changes occur with any changing of option, which can be simple enabling or disabling of certain features or can be the setting of specific changes, such as drawing parameters. Since the state machine only changes when told to do so, this state remains until any other changes are applied. This makes it simple to

document changes and simplifies the execution of multiple drawing operations which require the same configuration of drawing parameters.

4.6.3.2 OpenGL® Matrix Stacks

As described previously, the transformations applied to model geometry are done so with 4 x 4 matrices, in the form of an affine transformation matrix. It is convenient to consider the matrix as transforming an original coordinate frame to define a coordinate system with a new orientation and/or position. Figure 42 shows the layout of the matrix; the top left section holds three unit vectors representing the rotated x, y and z axes which define the frame orientation. The new origin of the coordinate frame is held in the top right hand corner of the matrix, with x, y and z coordinates respectively on rows 0, 1 and 2.

$$\begin{bmatrix} \text{Rotation of Frame} & \text{Translation of Frame Origin} \\ 0 \quad 0 \quad 0 & 1 \end{bmatrix}$$

Figure 42 – The layout of the affine transformation matrix.

Under OpenGL®'s state machine operation stacks of matrices are used to allow for ease of state changes. There are a number of matrix stacks, but the two that are of importance here are those which affect the transformation of model vertex data; these are the Modelview matrix stack and the Projection matrix stack whose position in the transformation pipeline has been illustrated in Figure 41.

The Modelview stack is responsible for moving model data from the object coordinate system to the eye coordinate system, replicating a physical displacement of the model. Essentially the matrix is a two part transformation, consisting of a transformation of the model data into a world coordinate system concatenated with a transformation to produce eye coordinates.

OpenGL® is in fact not viewed as having a world coordinate system and as such this notion is purely as an intermediate construct, rather than a formally recognised part of the transformation pipeline. The view transformation which is

applied at this intermediate stage is the inverse of a transformation which positions and orientates a camera in the world coordinate system. This is achieved by the gluLookAt() function from the utility library.

The Projection stack is responsible for producing clip coordinates. That is, it defines the size and shape of the view volume, hence determining the range of eye coordinates which will be visible. Vertex data outside of these coordinates will be clipped, i.e. not drawn to screen, a process which is handled by OpenGL® without the need for any other user intervention.

Only the top matrix in the stack affects the state of OpenGL® whilst the remainder of the stack allows the state definition to be returned to an earlier point. Any of OpenGL®'s range of matrix manipulation commands also are only performed on the top matrix in the stack. This is particularly useful for the construction of hierarchical models which require various model parts to be transformed to a range of locations known relative to some origin. Once the transformation is applied to the first model, it is drawn to a buffer and the previous state of the model transformation can be restored. The transformations unique to the next model can then be applied to tailor the top of the stack for its transformation.

Two key commands are used to exploit the matrix stacks, glPopMatrix() and glPushMatrix(). glPushMatrix() is called to record a stage of interest, such as a transformation which will be applied to all models. A good example is the camera view transformation, which will affect the entire scene. Upon this transformation being set, the glPushMatrix() command can be used to produce a copy at the top of the matrix stack, which will then subsequently be modified to affect the state of OpenGL®. The original matrix remains unchanged and occupies the next level of the stack below, being available to be reverted back to when the complete transformation of a different model is being calculated.

glPopMatrix() is the command used to work back through the matrix stack, discarding the top matrix and hence replacing it with the next matrix down in the stack.

4.6.3.3 Matrix Multiplication Convention

OpenGL® operations postmultiply a transformation matrix on to the stack, such that:

$$\begin{bmatrix}\text{Top Matrix}\\ \text{of Stack}\end{bmatrix}\times\begin{bmatrix}\text{Transformation}\\ \text{Matrix}\end{bmatrix}=\begin{bmatrix}\text{Top Matrix}\\ \text{of Stack}\end{bmatrix}$$

Figure 43 - Postmultiplication of the matrix stack.

Postmultiplying the transformation matrices has the effect of transforming the model to which they are applied about its own coordinate frame. The work here however also required transformations of the components in a world or reference frame, and so premultiplication was implemented by self programmed lower level matrix multiplication functions. Once multiplication is complete, the top matrix in the stack is replaced by the result of the multiplication.

A well recognised problem with applying a rotation about each of a model's own 3 axes in succession is the occurrence of gimbal lock, which is essentially caused by parallel alignment of two axes during the consecutive stages of rotation. Gimbal lock results in a 2D space, with a degree of freedom lost. The screenshots from the Wikipedia entry on gimbal lock (Figure 44) illustrate the occurrence of the problem during the rotation of an aeroplane model (Wikipedia, 2010). It can be seen that the first rotation on the red plane aligns the blue and the green planes (second frame). Subsequently, there is then no means of incorporating the yaw rotation in the second frame (the rotation about the aeroplane's vertical axis, i.e. in the blue plane of the first frame); a degree of freedom has therefore been lost. This can cause unexpected results and jerky movement during animation (Tremblay, 2004).

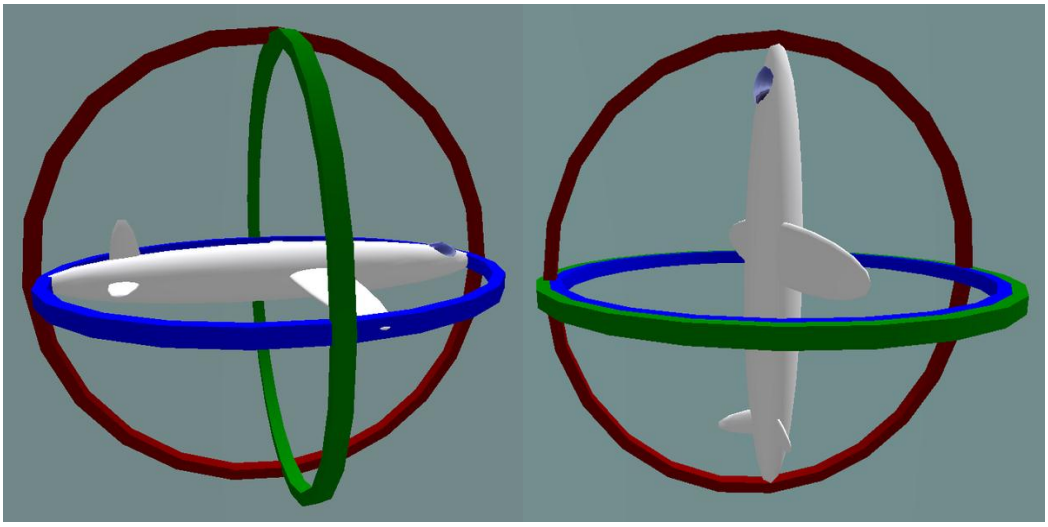

Figure 44 - Illustration of the occurence of gimbal lock.

The subject of 3D rotation is vast and the key to this work is simply for a robust way of applying rotations to the vehicle models. Therefore a quaternion based class developed from Baker (2010) which uses the so called Euler rotations about individual axes was used. Quaternions are in effect multi-dimensional complex number representations of rotations and their combination is efficient, allowing for various rotations to be combined easily (Tremblay, 2004). Three of the four numbers making up the quaternion represent a vector defining the heading and yaw of the object after rotation, whilst the fourth represents the roll rotation angle about this vector. It has been reported that gimbal lock is caused solely by the formation of rotation operators from Euler angle rotations, yet some sources suggest that the transformation of all axes together in the quaternion approach ensures no gimbal lock (Tremblay, 2004). The implementation employed here was tested and found to cause no gimbal lock issues with the data presented to it. As a method to illustrate the principles being investigated in this work, it was therefore deemed satisfactory.

Final application of the rotations had to be made to the OpenGL® matrix stack by a rotation matrix as described previously, which was a simple step as the quaternion class provided a matrix data member also.

4.6.3.4 OpenGL® Eye Coordinates

Upon application of the Modelview transformations, model geometry can be thought of having been transformed to eye coordinates. These coordinates are a transformation of the model in the intermediate world coordinate frame coupled with a translation associated with the camera location which views the scene. The convention for the coordinate directions is illustrated in Figure 45 with reference to the viewing screen.

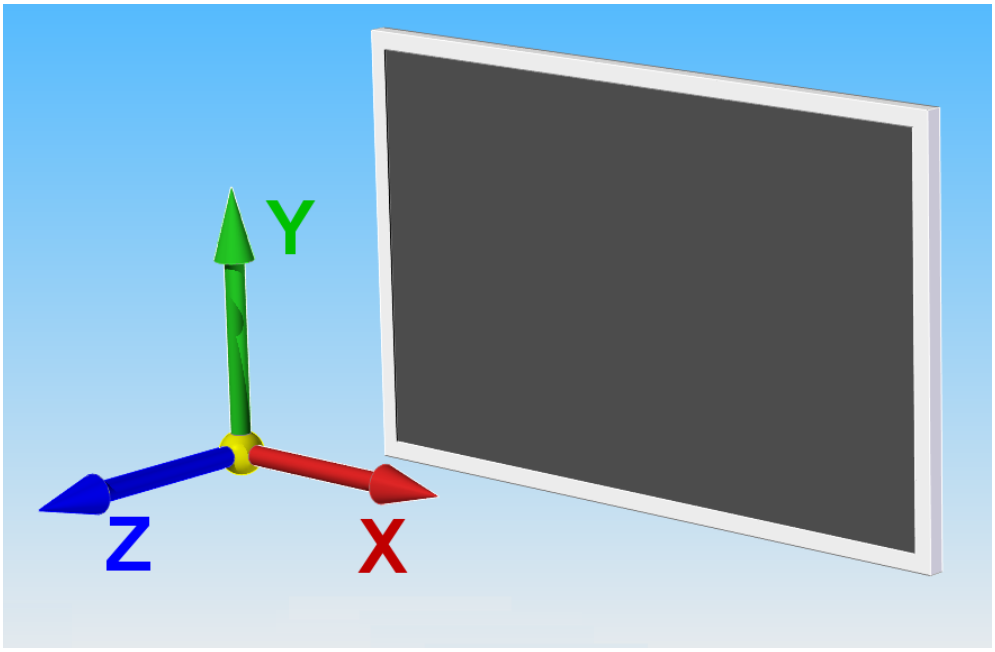

Figure 45 – The OpenGL® Eye Coordinate convention.

4.6.4 Loading Model Data with OpenGL

Guidance from a computer games programming student, who became involved in this work to a small extent recommended the use of a .3ds model loader programmed by Matthew Fairfax and which was freely available on the internet (Fairfax, 2001). This was programmed to utilise OpenGL commands through GLUT for recreating the surface data stored within the .3ds file. The loader fully supported the OOP of Visual C++ and simplified the use of .3ds model data within the main application as each model component was loaded as an instance or object of the .3ds model class. Within the main program, simple commands

such as Draw() and Load() applied to the object could be used to access the surface data within the file. Reconstruction of the surface data was performed by the OpenGL API polygon drawing functions called from the model loader class; GL_TRIANGLES drawing a triangle between the 3 vertices defined in turn by glvertex3f.

The .3ds file format approach of storing data as vertices for reconstruction by a graphics API to a mesh of triangles is known as polygonal modelling. It is a technique widely applied to real time rendering applications as it suits a scanline approach to visible surface determination; the process of determining which parts of an object are visible on the screen. This method allows for very specific control over what is drawn and hence good application optimisation which has lead to its proliferation (Shreiner *et al.*, 2008).

The polygonal approach to drawing the models in the visualisation application does not provide such a visually impressive recreation of the model as the renderers incorporated in the Solid Edge® modelling environment, as is clear from a comparison of the images in Figure 46. However, such an approach was used in the previous work leading onto this research (Parker 2004c) and was found to be extremely slow and not capable of real time rendering.

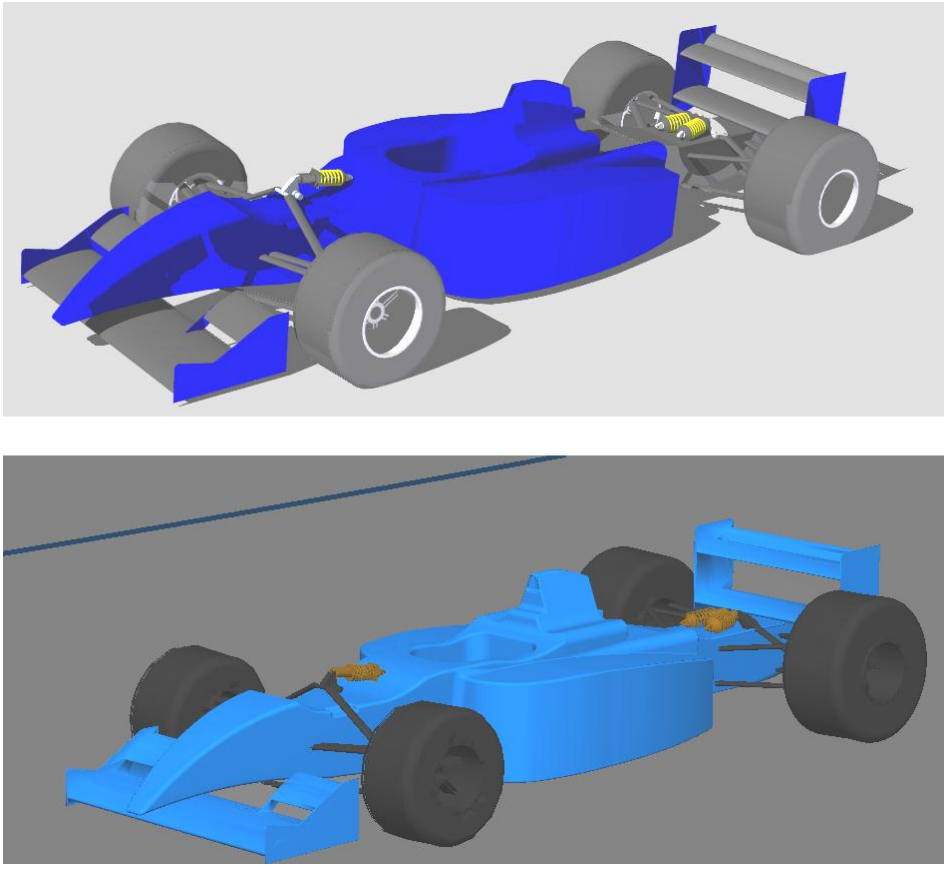

Figure 46 - Comparison of the Dallara T05 model rendered by the Solid Edge® renderer and by using a polygonal reconstruction with a .3ds version of the model in the visualisation application.

4.7 Display

A final aspect of creating the demonstration application was to design the layout presented to the user. The concept discussed in Chapter 3 for multiple windows, presenting different views of the data to the user would be tested here. It was decided that three windows would be a suitable arrangement, as illustrated in Figure 47, giving the user a wide view of the car following its calculated trajectory, a closer impression of the car itself and a window displaying data in a standard Cartesian graph format.

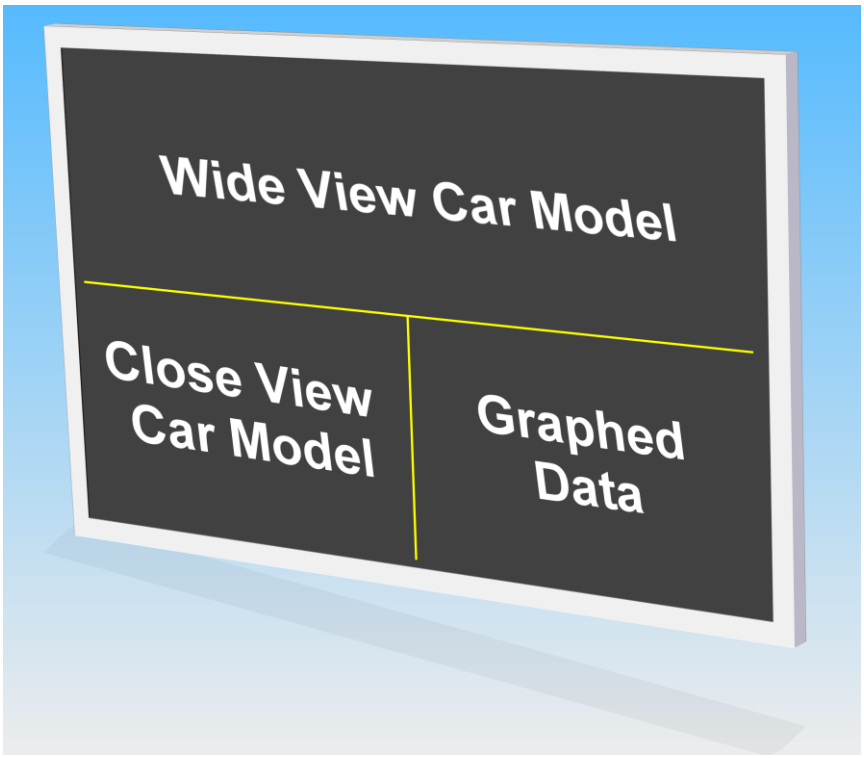

Figure 47 – The screen layout of the visualisation application.

Further to this layout, the nature of the views in the top and bottom left segments of the screen would vary slightly. The bottom left segment would feature a viewpoint moving with the car around the trajectory, replicating the close view which would be used to best illustrate suspension motion and such like. The top section would feature television style trackside camera views, cutting as the car reached different points of the circuit. The trajectory calculated for one particular lap, as detailed in section 4.5 is illustrated in Figure 48 with various markers indicating the location of cameras which would view the model as it traversed the calculated trajectory.

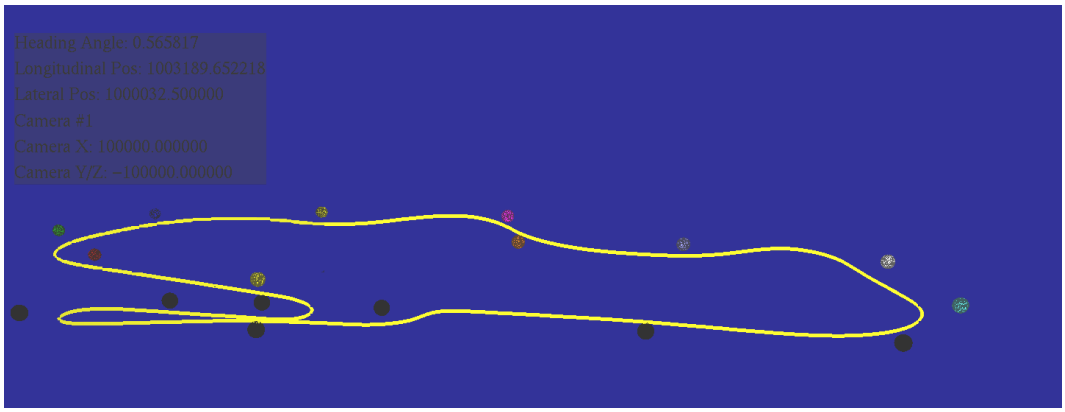

Figure 48 – Calculated trajectory with camera locations marked.

The data plot window was also designed as illustrated in Figure 28, which illustrates the comparison of two lap's speed traces. The animation would be synchronised with data markers illustrating the channel value and in keeping with the approach of video indexed data such as that produced by Pi Research (2000).

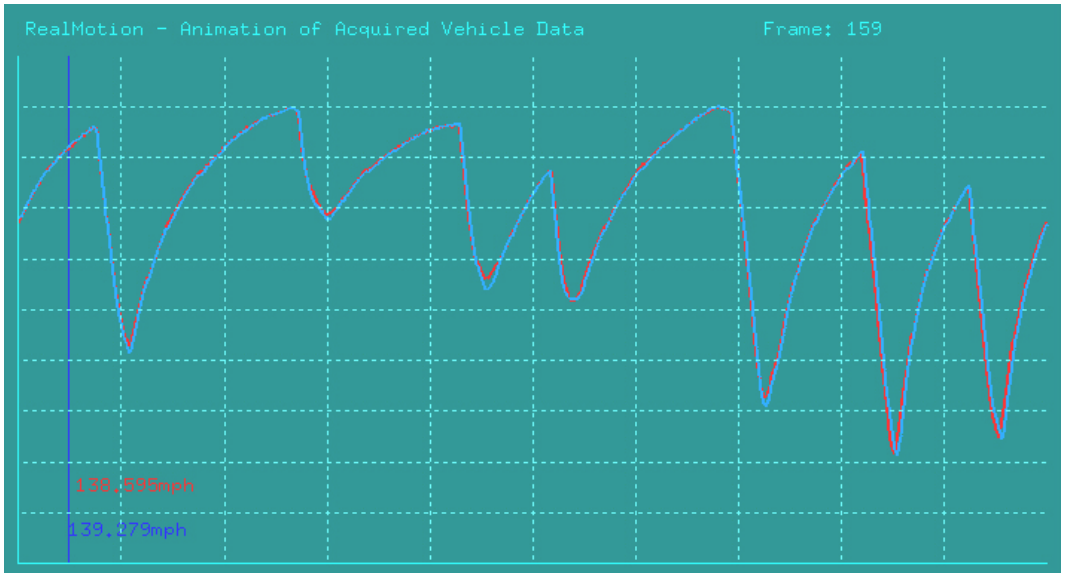

Figure 49 – The Cartesian data plot window from the display application.

4.8 Testing

The display was tested by a comparison of two laps of data recorded from the WSbR FR 3.5 driven by Alx Danielsson during qualifying for the WSbR meeting at the Donington Park circuit on September 10th 2006. The first is a 1 minute 18.600 second lap and the second is a 1 minute 18.060 lap, which secured pole position.

4.8.1 Test Configuration

Lateral acceleration, speed and distance data was extracted from Wintax 2, the Magneti-Marelli application used with the FR 3.5 car, at 50Hz. This naturally created some filtering effect on the noisy lateral acceleration data, whereas the distance and speed data tends to be naturally relatively smooth. A further filtering of the accelerometer data was required and this was achieved as might be expected of a typical team at the circuit; an averaging filter was used which was adjusted to an 11 point average (5 back and 5 forward points) to yield the best shaped trajectory from the data.

The two calculated trajectories and the speed and time data were then loaded into the visualisation application for display testing. Two models were used, one for each lap, with one being coloured red and one blue for distinction.

The model was positioned relative to the ground using the measured tyre contact patch centres, supplied by RST (Renault Sport Technologies, 2006). The concept of the tyre contact patch is illustrated in Figure 50, being the centre of the patch of rubber in contact with the ground. The deformation of the tyre combined with suspension motion causes the patch to change shape and for the centre to migrate in reality, however with this test involving no suspension motion the static contact patch could be used throughout. This can be seen to be essentially the intersection between the ground and a line from the wheel centre perpendicular to the ground (Rowley, 2004).

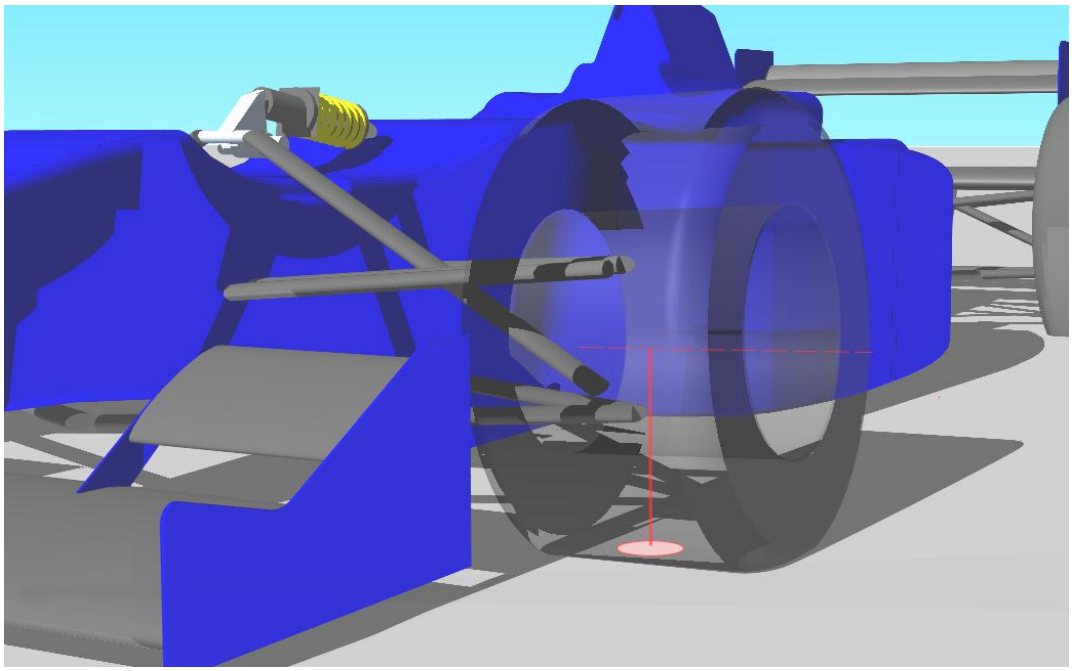

Figure 50 – Illustration of the tyre contact patch.

OpenGL® was set to match the 50Hz export rate of the data with a playback rate of 50fps. The application was tested on a desktop computer with the following specification:

Table 3 – Specification of the computer used for display application testing.

Processor	Intel® Xeon® E540	4 x 2.50GHz
System Memory		3Gb
Graphics Card	ATI Radeon ™ HD 3600 Series	512Mb

4.8.2 Test Results

The tests performed here were primarily in order to analyse the display application's potential for further development and incorporation of suspension motion.

The results are discussed with reference to a number of screen captures taken from the display application. It is also important to note that the application,

including its split screen operation and two models, produced 50fps playback successfully, validating the graphical approach as suitable in this sense for further development.

4.8.2.1 General Visual Impression

The following selection of screenshots (Figure 51 through Figure 53) depicts the visual impression presented to the user by the display. The corner names used on the aerial view in Figure 39 are again used to refer to parts of the circuit.

The difference in views between the two animation windows is clear. The top section giving a panning television style view allowing both blue and red laps to be visible in the same shot, whilst the bottom left gives a view focussed on the blue lap. It was envisaged that the focussed window would also allow a change in view to zoom in to the model, highlighting events of interest in a similar vein to the events driven and expert systems analysis described previously (Pi Research, 2004a; Vaduri and Law, 2000; Martin and Law, 2002).

The screenshots also illustrate the scrolling cursor in the data display window in the bottom right. One cursor moves to mark each lap position, whilst displaying a numerical value of the data at that point. This allows an additional visual impression of the time gap between two laps and the gains and losses which arise between them.

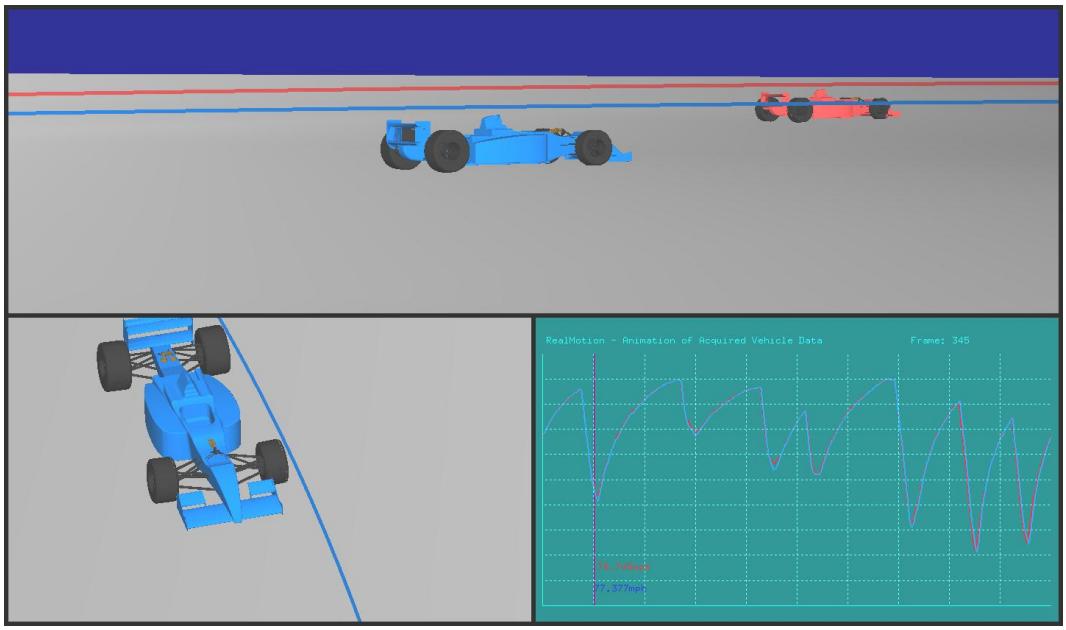

Figure 51 – Screenshot of display application illustrating the two laps approaching the apex of the first corner Redgate.

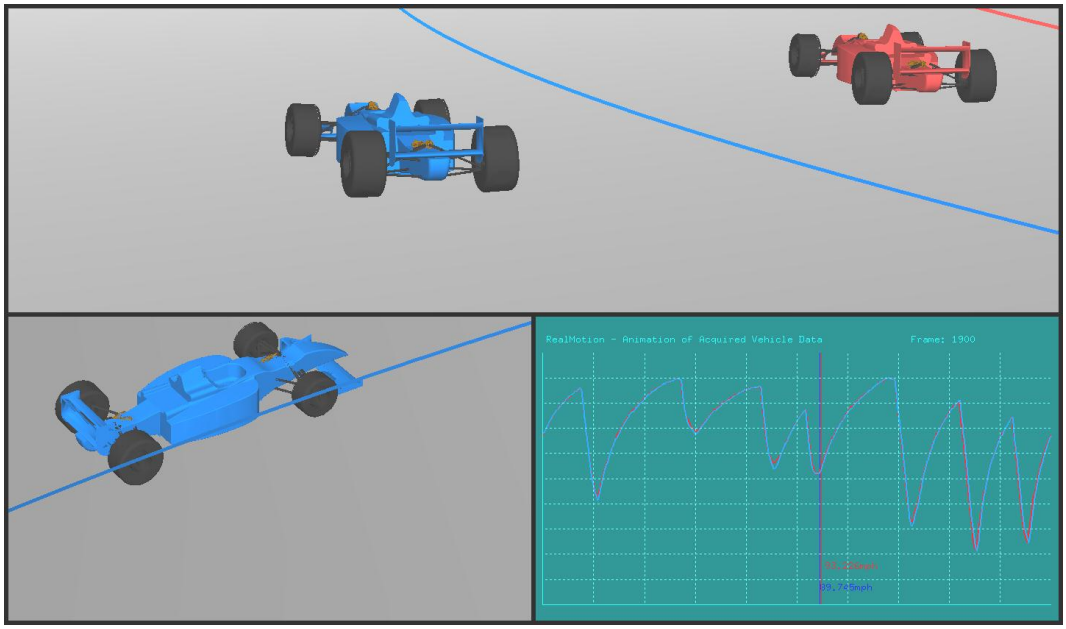

Figure 52 – Screenshot of display application illustrating the two laps at the apex of Coppice corner.

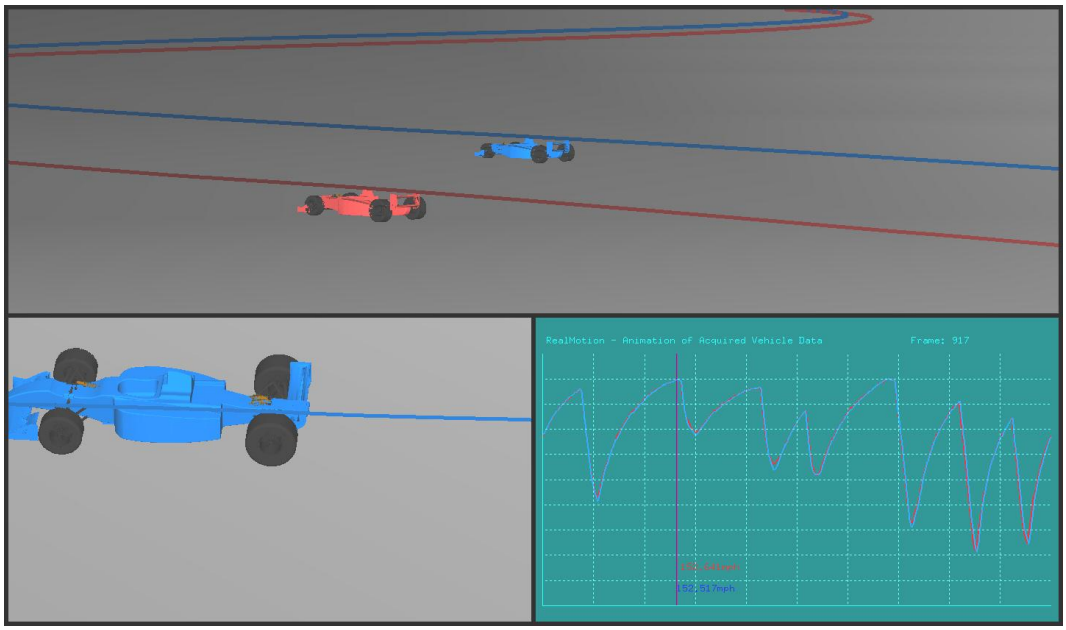

Figure 53 – Screenshot illustrating the two laps at the braking point for the Old Hairpin.

4.8.2.2 Comparison of Driving Lines

The driving lines or trajectories were calculated by the method described in detail earlier in this chapter. Both are displayed over the terrain for comparison as illustrated in Figure 54 through Figure 56. It is clear that the trajectories of the two laps suffer due to low accuracy, which was identified as issue previously, in the description of the calculation method (section 4.5) and by Casanova *et al.* (2001).

Consideration of the screenshots however should indicate to the reader the potential for such a display to assimilate and visualise driver approaches to corners, if the accuracy of the trajectory placement could be improved.

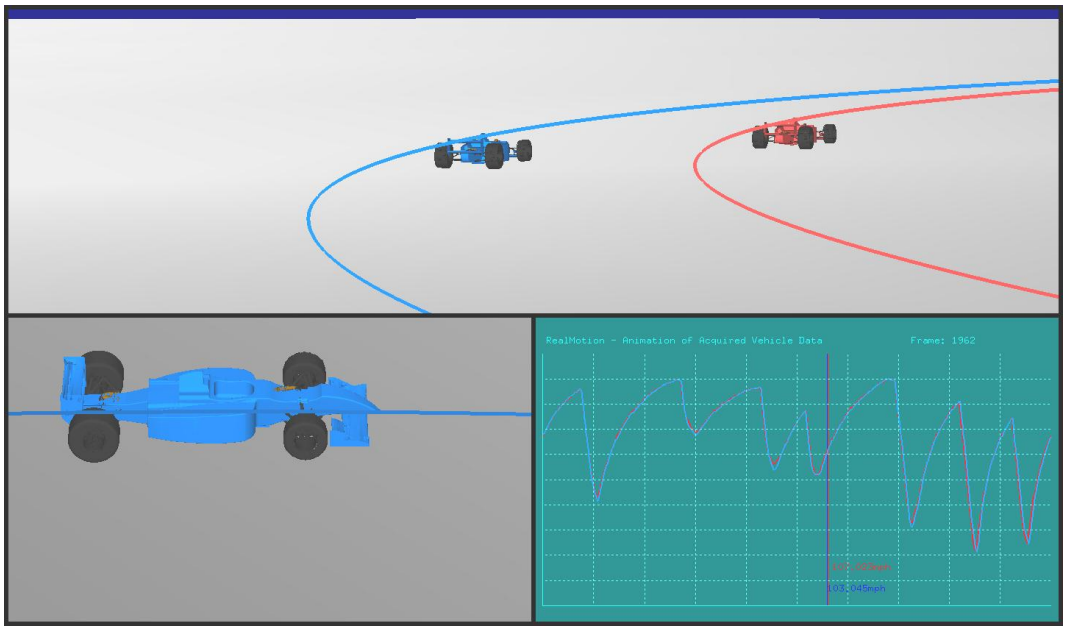

Figure 54 – Screenshot of the display application showing the comparison of two laps' trajectories at Coppice corner.

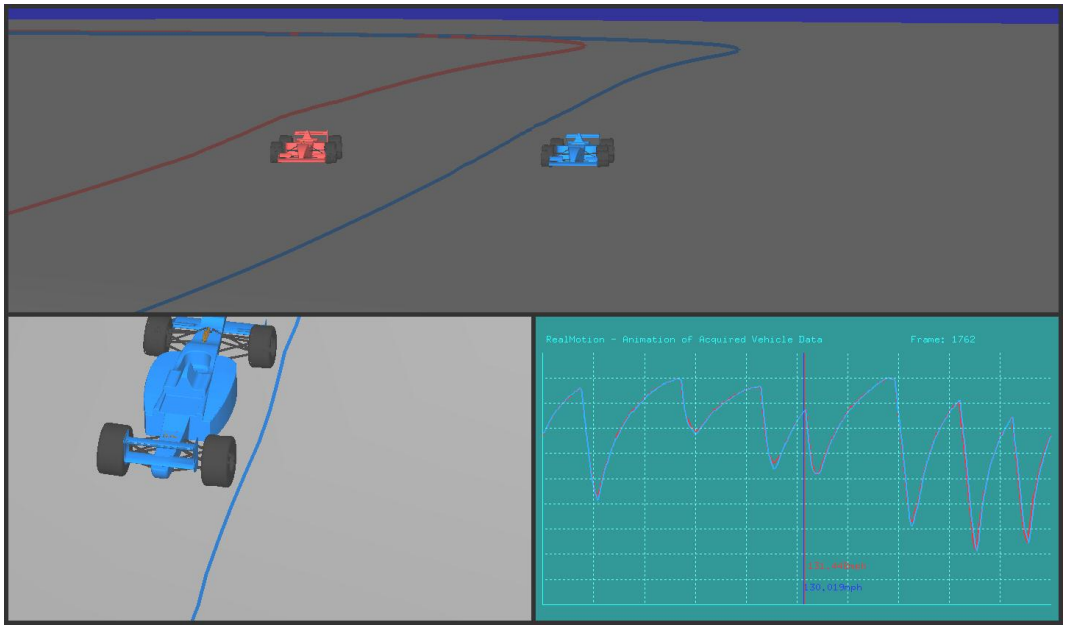

Figure 55 – Screenshot of the display application showing comparison of the two laps' trajectories at the braking point for Coppice corner.

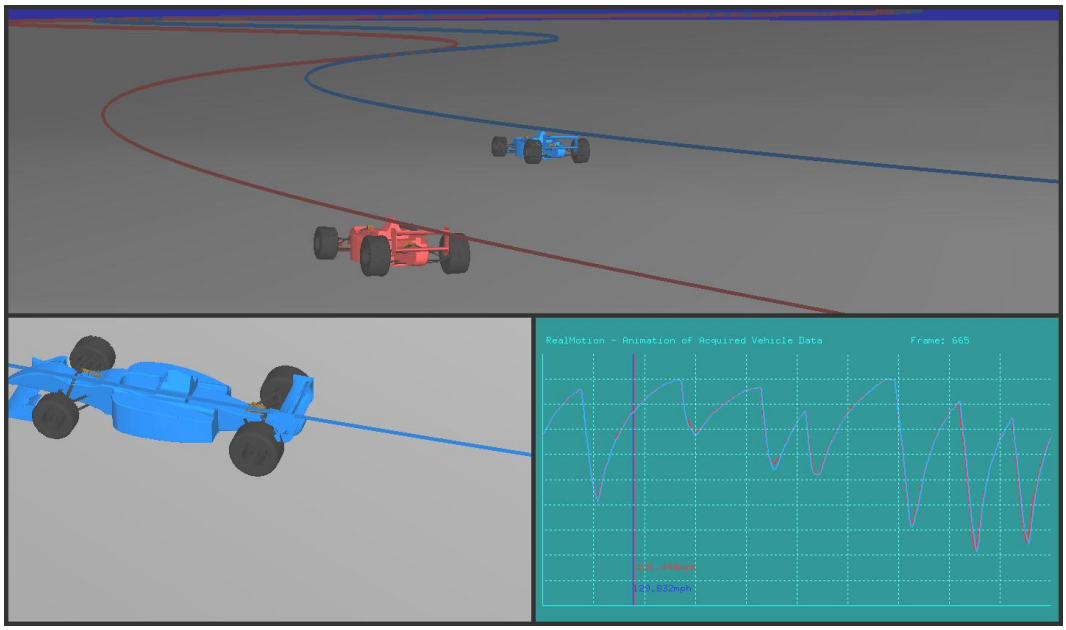

Figure 56 – Screenshot of the display application showing comparison of the two laps' trajectories exiting Redgate corner.

4.8.2.3 Television Style Camera

Three views of the display application are depicted in Figure 57, illustrating the camera panning to follow the car model past its position. This could easily be tailored to automatically zoom out the required amount in order to frame the other vehicle model.

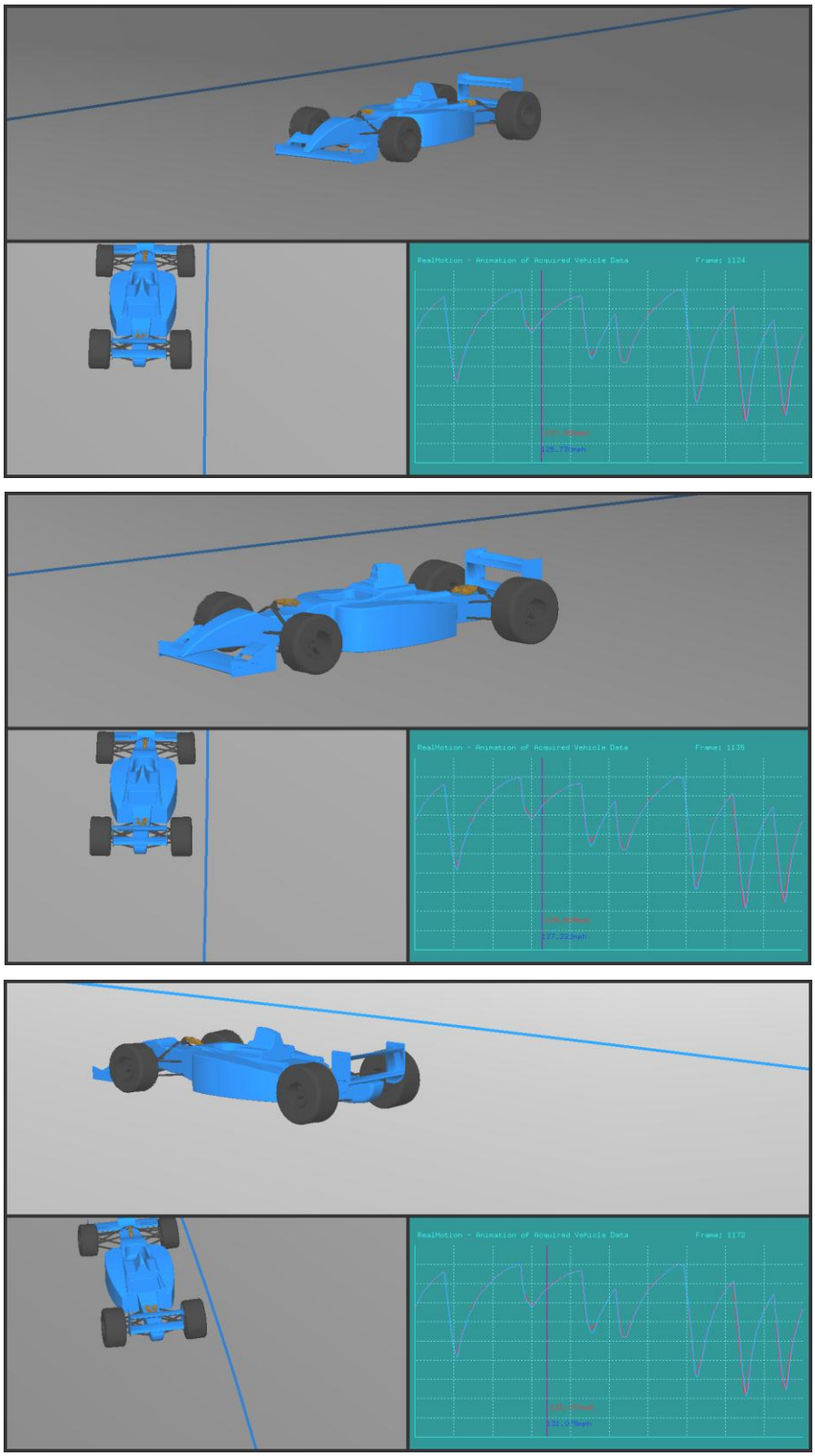

Figure 57 – Three screenshots illustrating the television style camera view.

4.8.2.4 Portrayal of Highlights

A single event which would be highlighted to the driver during a post session debrief is considered here, to illustrate the portrayal of an event of interest and how the display application could potentially complement driver/race engineer communication. The plot shown in Figure 58 illustrates the speed channel for both laps over the entire lap duration. The area of interest is at the Esses, the fifth trough in the data.

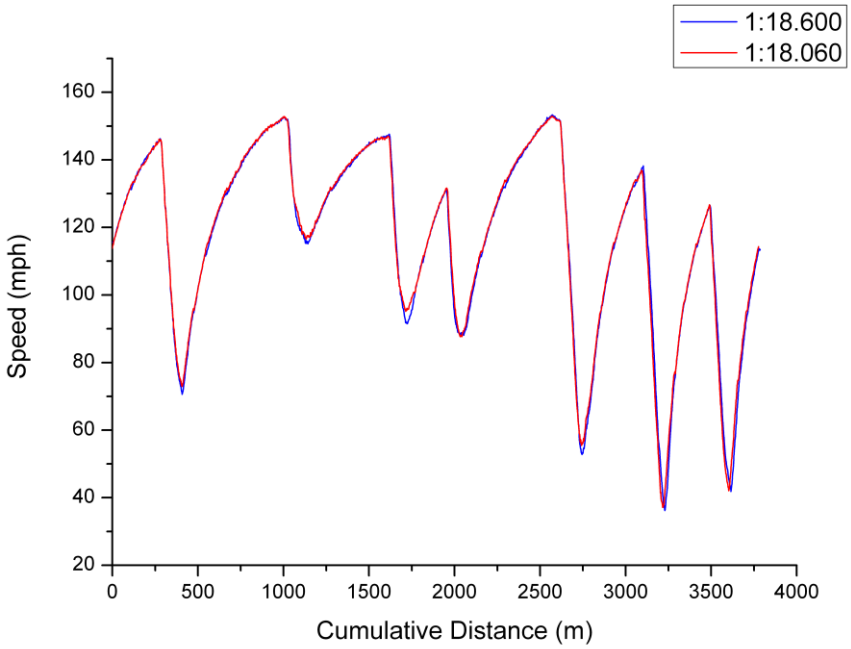

Figure 58 – Speed Vs. Cumulative Distance for the entire length of the Donington Park circuit.

Figure 59 shows the section of data at the Esses zoomed in to yield more detail. The event of interest begins with the braking of both laps, which occurs at a very similar lap distance of 2620m. The red lap illustrates good use of new tyres in qualifying as the driver (Danielsson) stops the car harder than on the blue lap, evident from the red trace dropping below the blue through most of the braking phase. This allows the blue lap to gain a little ground, however it enables the driver to release the brake sooner on the red lap and carry a greater speed into the corner and at the apex, maximising the lateral grip capability of the new tyres. This higher speed is carried through into a reasonable exit, with the slow apex

speed of the blue lap not allowing it to gain back a significant amount of time on the exit of the corner.

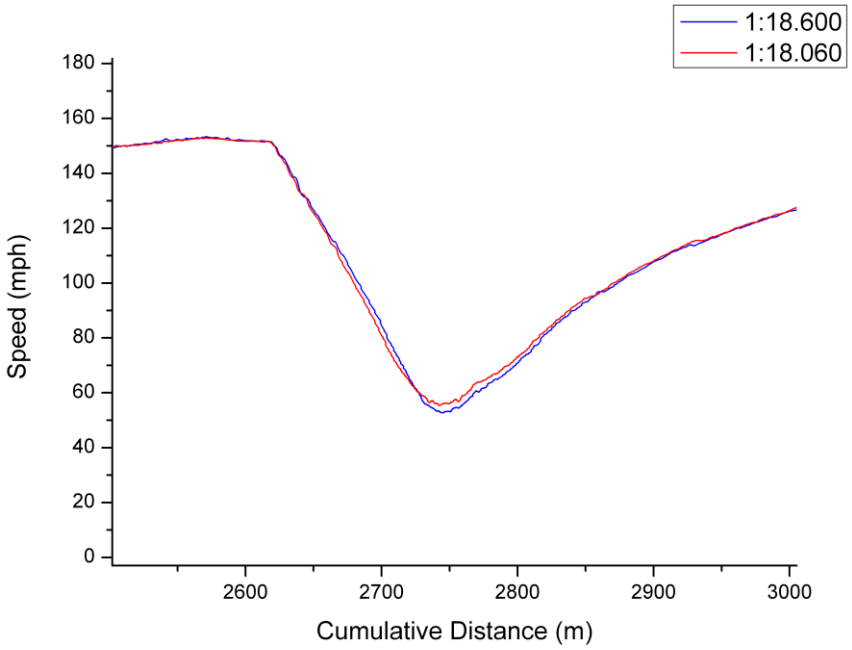

Figure 59 – Speed Vs. Cumulative Distance focussing on the Esses at the Donington Park circuit.

The series of screenshots in Figure 60 illustrate a number of key frames in the negotiation of the Esses.

A consideration of the screenshots should give the reader some impression of the assistance in visualising recorded data that the application can provide. For example, images such as B through F illustrate the closing of a time gap in a way which is immediately understandable to user. Meanwhile, images such as G through J illustrate the difference in corner turning in points and lines employed on the two laps, without having to extract these facts from a range of line graphs. A fuller description of the images is given in Table 4 with reference to Figure 60.

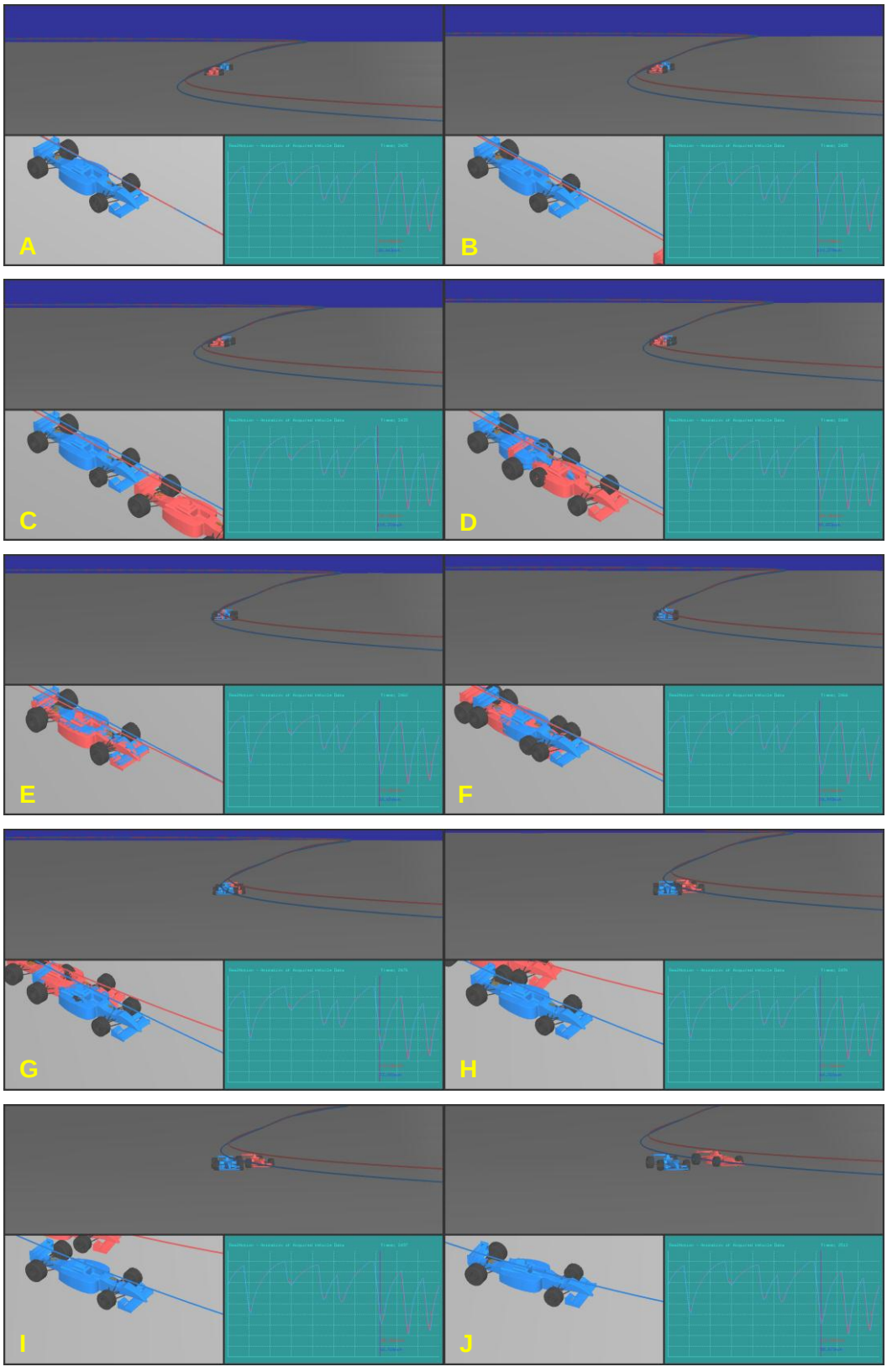

Figure 60 a - Sequence of frames showing the difference in approaches to Esses over two laps recorded by Alx Danielsson.

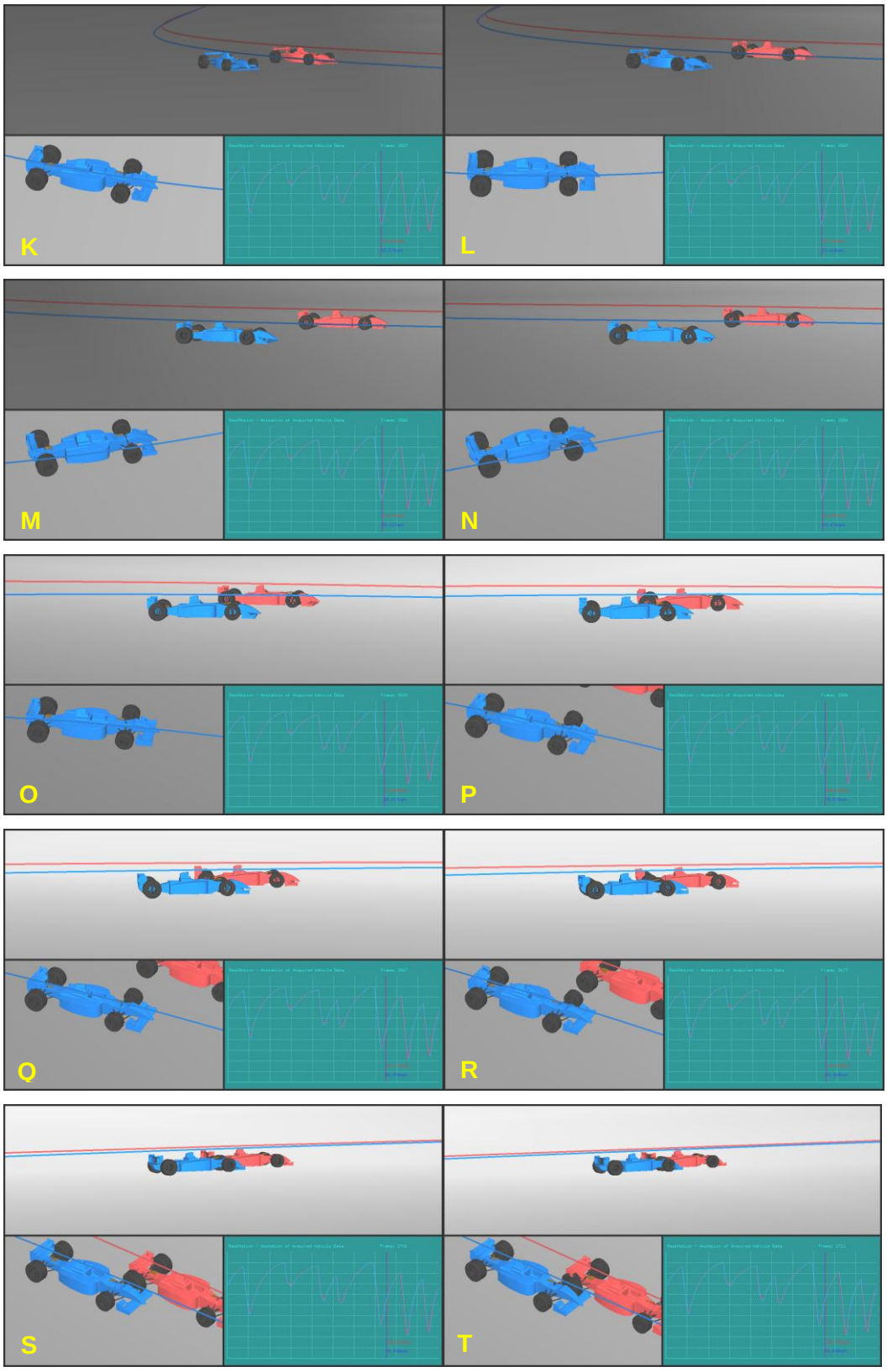

Figure 60 b - Sequence of frames showing the difference in approaches to Esses over two laps recorded by Alx Danielsson.

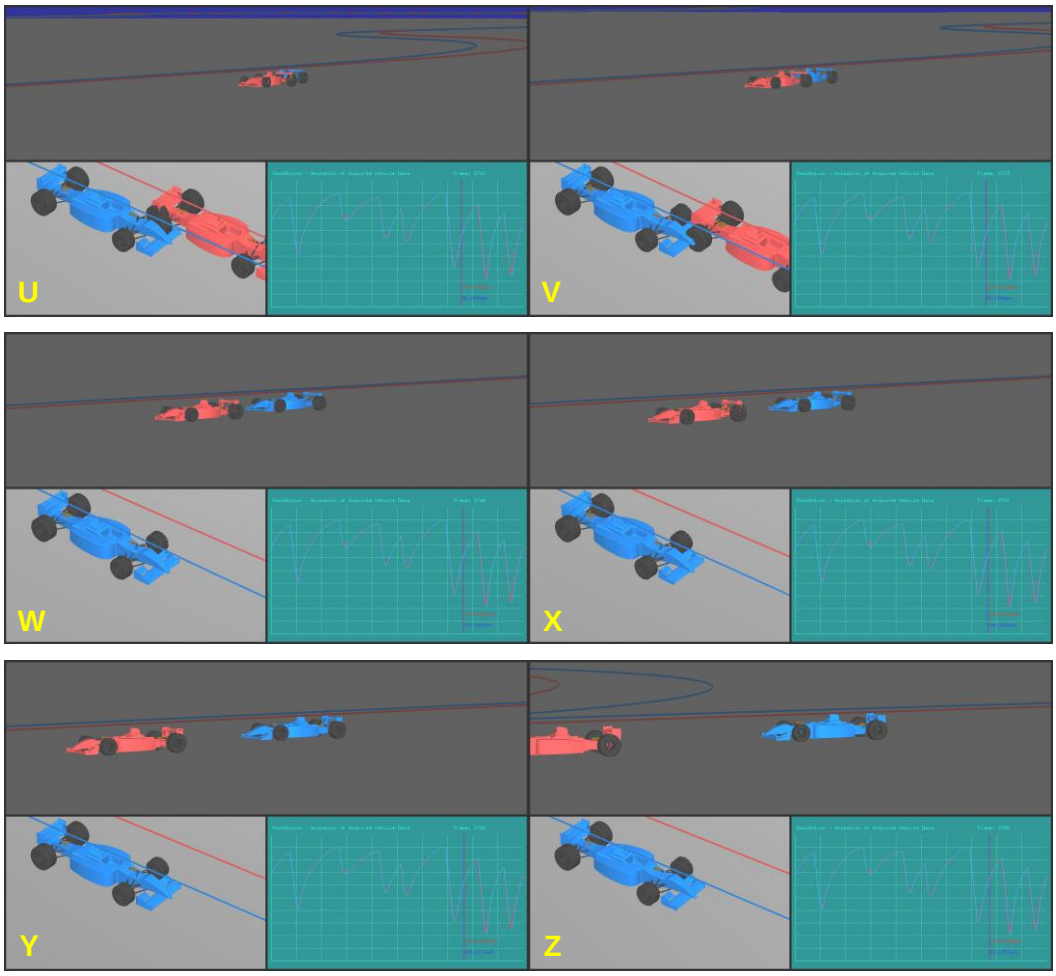

Figure 60 c – Sequence of frames showing the difference in approaches to Esses over two laps recorded by Alx Danielsson.

Table 4 – Description of key frames from the test animation.

Frame	Description
A	Both laps in the braking zone for the Esses.
B	Blue lap gains on red by braking more lightly.
G	Red lap turns in, whilst blue lap continues to run deeper into the corner.
K	Both laps approximately at their apex or minimum speed. The red lap carries a higher speed at this point.
M	The blue lap throttles well from corner, but appears to be on a wider line and does not gain any time back, just preventing further loss.
O	The blue lap appears to be gaining on the red. This is a problem caused by the inaccuracy of the trajectory calculation.
U	Camera cuts to next position.
V	Red lap gains time on exit of the Esses due to a higher exit speed.

The data displayed to the user in several of the screens depicted in Figure 60 is enlarged for ease of viewing in Figure 61. In screen A it is clear that the red lap has braked earlier as the displayed speed is considerably lower; a trend that continues at E. Screen J illustrates that red lap clearly has maintained a higher corner apex speed however, and has applied throttle sooner. The speed advantage at J has increased by screen O, confirming the earlier application of the throttle by the red lap.

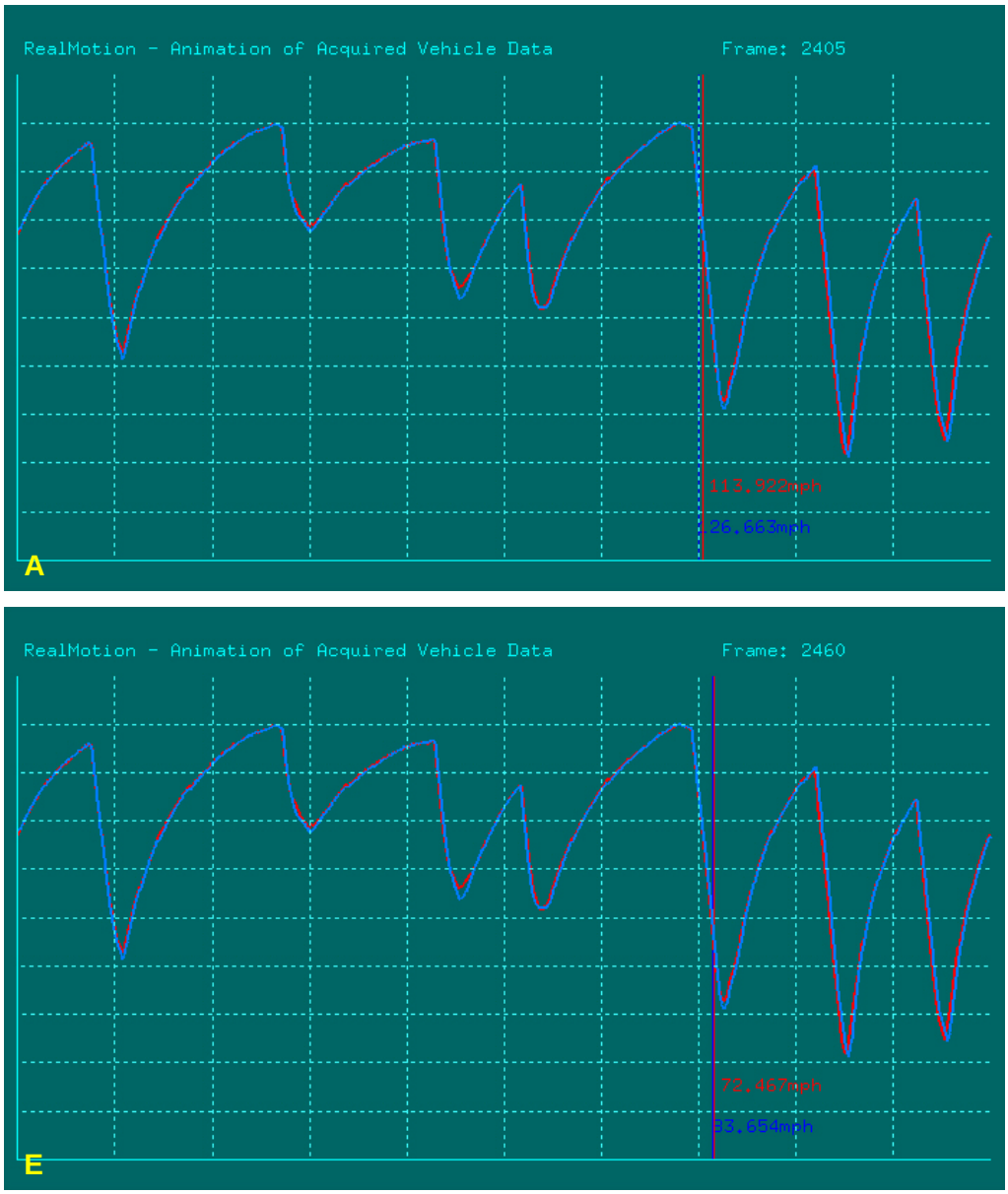

Figure 61a – The data display at different stages of event of interest potrayed.

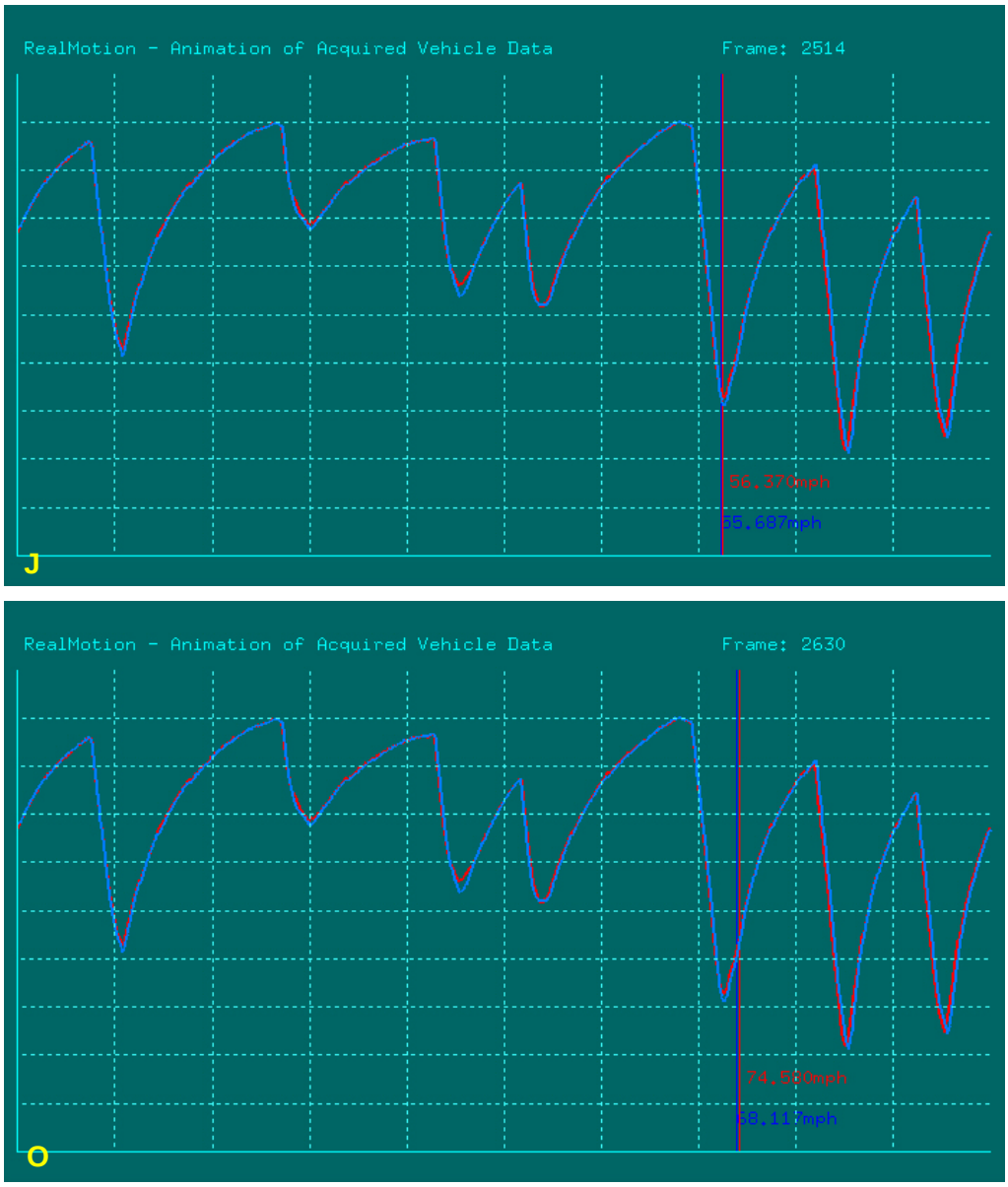

Figure 61b - The data display at different stages of event of interest potrayed

4.9 Conclusions

Through the development of an inertial data based trajectory approximation algorithm and of a 3D graphics display detailed in this chapter, several conclusions can be drawn:

- The comparison of trajectories can help the user of acquired motorsport data to assimilate the data to the vehicle itself;
- Despite the above point, accurate analysis of trajectories and particularly comparison is not possible with a trajectory calculated solely with the point kinematic approach described in 4.5.

The display animation has shown its potential for use in helping the user assimilate data. The preliminary version of the application has:

- Been able to attain 50fps playback of two models running under split screen operation;
- Allowed testing of display concepts on a simplified problem, by excluding suspension movement as well as body pitch and roll motion;
- Shown the potential of a split screen view of a model and plotted data as a useful tool for helping the user assimilate recorded data;
- Shown a useful means of illustrating gains and losses between two laps of data and differences in turn in point and driving lines, particularly with only a basic data set, already collected in all forms of racing. This illustrates its potential for application to junior racing, although it is clear that care has to be taken with comparison of trajectories however.

These conclusions in effect steered the remaining chapters presented in this thesis. The potential demonstrated by the display application warranted its further development, with the inclusion of suspension and body motion to enhance the data display further (Chapter 7). The system however ideally needed a more accurate means of calculating the vehicle trajectory, which lead to the investigation of an optical position sensor described in Chapter 6. The next chapter details the procurement, preparation and modelling of a test vehicle which would allow this sensor concept to be tested.

Chapter 5

The Test Vehicle

5.1 Introduction

The display application principle was well illustrated by the use of data recorded from a WSbR FR 3.5 car in the previous chapter. Although from a high level of racing, the data used represented that which would also be collected by the most junior teams and club level users. It was envisaged that an additional method of vehicle placement would be introduced to the application to improve positioning accuracy, which would require a test vehicle in order to be developed.

A kitcar was acquired, with funding from Norwich based Scion Sprays Ltd., which was instrumented and would allow for the controllable collection of data. The various aspects of acquiring, preparing and measuring the car are described in this chapter.

5.2 The Robin Hood 2B Plus

A kitcar was determined as the most feasible option of a test vehicle as many are designed in the vein of race cars, many are raced and they generally provide easy working access to attach instrumentation and so forth due to their tubular space frame design with removable bodywork.

Due to strict budgetary limitations, it was necessary put considerable effort into either secure funding, a reduced price on a kit or a technical partnership with a kitcar company who were prepared to provide the use of a car. Suppliers were canvassed with a promotional brochure which described the author's previous work and the aims of the research described here. Some interest was met, although ultimately an external sponsor had to supply some limited funding. Jeff Allen of Scion Sprays Ltd supplied this funding and covered the cost of an ex-demonstration Robin Hood 2B Plus (RH2BP). This was not an ideal car, being of

a low cost construction, featuring a relatively small number of large gauge tubes in the chassis construction, with minimal triangulation.

Extensive work had to be carried out to rectify a number of problems with the car which could not be determined at the purchase and to fully prepare it for the testing required in this research. This had a significant impact upon the previously anticipated time-scale for testing the vehicle. The work undertaken included addressing some serious safety flaws with the car, including the integrity of the steering column and the position of the fuel tank, which encroached into the cockpit of the car. Other major jobs included the complete rewire of the car's electrical system and replacement of the car's instruments.

The anticipated preparation of the car for testing involved a number of jobs such as the wiring of the data acquisition wiring harness, the design and manufacture of anti-roll bars for suspension adjustment, althought not ultimately used.

5.3 Measurement of the Test Vehicle Suspension Geometry

The kitcar required measuring for the calculation of the kinematics solution, which was to be part of the final display and for creating the 3D model of the car and its suspension components. An encoder based Coordinate Measurement Machine was used to measure key points on the vehicle and these were used as the basis of a car graphic model, created using the CAD package Solid Edge®. Unfortunately, the limitations of the CMM necessitated the additional design and construction of an alignment framework to help ensure that the measurement procedure was as accurate as possible.

5.3.1 The Coordinate Measurement Machine

Measurement of the car's suspension geometry was made using a Coordinate Measurement Machine (CMM) owned by the Wolfson School of Mechanical and Manufacturing Engineering. The system, a FAROArm bronze encoder CMM (see Figure 62) had a 2 sigma single point repeatability of ±0.305mm. The base was fixed and the measurements were made relative to an origin set using the stylus on the end of the jointed arm. At each subsequent measurement, the controlling software would determine the position of the stylus relative to the origin using the encoder readings and each arm joint.

Measurements were made of each suspension joint centre location using a variety of geometry fitting modes in the CMM software such as planes and 3D circles. The collection process was lengthy as a considerable amount of data had to be collected and analysed in order to determine the actual final data collection approach. The positions of a number of joints required their measurement to be made with the use of small jigs and measurement pieces, with a joint measurement being inferred after collection.

Figure 62 - The FAROArm Coordinate Measurement Machine, used to measure the chassis and suspension mounting points of the RH2BP.

5.3.2 Alignment Beam

The reach of the CMM arm was approximately 900mm, allowing for a span of around 1800mm. This was clearly too short to reach the length of the car, so the arm had to be moved around the car, making a series of measurement sets. At each movement, the alignment of the CMM's measurement frame had to be set as well as its origin. The alignment was set by defining a plane with the CMM stylus on a surface followed by two perpendicular lines, which the CMM software projected onto this plane, as two axes. A third mutually perpendicular line, originating at the intersection of these, would then be determined, giving the final axis of the coordinate system. A machined steel block, attached to the chassis

as an anti-roll bar mount, close to the left front suspension wishbones was used as the base origin for measurements.

At each movement, a means of setting the alignment equal to that derived from the anti-roll bar mount was required. An alignment beam was conceived and designed for this purpose (Figure 63). This would provide several points, positioned over a 2m length, which could be used to set the CMM alignment. As Figure 63 illustrates, the orientation of the bar could be set with adjusters at each end, adjusting all three reference points equally, as beam bending calculations had indicated a beam centre deflection of less than 0.3mm. This allowed the arm to be moved around the car, with offsets being determined at each step to transform the measurements to the base reference frame (the anti-roll bar mount alignment).

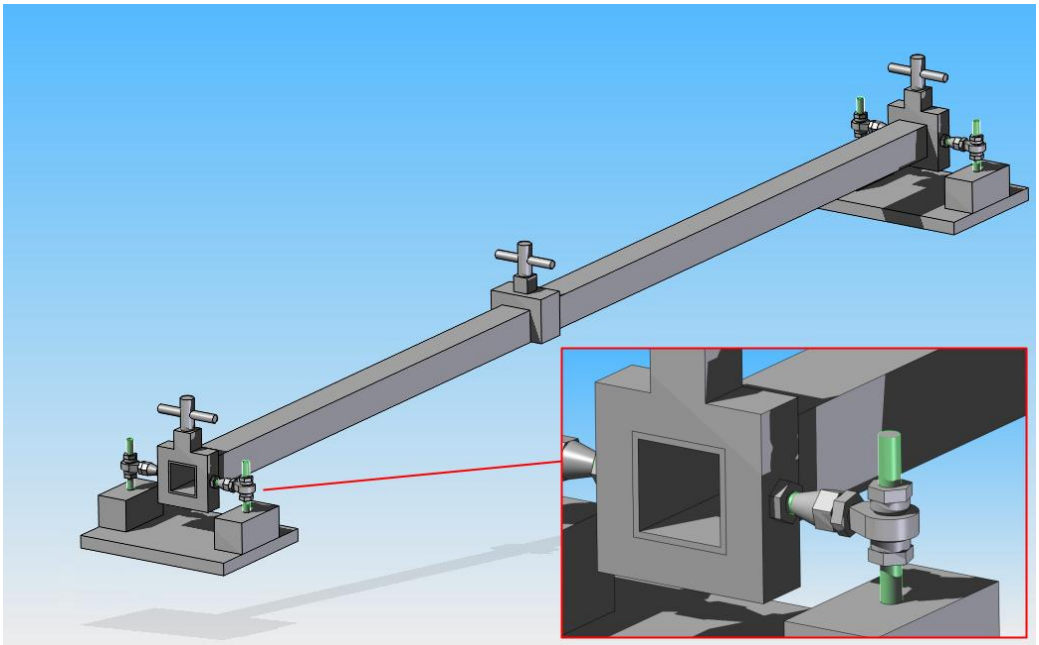

Figure 63 - The alignment beam and close view of one adjuster (insert).

5.3.3 Modelling of Suspension Components

The coordinates measured with the CMM were used in Solid Edge® to provide the basis for 3D models of the moving suspension components. These were

modelled to be visually representative of the parts whilst maintaining the dimensions between joint centres. The coordinates were entered into the 3D modelling environment to form the basis for modelling the various components. Figure 64 shows two swept extrusions used to form the legs of a suspension wishbone, between the measured outboard and inboard joint locations, for example.

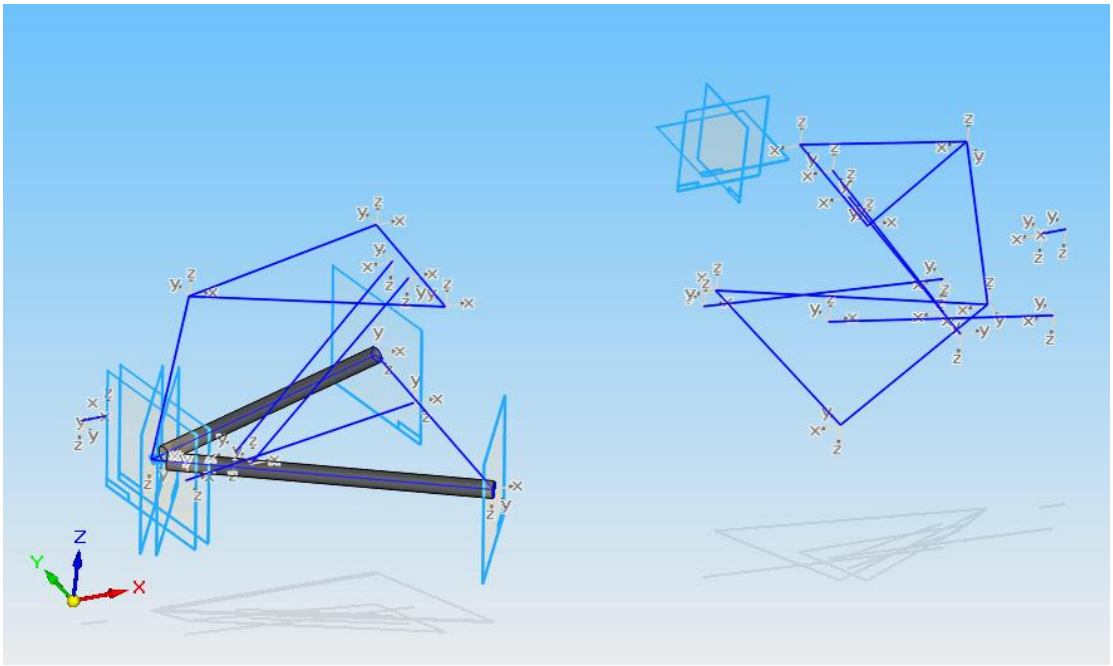

Figure 64 - Suspension geometry data in the Solid Edge® 3D modelling environment, in this example used to form a suspension wishbone.

Figure 65 illustrates the appearance of one corner of the car's suspension, viewed in the Solid Edge® environment and depicting suspension wishbones, damper, spring, track rod/steering arm, upright, wheel and tyre.

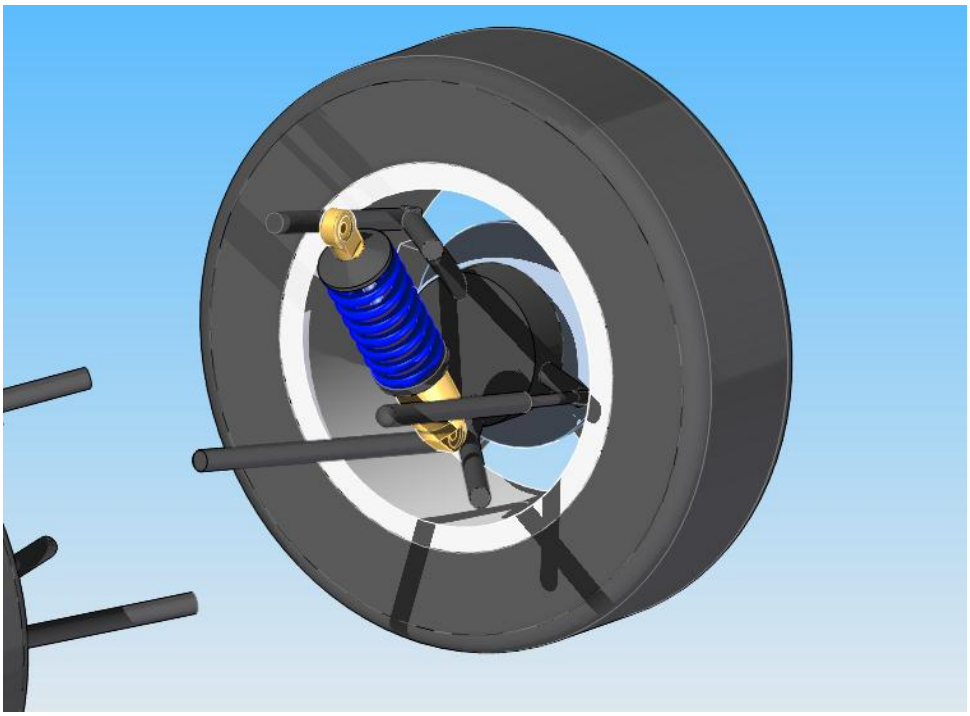

Figure 65 – Front left corner of the RH2BP, modelled in Solid Edge®.

All parts were subsequently converted to the 3D Studio Max 3DS file format, which allowed them to be read into C++ controlled OpenGL graphics routines in the same manner described for the WSbR models in the previous chapter.

5.4 Measuring and Modelling the Test Vehicle Bodywork

A key feature of the display application was to create a realistic impression of the vehicle's appearance. This gave rise to the need for a means by which to measure and model the bodywork. The CMM used for the suspension measurement was initially tested, but this was found to be difficult to position sufficiently to cover all of the bodywork. An alternative approach was found in the use of a Photogrammetry application, which used a series of cross referenced photographs to determine point locations. Its use and the results produced are described in more detail below.

5.4.1 Photogrammetric Measurement

Photogrammetry is a flexible camera based technique which allows for the non-contact measurement of any object or area which can be photographed from multiple angles. A series of images are required and captured using a camera calibrated for its optical properties, before being processed with a software application producing a model of the target object or area. The system first involves determining the camera locations using a method of resection, before a triangulation of the identified image points (Mikhail *et al.*, 2001).

A typical software system such as PhotoModeler 5® used here requires at least two images sharing six common points, which are identified by user mouse clicks within the software and cross-referenced. This allows the PhotoModeler 5® application to identify these points and to triangulate their position by intersecting lines originating at the identified camera locations image plane, ultimately producing a 3D coordinate of each point (Eos Systems, 2004).

The use of the technique for the measurement of the car bodywork involved covering the car with masking tape to which various dots were applied and highlighted with different colours for reference, as seen in Figure 66. The tape was applied in such a way as to provide enough points to define curves in the bodywork surface, but also to optimise the number of points used where possible to accelerate the computation of the point model. Since the bodywork model was to provide only an aesthetic function, only the left side bodywork was measured and subsequently mirrored. Despite these measures, the collection and modelling of data was lengthy as the process was somewhat painstaking.

Figure 66 - Masking tape applied to the RH2BP bodywork. This allowed dot markers to be added to aid referencing of the photographs.

Once the complete set of photographs were collected, they were introduced to the PhotoModeler 5® application and the points on the tape surface cross referenced in the working environment illustrated in Figure 67.

At the completion of the PhotoModeler 5® processing, a set of 3D point coordinate measurements resulted, as illustrated by Figure 68. This point data was used to define a series of 3D lines, which were subsequently imported into Solid Edge® for surface and solid modelling.

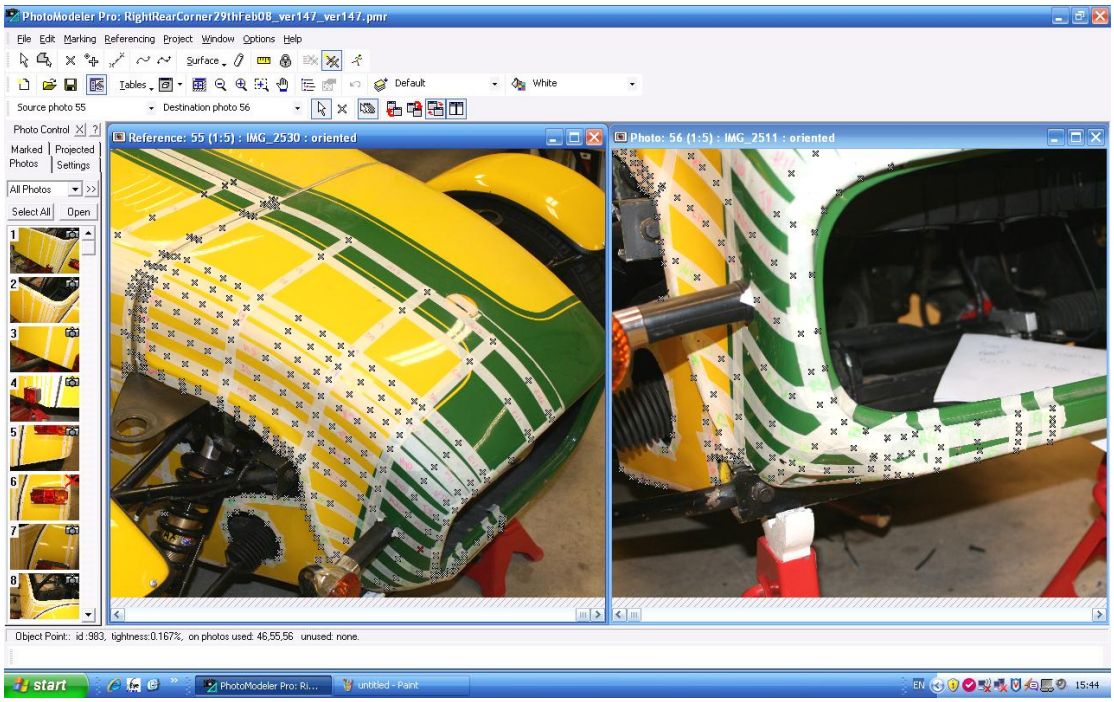

Figure 67 - Cross referencing points between images in PhotoModeler 5®.

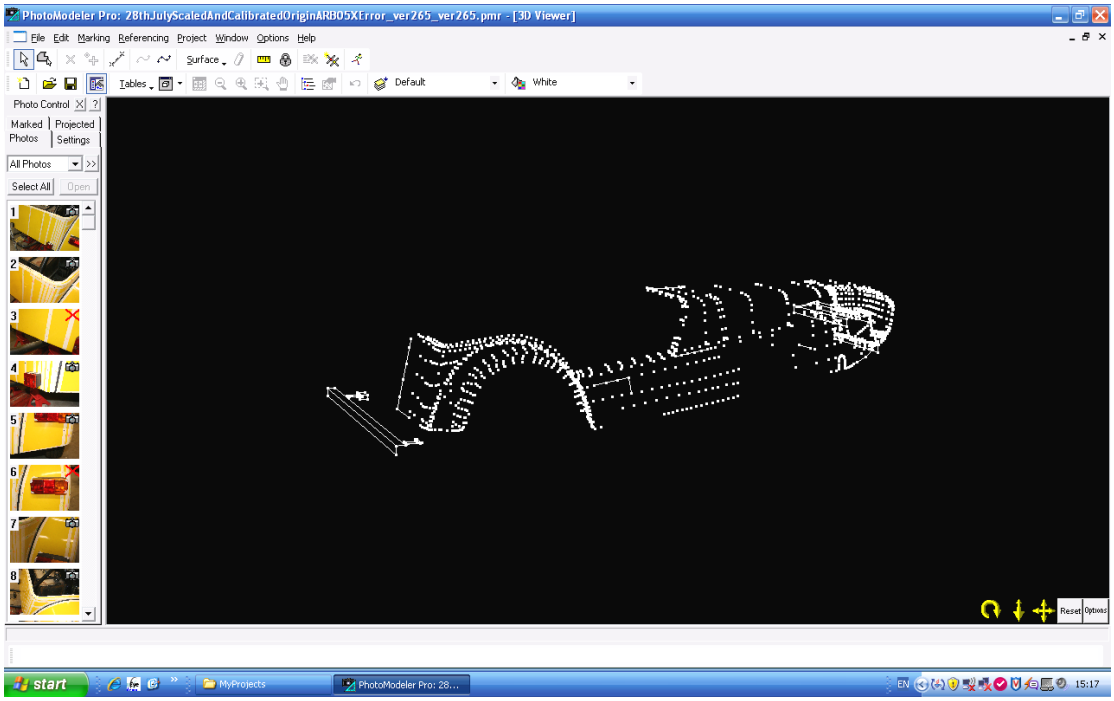

Figure 68 - The resulting point coordinate set after the image analysis in PhotoModeler 5 ®.

5.4.2 Modelling

As described previously, the point data was used to define a series of lines in the PhotoModeler 5® application, which could then be imported into Solid Edge® with the common IGES file format. Areas of more complex curvature, such as the nosecone and the rear wheel arches featured a much higher density of points in order to properly define bodywork in these areas, whereas across areas of less complex curvature the number of points was minimised. This is clear from consideration of the IGES import shown in Solid Edge® in Figure 69.

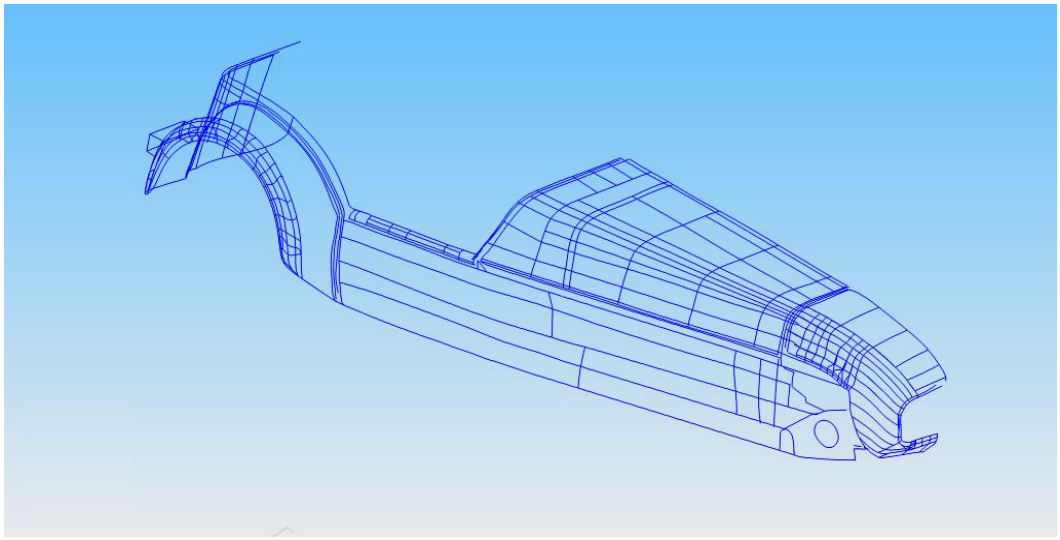

Figure 69 - The control lines defining the car bodywork, imported into Solid Edge®.

Once imported into the Solid Edge® modelling environment, the control lines were used to construct bounded surfaces which were subsequently converted to solid entities and defined key pieces of bodywork. This process is illustrated by Figure 70.

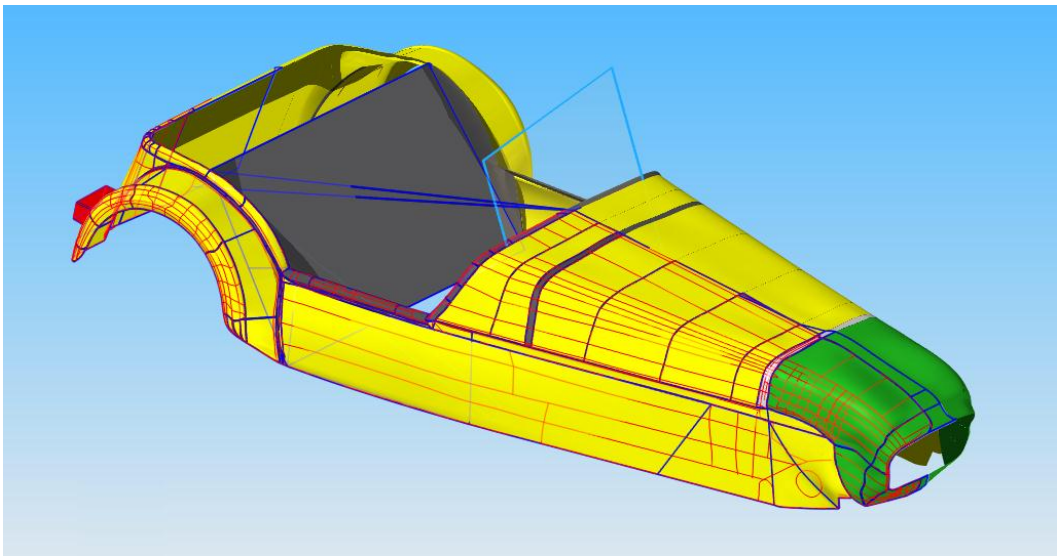

Figure 70 - Construction of bodywork surfaces in Solid Edge® using the point coordinate data computed by PhotoModeler 5®.

As with the WSbR models described in the previous chapter, the models were exported from Solid Edge® as IGES files and converted to 3DS files using 3D Studio Max®.

5.5 Combining Suspension and Bodywork Measurements

The combination of the bodywork surface data compiled using PhotoModeler 5® and the suspension data measured with the CMM required a common origin, which was selected as the front left corner of the front left anti-roll bar bearing housing base (see Figure 71). The inset of Figure 71 shows the plane drawn from the photogrammetric data in Solid Edge®, with the coordinate frame reference planes intersecting at the front left corner.

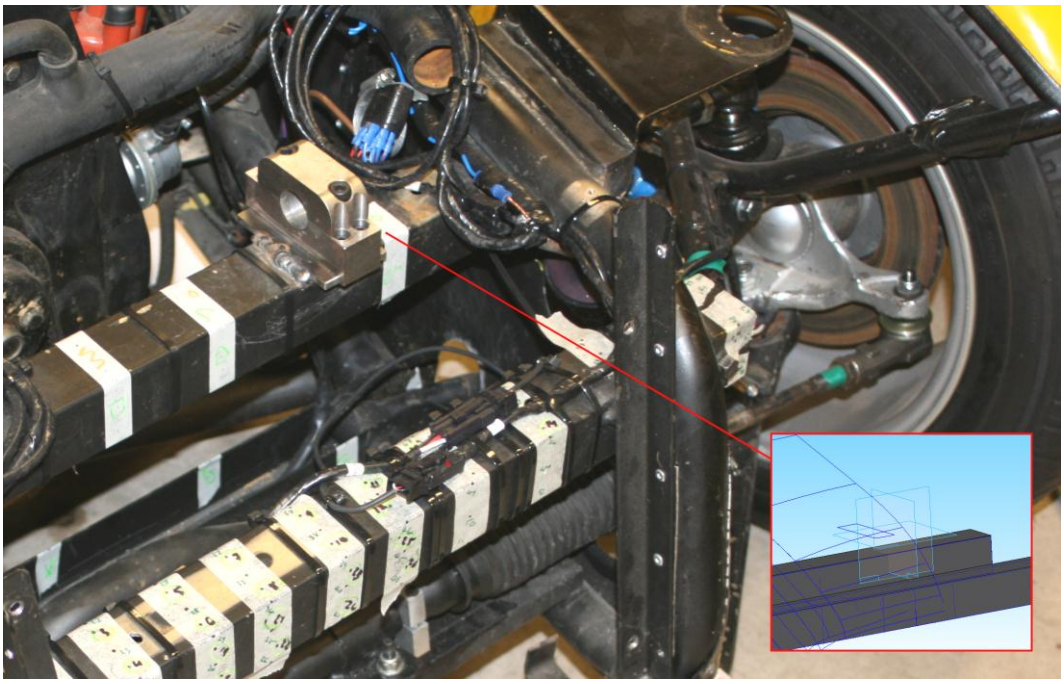

Figure 71 - The Front Left Anti-roll Bar Bearing Housing used to provide a common origin for combination of the CMM and photogrammetric data.

All suspension measurements made using the CMM were relative to this origin. The point data compiled in the PhotoModeler 5® software was automatically assigned an arbitrary origin and scale and so required shifting and scaling, based on a set of measured distances between recorded points. Once the bodywork data was shifted to match the origin of the suspension data, the two could be combined to produce the results shown in Figure 72.

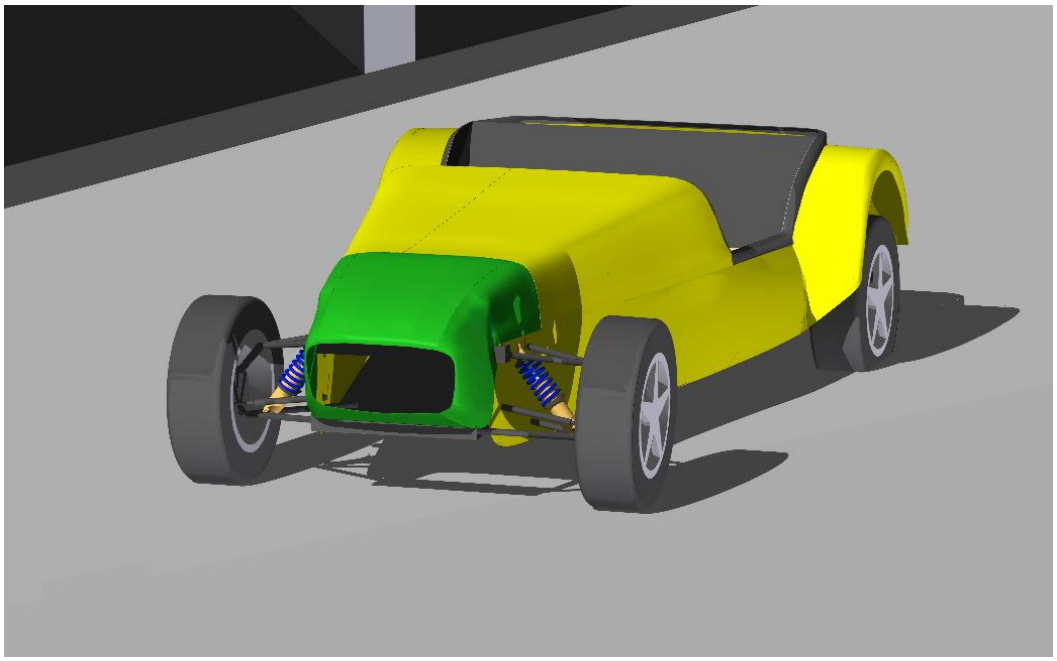

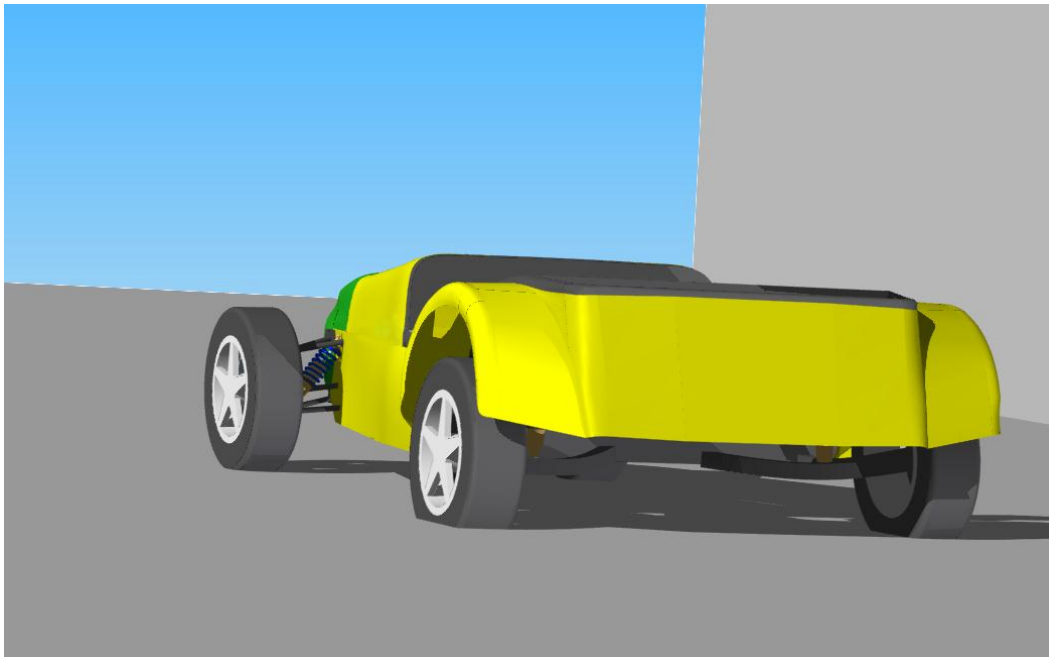

Figure 72 a - Images of the final RH2BP model, with combined bodywork and suspension measurement data.

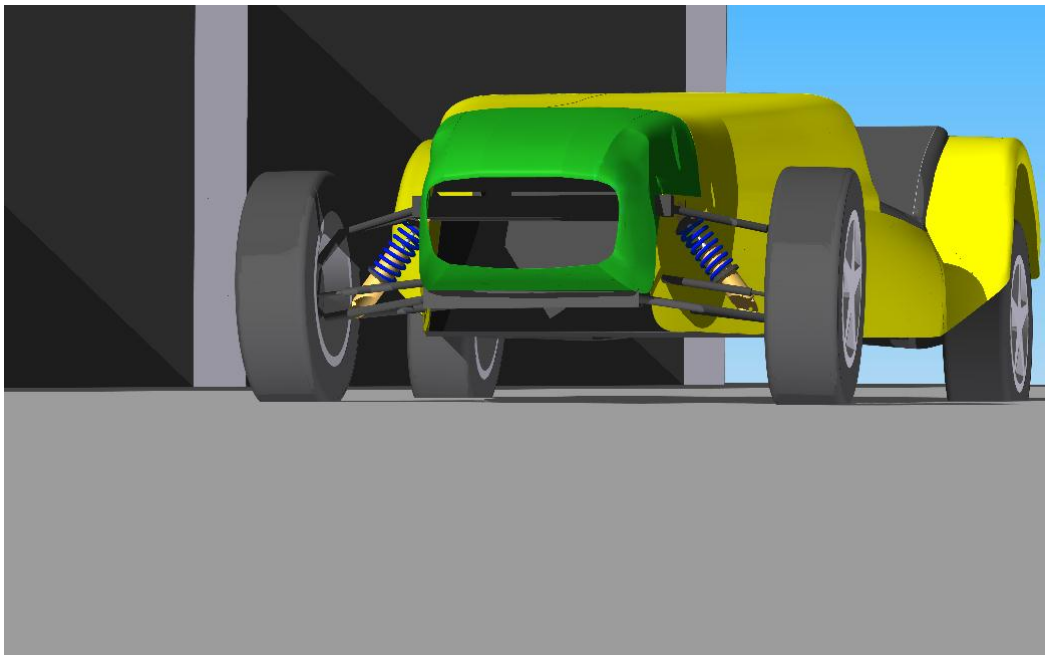

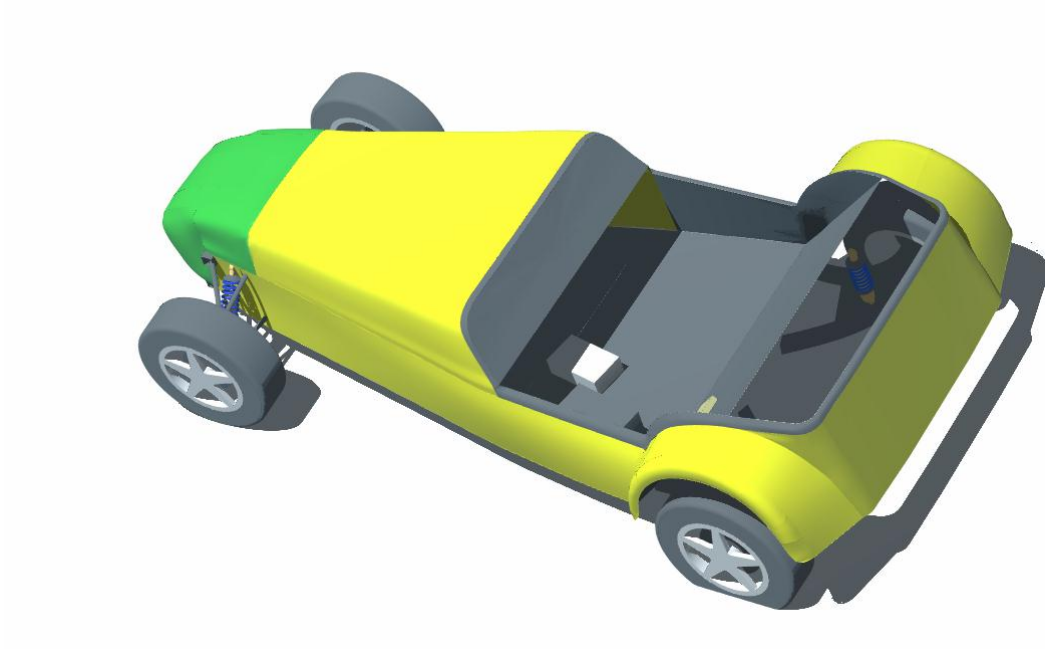

Figure 72 b – Images of the final RH2BP model, with combined bodywork and suspension measurement data.

5.6 Data Collection

Motorsport data acquisition and sensor technology have previously been introduced. This section introduces the reader to the measurands to be recorded from the RH2BP during testing, the data acquisition system fitted to the car and the specific sensors chosen and their installations.

5.6.1 Measurands to be Sampled

The data to be collected during the tests was to closely replicate that collected from a typical single seater racing car. Section 2.2 gave the reader some background on the various sensing approaches used in racing and those which are emerging or used by large manufacturers. The same section also identified which of these were likely to be used at a junior racing level, which gave rise to the following channel list, aiming to replicate the core logging setup of a junior category single seater:

- Suspension displacement,
- Steering movement;
- Road speed;
- Lateral acceleration;
- Throttle position;
- Brake position.

The suspension and steering movements were key to the fundamental purpose of the display tool of illustrating the car's behaviour around a lap whilst the road speed and lateral acceleration would give the data required to compute a point kinematic vehicle trajectory, as described in the previous chapter. Throttle and brake application were recorded to provide other channels required for the accurate analysis and validation of events recorded during testing.

The next chapter introduces the development of an optical sensor used to measure vehicle position, which has been briefly discussed previously. As part of the operation of this sensor, a series of trigger signals marking image captures by the sensor were recorded on the data logger also.

5.6.2 National Instruments USB-6211 Data Logger

Initially a standalone DAS was investigated as the most ideal solution for packaging in the confines of the vehicle. Cost drove the attempt at trying to use a bespoke data logger developed within the Wolfson School. This wrote to a removable Compact Flash (CF) card and data was downloaded by copying the contents of the card to a computer with a VB application. This data logger was developed partly during work with the Loughborough University Formula Student team, but was ultimately abandoned because of reliability issues in favour of an off the shelf (OTS) data logger, the National Instruments USB-6211.

The National Instruments (NI) USB-6211 data logger, shown in Figure 73 was chosen as a suitable data acquisition device for the project, although it carried the disadvantage when compared to the CF data logger of requiring a laptop computer onboard for operation. The key performance parameters of the NI logger are summarised in Table 5.

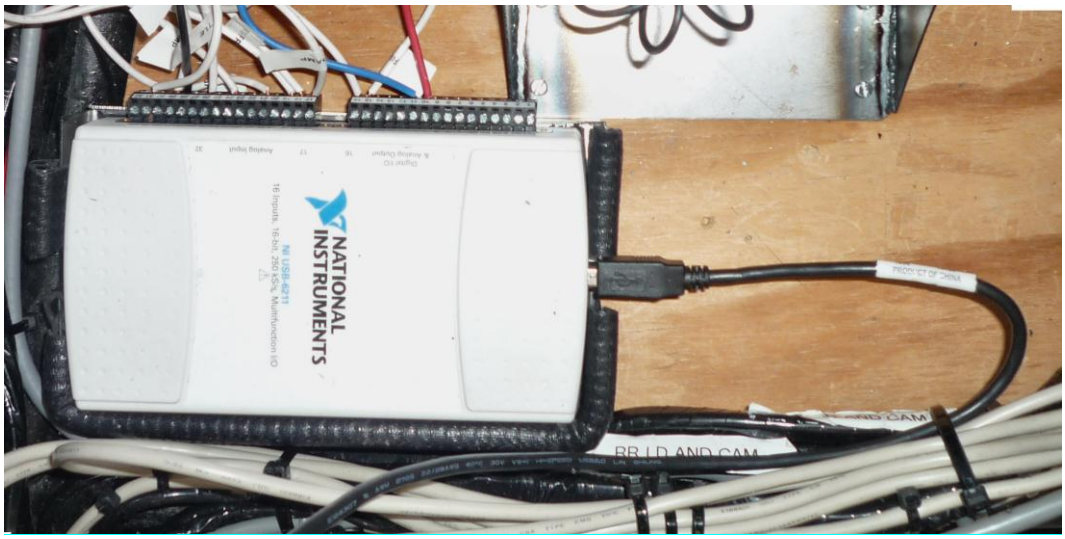

Figure 73 - The National Instruments USB-6211 USB data logger.

Table 5 - The performance parameters of the National Instruments NI USB-6211 USB 2.0 Data Logger (National Instruments, 2009).

Parameter	Value
Number of Analogue Channels	16
Sample Rate	250kS/s
Sample Resolution	16 bits
Accuracy Over Maximum Range (-10 to 10V)	2.69mV
Sensitivity Over Maximum Range (-10 to 10V)	91.6µV
On-Board Memory	4095 samples
Timer/Counter Resolution	32 bits

It is a USB data logger which contains an Analogue to Digital Convertor (ADC) but uses a computer's memory for storage. The data logger could be used with National Instruments' LabVIEW programming language but also functioned with a basic data logging application supplied. This restricted the sampling to analogue signals, but it was envisaged that the there would be sufficient sampling bandwidth with the specified figure of 250kS/s (see Table 5) to capture measurands as analogue signals which in nature were potentially better captured

on a digital channel. The two examples being the passing of wheel speed triggers described in 5.6.4 and the optical sensor trigger signals.

Post processing of these analogue captures of digital phenomena (described in section 5.8) was found to need a well defined rising signal edge. Trial and error duly found 2kHz to achieve this, a figure that was partly prescribed by the limitations of the data logger and the available increments of logging rate. This sample rate had to be assigned to all channels but still kept the total logging requirement within the system's capability and exceeded the recognised limit of twice the Nyquist frequency of any sampled channel; this being quoted as a likely maximum of 200Hz, for a race car's suspension (Segers, 2008).

The exact architecture of the DAS is unknown, but due to its cost and because of some results, obtained during testing, of empty channels recording previous channel's signal output, it can be assumed to have a shared ADC. Therefore the channels have to be multiplexed for sequential sampling. It is not known how the logging software was designed to account for this phenomenon, whether it has a time based interpolation from a previous recorded value or whether it assumed the sampled values are all recorded together. For the purposes of the software illustration proposed here and with account of the budgetary limitations, it was considered acceptable to proceed with this potential small inaccuracy.

5.6.3 Data Acquisition System Wiring Loom

The data acquisition wiring loom was originally designed for use with the CF data logger described previously, but was easily adapted to the USB data logger. The loom, which is illustrated by a schematic diagram in Figure 74, was constructed in two main braches; a front and a rear loom branch. These were routed together at a terminal block rail section used for making sensor grounds and power supplies common.

Each sensor channel consisted of three separate runs of single core 1mm^2 5A cable, colour coded as Table 6.

Table 6 – Wiring loom colour scheme

Insulation Colour	Function
Red	Sensor power supply (5V)
White	Sensor signal (0 – 5V)
Black	Sensor ground

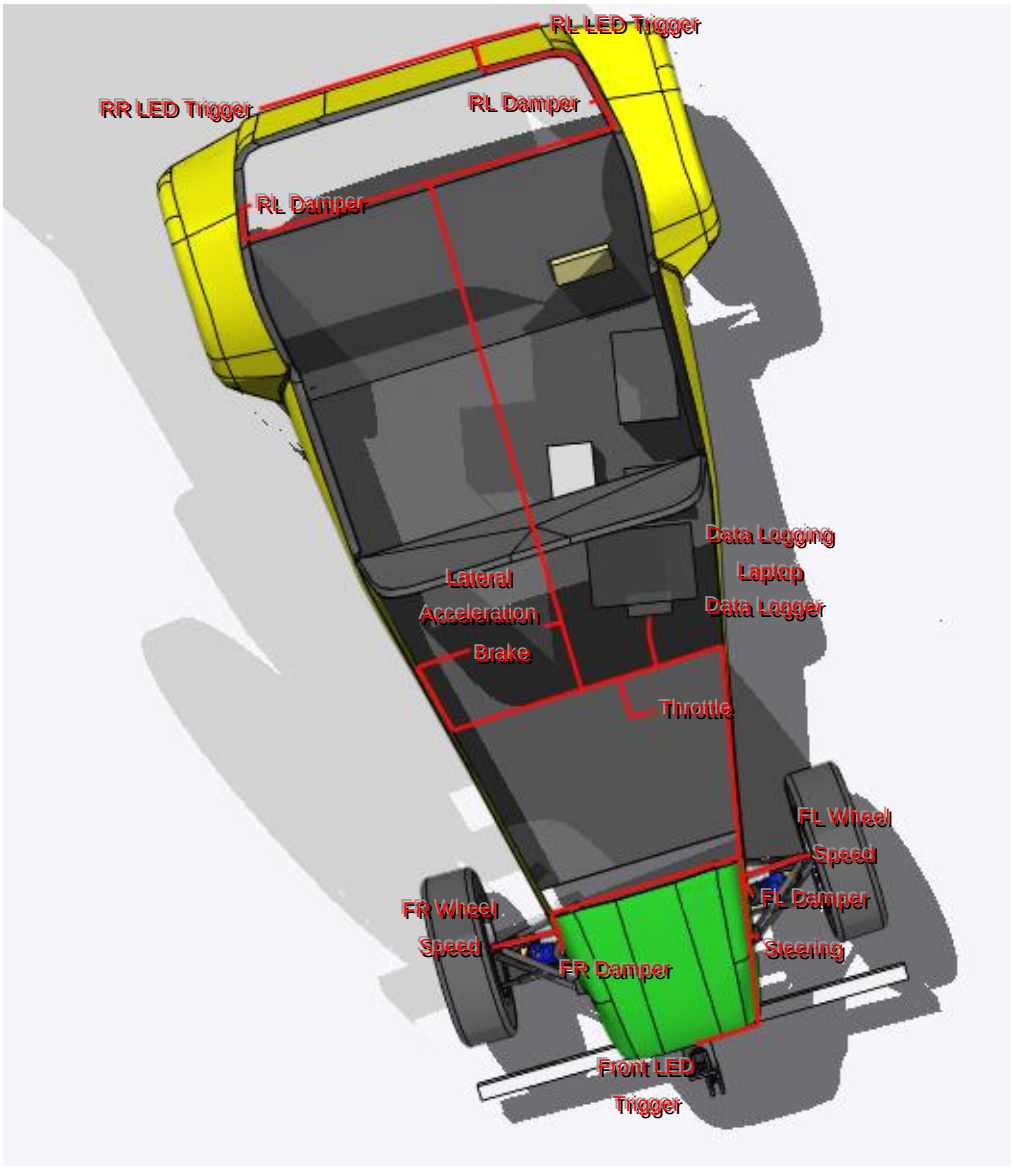

Figure 74 - Schematic illustration of the layout of the DAS wiring loom.

A pin and socket type connector featuring a clip was sourced from RS components, with the socket used to terminate the loom channels to reduce the risk of shorting, as they featured a 5V power supply, whilst the sensors were terminated by the plugs. The plugs were only connectable one way so would reduce the likelihood of subsequent misconnection and also help to ensure good contact from their clip system. The loom channels themselves were wrapped with insulating tape and bundled and wrapped together where possible, to reduce the likelihood of chaffing and wearing through of the cable insulation itself. A complete data channel, with plug and socket termination is illustrated in Figure 75.

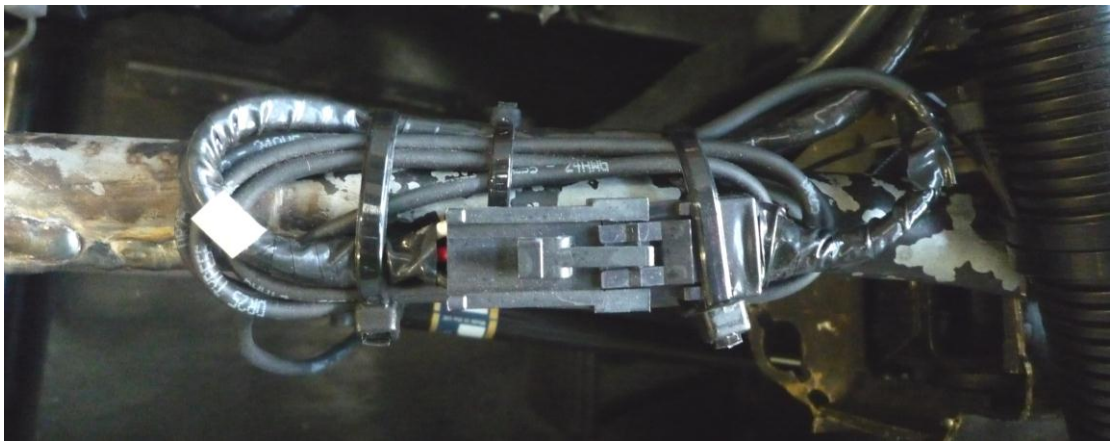

Figure 75 - A complete data channel of the wiring loom with plug on sensor end and socket on loom end.

The two main ‘branches’ of the data logger connected around the passenger foot well, where the data logger was mounted (Figure 76). Also located here and shown in Figure 76 along with the data logger itself was a run of terminal blocks in a rail. Each terminal block provided four male spade terminals, all connected together electrically. By connecting a series of blocks, a large number of spade terminals could be made common. In Figure 76 it can be seen that there are two distinct sections, with the sensor black ground cables connected on the left, to which the data logger ground is also connected and the sensor red power lines connected in the same fashion to the data logger 5V dc supply on the right. As viewed, the block’s terminals are common from top to bottom of the picture and the wire jumps to interconnect them are from left to right. The white sensor signal

connections can be seen connected to the screw terminal block of the USB-6211 data logger and the wiring loom is clear in the right of the photograph.

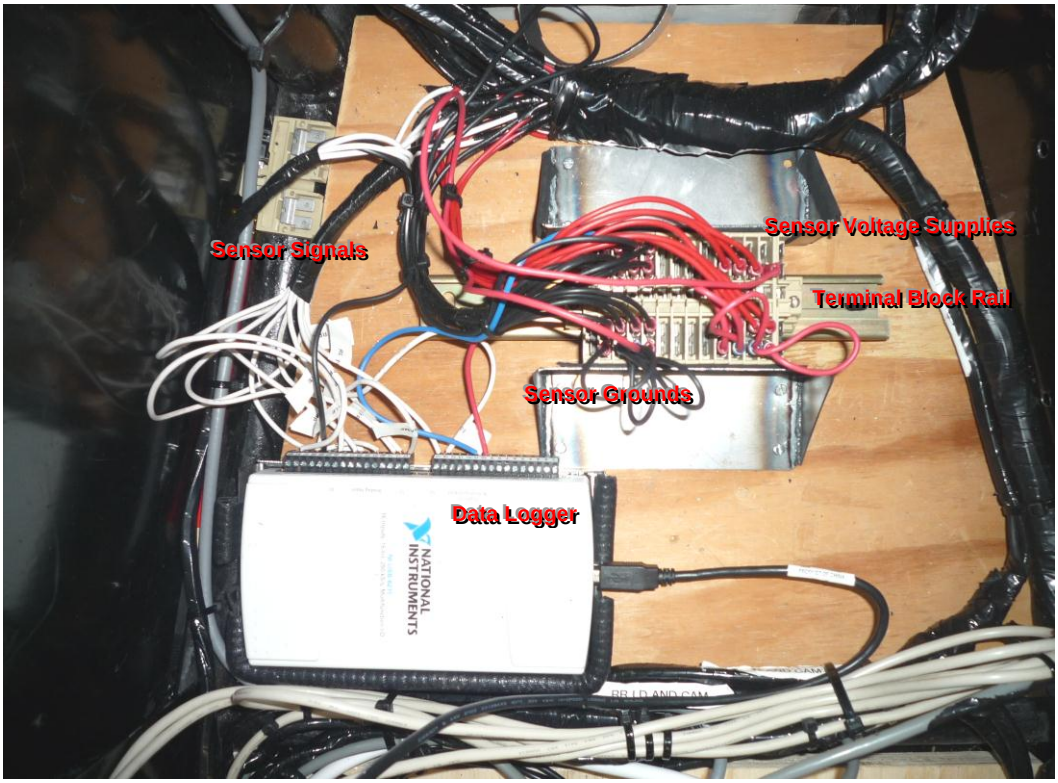

Figure 76 - The passenger foot well of the test vehicle containing the USB-2611 data logger, the jumper bar section for making sensor voltage supplies and grounds common.

Initial tests of the wiring loom using the CF data logger highlighted issues with one particular section of the loom running alongside the engine bay. Figure 77 illustrates the extent to which this section suffered from electrical interference from the proximity of the ignition coil and distributor which rapidly switches a high voltage and therefore creates electrical noise. The figure also shows the success of the foil screening employed to this section of loom, grounded to the chassis at both ends (Figure 78).

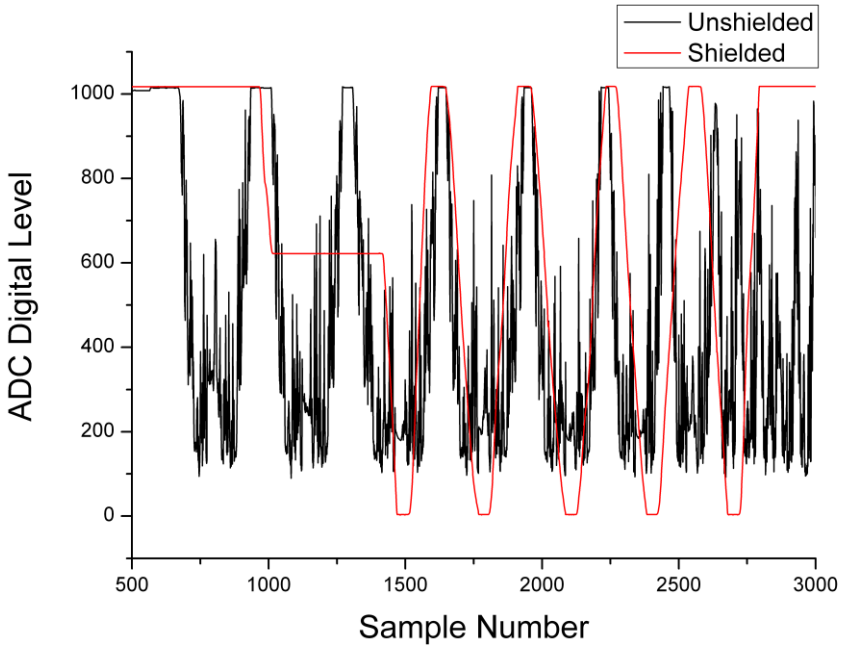

Figure 77 – Comparison of channel routed alongside engine bay before and after screening.

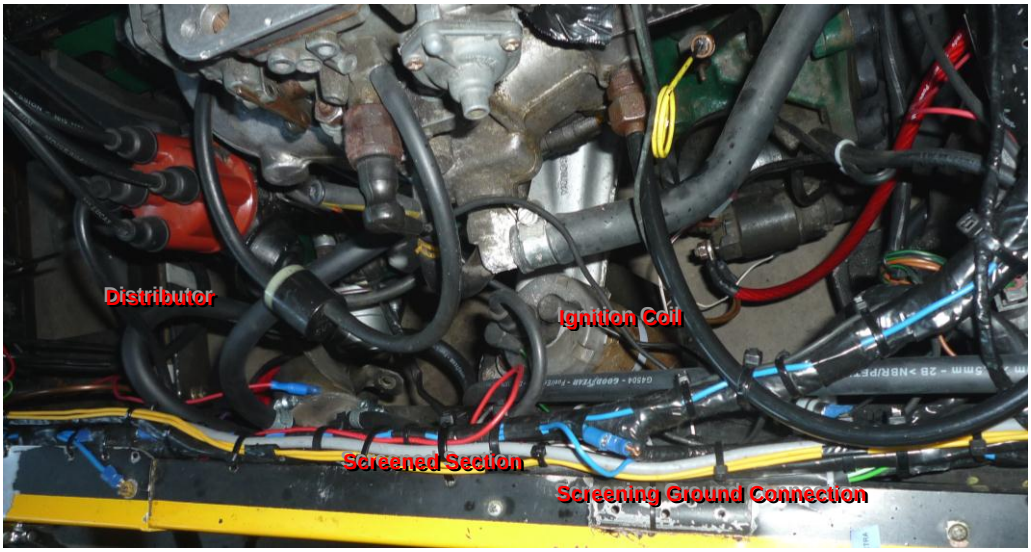

Figure 78 - The section of wiring loom screened from electrical noise.

5.6.4 Wheel Speed

The typical approach to wheel speed measurement from a race car was adopted; a magnetic proximity pickup to count the passing of a ferrous trigger attached to the wheel. This would give direct comparison between speed data obtained by this established method with that collected from the optical displacement sensors which are described fully in the next chapter. Typically it involves a round plate with a number of fingers attached to the back of the stub axle. As this rotates, the fingers move close to the pickup which is attached to the upright that carries the stub axle running inside a set of wheel bearings. Every passing of a trigger can then be recorded and used to determine the distance covered by the wheel and its speed by knowledge of the tyre circumference and the number of trigger fingers in a total rotation.

Initially an inductive magnetic proximity pickup was trialled. This required no power but relied on the voltage induced by the interaction of the magnetic field surrounding its coil wound magnetic core with the passing ferrous trigger. The operational principle is well described by Figure 79.

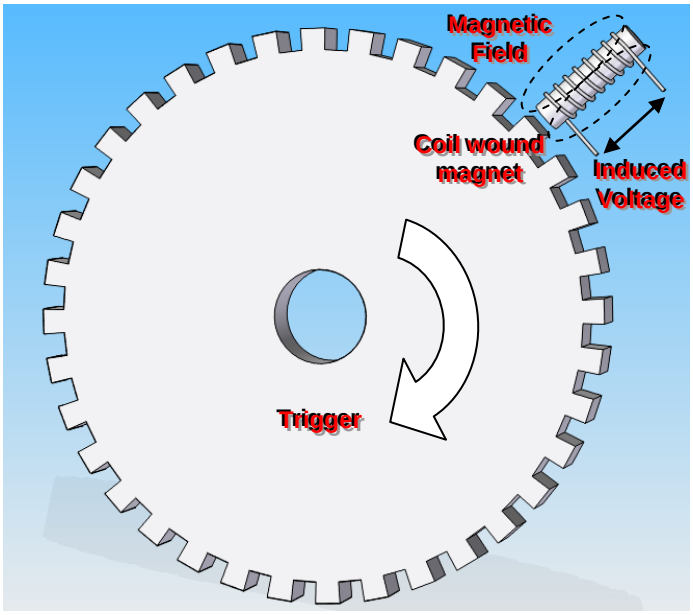

Figure 79 – Principle of the inductive magnetic proximity pickup, adapted from Ramsay (1996).

This was arranged to sense the passing of the rear of the wheel studs which stood proud of the back face of the stub axle and was mounted using a small aluminium bracket to the cast upright. The four wheel studs gave eight voltage pulses for every revolution of the wheel; one each side of the four passing wheel studs.

The key issue with an inductive pickup was that the signal is proportional to the rate at which the ferrous trigger passes; hence the voltage level associated with a trigger passing is not constant, complicating post processing. Further to this the early tests indicated the voltage levels attained were not distinguishable at very low speed.

A Hall Effect switch was instead used to pass a constant voltage level to the data logger upon sensing of a ferrous trigger. The Hall Effect is a phenomenon whereby the interaction of a magnetic field though a conductor with a flow of current causes a voltage to be produced perpendicular to both the magnetic field and the direction of current. This is caused by a deflection of the charge carriers by Fleming's left hand motor rule and can be better understood by Ramsay's (1996) diagram in Figure 80.

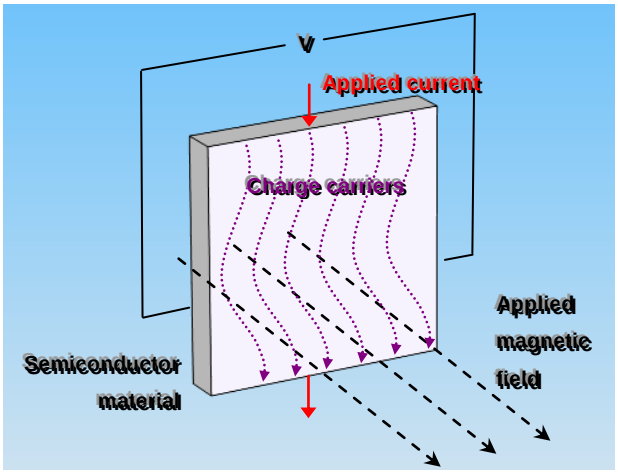

Figure 80 - The Hall Effect, creating voltage V, adapted from Ramsay (1996).

The switch mounting was identical to that described for the inductive pickup and can be better understood by Figure 81. Although conventionally used to produce

a digital signal, the limitations of the data logger meant it was necessary to configure as a switch to a voltage supply, recorded on an analogue input. The sensor was configured electrically as depicted by the schematic illustration in Figure 82.

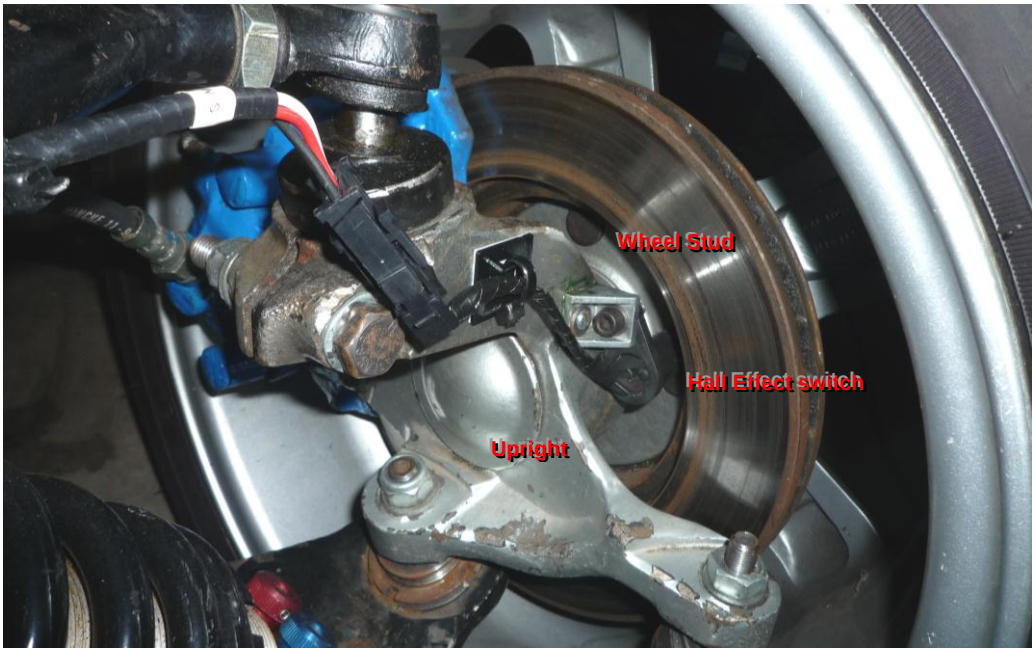

Figure 81 - The installation of the Hall Effect front wheel speed sensors.

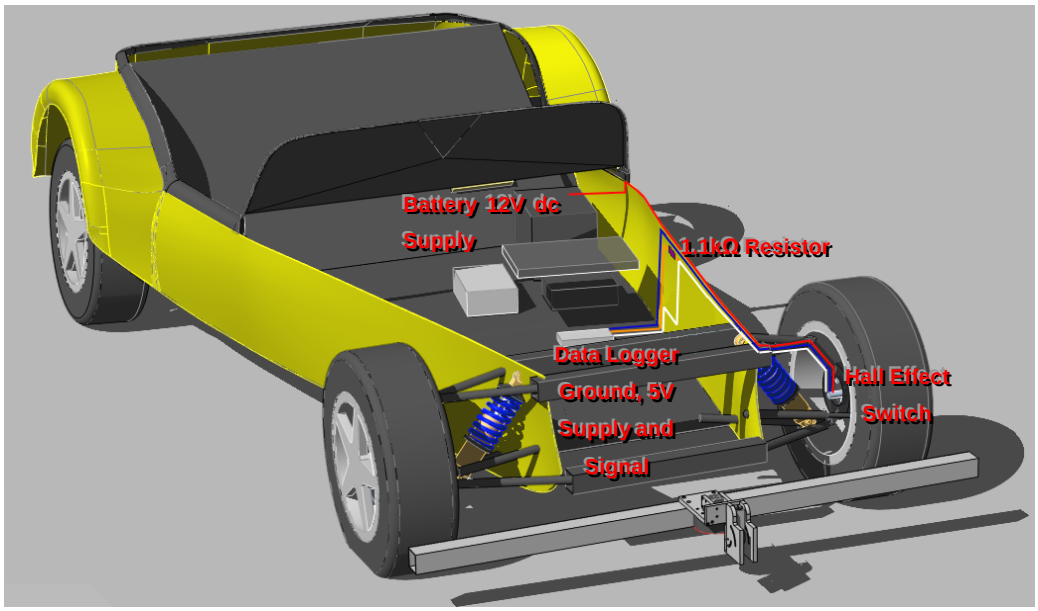

Figure 82 – The electrical arrangement of the Hall Effect switch for wheel speed measurement.

The wheel speed switch was powered by a 12V supply from the auxiliary battery, providing the flow of charge required as part of the Hall Effect phenomenon. It had a common ground with the all other sensors via the data logger whilst the signal channel was also connected to the 5V data logger supply, through a 1.1kΩ resistor. When the switch was closed, the data logger supply flowed directly through the resistor back to the logger and 5V was logged. When the switch sensed a wheel stud passing and opened, the 5V supply flowed straight to earth and 0V was logged. The characteristic trace produced is depicted in the data excerpt shown in Figure 83.

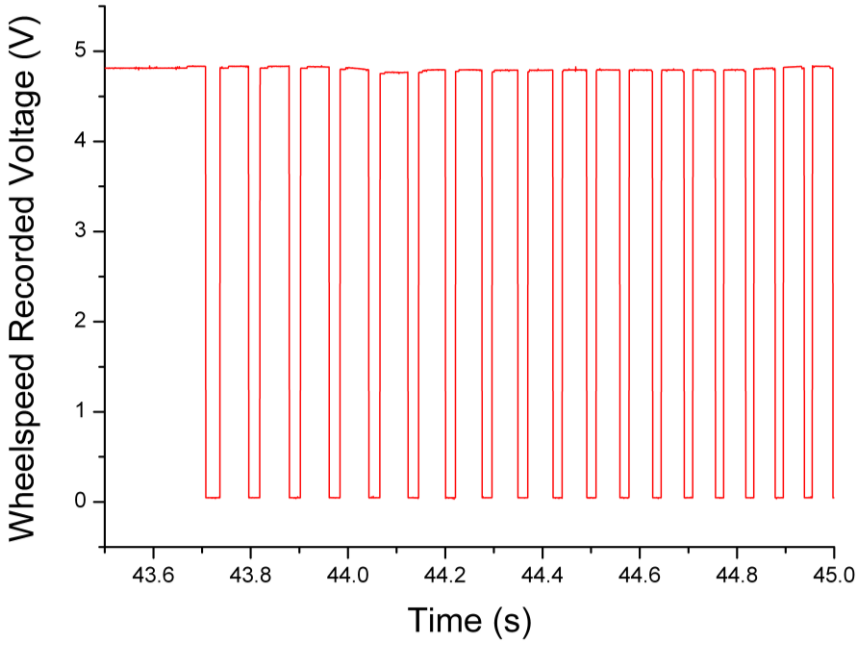

Figure 83 - Data excerpt depicting the wheel speed signal produced by the Hall Effect switch.

Wheel speed sensors were fitted to each of the two front wheels, as is common practice to mitigate for the effect of a wheel locking under braking. The signals produced were post processed as part of the data calibration software discussed in section 5.7.

5.6.5 Suspension Movement/Damper Displacement

Damper displacement was measured using linear potentiometers, previously introduced in section 2.2.2 as a common and cost effective method of measuring displacement on a race car. They are used in GP2, WSbR and other all other categories below in favour of more expensive non-contact Linear Variable Differential Transformers (LVDT). The sensors were mounted such that their axis of measurement was parallel to the axis of the spring and damper units, as depicted in Figure 84.

Figure 84 - Linear potentiometers mounted to the coil over damper units for measuring damper displacement/suspension deflection.

The diagram in Figure 85 adapted from Segers (2008) illustrates the principle of operation of a potentiometer. The sensor works as a potential divider, with a slider or wiper connected by a shaft to the system being measured. The body of the sensor is attached to some fixed reference and contains a track way along which the wiper sweeps when the system moves. The track is grounded at one end and supplied with a voltage (typically 5 V) at the other.

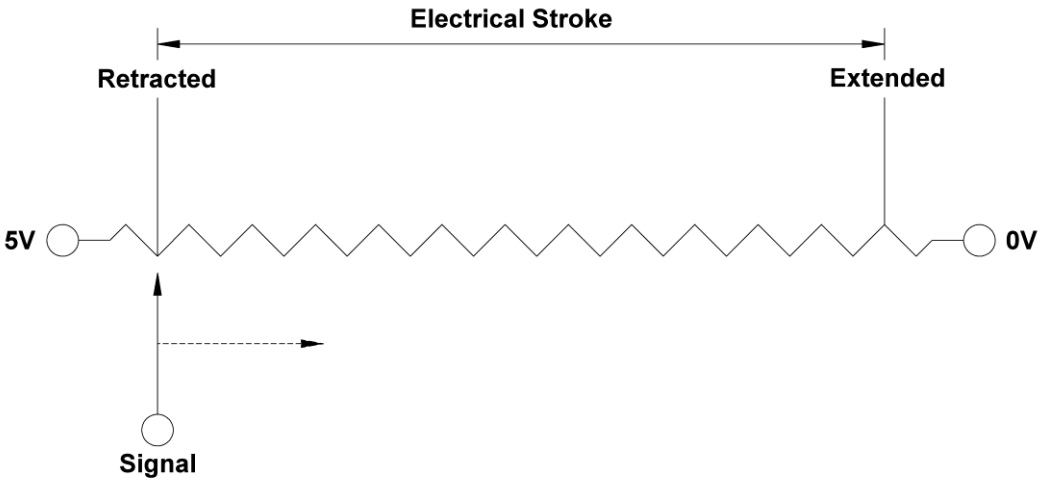

Figure 85 – The operational principle of a potentiometer (adapted from Segers, 2008)

The wiper, which is electrically connected to the data logger and the same earth then picks off a fraction of the potential difference of the track way as a signal, in proportion to its position since the track resistance is directly proportional to its length (Equation 21 and Equation 22).

$$V = V_S\left(\frac{R_W}{R_T}\right) \qquad \text{Equation 21}$$

Where V is the voltage picked off (V), V_S is the voltage supplied to the potentiometer (V), R_W is the resistance between the wiper position and ground/0V (Ω), R_T is the total resistance of the track way (Ω).

Since resistance is linearly proportional to the length of the conductor,

$$V = V_S\left(\frac{L_W}{L_T}\right) \qquad \text{Equation 22}$$

Where L_W the physical length between the ground connection and the wiper position (mm) and L_T is the physical length between the ground and voltage supply connections (mm).

Since the resistance variation is linear, the sensor output could simply be calibrated with a linear length to voltage relationship as discussed in section 5.7

The particular sensor employed for damper displacement measurement was an Active Sensors CLS1322-75, with a 75mm stroke and a quoted non-linearity of ±0.15% (Active Sensors, 2008).

5.6.6 Steering Angle

Steering angle was measured using a linear potentiometer mounted to the steering rack, shown in Figure 86. The potentiometer used was of the same series as the damper and brake potentiometers but of a longer stroke (CLS1322-150, with 150mm instead of 75mm stroke). This was necessary for the range of motion of the steering rack but resulted in a lower measurement resolution as the each ADC measurement level equated to a greater increment of physical distance.

Figure 86 - The linear potentiometer mounted to the steering rack for measurement of steering angle.

The calibration of the steering sensor was slightly more complicated than that of the damper potentiometers as it was to give a 3D coordinate of the steering rack joint locations as described in section 5.7.

5.6.7 Throttle Position

The throttle position was measured using a Vishay Spectrol 971 rotary potentiometer sourced from RS Components, which was attached to the shaft of the throttle itself as shown in Figure 87. The rotary potentiometer worked in the same way as the linear version, except that the track way and the wiper motion were circular. The sensor output here was simply calibrated to provide a percentage measure of full throttle. This was included as being one of the driver controls and so is intrinsically linked with the car's behaviour. It is an important measurement for a team to help associate the driver and car behaviour and their effect on each other, but was not as critical as the damper data for this research, so the quoted non-linearity of ±2% was accepted (Vishay Spectrol, 2002).

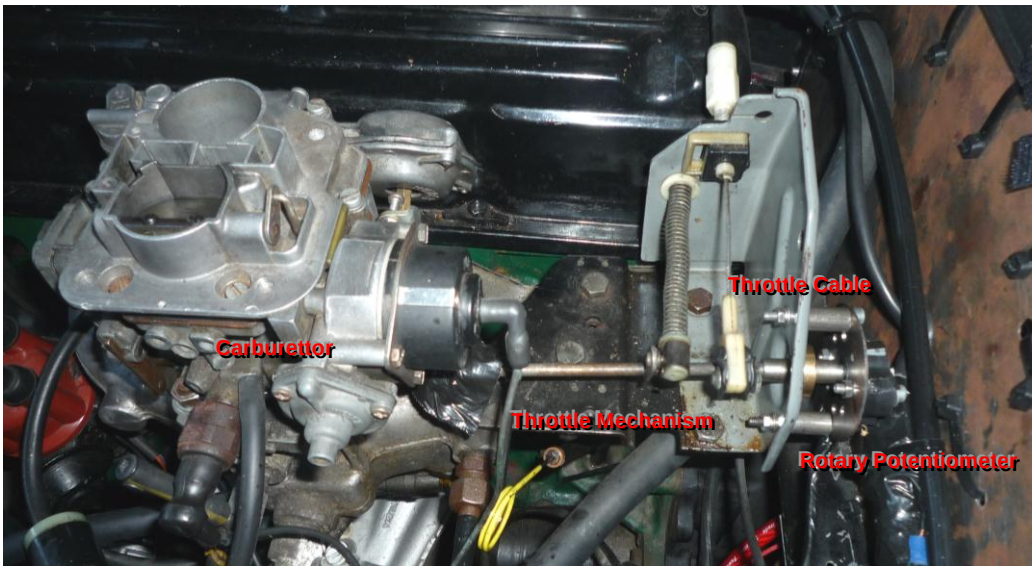

Figure 87 - The rotary potentiometer attached to the throttle mechanism for measuring throttle angle.

5.6.8 Lateral Acceleration

Lateral acceleration is a universally measured performance parameter in motor racing. It can firstly be used as part of an analysis of a vehicle and driver's performance, as a direct measure of the utilisation of the tyre's cornering performance. Secondly, it is an integral aspect of inertial trajectory approximation algorithms described in the previous chapter.

An acceleration transducer, featuring an Analog Devices ADXL330 three axis accelerometer was purchased, which provided three voltage signal outputs, one per axis. An AA battery holder with integral dc to dc converter was also sourced to provide the accelerometer with a 3.3V supply. The accelerometer had a non-linearity of ±0.3%, a sensitivity of 300mV/g and a maximum bandwidth of 1600Hz (Analog Devices, 2006)

For mounting it was housed in a small box which was filled with resin and mounted to the car with small aluminium brackets, with the longitudinal and lateral axes aligned with those of the car.

Ideally the accelerometer would be mounted at the car's centre of gravity where the combined forces on the car can be assumed to act (Fey, 1993). However, packaging constraints meant it had to be placed 200mm fore of the longitudinal position indicated from a corner weight measurement.

Figure 88 - The Analog Devices ADXL330 Accelerometer

5.6.9 Brake Application

Brake application is typically measured as a change in the brake line pressure in race car applications (often divided as the front and rear brake circuits) and allows a significant amount of insight into the driver's use of the brakes to be gleaned (McBeath, 2008). However, for this work; the proof of the data visualisation and optical displacement sensor technologies, it was sensible to minimise cost and use a potentiometer to simply indicate when the brake pedal is depressed for helping to understand the other data collected. The test vehicle was therefore fitted with a linear potentiometer mounted between the brake pedal and a plate welded to the pedal box brace (see Figure 89). This was a CL1322-75 type potentiometer, as used for the damper displacement measurement.

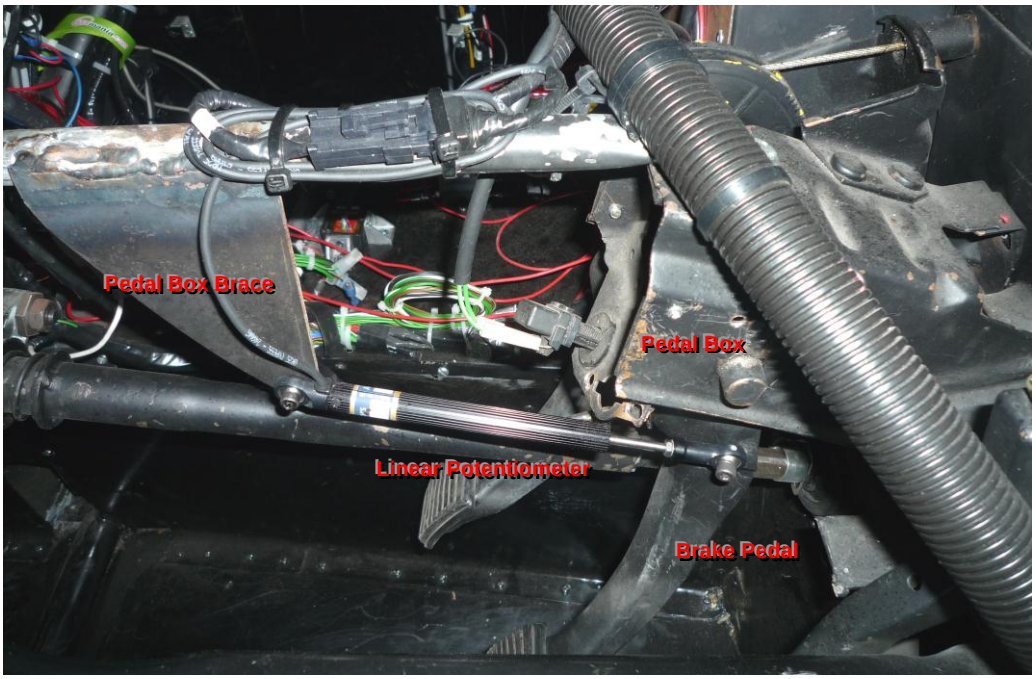

Figure 89 - The linear potentiometer connected to the brake pedal of the test car.

5.6.10 Optical Displacement Sensor LED Triggers

A final set of measured channels were the trigger signals used as part of the optical displacement sensors, which are discussed in more detail in Chapter 6.

These were 5V signals used by each optical sensor to trigger their lighting and also used as a very close approximation to the start of the image capture process of a frame.

5.7 Sensor Calibration

The USB-6211 data logger recorded raw voltages, which were subsequently calibrated in a post processing application to yield meaningful physical values. In most cases this was a length measurement of a linear potentiometer which provided initial conditions for the kinematic solution of the suspension joint positions required for the vehicle animation previously mentioned and more fully described in Chapter 7. In the case of the brake and throttle application, the measurement was converted to a percentage of full application, whilst the accelerometer data was converted to provide the vehicle lateral accelerations in $m.s^{-2}$.

This section describes the procedures applied to determine these calibrations.

5.7.1 Dampers

The damper potentiometers had a low non-linearity and so a linear calibration was applied, converting their measured voltage to their total length for input to the suspension kinematic model which has been described previously and is discussed fully in Chapter 7.

Calibration data was collected as a series of physical measurements of the potentiometer and measured signal voltages viewed through the NI software supplied with the data logger. The collected points produced strong linear relationships in all cases (Figure 90), the equations of which were used to calibrate the measured voltages (see section 5.8).

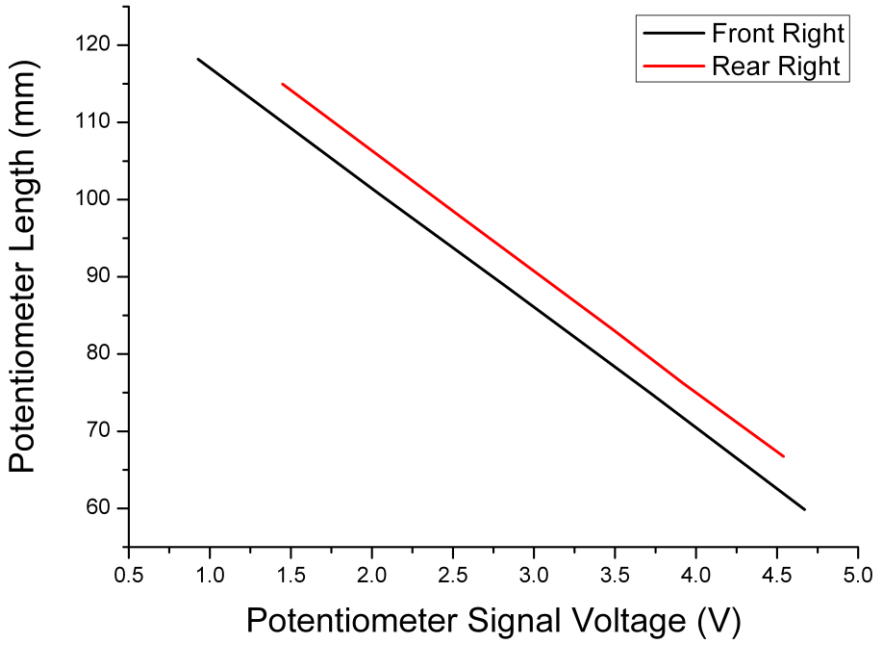

Figure 90 – Comparison of calibration curves for front and rear damper potentiometers.

5.7.2 Steering

The calibration of the steering rack potentiometer differed from that of the damper potentiometers in that the voltage measurements recorded were ultimately set against a 3D location of the steering rack inboard joints. This was achieved by initially measuring the potentiometer length and signal voltages across a sweep of movement. The vehicle model described earlier in this chapter was then used in Solid Edge® to construct the movement of the joints with the sensor reading. This resulted in three calibration curves for each of the left and right hand inboard trackrod joints (Figure 91).

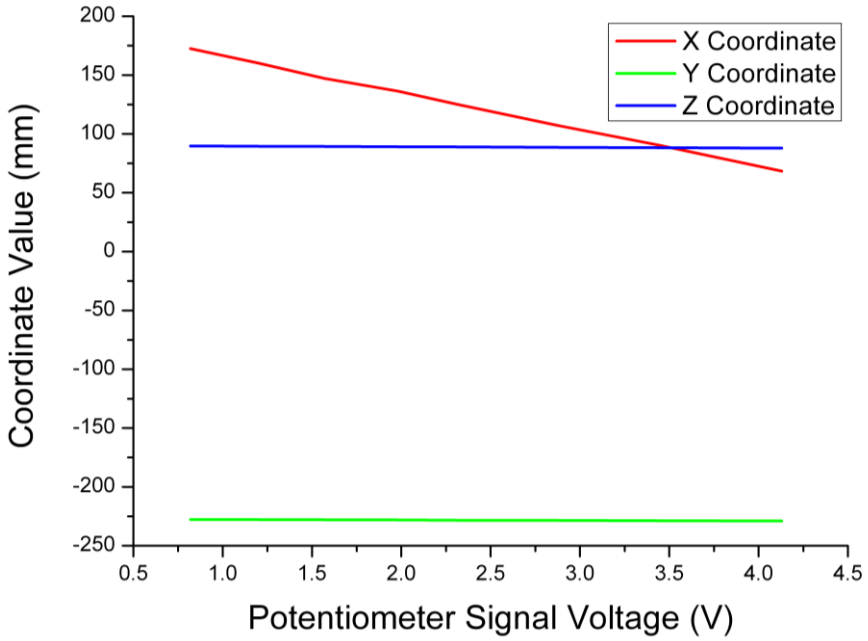

Figure 91 – The calibration of the front left trackrod inboard joint for steering potentiometer displacement.

5.7.3 Throttle and Brake

With the exact definition of both throttle and brake levels being difficult to make, both sensors were calibrated against a percentage of their application. This however did make the calibration less accurate than that of the dampers as only two points at 0 and 100% application could be set.

5.7.4 Lateral Acceleration

The accelerometer was calibrated by positioning on a flat surface so that the lateral acceleration axis was normal to the surface and therefore subjected to an acceleration of 9.81m.s^{-2}, for which the voltage output was recorded. By flipping the sensor so that this axis was still normal but facing the opposite way, the voltage associated with the same acceleration in the other direction could be determined. A zero point was found, with the accelerometer positioned such that the lateral axis was parallel to the surface.

5.7.5 Wheel speed

The tyre rolling circumference was required for the calibration of the pulses collected from the wheel speed sensor. This was measured by both tape measure and inferred from a diameter measurement by height gauge on a surface table, as 1.826m.

5.8 Sensor Output Post Processing

A VC++ application performed the sensor signal voltage post processing. This read a CSV file created by the NI data logger software and stored the extracted data into arrays for processing. There were three distinct processing routines required for the data collected by the DAS. Two are described here for the data from the standard OTS sensors, whilst a third for the optical sensor trigger signals is described in the next chapter.

5.8.1 Dampers, Steering, Throttle, Brake and Acceleration

The post processing of much of the data, collected by potentiometers and the accelerometer, involved the simple application of a calibration relationship to sensor signal values. In all cases these were linear relationships which had been defined by collecting potentiometer signal readings and physical measurements.

5.8.2 Wheel speed

The post processing of the wheel speed data was more complex than that of the potentiometer and accelerometer data. The nature of the data collected from the wheel speed sensors was presented in Figure 83. Each drop in the trigger signal level represented the passing of a wheel stud, of which there were four.

The post processing application first thresholded this data at a voltage level of 4V, giving a digital on/off signal illustrated in Figure 92.

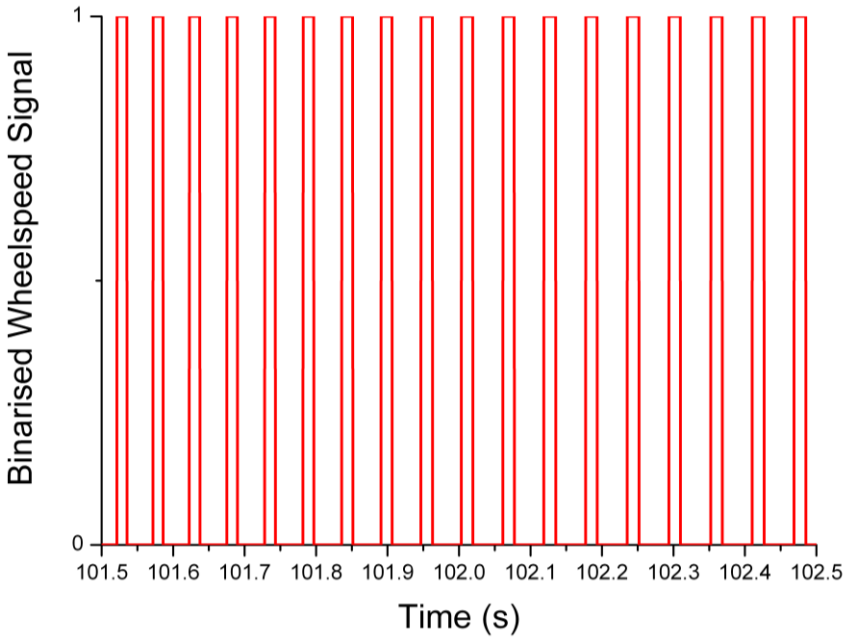

Figure 92 – Binarised wheel speed signal.

The times associated with each trigger passing were identified in one pass of the binarised data. The time increments associated with the passing of one quarter of a wheel revolution were then found at each point by subtracting the preceding time from the current. A four point average of these then replaced each point.

The determination of actual speed is made by dividing the time averaged (smoothed) increment for a quarter wheel revolution at each point by one quarter of the tyre circumference.

5.9 Closing Remarks

This chapter has presented the reader with the work undertaken to provide a test bed for a software concept previously discussed and which was already tested in a simplified form in the previous chapter. It also provided the means for testing a

sensor concept which, although strongly linked with the preparation of the car, is considered in a chapter of its own owing to the considerable and time consuming volume of work undertaken in its implementation; this chapter follows.

Chapter 6

Optical Displacement Sensor

6.1 Introduction

A method for positioning a vehicle in a global space was previously introduced as a key part of the data visualisation application. The universally employed method of approximating vehicle trajectory from wheel speed and lateral acceleration was described in chapter 4, whilst other approaches and sensors for measuring trajectory and vehicle displacement were discussed in section 2.7.3. All of these are summarised below (Table 7):

Table 7 – Overview of trajectory reconstruction and vehicle displacement measurement methods.

Method	Comments
Lateral acceleration and wheel speed trajectory calculation	Uses universally employed sensors and calculation is rapid, but results in low accuracy (magnitude of 10^1 m).
GPS code-phase measurement	Low accuracy (>3m) dependent on coverage also.
DGPS /augmentation Systems	Better accuracy (≈1m) but still too low on its own for trajectory comparison. Also can require additional cost and still dependent on coverage.
GPS carrier-phase measurement	Accuracy good (<20cm), but requires additional cost and time to determine carrier-phase ambiguity. Does not appear robust enough for operation at a race circuit.
Inertial and GPS Kalman filter based navigation systems	Use a range of GPS approaches fused with INS data to give a more accurate trajectory approximation. Can use any of the GPS approaches and potentially achieve 0.02m accuracy. However, practically they would achieve 1m accuracy when used by a racing team.

GPS phase Doppler measurements	Appears a good method of attaining a reported 0.05m accuracy, but still reliant on good satellite coverage.
Doppler shift speed sensors	Have been in existence for some time, but not employed in racing. Appear to suffer issues with smooth surfaces, making their application to racing questionable.
Correvit® sensors	Optical sensor, using a grating to produce a modulated ground image for photo detection. The intensity of the signal can be used to determine velocity from its frequency. Extremely high accuracy (≈0.002m) but too expensive for use in all but the highest categories of racing.
Image based sensors	A single axis correlation and dual axis neural network approach have been applied to farm machinery. They both required large images and did not account for height. Also the approach of rolling capture would not work at high speed. At slow speeds errors were already apparently too high.

A consideration of this table suggested that there was potential for investigating a means of determining vehicle displacement with sensor hardware whose cost could be minimised and whose use at a race circuit would be more practical than the more accurate GPS methods.

The concept of a sensing method to achieve this is presented in the following section before background to the technique of Particle Image Velocimetry, which provided some of the inspiration for the sensor concept.

6.2 Sensor Concept

An approach of using 2D cross correlation analysis of captured images was conceived which would build on the work of Stone and Kranzler (1992) and Kim and Slaughter (2008) and aim to develop a 2D image based displacement sensor. This would endeavour to achieve greater accuracy than Kim and Slaughter's approach by applying a complete image correlation and provide accurate placement in 2D unlike Stone and Kranzler.

These previous works were only concerned with slow moving farm machinery and used rolling camera capture. This sensor design would have to be far more robust in its operation as it would be subject to a much harsher environment and would measure higher velocities. Lighting methods were cited as a means of addressing these requirements and allow operation at higher vehicle velocities and with potentially high camera vibration.

Finally the previous work described was not concerned with the sensor height from the ground, presumably because of the level of accuracy required. However, in order to achieve the accuracy required for trajectory comparison, the concept proposed here would also determine the sensor's height from the ground. This would link with an accurate calibration methodology of the pixel displacements recorded.

The use of imaging for sensing movement has also seen application in optical computer mice. These generally feature a small CMOS (Complimentary metal-oxide-semiconductor) chip, typically of size 18 x 18 pixels imaging a surface illuminated by an LED (Ng, 2003). Generally, only 5 x 5 pixels are used for an image correlation between successive captures of the sensor, allowing displacement between images to be calculated at approximately 1500 Hz. They can achieve good positional accuracies, but their ability to measure displacement from different working heights has previously been found to fail above 1.25mm working distance, due to complete image defocussing (Ng, 2008). Therefore, as with the farm machinery displacement measurement techniques, the use of

current optical mouse technology was also not directly applicable for race car displacement measurement in its current form.

Ultimately, and after considerable modification and development of the original design, as described in the remainder of the chapter, the sensing approach was a success. This utilised a small USB 2.0 camera for image capture, synchronised with a LED ring illumination source, strobing on each frame.

A network of three optical sensors would in fact be used, individually giving data measures of vehicle speed and also ride height for calibration at each of three locations. Combined they provided an alternative method of approximating vehicle position within a global coordinate frame.

The approach in general built upon the expertise of the Wolfson School at Loughborough University, who were highly regarded in the field of Particle Image Velocimetry, a technique commonly applied to the measurement of fluid flows and which uses image correlation techniques.

6.3 Background Overview of Particle Image Velocimetry

Particle Image Velocimetry (PIV) is a whole field velocity measurement technique applied to fluid flows. Anandarajah (2005) gave a review of Particle Image Velocimetry's development and application, describing its origins in Laser Speckle Photography (LSP) and its development towards a measurement technique. The approach can simultaneously measure the velocity of a whole flow region by illumination with a 2D light sheet and as such is non-intrusive, unlike measurement apparatus such as hot wire anemometers and pitot tubes which both disrupt the flow and give only a single measurement point (Anandarajah, 2005; Grant, 1997).

The basis of the approach is the use of multiple-exposure photographic methods to capture images of flow with a known time between consecutive frames. The flow is generally illuminated by a laser light source allowing the light to be shaped into a sheet, illuminating a plane through the flow. The flow is seeded with particles which are chosen to be as close to neutrally buoyant as possible and which scatter back light for imaging purposes. Capture of two images of the flow allows for measurement of the imaged particle displacements and an inference of the fluid velocity to be made using the known time gap (Grant, 1997).

The use of photographic film remained common place for a time because of the high image resolution it offered, but developments in digital camera technology led to the natural progression towards Digital Particle Image Velocimetry (DPIV) and a move away from the inherent issues associated with processing large amounts of film. DPIV has a significant advantage in the potential for acquiring images straight to a computer for digital processing, without the need for manual processing and scanning, which presents part of the opportunity investigated in this work, for the system to be mounted on a moving vehicle.

Further, the combination of digital cameras and laser illumination allows for extremely high capture rates in the order of kHz as lasers commonly have a pulsed output allowing for their use as a stroboscopic illumination source (Anandarajah, 2005; Grant, 1997).

Both sources described correlation techniques applied to PIV images, which followed from the initial use of Young's fringe analysis. These are given more consideration in the section 6.9 having been considered as viable for application to images captured from a vehicle mounted car.

The brief introduction to PIV presented here and the review of current vehicle displacement sensors prompted the investigation of applying DPIV derived correlation techniques to ground surface images recorded from a car. The technique was envisaged to rely on ground texture rather than seeding particles in a flow. Images would be analysed by correlation techniques as they were most readily implemented with relatively low cost equipment. Pixel

displacements would be converted to actual displacements by a calibration and to velocity by knowledge of the time between frames.

6.4 System Specification and Procurement of Parts

Table 8 details the specification of the optical displacement sensor system which was defined before commencement of the design. These specifications were agreed after consideration of existing displacement measurement solutions, available finances and time and consideration of the performance required of the system to prove its concept.

Table 8 - Design Specifications of the Optical Sensor System

System Capture Operation	Continuous/Real Time
System Processing Operation	Post Test Processing of Raw Data
Target Frame Rate	50 samples/s
Target Maximum Speed	50 mph/22.347 m/s
Target Ride Height Measurement	>50 mm
Positional Accuracy	<5mm
System Running Time	15 min
Overall Dimensions	Ideally <250 mm^3

The following sections detail the procurement of key pieces of hardware forming the system, driven by the specifications described above. The physical design of the housing for these components is considered in section 6.5.

6.4.1 Image Capture

Initially the concept of using an OTS webcam was considered as the lowest cost means of implementing a camera based sensor. This would use a red, green, blue (RGB) LED lighting system to double the effective capture rate. If each

colour of LED fired independently at a known time separation, three separable images would be captured on the frame, providing two image pairs in each frame for cross correlation. This was not implemented ultimately however due to difficulties in camera control.

An alternative solution was found in a USB 2.0 camera manufactured by the German company Imaging Development Systems GmbH (IDS). The UEye® 1220-C model selected was compact and capable of recording images at 78fps at a resolution of 752 x 480 pixels. The cameras were shipped with a full Visual C++ 6.0 Software Development Kit (SDK).

An 8mm focal length C-Mount lens was used, providing a field of view of 120 x 90mm at the expected operational height of 200mm.

6.4.2 Illumination

The IDS USB 2.0 camera had a maximum quoted frame rate of 78fps running in free mode with no image storage. The design specification of the sensor described previously required storage of the images for post processing, which would slow execution. A method of increasing the effective frame rate by the illumination strategy employed was required in order to surpass the target sample rate.

A Signatech S6000A strobe controller unit was sourced as a suitable control unit for illumination, although it limited the illumination to Signatech lightheads and only either red or white light. The light outputs of the strobe unit could be controlled by a trigger input and were capable of delivering a minimum pulse (i.e. on time) of 1µs which at the maximum estimated vehicle speed of 50mph (based on the available test facilities) would equate to 0.02mm vehicle displacement, which was considered to be acceptable for a clear image. Red light (660nm) was duly used in an attempt to only expose red pixels in the camera, with the illumination strategy becoming one of doubly exposing each frame by strobing the light in each frame.

The capture of two images in a single frame dictated that the correlation would be by an autocorrelation technique, which involves correlating two copies of the same image data. The use of doubly exposed images increased the measurement sample rate to match that of the camera frame rate since every image would produce a displacement measurement rather than every two images, as would be the case with cross correlation of single exposure frames.

6.4.3 Laser Diode

The ride height would be measured by angling a light source into the camera frame. The dot image produced would then migrate with a change in height as illustrated by Figure 93 and explained more fully in section 6.11, allowing the ODS height from the ground to be inferred. A laser diode was selected as the best source for creating the dot image, owing to their compact size and high energy outputs. A class 3R laser diode of 670nm wavelength and 3mW power was selected. The relatively high output for a small light source would help ensure the largest possible contrast between the dot image and the double exposed image of the ground, which was envisaged to aid separation of the two images.

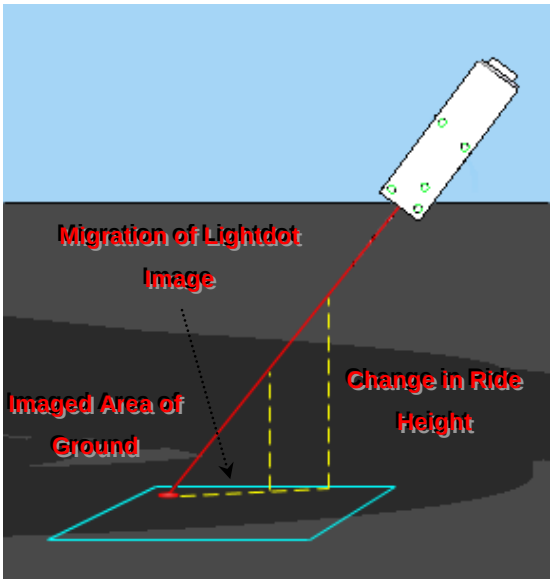

Figure 93 - The sensing principle employed for measurement of vehicle ride height.

6.4.4 Optic

A 90˚ beam deflector optic with a 10mm square base was sourced for the initial design as part of an adjustment system for positioning the light source. This was abandoned for the final version of the ODS housing however, since a close to 90˚ deflection of the laser diode beam was required as explained in the following section.

6.5 Sensor Housing Design and Assembly

Once the main components of the sensor had been specified it was then possible to design the housing which would allow rigid fixing of the components relative to one another and also mounting of the whole assembly to the test vehicle. For ease of machining and its light weight, aluminium plate and bar were used.

An initial housing design was created which would allow for considerable adjustment of the hardware configuration and would be used on the laboratory bench during the code development. It was envisaged that a second design would remove this adjustment in favour of increased rigidity and strength for the final stages of development and actual on vehicle operation of the sensor. As could be expected several additional modifications were also made to the second design relative to the first. Both of the designs are discussed below.

6.5.1 Initial Design

The first aluminium housing design was only used as a laboratory test mount, but allowed proper and consistent fixing of the sensor hardware components relative to one another.

The complete configuration is depicted in Figure 94 before a discussion of the key design features.

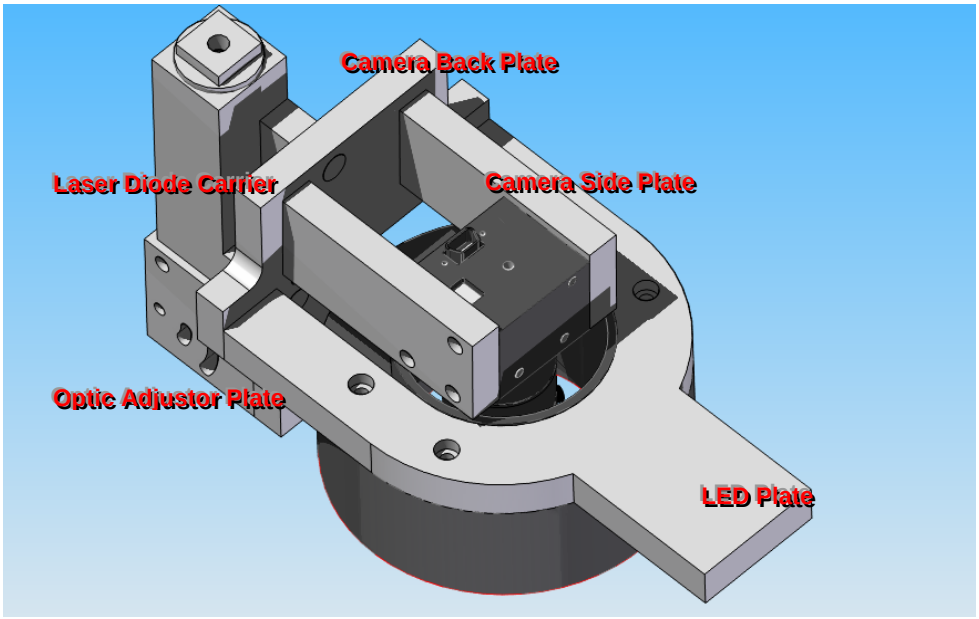

Figure 94 – The initial design of the ODS housing.

6.5.1.1 Laser Diode Carrier

The laser diode carrier shown in more detail in Figure 95 was designed to provide protection to the laser diode itself whilst also providing a method of attaching it rigidly to the camera and LED mounting plates. In this first configuration the laser diode was mounted perpendicularly to the LED plate and shone through a beam deflector optic housed below, which was able to adjust to change the light dot position. The carrier featured a screw cap with an internal collar to locate a spring used to apply pressure on the laser diode and ensure proper seating, which can clearly be seen in the cutaway view in Figure 95.

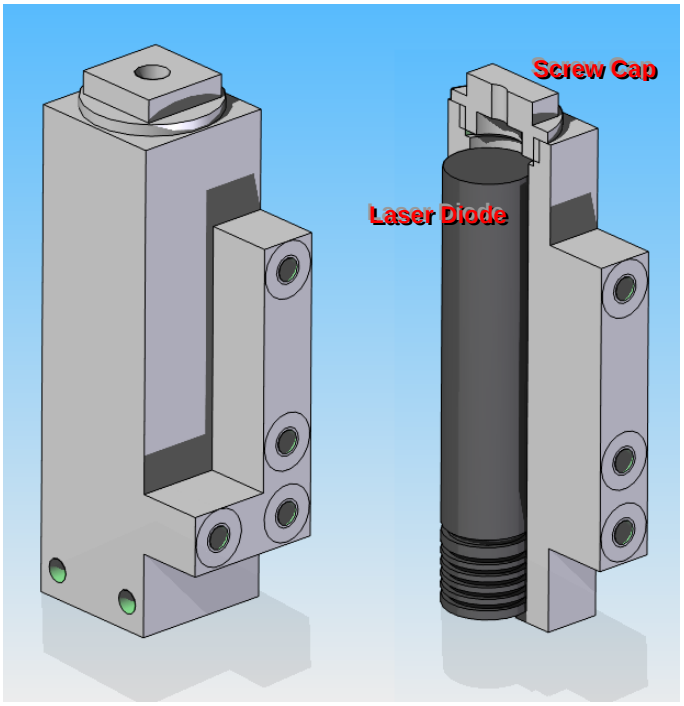

Figure 95 - The laser diode carrier of the initial design OSD housing.

6.5.1.2 Optic Adjustor System

The system for adjusting the angle of the laser diode beam in the first design involved the use of 90º beam deflector optic. This is not shown in Figure 96 but was mounted on the small optic plate shown in the cutaway view. The beam was delivered to the optic vertically as shown in Figure 96 whilst the angle of its deflection relative to the laser diode could be adjusted by movement of the optic plate securing bolts in the curved slots of the optic adjustor plates.

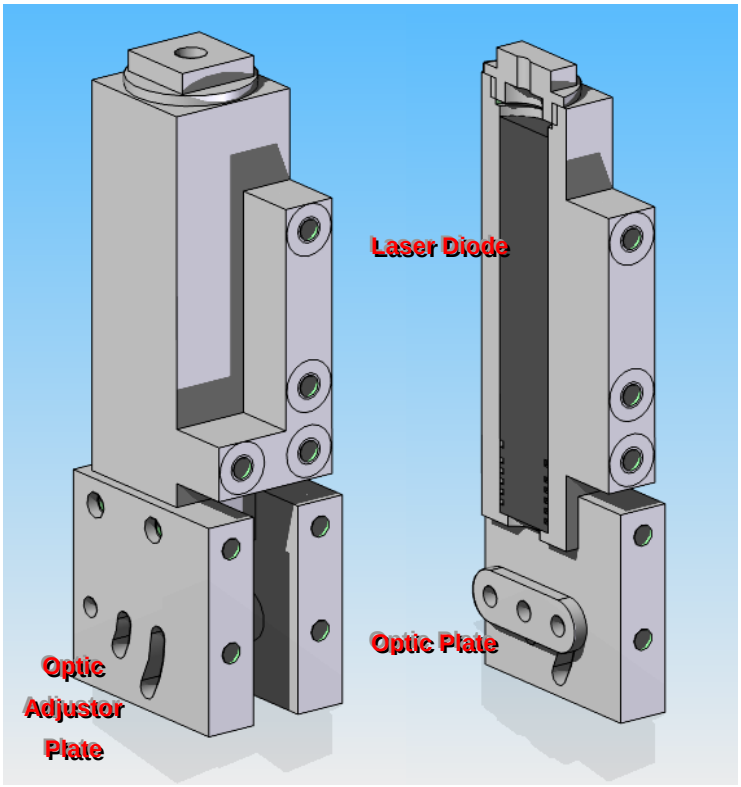

Figure 96 - The optic adjustor system of the ODS housing initial design.

6.5.1.3 Camera Height Adjustment

In the first design the LED ring and laser diode's position was fixed relative to the LED plate, but some adjustment of the vertical height of the camera relative to the rest of the assembly was incorporated, by way of linear slots for attachment of the camera side plates to the camera back plates, as shown in Figure 97. The height of the camera and angle of the laser diode could then be adjusted to the most suitable position for capture of the ride height image.

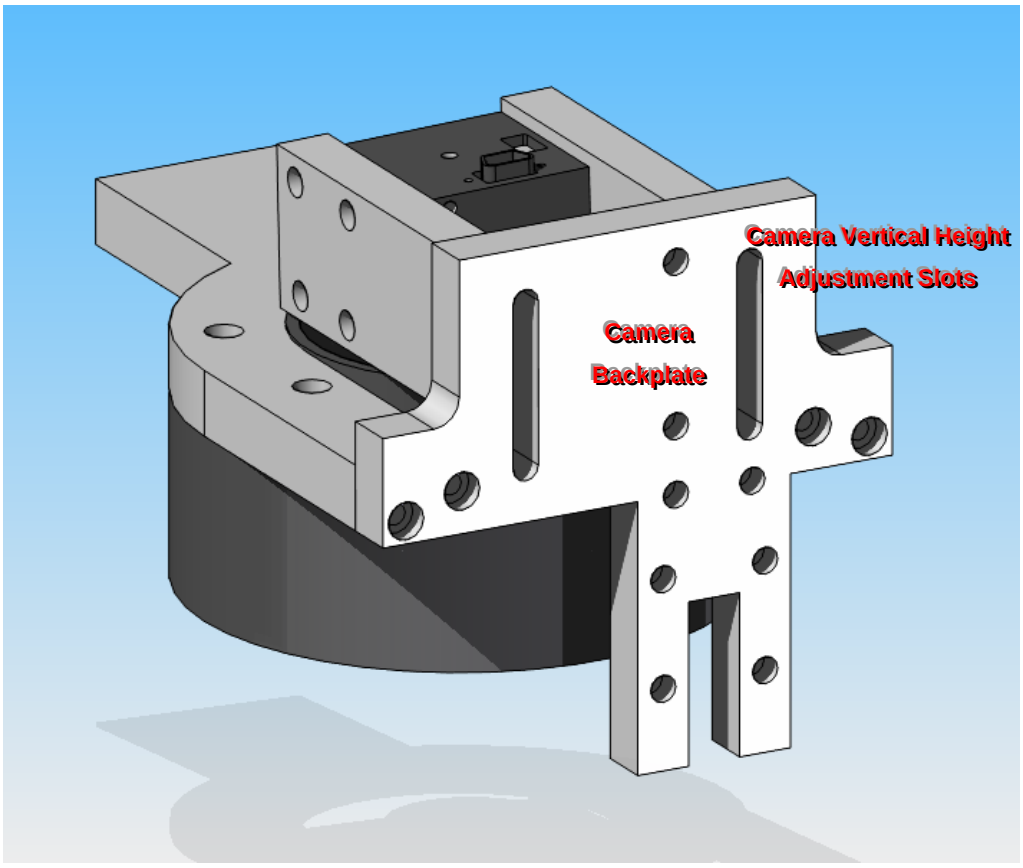

Figure 97 - The camera back plate of the ODS housing initial design, allowing adjustment of the vertical height of the camera relative to the LED ring.

6.5.1.4 Performance of the Initial Design

The first design was used during the initial code development described later and during which a key issue was identified with the delivery of the laser diode beam to the image area. Difficulties in securing the beam deflector on the optic adjustor plate meant its angle was rotated in all axes and therefore it was difficult to contain the laser diode image within the desired portion of the frame. Also it was difficult to fully secure the optic and it appeared that vibration caused some movement of the laser diode image within the camera frame.

6.5.2 Final Design

The final design of sensor housing removed the adjustment from the previous design with the exception of the laser diode angle adjustment, necessary to allow the initial dot position in the image to be set for the desired mounting height on the car. It was felt that there was no distinct need to allow the camera to move relative to the LED ring and in effect height adjustment of the camera could be achieved by spacing of the whole sensor assembly on its car mounts.

The integrity of the laser diode adjustment itself was increased in the design, to help reduce the possibility of any movement of the laser diode relative to the camera during operation. This involved removal of the optic adjustment of the laser diode beam in favour of adjustment of the whole laser diode itself, which now shone directly onto the ground. The result was a more cumbersome design, but one which was felt to best ensure reliable operation of the sensor in tests. The complete design is illustrated by Figure 98 before more detailed description of the redesigned laser diode adjustment system.

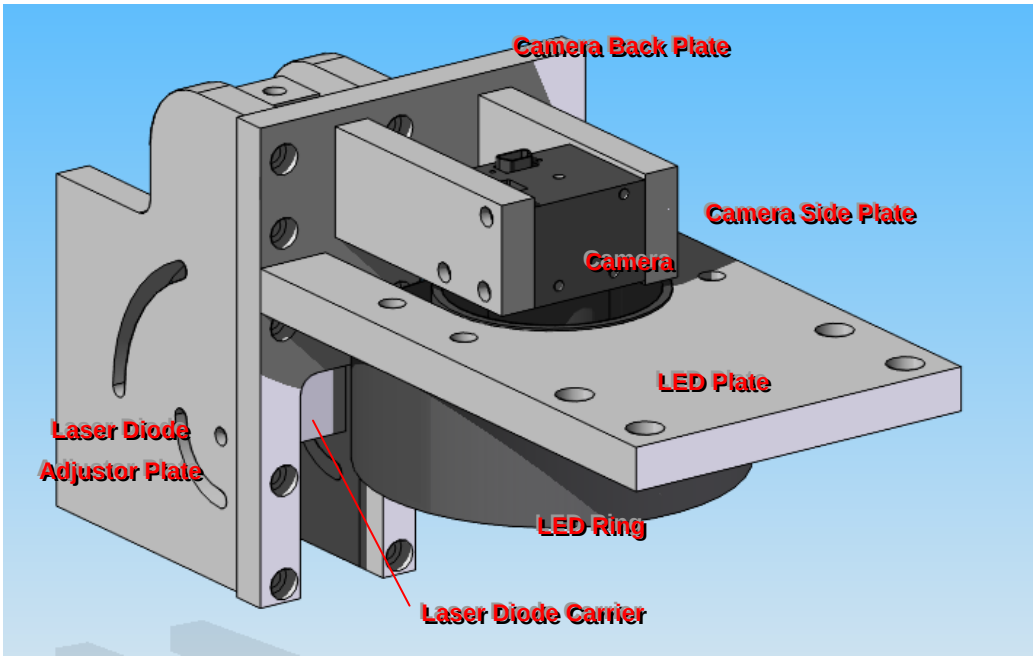

Figure 98 - The final design of the sensor housing.

6.5.2.1 Laser Diode Adjustor Plates

The laser diode adjustment system on the final design is more clearly illustrated by Figure 99. The laser diode carrier was held between two aluminium plates, with curved adjustment slots allowing the laser diode to be pivoted about the front bolt and secured through the slots at any desired angle up to 67º from the vertical. Light shone directly from the laser diode to the ground.

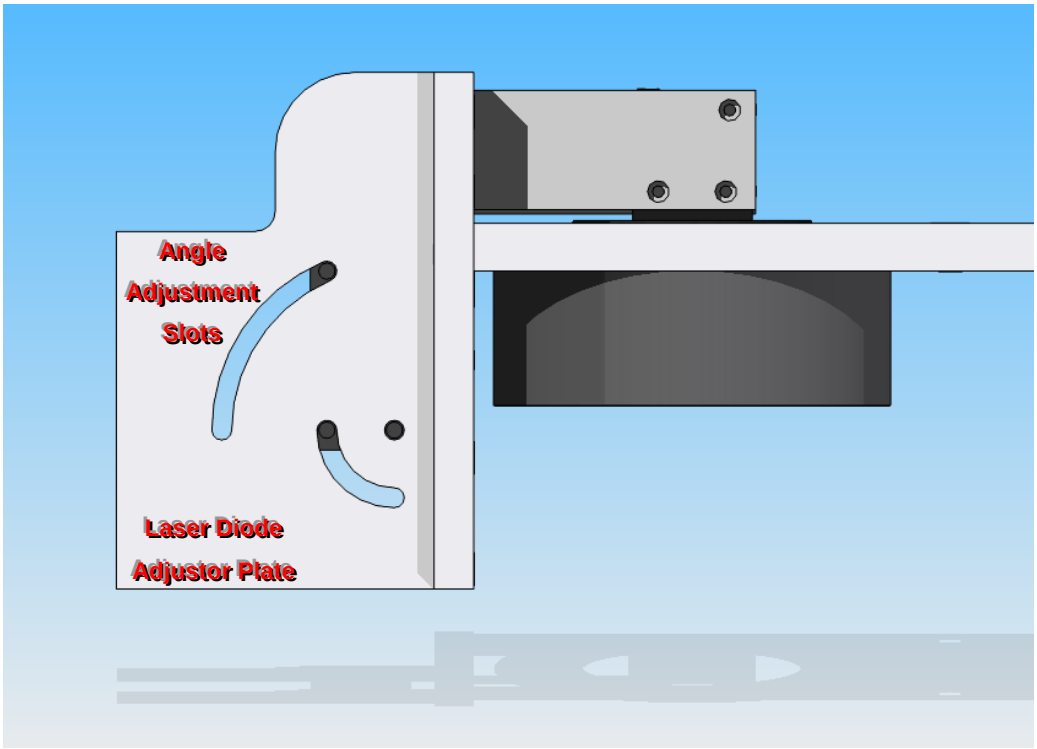

Figure 99 - Final design laser diode adjustor plate.

6.6 System Electrical Specification and Arrangement

The arrangement of the optical displacement/velocity sensor hardware was a concurrent design consideration to the mount itself and had to take into account a number of aspects. These could broadly be divided into those connected to the electrical operation of the sensors, forming the largest area of focus and those

associated with the physical dimensions of the car. These key design considerations are discussed below, before an illustration of the system arrangement on the car is presented.

6.6.1 Collecting Image Data

A key target of the ODS from the outset was to maximise the capture rate of the sensor in order to reduce the time between frames since the data was not continuous. The autocorrelation image analysis technique employed for analysing the captured images, and discussed in more detail in section 6.10, analysed the frames individually. Therefore there was no continuous record of displacement, rather measurements taken at discrete time intervals. In order to track the complete vehicle trajectory, as was aimed with the use of these sensors, interpolation between the discrete measurements would be required. Increasing the capture rate and hence reducing the time step would therefore reduce this interpolation between sample points and improve accuracy.

The IDS SDK could utilise multiple cameras connected to the same computer, but the USB bandwidth available to each camera on a single USB bus was divided evenly. Therefore, in order to achieve the optimum frame rate for a given range of settings, the full USB bandwidth of 480Mbits/s (equivalent to 60Mbytes/s) was required for each camera.

Camera control was by laptop computer, due to their portability and ruggedness in comparison to a desktop computer. As described in more detail in section 6.6.5, three cameras were ultimately used in the sensor system; with expansion of laptops being fairly difficult, a single laptop was devoted to each camera, therefore allowing each the full bandwidth of a USB bus.

Another advantage of the use of laptop computers was the removal of the power demand of the use of a desktop system, estimated to be around 150W with a LCD monitor included (Bray, 2006).

6.6.2 Powering the System

The decision to use laptop computers to control the USB cameras greatly reduced the overall power demand, however it was decided as a matter of course that the car's main battery should remain dedicated to the standard vehicle systems, so an auxiliary was installed for powering the sensor hardware. The hardware requiring power from this battery was:

- 3 Laser Diodes;
- 3 Signatech S6000-AS Strobe Controllers.

6.6.2.1 Laser Diodes

The laser diodes were dc powered and so were connected directly to the auxiliary battery without any need for inversion. They also only required connection in a simple manually switched on-off circuit, as they would remain powered on for the duration of a test. Owing to the battery voltage of 12.3V being very close to the laser diode's maximum operating voltage, a potential divider was also incorporated into the circuit to reduce the voltage supplied and protect it from damage during switching on of the system. The potential divider operated on exactly the same principle as the potentiometers used for sensing, with a reduced voltage being picked off for supply to the laser diodes.

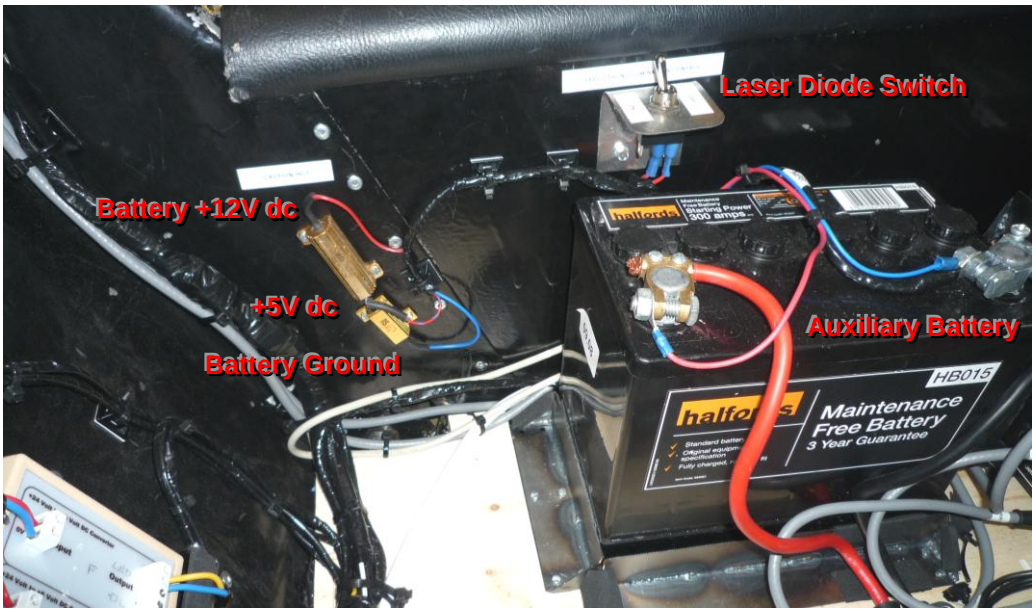

Figure 100 - Photograph illustrating the potential divider used to step down the voltage supplied from the car battery from around 12V to 5V.

6.6.2.2 Strobe Controllers

Three strobe controllers were required for the complete sensor arrangement in order to maximise the intensity of light produced. Each of these operated from a power supply, fused at 1.25A and supplying 24VDC, consuming a maximum power of 30W each.

The power supplies were mains terminated, so an inverter was required to produce an ac supply from the auxiliary battery's dc output. With a combined power demand of 90W it was relatively simple to procure an inverter capable of meeting this demand. The components of this part of the electrical configuration are illustrated by Figure 101.

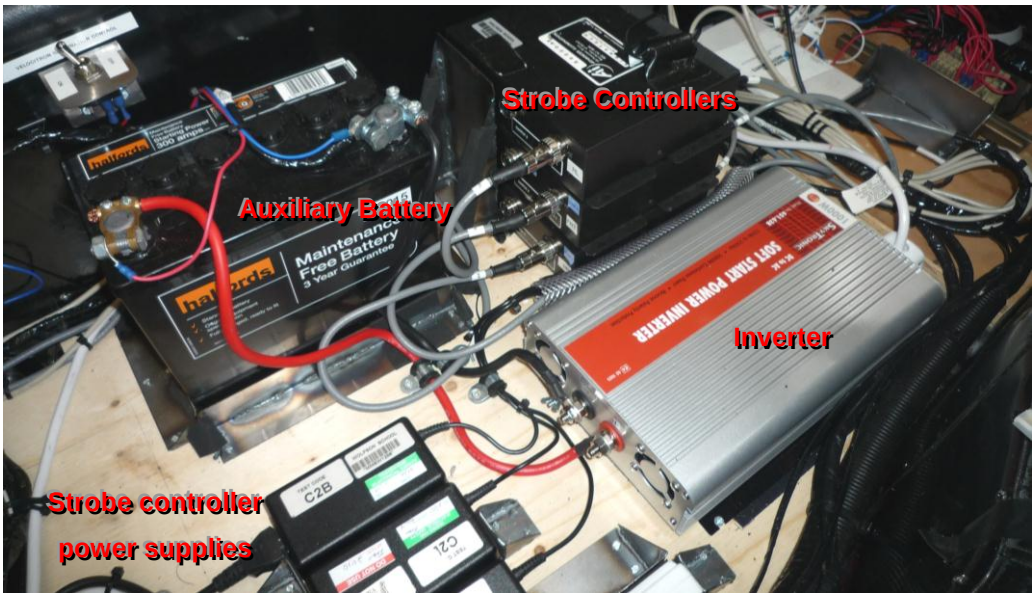

Figure 101 - The strobe controllers and associated parts for powering.

6.6.3 Light Triggering

The triggering of the LED illumination was performed using the IDS USB cameras and their SDK trigger command. However, the command only operated a switch on the cameras and so they required a suitable external voltage supply, which was achieved by the hardware arrangement in Figure 102.

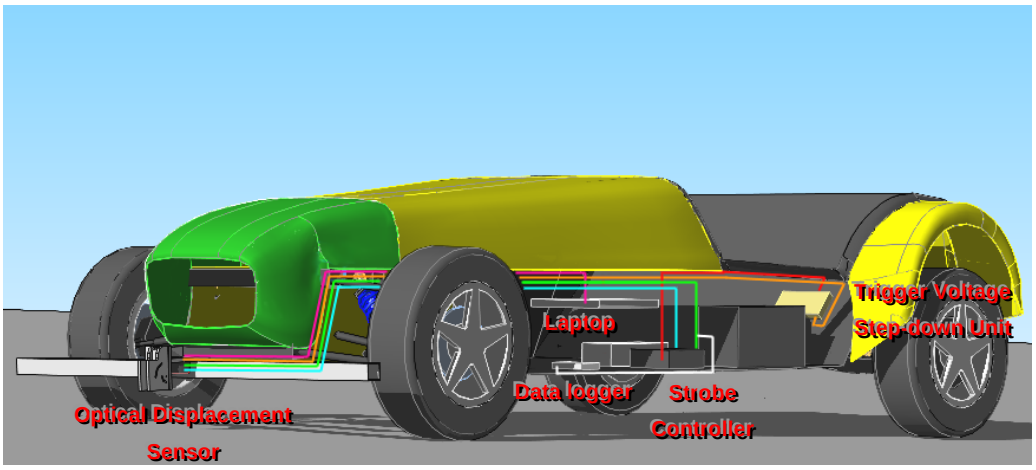

Figure 102 Schematic illustration of the trigger configuration of the LED illumination.

Figure 102 shows the key components in the triggering of LED light rings. The camera making up part of the sensor is supplied by a constant 24V dc supply from the strobe controller. This is shown as the red line, which is first routed through the trigger voltage step down unit, a potential divider described in section 6.6.4. This lowers the voltage supplied to camera to 5V reducing the potential for voltage overloading of the camera and allowing the signal to also be fed to the data logger. The 5V supply shown as orange is then fed to the camera. The USB command from the laptop computer to trigger the LEDs is shown as pink. On receipt of this command the camera switches its trigger output and 5V dc flows back to the strobe controller, shown green. This signal also branches off and is fed to the data logger (shown white) and recorded for timing purposes as described in section 6.6.4. The strobe controller's output is set to wait for a rising edge voltage signal on its trigger input and upon receipt of this, discharge to the LEDs shown in light blue, which subsequently followed the predefined output pattern described in section 6.9.

6.6.4 Interfacing with Data Logging Hardware

The data logger was utilised as a means of time stamping the images captured from each of the three cameras and comparing the three streams of data against a common reference point in time, which clearly also matched with the other streams of data acquired from the standard sensor set.

As described in section 6.6.3 the voltage signal triggering the output of the strobe controllers to the LEDs was also fed to the data logger. This trigger output is switched in the line of code immediately preceding the one commanding the image capture, and so was assumed to also represent the time of the image capture commencing. The time assigned to the computed displacement from the sensor could then be calculated by addition of half the exposure time (1ms). Code described in section 6.13.1 was developed as part of the data pre-processing routine to detect the occurrence of a rising edge in the trigger signal.

A potential divider step down unit, shown in the photograph in Figure 103 was assembled by the Wolfson School Electronics workshop, which would step the 24V trigger signal down to 5V, making it safe for use with the data logger.

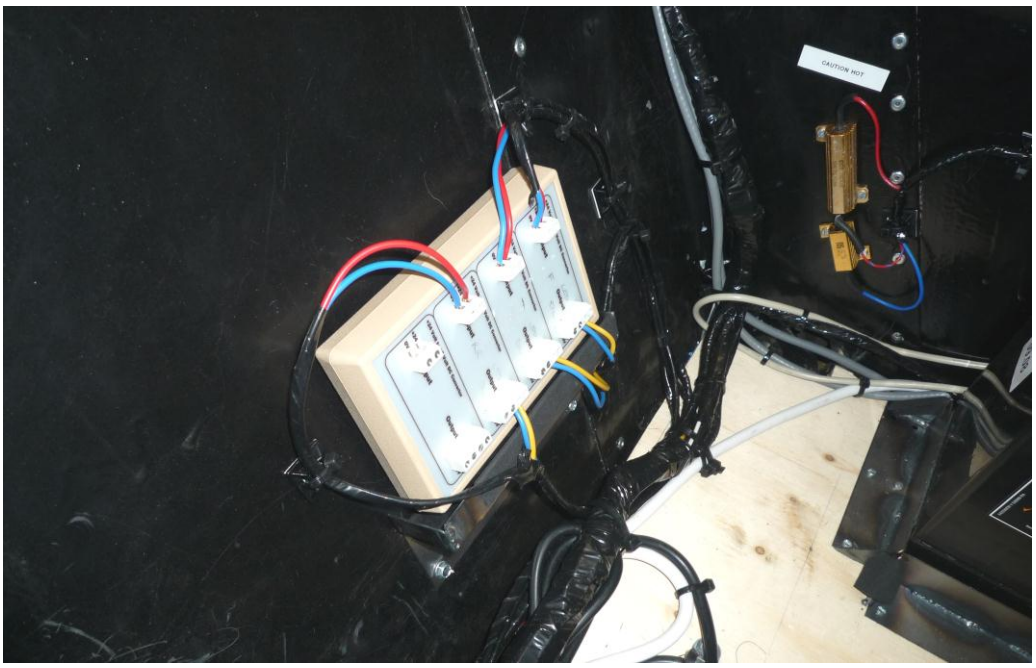

Figure 103 - The step down unit for the strobe controller trigger signals; converting a 34V dc signal to a 5V dc signal.

6.6.5 Vehicle Layout

It was a requirement to minimise the length of the USB cables used in the system in order to reduce the risk of USB time out errors. The USB 2.0 specification (Compaq Computer Corp. *et al*., 2000) stipulates a maximum one way signal propagation delay of 30ns, with 26ns assigned to the cable delay. With a specification of a maximum cable delay of 5.2ns/m this allows for a 5m cable without the addition of a hub. These limits are specified in order that the host controller of a USB system can determine if a command is received by the device it controls. If the host does not receive an answer from a device in 1700ns it considers the command sent to be lost.

As will be described in section 6.7.1, the optical sensors themselves were positioned with one at each rear corner and a single sensor at the front of the car,

centrally mounted. For packaging reasons, the laptops were all mounted at the same location, meaning there were a range of cable lengths required between each camera and laptop pair. Careful attention was paid to routing the cables with the minimum number of extensions, although it was found that there were communication issues between the rear right sensor and its computer, these being the farthest apart. The occurrence of a single communication time out ruins a complete set of data as the camera SDK has no way of catching the error and proceeding with the next capture. Attempts were made to reduce the length of cable used and eventually a workable solution was achieved. This was found to largely rectify the issue.

6.6.6 Optical Displacement/Velocity Sensor System Arrangement

A final consideration of the arrangement of the electrical equipment making up the ODS system was the physical dimensions of the test vehicle. With the boot space entirely filled by the fuel tank, the passenger side of the cockpit was the only remaining suitable mounting location.

Another consideration with the mounting of electrical equipment was the vibration inherent in a moving vehicle (particularly one that it relatively stiffly sprung such as this). So adequate anchorage of all components and various precautions to ensure that cables were sufficiently protected and secured, so as to prevent chaffing and possible shorting, were required.

Ply was cut to the shape of the passenger side cockpit floor plan and placed on the floor with foam backing. The foam acted as some vibration attenuation whilst the ply gave a large area suitable for mounting and securing brackets and such like. The components were eventually laid out as illustrated by the photograph in Figure 104, where it can be seen that the packaging of all components is extremely tight, requiring an additional shelf above the foot well area for the laptop computers to be housed.

The components visible in Figure 104 are largely those which were expected to be accessed most frequently, such as the auxiliary battery for replacement and the strobe controllers for powering on and off. The data logger was housed in the foot well as shown in Figure 105 as it was to be accessed less frequently along with the terminal block rail used to make all sensors' earths common and to split the voltage supplied by the data logger to each sensor requiring power.

Figure 105 also illustrates some of the key aspects of securing the electrical equipment to the car. The terminal block rail can be seen secured between two steel brackets, which were laser cut and folded before being secured to the ply base board. The use of cable ties to secure wiring where possible is also evident, as is use of foam tape on sharp edges and of plastic hose as cable conduit in the left of the frame to reduce the likelihood to chaffing between wires and sharp edges.

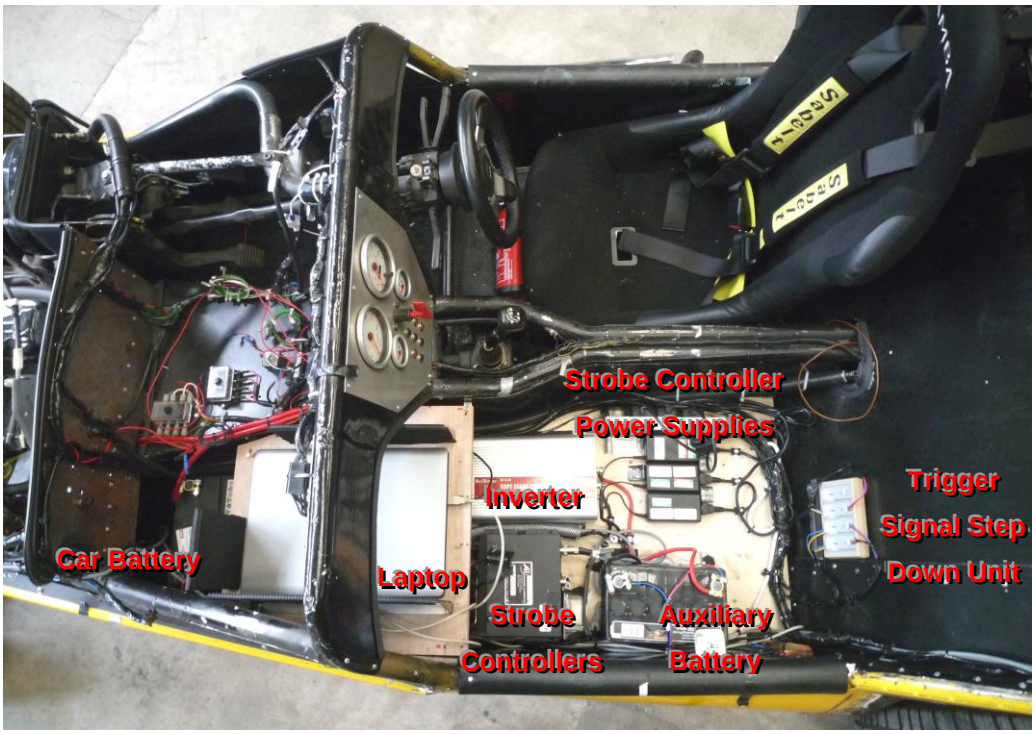

Figure 104 - Overhead photograph showing the electrical components mounted in the passenger side cockpit area.

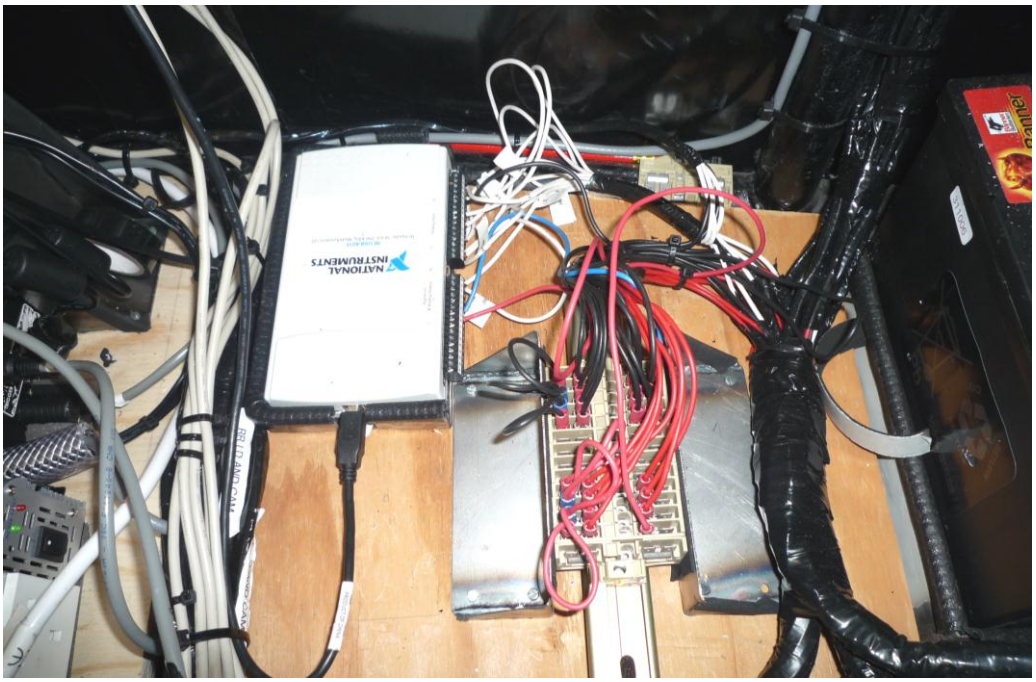

Figure 105 - The data logger and terminal block rail for making sensor grounds common and splitting sensor voltage supply, located in the passenger side footwell.

6.7 Vehicle Mounting

The last stage of the optical displacement sensor development was to finalise the method of mounting the sensors to the car. There were two key aspects to the mounting process to be considered. Firstly, was the arrangement of the sensors on the car in order that they produced the desired data. Secondly the physical means by which this arrangement could be achieved. The following section describes both these aspects.

6.7.1 Layout

The method of approximating the vehicle trajectory from the displacement measured by three sensors is given a full consideration in section 6.14. However, the system used the three sensors to make a triangle plane which approximated the car. Two cameras were located at the rear and one at the front, as Figure 106 illustrates.

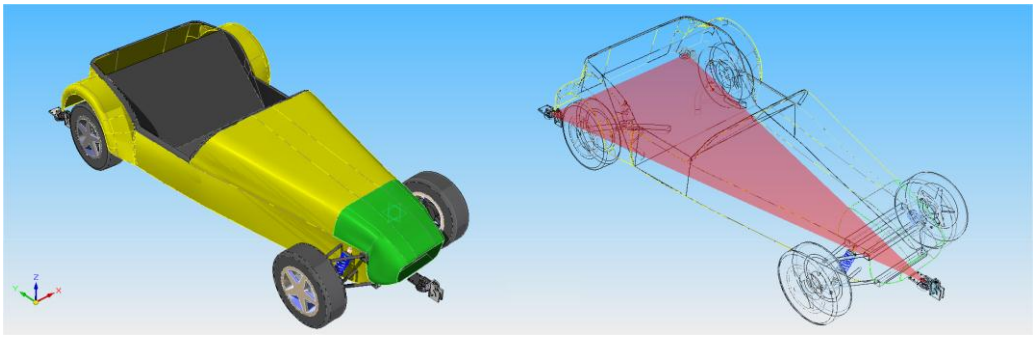

Figure 106 - CAD screenshots illustrating the optical sensor locations and the plane formed and used to approximate the motion of the car.

6.7.2 Mounting Beams

The mounting configuration of the optical displacement/velocity sensors described in the previous section was achieved using 1.5m lengths of 2” steel box section.

Figure 107 shows the front mounting beam, which was a simpler configuration than the rear. Two strips of 5mm thick steel plate were welded to the beam. The beam was then fastened to the front-most chassis tube by these plates with M8 bolts, through holes drilled in the chassis tube and reinforced with steel tube to prevent crushing. Because of the central mounting location and position of the sensor, the front mounting did not suffer from any significant vibration issues.

.

Figure 107 – The front displacement/velocity sensor mounting beam.

The rear mounting beam was suspended on two lengths of M8 threaded bar which were located through holes drilled in a plate welded to the spare wheel frame, as can be seen in Figure 108. Because of the outboard location of the sensors at the rear and the central mounting position of the beam, the sensors were prone to vibration, so braces were incorporated with thin steel tube bolted to the roll over bar on the chassis and welded to the ends of the beam.

Figure 108 – The rear optical displacement/velocity sensor mounting beam.

6.8 Initial Testing and Development

A series of preliminary tests were used in order to determine the settings used for the camera, which also led to the introduction of two design developments.

The reader should consider Figure 109, which depicts the trigger and LED or strobe controller outputs. The double pulse light wave form described previously can be seen and the key timing parameters are labelled as follows:

A. Delay time;
B. On time;
C. Separation time.

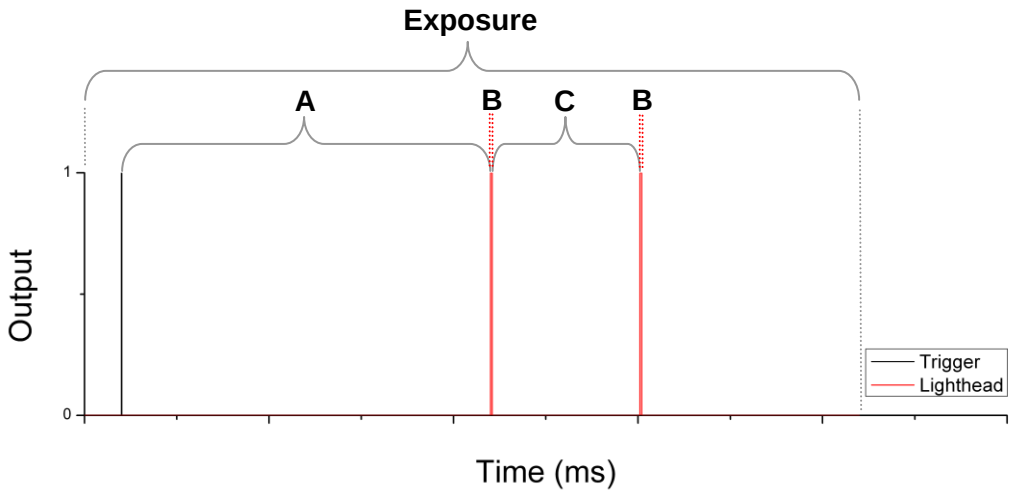

Figure 109 – Output Vs Time plotted for the trigger and LED lighthead, illustrating the timing parameters controlling the light output.

The series of tests involved driving the car around a concrete compound at approximately 30mph. A range of settings on both the camera and lighting controller were trialled and a subjective assessment of the image data captured was made. At the conclusion of the seven tests, the settings used for the main testing detailed in Chapter 8 were determined.

The test settings are detailed below in Table 9 and a selected representative image from each is presented in Figure 110. All tests had a delay (A) of 1ms. The delay time placed the measurement towards the centre of the frame and also ensured the illumination fell within the camera exposure. Preliminary tests suggested that too short a delay time resulted in the first light pulse being lost.

In terms of the ride height images, depicted on the right of Figure 110, all test settings produced an image which could be successfully thresholded to allow the software developed and discussed in section 6.11 to determine the sensor height. The dot appeared larger as one would expect in the tests using the longer exposure time of 6ms (1 and 2) but was usable in all tests.

In terms of the ground displacement images, shown on the left of Figure 110, the single biggest influence can be seen to be the exposure of the camera; tests 1 and 2 with a longer exposure feature heavy motion blurring.

Test 3 produced very clear results, but the stop time C being so long meant the double pulse was only just captured within the exposure and the potential separation of the two images was also considered consequently too high, increasing the pixel displacement range which must be considered in the correlation process explained later. The separation was therefore reduced for test 4, which can be seen to result in a darker image as the strobe controller has less time to charge its capacitor.

The effects of reducing the on time B are clear between tests 4 and 5. The shorter on time produces a much darker image, presenting less detail in its unprocessed form.

Test 7 introduced an ambient light and lens shield to the sensor and tested this in combination with a further slight reduction in the stop time C, to further reduce the pixel shifts encountered. This results in a darker image as ambient light is blocked, there is some attenuation by the lens shield and the strobe controller can only charge to a lower current than test 6. However, the images captured produced usable results and proved to be the sensible limit of the reduction in stop time. These settings with the aforementioned design developments were the final configuration used for testing. These design developments are discussed in more detail below.

Table 9 – Camera and strobe settings used during preliminary tests

Test	Strobe Settings						Camera/Software Settings	
	Output Current (mA)				Output Waveform			
	Ch 1	Ch 2	Ch 3	Ch 4	B - On Time (µs)	C - Separation Time (µs)	Exposure (µs)	Ride Height Threshold (pixel value)
1	1922	1922	0	0	10	1000	6000	255
2	2863	2863	2863	2863	5	1000	6000	255
3	2863	2863	2863	2863	5	1000	2000	255
4	1922	1922	1922	1922	5	500	2000	252
5	3255	3255	3255	3255	2	500	2000	252
6	1922	1922	1922	1922	5	500	2000	240
7	1686	1686	1686	1686	5	400	2000	240

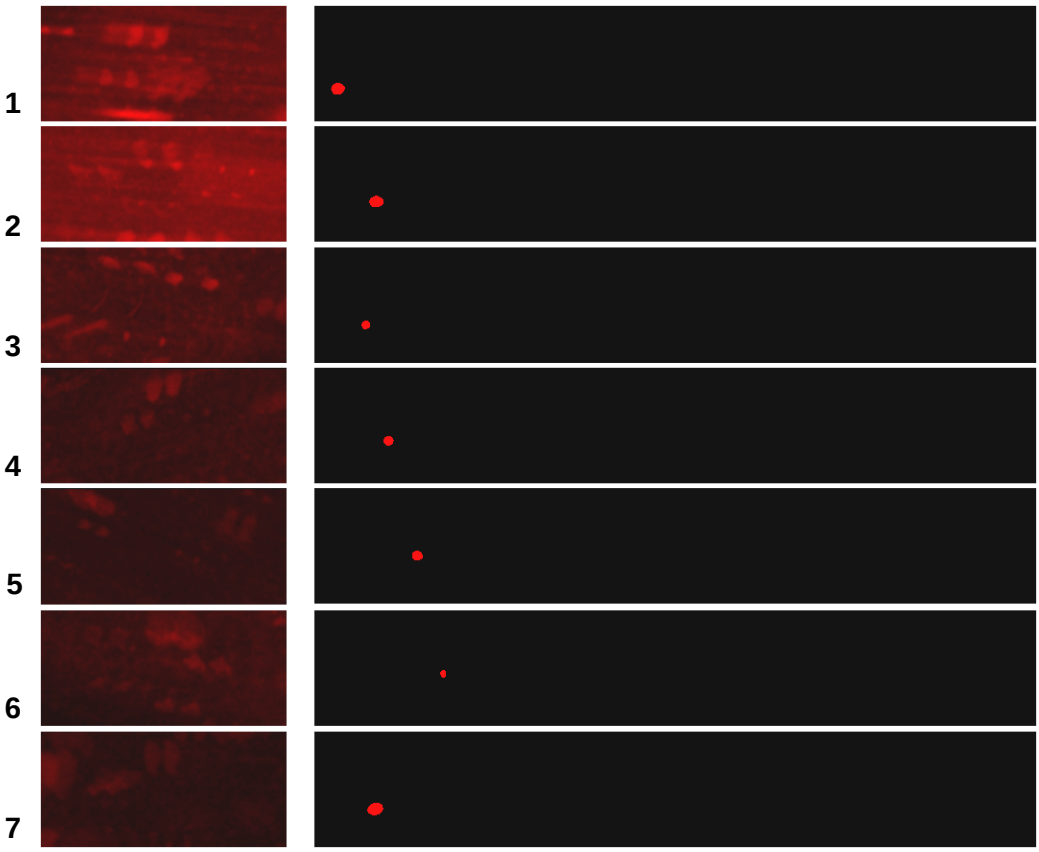

Figure 110 – Selected images captured from the settings tests.

6.8.1 Ambient Light Shields

The preliminary tests described above had indicated a reduction of exposure from 6 to 2ms as drastically reducing the effects of motion blur in the images collected. However, it was found that this was still affecting the images under certain conditions during a test at a 2ms exposure, which prompted development of an ambient light shield.

An extreme example of the effect of motion blur from a long exposure (6ms) test is shown by Figure 111 to illustrate the effect. The result is the masking of some feature image pairs which could positively contribute to the correlation result.

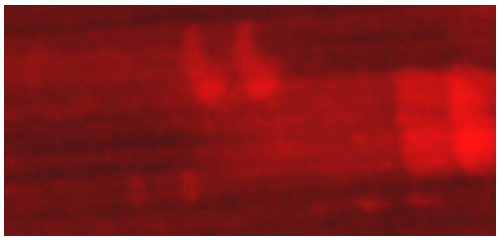

Figure 111 - A motion blurred image produced by the sensor running unshielded.

A system of shielding was investigated and the solution of an inverted plastic washing bowl was quickly decided upon as a cost effective and rapid solution. These were attached to main mounting beams using thin steel brackets as shown in Figure 112, and featured a hole allowing the top of the sensor to protrude for wiring purposes. By having the shield attached independently of the sensor it ensured that any contact of the shield with the ground would not damage the sensor itself.

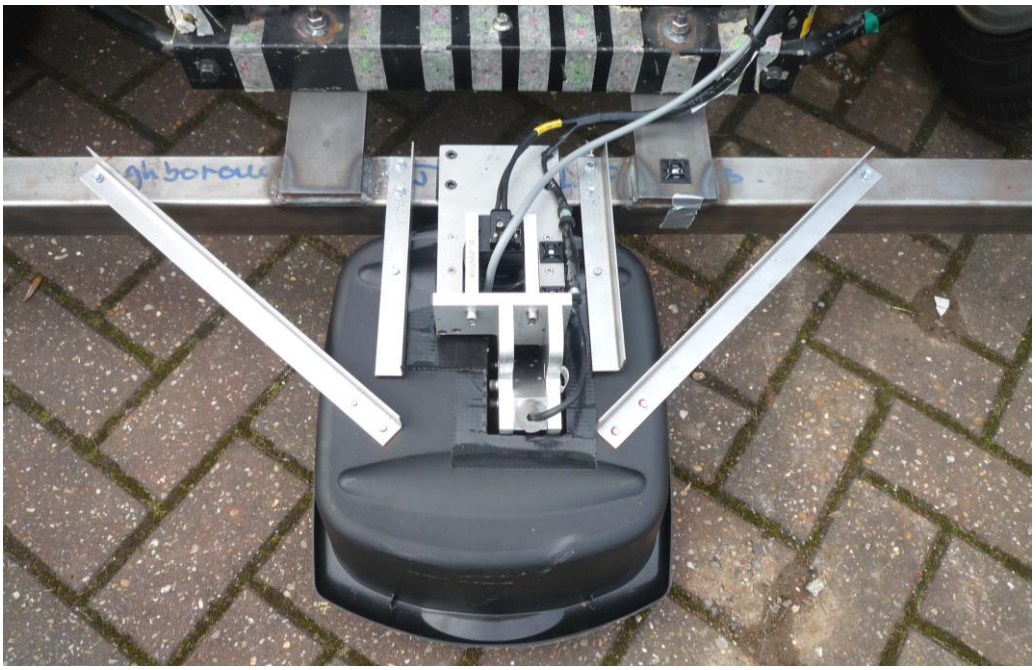

Figure 112 - The mounting of the ambient light shields.

To help improve the shielding, a flexible skirt made from a heavy gauge waterproofing polythene was attached around the plastic bowl as shown in Figure 113.

Figure 113 – The skirted ambient light shields in use during testing.

6.8.2 Lens Shield

A lens guard was added to the design prior to actual mounting after tests of the mechanical operation of the car made apparent the amount of surface debris that was lifted by the car's tyres.

The shield screen itself was a laser cut 110mm diameter clear Perspex® circle. It was mounted onto a section of household waste pipe with an outer diameter of 110mm and an inner diameter of 102mm, which was slightly larger than the outer diameter of the LED ring (100mm). This meant with a small amount of foam inside the pipe section it would push over and grip the light ring, protecting both the light and camera lens from debris as shown in Figure 114. A number were made and were intended to be continually changed between test runs.

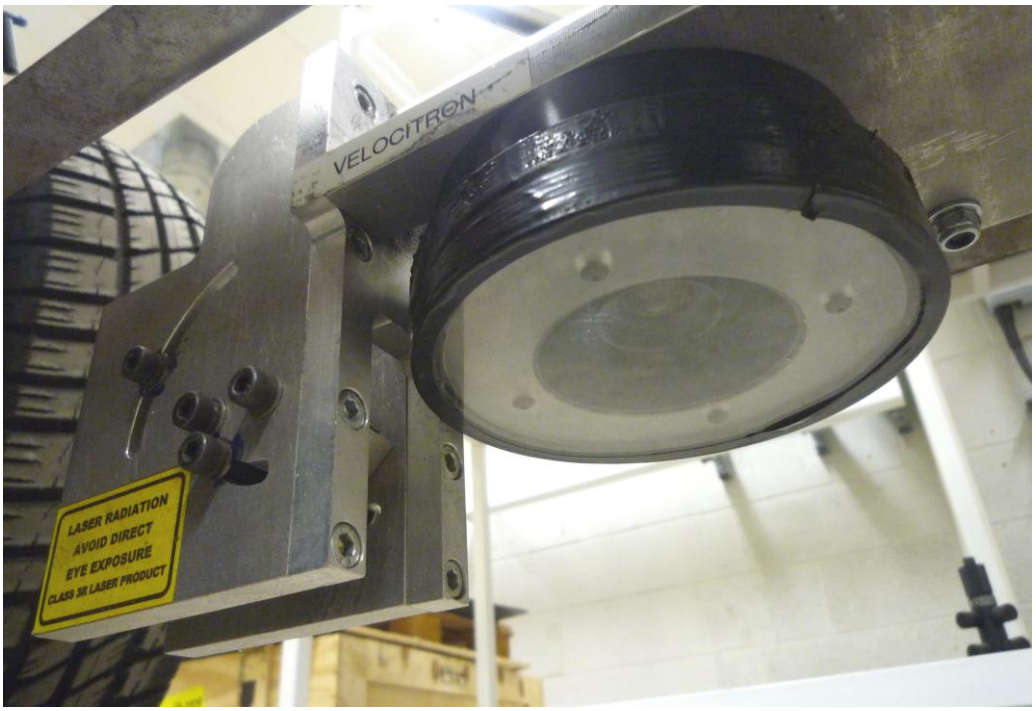

Figure 114 – Lens shield in situ over the LED light ring.

6.9 Development of Image Capture Routine

The camera used in each optical displacement sensor captured data which was used for lateral, longitudinal and vertical displacement approximation. The cameras were each controlled by a single laptop computer executing a controlling software application. This application provided the user with various options for setting the capture routine as well as executing the image capture itself. Both these aspects of the application are discussed below.

6.9.1 User Interface

The Graphical User Interface (GUI) used standard C++ libraries to create a functional form for controlling the IDS cameras, defining capture and analysis

settings, opening and writing files and also for reviewing data. The appearance to the user is depicted in Figure 115.

The three main areas of the application were divided. Section A marks the area concerned with capture controls, where capture size, interrogation region size, image thresholds and the project name can be set. Section B is the analysis section, giving the controls for loading image data and for adjusting the analysis regions for both the ground displacement and height images. Finally section C is the review section, mainly used during the preliminary tests described above, which allowed the user to review and play captured images to subjectively check their quality.

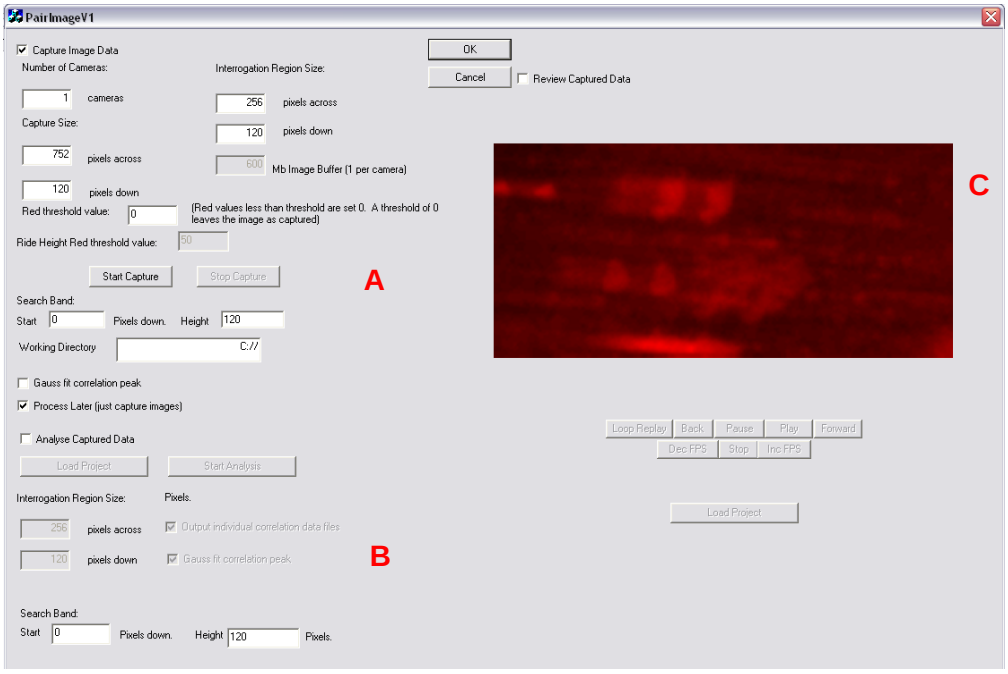

Figure 115 – The GUI of the camera capture programme.

6.9.2 Capture Routine

The underlying capture routine, which was introduced previously and was responsible for collecting the images for both ride height and ground displacement measurement, had to perform a number of tasks:

- To call the capture of an image;
- To trigger the double pulsed illumination of the camera frame;
- To store both the ground displacement and ride height images for subsequent analysis.

The capture routine is illustrated well by the program development flow chart in Figure 116.

In order to optimise performance of the system during testing, images were stored to RAM to avoid slowing from hard drive writing operations. As depicted by the flow chart, the capture was performed in a loop which was executed until the user exits. The routine would loop as quickly as was possible, which meant the instantaneous frame rate could vary slightly depending on the performance of the controlling computer, but as tests discussed later in this section showed, this variation was small.

The storing of images is illustrated by Figure 117. The position in a large storage buffer was maintained by a pointer variable (CutPointer) initially set to 0. As each image was captured the CopyPointer variable was set to indicate the pixel to be copied from the captured image buffer (which must be overwritten at the next capture). This was achieved by using a set of variables set by the user on the GUI which define the section of the captured image to be stored. These control a nested for loop routine going through the effective rows and columns of the image (which is actually stored as a 1D array). The CopyPointer variable was calculated at each loop to cut the necessary section from the image and store it in the storage buffer at the location pointed to by CutPointer. Only the red pixel value was stored, since red illumination was used; this triples the length of capture possible with the system. Once stored, the CutPointer is incremented to point to the next storage location and the copy code loops to the next target pixel. Once execution of the capture loop was complete, the image routines were then run. These are illustrated by the flow chart in Figure 116.

A counter variable, incremented in the overall capture routine (Figure 116) recorded the total number of frames captured and was used as a control variable in a for loop cycling through the stored images. For every image, a file pointer

was first created in order to output data as a 24-bit bitmap file. The image data was then cycled through by a nested for loop moving again through image rows and columns. At each step, a pointer to the image was calculated and used to extract the data. The location was calculated by multiplication of the current frame and individual frame storage size to offset the pointer by one frame each storage operation. The red pixel data was then written to a bitmap, with zeroes written for blue and green bytes in order to match the bitmap format.

Consideration of the three flowcharts presented in the following pages will indicate to the reader that the ground displacement image data and the ride height image data are considered separately. There were different functions for each, but they follow exactly the same format, so the storage and saving routine flowcharts depicted are effectively generic. The data collected for both was captured in the same frame using different sides of the frame width. The sections were then cut to the appropriate storage buffer by the form of routine illustrated by Figure 117. This was efficient since the command for extracting the image data from the camera buffer to a separate holding buffer (not depicted for brevity) involved reading complete lines of data, so this image width was well utilised.

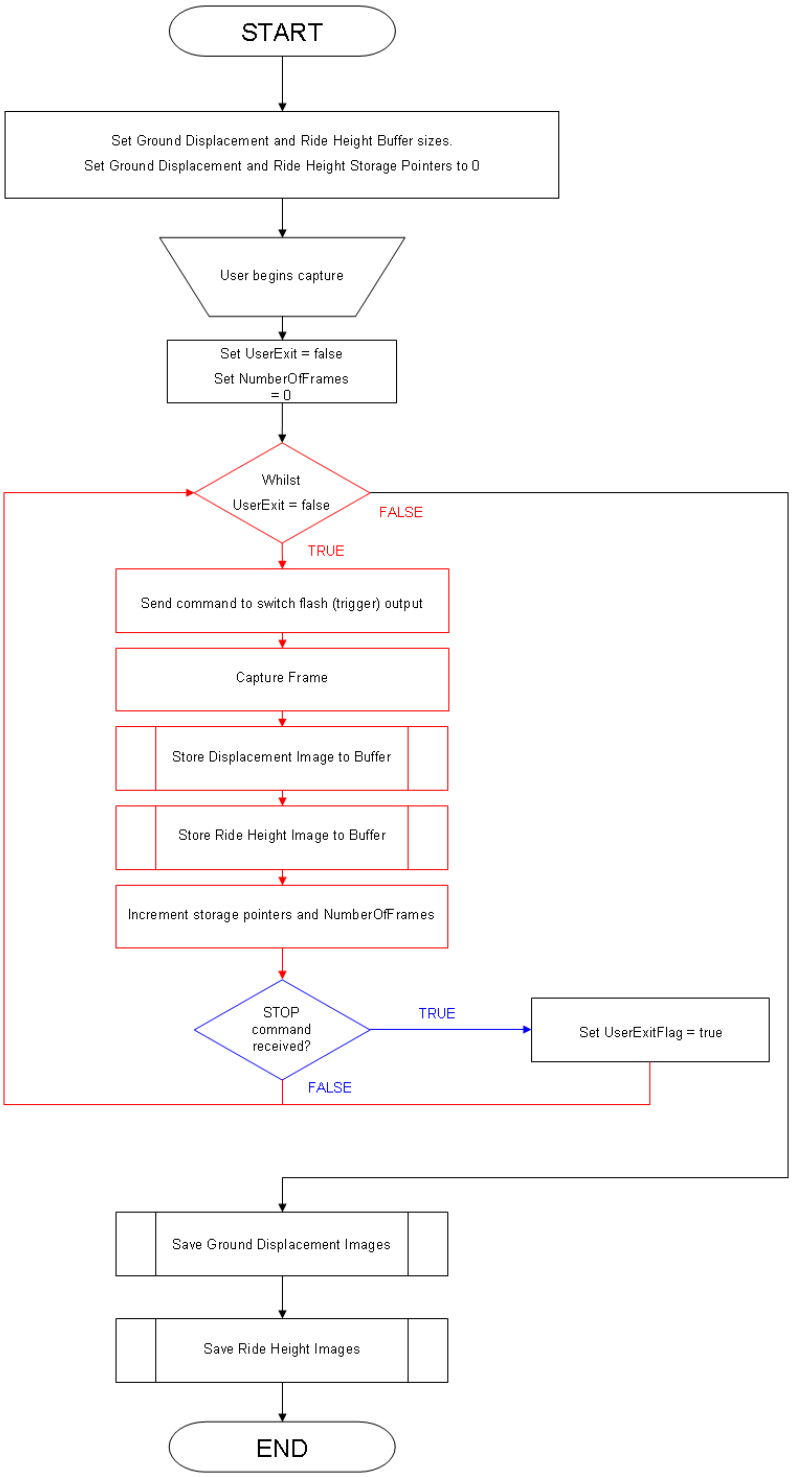

Figure 116 - Program development flowchart for the image capture routine.

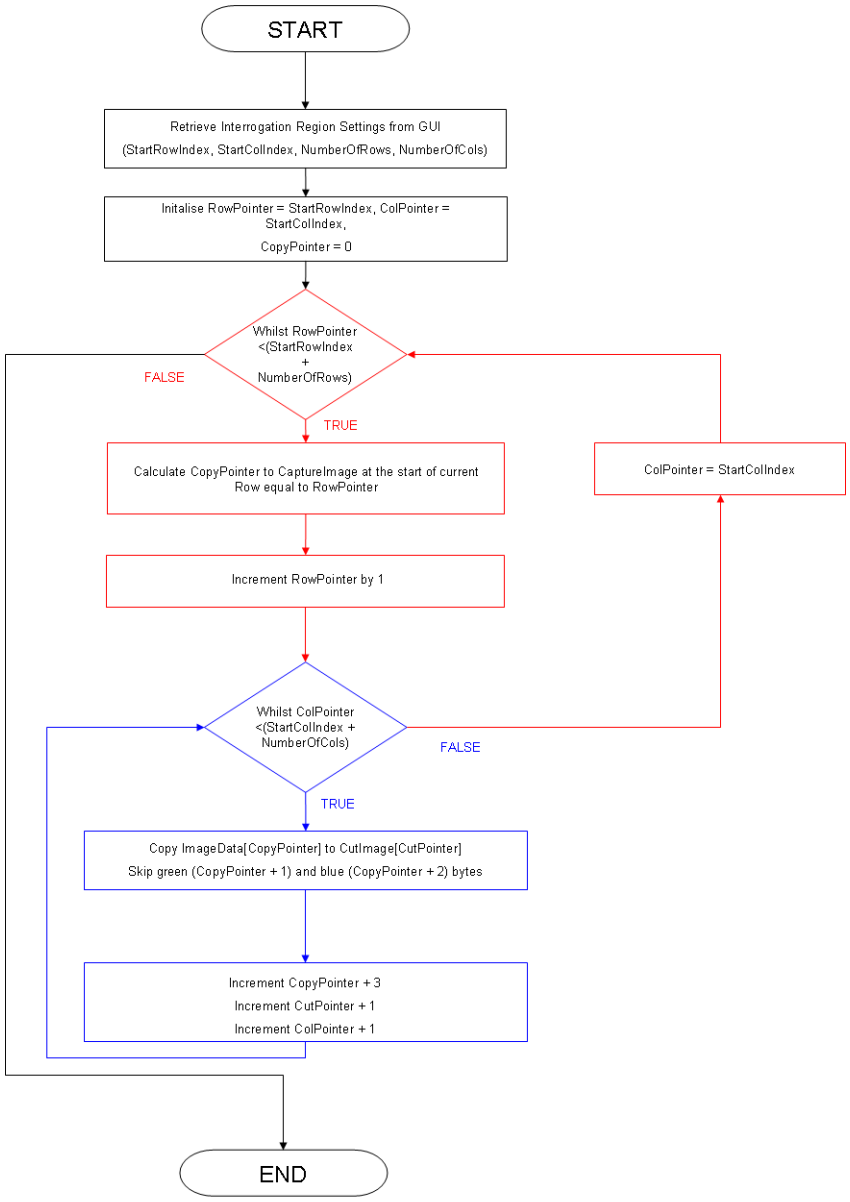

Figure 117 – Flow chart illustrating the image storage routine.

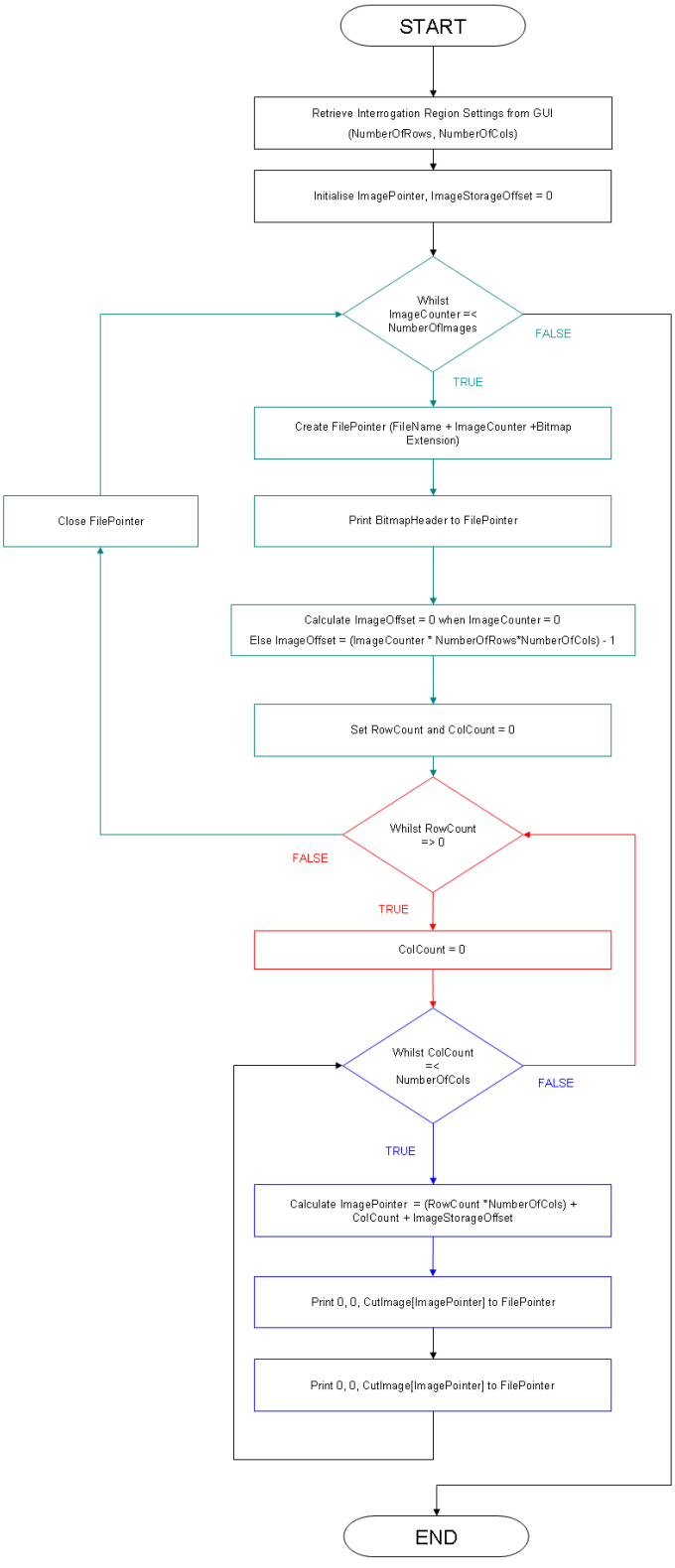

Figure 118 – Flow chart illustrating the image save routine.

The code also commanded the triggering of the illumination prior to the capture image call (see Figure 116) by a call to the camera to switch its trigger output. When received by the strobe controller, this trigger signal prompted it to execute a predefined lighting output characteristic which is illustrated by Figure 119. A series of trial and error tests recording images with a range of exposure and light pulse durations and separations resulted in this particular configuration (these were preveiously illustrated by Table 9).

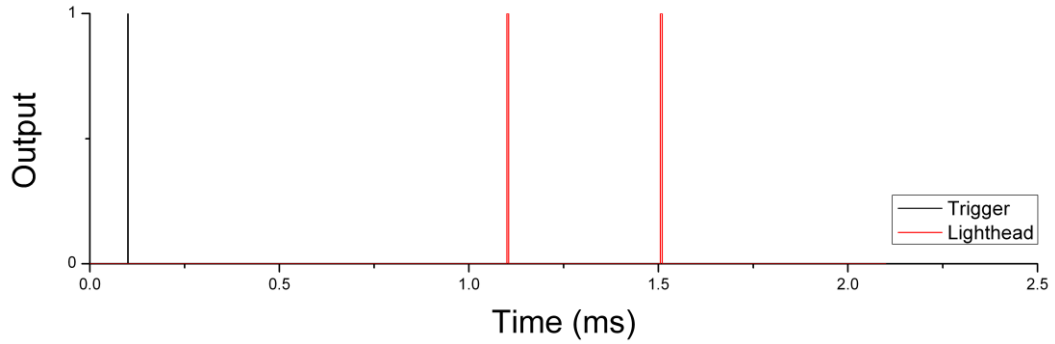

Figure 119 - The trigger and lighting output characteristic.

The trigger signal was followed by a delay from the light unit of 1ms in order that the exposure of the camera could then be commanded before the light head fired the double pulse of light. As described previously it was this trigger signal which was recorded as the time stamp for the image, as it was considered that the time between the trigger command and the capture command which immediately followed would be negligibly small. The time assigned to the image captured was this trigger time plus half the exposure (1ms).

The imaging timing was verified by a series of tests with a Photron high speed camera. Figure 120 shows four images captured from one ODS LED ring at 10000fps and representing two consecutive captures. The times displayed indicate 400µs separations between the double pulses (images 1 and 2 and 3 and 4), and a time of 18.9ms between the capture of the two frames (2 and 3), suggesting the target capture rate of 50fps is met. These results held true for all three ODS.

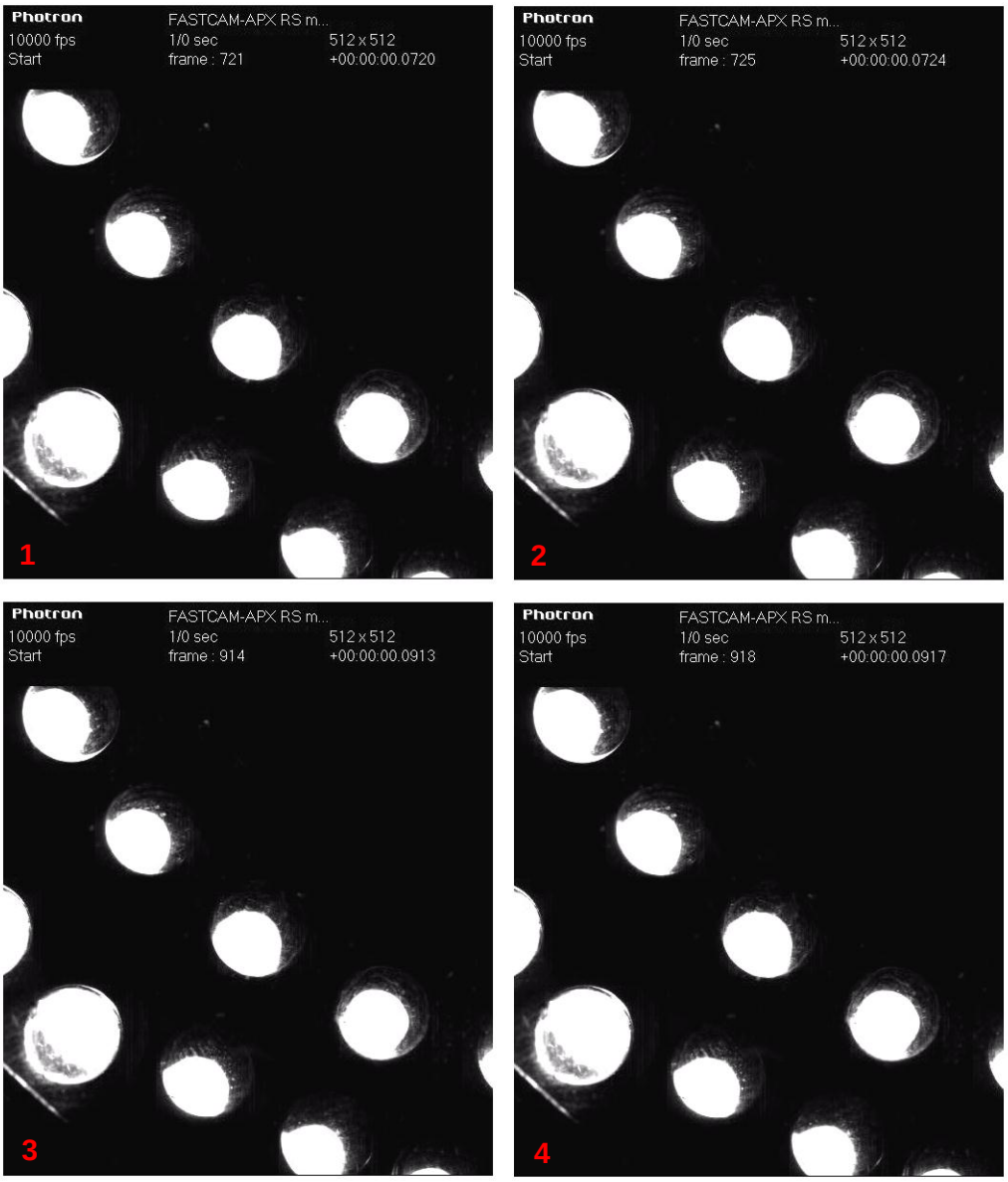

Figure 120 - High speed capture of the LED output, verifying the lighting settings.

6.10 Ground Displacement Analysis Code

In the previous section, the hardware and image capture control was introduced. The other key aspect of the overall functionality of the measurement system was the processing of the captured image data. This section (6.10) considers the

ground displacement analysis, whilst the next (6.11) considers the ride height analysis.

The consideration of the ground displacement analysis code begins with a background of image correlation techniques, before describing the implementation and the necessary image enhancement and solution detection code which was required.

6.10.1 Background

Particle Image Velocimetry (PIV) was introduced at the beginning of this chapter as an application of image correlation techniques, which had partly inspired an investigation of their application to vehicle displacement measurement

As described previously, this system would employ autocorrelation, which involves a pixel by pixel shift of a copy of the double exposed image (I_1) relative to a second static second copy (I_2). At each shift of the image I_1, a statistical correlation of overlying pixels in each image is performed, to give a correlation factor, R. In its direct form described here, it is known as *R(m,n)* and is defined by the following equation (Gonzales and Wintz, 1987):

$$R(m,n) = \sum_i \sum_j I_1(i,j) I_2(i-m, j-n) \qquad \text{Equation 23}$$

Where I_1 is the first image, I_2 is the second image, i is the location in the x (horizontal) direction, j is the location in the y (vertical) direction, m is the shift in the x direction and n is the shift in the y direction.

I_1 is moved relative to I_2 within prescribed limits in both x and y directions. With each shift, R is calculated and recorded to produce the correlation plane described later.

When used for autocorrelation, the static image is typically zero padded with a border of black pixels to the size of the correlation plane (the 2D space containing

the $R(m,n)$ results for the autocorrelation), so that the contribution of a pixel from I_1 not overlapping a pixel in image I_2 is zero. Figure 121 illustrates that the padding only needs to be applied to the right and bottom sides of image I_2 as image I_1 is moved from the top left of I_2 and any location before this starting point would only produce an R value of 0. Therefore the correlation plane produced can be seen to be twice the width and height of the actual image size.

Figure 121 – The unpadded and zero-padded images

The autocorrelation process produces three characteristic correlation peaks (see Figure 122). The largest is formed by the padded and non-padded images overlying each other exactly. The two secondary peaks are equal and symmetrical about the centre of the correlation plane. These represent the two potential correlation results caused by each of the two exposures aligning with their counterpart in the other image, i.e. the second exposure of I_1 aligns with the first exposure of I_2.

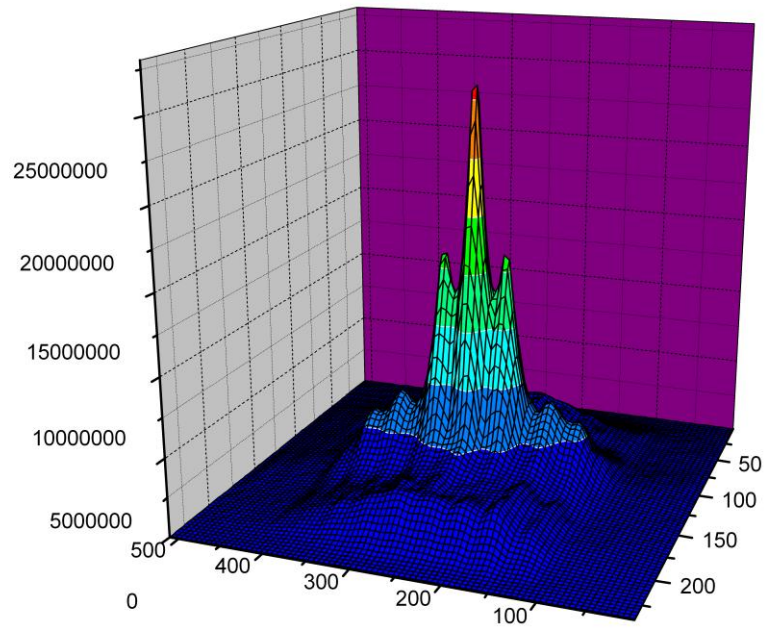

Figure 122 - A plotted 3D colour map surface showing the R correlation value for an autocorrelated double exposed image.

The area imaged with the 8mm focal length lens was approximately 25 x 12mm causing ground features to appear particularly large. This prompted the use of the full 256 x 120 pixels available to maximise the ground detail captured for a successful correlation. This would slow analysis potentially but would allow for a maximum velocity measurement of 50m.s^{-1} (112mph) which exceeded the speed intended for testing.

A typical commercial application would not perform a direct image correlation but would instead perform a Fast Fourier Transform (FFT) to generate the correlation plane in the frequency domain (Anandarajah *et al.*, 2004). This technique is not discussed in significant detail here as its application is impractical because of the requirement of square interrogation regions of dimensions to the power of base-2 (i.e. 16 by 16, 32 by 32 etc). The nature of the motion of the car ensured that the displacement in the longitudinal axis of the car was far greater than that in the lateral axis and therefore it was practical to configure the sensors with the camera frame width aligned with the forward direction of the car. The capture of

256 lines of the frame to make a square interrogation region required by FFT would have likely halved the capture rate of the sensor by more than doubling the pixel data to be read from the camera at each frame. The quantifiable gain of employing a FFT technique however would be a less computationally demanding analysis process with only small error increases. However, the analysis was less significant to this work than the actual capture rate, so it was not employed.

Another consideration when performing correlation analysis of digital images is the two layer discretisation of the process. Both the shift and the image data are discretised and the peak position itself is therefore locked to an integer pixel location. Where necessary a peak fitting algorithm can be applied to the correlation plane peak location to approximate the peak location to sub-pixel accuracy (Anandarajah *et al.*, 2004). However, as the effective resolution was high, with 1 pixel equal to approximately 0.1mm ground displacement, the use of a peak fitting routine was considered unnecessary.

6.10.2 Autocorrelation Code

The autocorrelation code essentially implemented the methodology presented in the previous section. A program development flow chart in Figure 119 illustrates the operation. In order to obtain sufficient image information, the correlation was performed on the entire section of image captured and set aside aside for ground displacement image (rather than a reduced section as hoped), but the pixel shift was limited in order to accelerate processing times, with the shift being greater in the longitudinal direction. Each frame was loaded into two image arrays; one representing the padded and one the non-padded version of the images. Another array, twice the size of each dimension of the image was created to hold the correlation data. A nested for loop was executed for the shift in each dimension, with the correlation being performed within a nested for loop of its own at each shift. The code determined the limits of overlapping pixels within each image so that execution time could be saved by only considering contributing pixels.

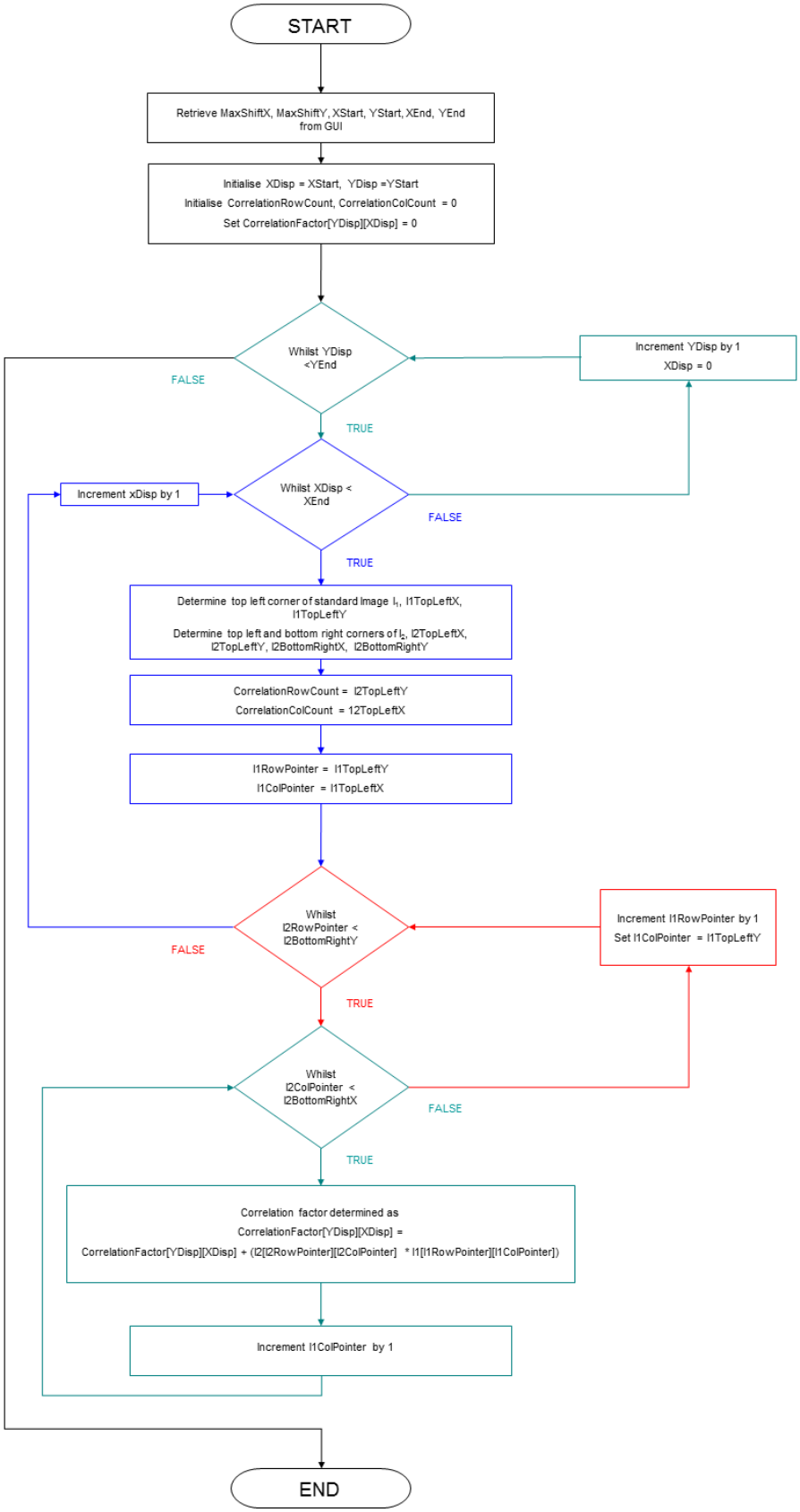

Figure 123 - Program development flow chart of the autocorrelation code.

6.10.3 Image Enhancement

Through testing with preliminary data collected during the hardware development, the software included an image enhancement routine to improve the performance of the correlation. Consideration of an image as collected from the car in Figure 124 illustrates how there is minimal contrast of distinguishable features which can be used as correlation pairs. Figure 125 depicts the same image after the contrast enhancement routine has been applied.

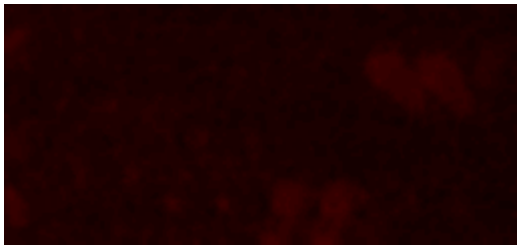

Figure 124 - An image collected for analysis and measurement of the vehicle's x-y displacement, shown as captured.

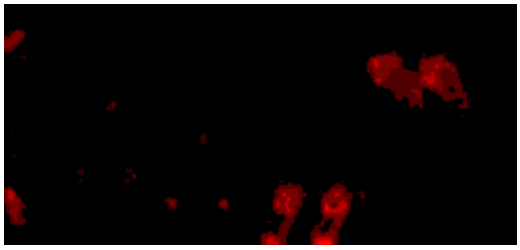

Figure 125 - An image collected for analysis and measurement of the vehicles x-y displacement, shown after contrast enhancement processing.

Figure 126 illustrates the routine for boosting the contrast of an image as a program flow diagram. It essentially normalised an image by the maximum red value present, therefore giving a theoretical red scale of 0 (black) to 1 (full red). The theoretical red scale values were raised to a power, typically 4 as found by trial and error, thus attenuating lower pixel values by an increasing degree. Once the contrast was enhanced the image was scaled back to 0 to 255, to be saved as a bitmap and low pixel values were removed by thresholding to leave key distinguishable features as shown in Figure 125.

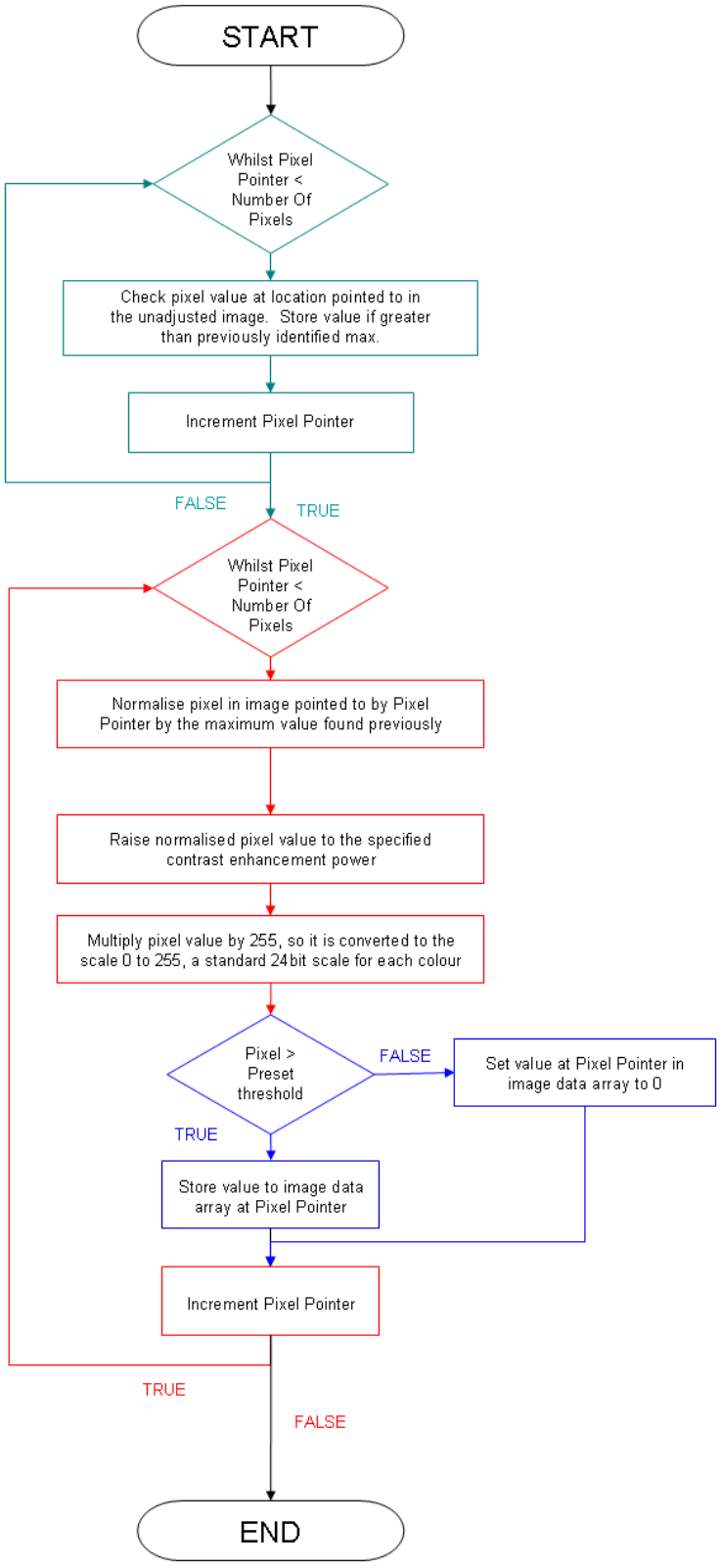

Figure 126 - Flowchart illustrating the execution of the contrast enhancement code.

Although the contrast boosting algorithm increased the number of images in a data set successfully correlating, it was found to not be sufficient to ensure the correct correlation of all images. A series of approaches to rectifying this short-coming were investigated, but ultimately it was determined to be beyond the scope of this work to implement the use of edge detection or similar, which emerged as the most likely next course of action.

A subjective appraisal of images failing to correlate such as Figure 127 illustrates the occurrence of a key issue with the contrast boosting algorithm. The features denoted with the label (A) are paired images of ground features which would likely produce a good correlation. However, it can seen that the large area of pixel data labelled (B), which does not display an image pair, is of a higher intensity. It is believed that this area had the effect of shifting the correlation away from its true location. Therefore, the contrast boosting algorithm was successful at lifting paired features from the background intensity level and hence improving correlation performance generally. However, clearly it had a negative effect when non-descript pixel data existed at a higher intensity than paired features as it was boosted to a higher contrast separation by the algorithm. This is therefore an issue of insufficient signal to noise ratio (SNR).

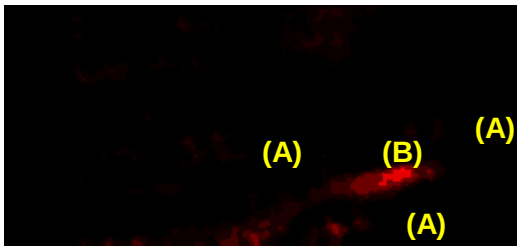

Figure 127 - A contrast boosted image which failed to successfully correlate. (A) denotes features subjectively identified as contributing towards a successful correlation result, whilst (B) denotes the area of high intensity pixel data which was deemed likely to have overpowered the correlation of the other features.

There are various potential solutions to the SNR issue. A higher light intensity would allow a smaller camera aperture to be used, consequently ensuring a sharper focus through the movement range, which would help alleviate blurring and merging of features. A sharper delivery of light, again perhaps from the use of a higher intensity source, would also prevent any motion blur causing these issues. Finally, it is possible that edge detection and enhancement in the image

processing could help address the issue, but this would clearly lead to an increase in computation time for a data set.

6.10.4 Peak Identification

The peaks in the correlation data were identified by a function which scanned through the correlation plane data for a frame, considering the neighbouring points of each location in order to determine the peaks present. It considered the magnitude of all these peaks, excluding the centre peak and took the two next largest as the displacement solutions. The solution with the vehicle travelling forwards was then selected from the two as the final frame solution.

6.11 Development of the Ride Height Measurement Code

The predominant focus of implementing the ride height measurement technique was the identification of the location of the ride height light dot in an image frame. Triangulation of a light source reflecting from the ground surface at an angle was introduced in the literature survey as a principle used to measure height in a range of vehicle ride height sensors. A similar principle was adopted, utilising available image resolution on the camera CCD not required by the ground displacement measurement. Figure 128 illustrates the principle more clearly. It can be seen that as the height of the vehicle changes, the position of the image of the angled light beam in the frame changes. An identification of the location within the frame can be used as a basis for inferring the sensor height from the ground. It was assumed that the height change in the 2ms exposure of a frame could be neglected and so the laser diode was permanently illuminated giving sufficient time to capture a region of full intensity pixel data.

The software development involved identified the location of the dot image along a predefined line through the frame, determined during calibration. This line was

2D due to the effect of the lens-camera cone configuration with a variation in height. The migration and identification of the light dot by the code is illustrated in Figure 128, taken during calibration. The light dot centre was approximated as the centre of the located red pixel data.

The final stage of the height measurement was to convert the identified image centre to a height measurement, based on calibration data collected in the laboratory and described in the following section.

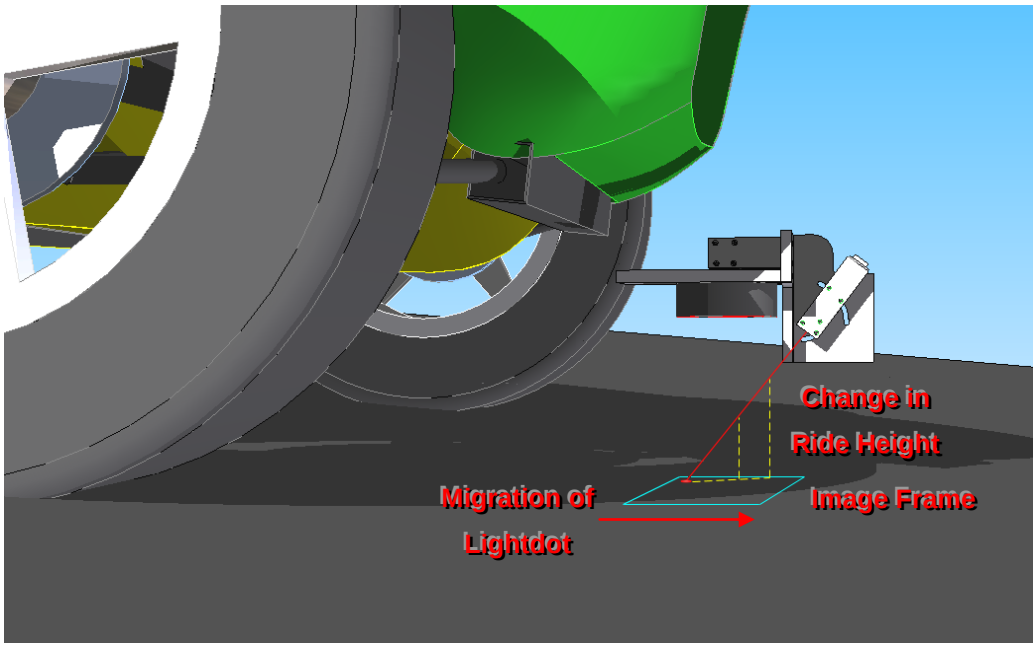

Figure 128 - The sensing principle employed for measurement of vehicle ride height.

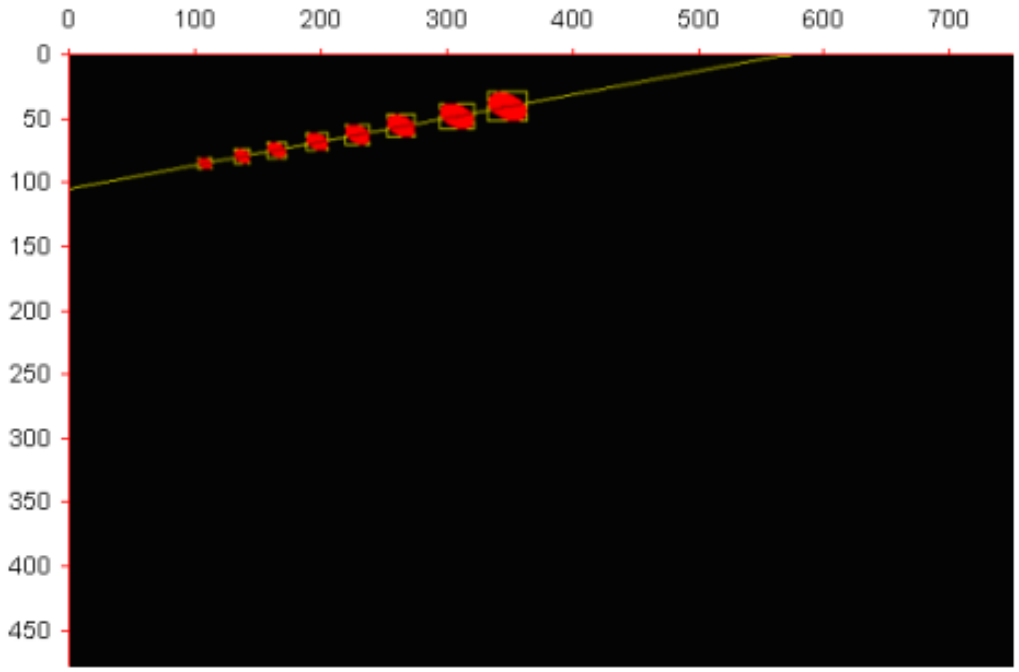

Figure 129 - The migration of the ride height laser diode dot image through the frame during calibration of a sensor.

6.12 Sensor Calibration

Both the ground displacement and ride height measurement required laboratory calibration. The ride height calibration, desecribed first produced a height measure which was subsequently also used as the independent variable in the to calibrate the ground displacement measurement.

6.12.1 Ride Height Calibration

Each assembled ODS was clamped to a piece of steel box plate, facing down towards a laboratory jack, which featured a matte white disc to act as a surface for the light dot image. Figure 130 shows the complete configuration with the insert illustrating the point chosen as the measurement origin; the outside corner of the camera side plate, farthest from the backplate.

Figure 130 - The laboratory calibration setup and origin point.

The height between this reference and the image surface at the location of the light dot could then be easily measured by the CMM in a coordinate frame alignment set on the reference point's camera side plate. The ODS height was determined by measuring planes on both the side plate and image surface, determining a vector distance between the two and taking the z component as the height.

The height of the laboratory jack was then adjusted to effectively change the height of the camera from the image surface. Eight heights were used, with an approximate separation of 5mm and three separate measurements taken at each height to produce an average. The camera was focussed prior to the calibration at 0.2m from the image surface with the largest aperture of F1.4. This represented a good approximation to the working height and the aperture configuration which would be used in testing.

A small VC++ application was created and used to interface with the cameras, collect the pixel coordinates identified and output them as a text file along side measured calibration heights for curve fitting using Origin Lab® 7.5. Two fitted curves were actually required to fully define the calibration of the camera. The

first of these described the lateral and vertical pixel locations of the dot image path traced through the frame, which was used as the search basis for locating the dot image in a recorded frame for measurement. The second curve was of the camera height against the dot image horizontal pixel position and was used with the located dot image centre to determine a corresponding height of the ODS.

A straight line was sufficient to define the horizontal and vertical pixel coordinates of the light dot trace whilst it was found that a second order polynomial was required for defining the calibration curve of the height to horizontal light dot position within the frame.

A comparison of the vertical height to laser diode image centre location calibration curves for the 3 individual sensors can be seen in Figure 131 and shows a good agreement between the three curves, suggesting the calibration was repeatable and one could be confident in each individual set of results.

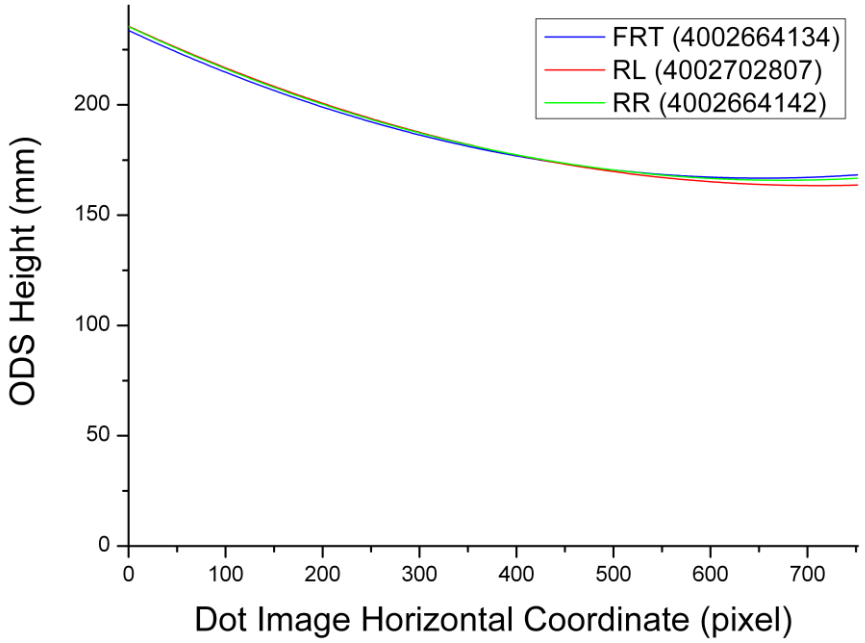

Figure 131 - ODS Height Vs Dot Image Horizontal Coordinate for the three cameras used (identified by the camera serial number).

Further laboratory tests with an application using the code described previously for a single captured frame, showed the calibrations to be accurate with heights measured to within an average error of 0.12mm. These results for the three cameras are displayed in the following table.

Table 10 - Height calibration check results.

FRT – 4002664134

Image	CMM Measures of Height (mm)				Software Height (mm)	Height Error (mm)
	Height 1	Height 2	Height 3	Average		
1	219.58	219.60	219.71	219.63	219.41	-0.22
2	209.35	209.33	209.40	209.36	209.40	0.04
3	199.86	199.81	199.88	199.84	199.87	0.03
4	190.90	190.82	190.90	190.87	190.80	-0.07
5	181.54	181.49	181.55	181.53	181.79	0.24
					Average	**0.12**

RL – 4002702807

Image	CMM Measures of Height (mm)				Software Height (mm)	Height Error (mm)
	Height 1	Height 2	Height 3	Average		
1	219.15	219.03	218.94	219.04	218.88	-0.16
2	209.68	209.54	209.44	209.56	209.64	0.08
3	197.93	197.89	197.85	197.89	197.78	-0.11
4	189.19	189.09	189.07	189.12	188.89	-0.23
5	179.05	179.01	178.97	179.01	179.10	0.09
					Average	**0.13**

RR – 4002664142

Image	CMM Measures of Height (mm)				Software Height (mm)	Height Error (mm)
	Height 1	Height 2	Height 3	Average		
1	219.84	219.88	219.82	219.85	219.71	-0.14
2	210.21	210.17	210.19	210.19	210.18	-0.01
3	200.91	200.89	200.90	200.90	200.84	-0.06
4	190.90	190.86	190.88	190.88	190.84	-0.04
5	180.38	180.39	180.35	180.38	180.65	0.27
					Average	**0.10**

6.12.2 Ground Displacement Calibration

The ground displacement calibration was performed with the same apparatus as the height calibration, with the exception that a section of graph paper was mounted to the imaging surface. Single images were collected from the ODS at

5 heights, again measured by the CMM. The horizontal and vertical pixel to distance ratio was determined manually using Paintshop Pro® 8 and measuring the distance across the same 10mm square appearing in the image. Across the three sensors, the horizontal and vertical values at each height were extremely close allowing the three sets of results to be averaged, producing a single horizontal and vertical value at each height. A 2nd order polynomial displacement calibration curve fitted in Origin Lab® 7.5 to this data gave the lateral and longitudinal vehicle displacement equivalent of a pixel for a given height of the camera/sensor above the ground, as shown in Figure 132.

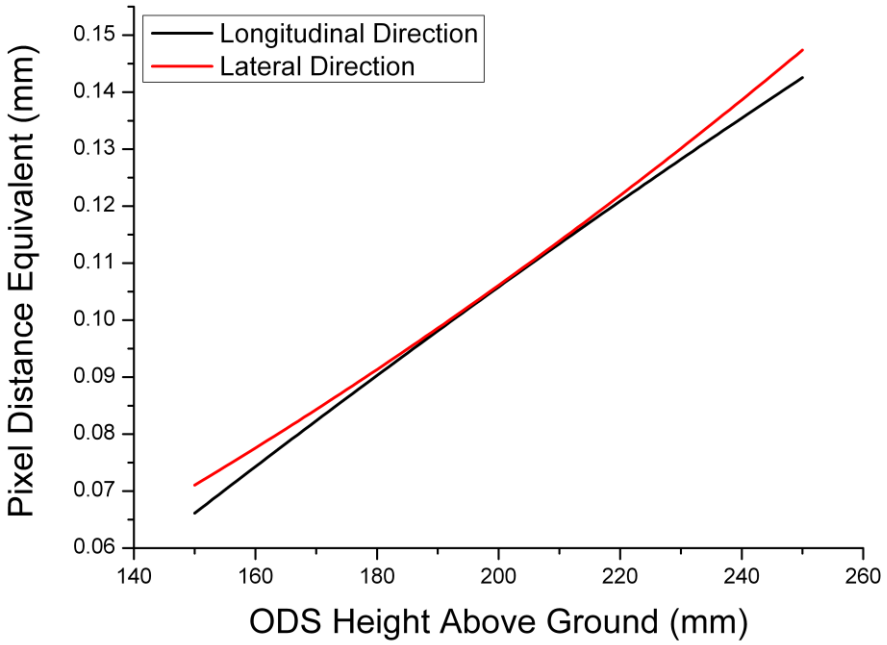

Figure 132 - Distance equivalent calibration curve for 1 pixel displacement at a given sensor height.

6.12.3 Application of Calibrations to Raw Data

The three curves used in the calibration procedure were introduced in the previous sections. The following flow chart (Figure 133) summarises the combination of these to produce calibrated data.

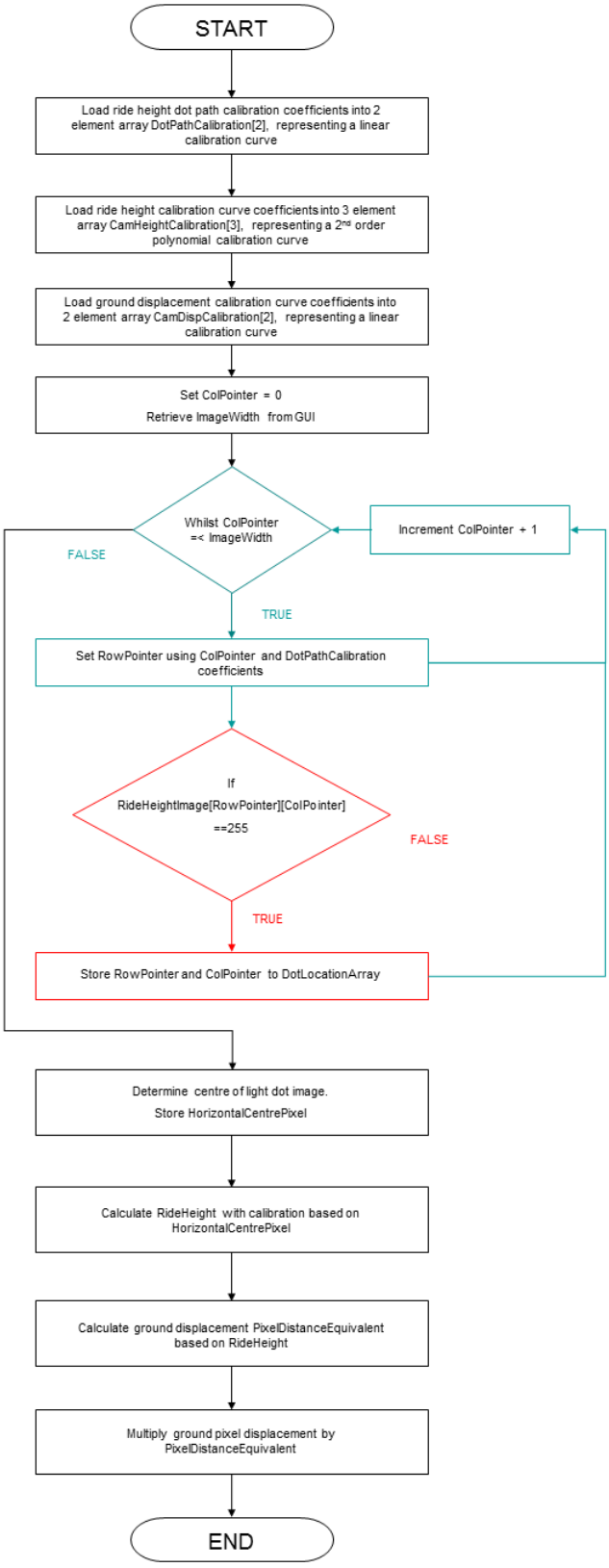

Figure 133 - Flow chart showing the complete process of calibration of raw pixel displacements to measured distance displacements.

The effect of the ground displacement calibration can clearly be seen in Figures 134 and 135. The former shows the pixel displacements measured by the three sensors and determined by the analysis software. There can be seen to be considerable differences between the traces at certain points, primarily during the increase from the start at approximately 39 seconds to greatest peak at approximately 43 seconds. Application of the full calibration routine described in Figure 133 results in the plot of Figure 135. It should be noted that the data describes a straight-line test, so the velocities would be expected to be identical at each point on the car. With the exception of some small deviations, which could be expected from any measurement technique and lateral movement of the car during the very early part of the acceleration when the tyres are establishing grip, the calibration routine can duly be seen to have achieved this.

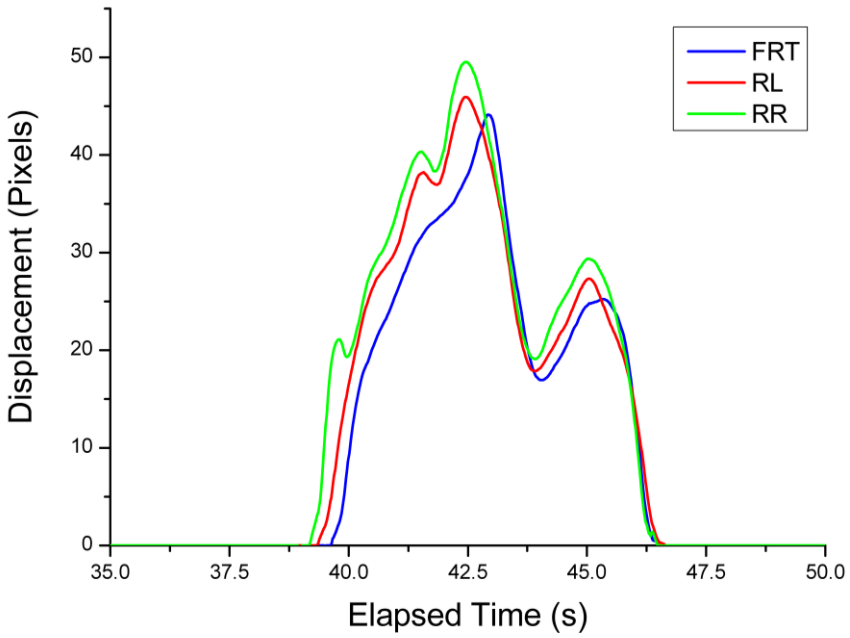

Figure 134 – Pixel Displacement Vs. Time for all three ODS during a straight-line test.

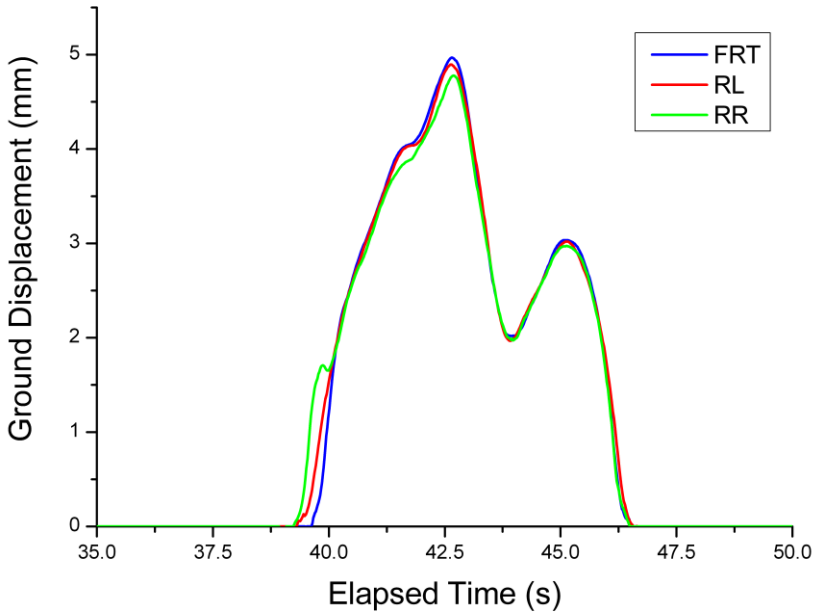

Figure 135 - Calibrated Distance Displacement Vs. Time for all three ODS during a straight-line test.

6.13 Image Timing and Analysis

There were two key issues with regard to the image time; firstly was time stamping images to a common reference, which was achieved by the data logger described in section 6.9.2. This signal required post-processing to extract the actual time as described in section 6.13.1. The second issue was that the trajectory approximation required displacements to be measured against the same instance in time. Since the data logger was sequential and each computer ran at its own frame rate, code was developed to interpolate between measured points to obtain values at the same instance of time from each of the three sensors, as described in 6.13.3.

In between the two sections, to reflect the order that the data is manipulated in the analysis software, the code which catches erroneous results is introduced in section 6.13.2.

6.13.1 Image Timing

The calibration software described in Chapter 5 was expanded to include the frame time stamping based on the identification of rising edges in the recorded trigger signal. A typical signal is shown plotted blue against time in Figure 136, with the rising edges indicated in red. It was determined that the accurate recording of this signal necessitated a capture rate of 2000Hz to ensure that the very short “off time” of the trigger signal was not lost. Identification of the rising edge was by simple sequential comparison of points, which were initially thresholded to two levels, 0 and 1.

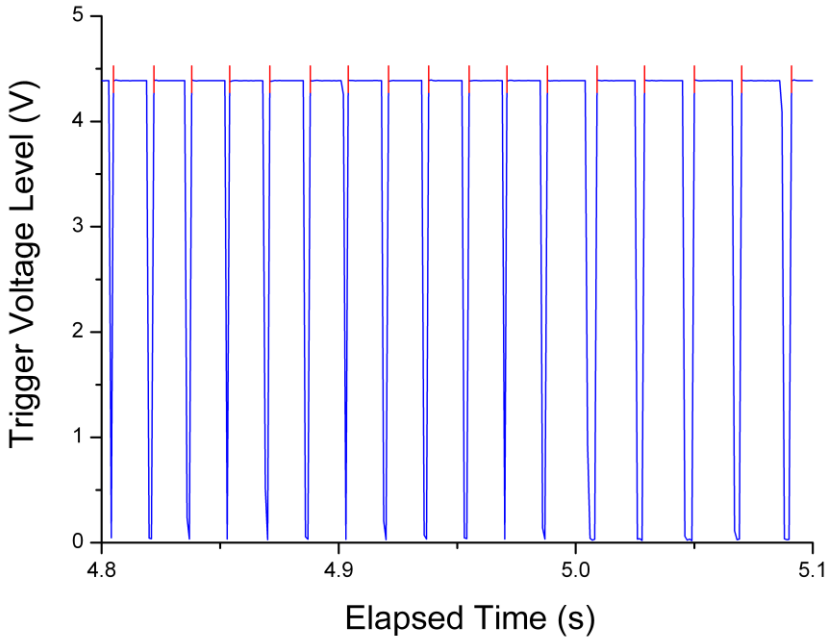

Figure 136 - Graph of raw Front Trigger Voltage Vs Time during 2000Hz sample rate tests. Red markers indicate the calibration software's identification of a rising trigger edge and hence start of a frame.

The process of timing of all trigger signals with the data logger and combining them with the captured images during post processing solved the issue of all three controlling laptops’ clocks being asynchronous to one another.

6.13.2 Treatment of Erroneous Displacements

A separate application completed the post-processing of the recorded displacement image data, albeit without the application of filtering. This outputted the raw ODS data, with erroneous points handled.

Erroneous ground displacements were identified on the basis of a number of criteria which were found to give good indicators of a false result. These included:

- Displacements which exceeded certain preset limits (automatically considered a non-result during the analysis);
- Displacements which were not mirror images of each other within a pixel tolerance (for rounding);
- Displacements which varied too much from the previous result, based on a preset tolerance.

In each of these cases, a result was marked as erroneous and, as the closest approximation of its value, was replaced with a linear interpolation between the accepted solutions laying either side of it. Since the calibrations were all continuous, the interpolated values maintained sub-pixel accuracy.

Ride heights were checked for undetermined results based on their change from the previous measured height. Similarly, if the dot image was not detected, the image was marked as erroneous.

6.13.3 Combining Temporal Data from the Complete ODS System

The three ODSs were all measured against the same temporal scale through the use of a common clock on the data logging laptop. The trajectory reconstruction described in the next section, however required displacement measurement from

each ODS at the same instance in time. Since the three ODS were each run on an independent laptop, a simple post-processing means of achieving this was developed. A VC++ application took the lowest measured time from the three ODS sensors as the starting time and linearly interpolated between the measured points in 0.02s time steps (equivalent to the 50Hz sample rate of the sensors). This accounted for both differing start times and execution rates of the individual sensors.

6.14 Estimating Vehicle Trajectory from ODS Data

This section describes the reconstruction of a 2D trajectory traversed by the car using the measurements recorded from the three ODS, arranged as Figure 137 to form a triangular approximation to the vehicle. It firstly describes the method of reconstruction before also describing signal conditioning applied to the raw error interpolated data.

6.14.1 Trajectory Reconstruction

The level of trajectory reconstruction was maintained at its most basic for this work, but developments of the approach which include the approximation of handling imbalances are described in Chapter 9 as further work.

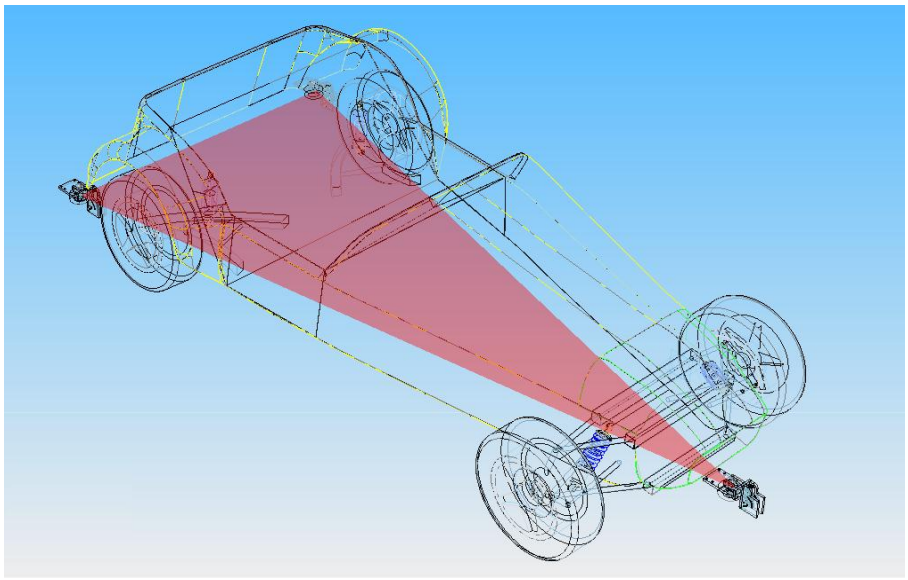

Figure 137 - Illustration of the three ODS locations, forming a plane approximation of the vehicle.

The ODS produced a 2D ground displacement measurement in a frame of reference attached to the vehicle chassis. Therefore the ODS saw all displacements relative to the initial chassis position at the start of the frame rather than a global reference. A simple method was devised for transforming the measured displacements from the car's frame of reference to the global frame of reference.

Figure 138 illustrates part of the principle; the pink triangle overlaying the car is the reconstruction between the measured ODS locations at the start of a frame. If each ODS location is then transformed by the 2D displacement it measured during the frame (assumed to be constant between sample points, so scaled accordingly) the blue triangle results. The vehicle is assumed to have moved a displacement of ds, determined as the distance between the centre of gravity/accelerometer location at each instance in the frame, which is reconstructed relative to the ODS points and used for comparison with the inertial approach also employed.

The heading angle change of the car, $d\psi_t$ is determined as the angle between the line traced from the front ODS to the lateral centre of the line between the two rear ODS at the start and end of the frame. Since the ODS exposure is so short, it is assumed that the same heading angle is maintained throughout the frame.

By this reasoning, the total heading angle of the car, ψ_t can be determined by cumulatively adding each incremental change, i.e. effectively integrating the heading angle change around the lap, in the same vein as for the inertial trajectory approximation routine described previously.

Finally, the heading angle is used to determine the transformed coordinates, by projecting the displacement magnitude ds at this angle. The coordinates of the end point of this line after transformation represent the new trajectory coordinates of the car.

It should be noted that the origin and initial heading angle of the car are as the first frame, therefore in this work they are arbitrary, although attempts were made to ensure they were similar in the lap tests described later. A potential low cost and simple method for allowing the reconstruction to be relative to one point and therefore more directly comparable with another trajectory is given in Chapter 9 during the discussion of further work.

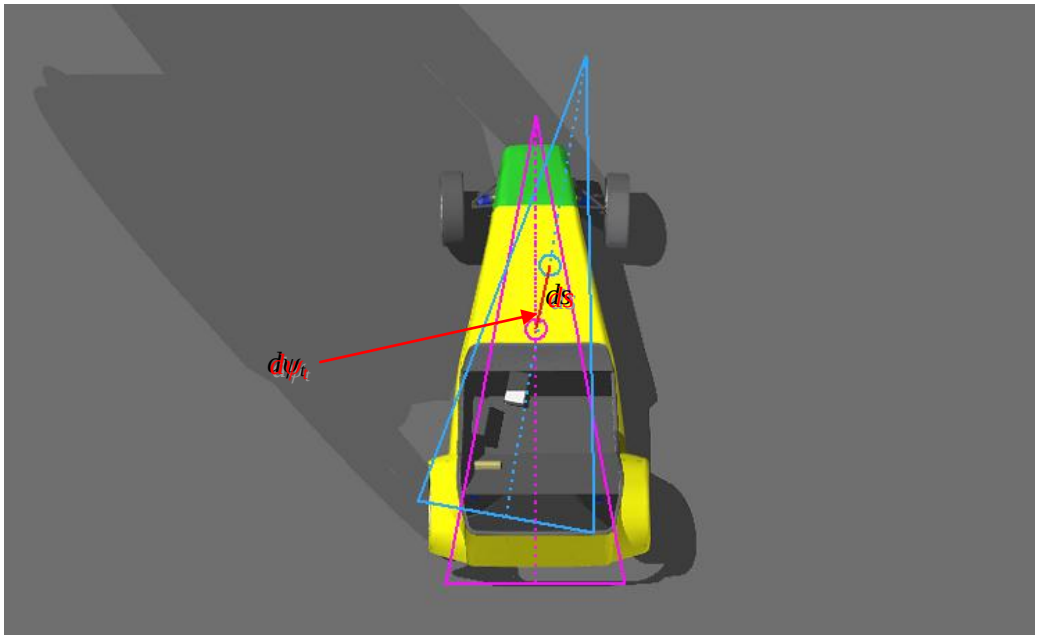

Figure 138 – Plan view illustrating the construction of the triangle representation of the car at the start (pink) and end (blue) of a frame.

6.14.2 ODS Data Signal Conditioning

As one might expect, the data produced by the ODS was extremely noisy and required some signal conditioning before a smooth trajectory could be approximated. This was implemented using Matlab® and the inbuilt RLOESS filter, which subjectively appeared to produce smoothed results whilst maintaining the gross trend of the data.

The filter is based on a regressive linear least squares fit with weighting to reduce the influence of outlying points. It uses a 2^{nd} degree polynomial expression as its curve model. Data was filtered over 50 sample points, representing 1 second of data.

6.15 Closing Remarks

This chapter has presented considerable detail of a system intended to prove the concept of an optical camera based measurement method, inferring displacement from captured ground images. The hardware, measurement principle and the software based methods of achieving this aim have been described.

The next chapter describes the final version of the data visualisation tool which would in part be driven by the data produced by the ODS described here. Chapter 8 describes tests of the ODS system and of its incorporation into the data animation.

Chapter 7

Development of the 3D Data Display Final Version

7.1 Introduction

Chapter 4 presented the development of a graphical data visualisation application which utilised a trajectory approximation method based on lateral acceleration and wheel speed data. Presented here is a development of that system, modelled on the RH2BP and which features two significant advances from the previous version:

- Vehicle trajectory placement is based on the ODS system, described in the previous chapter;
- The suspension and body motion of the car is included, derived from a kinematic model using measured damper displacement and from the ODS ride height measurements respectively.

The computation of the suspension kinematics relative to the car chassis are presented first, prior to a consideration of the vehicle's body placement and motion.

7.2 Suspension Solution

Both kinematic and dynamic models were investigated, their difference being defined by the freedom of the model (Rahnejat, 1998). A kinematic model features purely prescribed motion and no force or torque inputs. A dynamic system has fewer constraints and force or torque inputs are required to calculate the position of those components whose paths are not completely prescribed. The exact configuration of these constraints can vary and there are a number of different possible dynamic models of the same system.

A vehicle will inherently experience compliance in all stressed components during cornering and therefore is more accurately described by a dynamic model

(Blundell and Harty, 2004). However the implementation of a kinematic approach in comparison to a dynamic one is far quicker (Nikravesh, 1988).

Allied to this was the fact that the force measurement required for a multi-body model would require the additional use of strain gauged pushrods to infer the wheel loads. These are seldom used in junior categories because of their cost and their vulnerability in the event of an impact.

Lotus Engineering Software had also developed a kinematic application which overlaid compliance data if required, based on the computed spring deflection (Williams, 2004; Clarke 2005; Lotus Engineering, 2004). This appeared to be a straightforward approach to modelling the vehicle compliance if this was required at any stage.

For these reasons combined, a kinematic approach was developed, in order to best achieve a representative application in the time frame of the research.

7.3 Kinematic Solution Routine

The kinematic routine employed is described in this section. Firstly some additional background to the approach is given, before a description of the implementation is presented.

7.3.1 Background

The Lotus Engineering suspension analysis application could achieve real time calculation of suspension system geometry as well as incorporating the aforementioned compliance of suspension bushes (Williams, 2004; Clarke 2005; Lotus Engineering, 2004).

Reasonably detailed insight into the operation of the suspension analysis application, dubbed SHARK (for Suspension Hardpoint And Real-time

Kinematics) was provided in an SAE paper by Burgess *et al* (2004). The solution to the suspension kinematics is handled in the following stages;

- Firstly the new position of the suspension is calculated from a vector approach, in Cartesian coordinates, after a new input motion constraint is applied. The system is assumed 'pin jointed' (i.e. has spherical bearing type joints) and the kinematics can be solved rapidly. This is incorporated in the formulation approach, using the vector distances between joint locations;
- At each new position of the suspension, the input forces are calculated based upon the spring deflection. The orientation of the suspension bushes are then considered and a calculation of the resulting deformation is the made, based upon the component of force acting on them (dependent on the angle of suspension members and the bushes themselves) and their known stiffness;
- The overall movement of the suspension is determined from the superposition of the kinematic and compliant motion.

It should be noted that this method only considers the vertical force reacted by the spring (determined from its deflection) and not the deformation produced from lateral loads when determining bush compliance. However, the inclusion of this one component of the compliance should theoretically improve the overall accuracy of the software's results.

Burgess *et al* (2004) argued that this multi stage approach was favourable to the strategy of ADAMS, for example, which formulates a single equation including the bush orientation, suspension orientation and so forth. These equations are complex, non-linear and would need an iterative solution technique, which would prevent a real time solution.

The kinematic equations formulated by Burgess *et al* (2004) resulted in 15 individual non-linear equations at each step, for each wheel. They suggested the potential for using many different solvers, but they utilised the Powell Hybrid Method.

As a final stage, various suspension performance parameters, such as camber and castor angles, could be calculated by working out various angles between two points attached at different positions along the stub axle.

A similar technique to this was discussed by Blundell and Harty (2004). However, they suggested the use of the quadratic formula to solve the quadratic equation that arises for a coordinate of each point.

In conclusion, the approach described here appeared to offer the potential of a fast solution routine which would be simple to implement and, if required, provided the flexibility to better represent the vehicle suspension motion later in development by the inclusion of a compliance approximation.

7.3.2 Implementation

The solution strategy used was based upon work described by Blundell and Harty (2004) and by Burgess *et al* (2004). At each stage of movement, three points of known coordinates, which had known fixed lengths to an unknown point, were used to find the coordinates of that unknown point. The formulation was based upon equating the expression for the vector length between each of the unknown points and the one known point with the known length measurements (Equation 24), to yield three expressions of the form shown in Equation 25.

$$|FL| = \sqrt{(KPx - UPx)^2 + (KPy - UPy)^2 + (KPz - UPz)^2} \qquad \text{Equation 24}$$

$$|FL|^2 = (KPx - UPx)^2 + (KPy - UPy)^2 + (KPz - UPz)^2 \qquad \text{Equation 25}$$

Where KP is the known point, UP is the unknown point, x, y and z refer to the coordinates of each point and FL is the fixed length between the known and unknown point.

Values for the coordinates and lengths are then substituted into Equation 25 and when expanded and rearranged give the form in Equation 26 where α, β and χ

are coefficients of UPx, UPy and UPz terms respectively, arising from multiplication of the known points.

$$UPx^2 + UPy^2 + UPz^2 + \alpha UPx + \beta UPy + \chi UPz + C = 0 \qquad \text{Equation 26}$$

There will be three equations of the form of Equation 26, one deriving from each of the known points used in the formulation. If these are denoted equations A, B and C, a further three equations D, E and F are formed by subtracting these equations from one another as Equation 27, eliminating the squared terms in doing so, to result in the form of Equation 28.

$$\begin{aligned} &\text{Equation D} = \text{Equation C - Equation A} \\ &\text{Equation E} = \text{Equation B - Equation C} \\ &\text{Equation F} = \text{Equation B - Equation A} \end{aligned} \qquad \text{Equation 27}$$

$$\phi UPx + \psi UPy + \lambda UPz + D = 0 \qquad \text{Equation 28}$$

Where ϕ, ψ and λ are the resultant coefficients from subtraction of the respective α, β and χ coefficients and D is the equivalent for the coefficient C.

A further equation, labelled Equation H is formed, as illustrated in Equation 29, by subtraction of an interim formulation Equation G from Equation D. This two stage process eliminates the unknown coordinate UPx and is subsequently rearranged in to the form of Equation 30 with UPy expressed in terms of UPz.

$$\begin{aligned} &\text{Equation G} = \text{Equation E} \times \left(UPx_D / UPx_E \right) \\ &\text{Equation H} = \text{Equation D - Equation G} \end{aligned} \qquad \text{Equation 29}$$

$$UPy = \frac{\mu UPz + E}{\xi} \qquad \text{Equation 30}$$

Where ξ is the resultant coefficient of UPy, μ the coefficient of UPz and E is the resulting constant term.

The same approach is repeated, however this time using Equation E in place of Equation D and Equation F in place of Equation E in Equation 29 and instead eliminating y to give Equation 31 with UPx in terms of UPz. Once UPz is determined these equations will give the means of calculating the other two coordinates directly.

$$UPx = \frac{\sigma UPz + F}{\varepsilon} \qquad \text{Equation 31}$$

Where σ is the resultant coefficient of UPx, σ the coefficient of UPz and F is the resulting constant term.

Equation 30 and Equation 31 are substituted in place of UPy and UPx in Equation 26 to give a quadratic expression containing only UPz as an unknown variable, as Equation 32.

$$|FL| = \sqrt{\begin{array}{l}\left(\frac{\sigma^2}{\varepsilon^2}\right)UPz^2 + 2\left(\frac{F\sigma}{\varepsilon^2} - \frac{KPx\sigma}{\varepsilon}\right)UPz + kPx^2 + \frac{F^2}{\varepsilon^2} - \frac{2FKPx}{\varepsilon} + \\ \left(\frac{\mu^2}{\xi^2}\right)UPz^2 + 2\left(\frac{E\mu}{\xi^2} - \frac{KPy\mu}{\xi}\right)UPz + KPy^2 + \frac{E^2}{\xi^2} - \frac{2EKPy}{\xi} + \\ UPz^2 - 2KPzUPz + KPz^2\end{array}} \qquad \text{Equation 32}$$

And rearranged to the quadratic form:

$$0 = GUPz^2 + HUPz + I \qquad \text{Equation 33}$$

Where:

$$G = \left(\frac{\sigma^2}{\varepsilon^2}\right) + \left(\frac{\mu^2}{\xi^2}\right) + 1$$

$$H = 2\left(\frac{F\sigma}{\varepsilon^2} + \frac{E\mu}{\xi^2} - \frac{KPx\sigma}{\varepsilon} - \frac{KPy\mu}{\xi} - KPz\right)$$

$$I = kPx^2 + \frac{F^2}{\varepsilon^2} - \frac{2FKPx}{\varepsilon} + KPy^2 + \frac{E^2}{\xi^2} - \frac{2EKPy}{\xi} + KPz^2 - FL^2$$

Coefficients G, H and I are all known so it can be seen that Equation 32 is a solvable quadratic which will return two solutions of UPz. The two solutions of UPz can then be substituted into Equation 30 and Equation 31 in turn, to yield UPy and UPx respectively. Two possible solutions will therefore result for each point, the correct one being selected by an inspection method described in the next section.

Although not quickly adaptable to different suspension configurations, this solution method was employed as the application was to be totally specific and it would allow rapid direct solution, without the need for iteration, which would greatly slow the solution (Blundell and Harty, 2004). The method would also find a solution, which iterative techniques, such as the Newton Raphson method, do not always guarantee (Papegay *et al*, 2005; Nikravesh, 1988).

This approach was also employed in commercial level software, which gave some support to its use, with Lotus Engineering's suspension analysis application employing the same approach and being able to achieve real time calculation of suspension system geometry (Williams, 2004; Clarke 2005; Lotus Engineering, 2004). It could also incorporate the compliance of suspension bushes as described in section 7.2, which although not incorporated in the final level of the research presented here, was seen as providing a useful capacity for expansion.

The solution of the vehicle suspension points after movement was conducted in a local coordinate frame, which was dictated by the vehicle measurement described in section 5.4. Displacement of the vehicle across the ground and

about its own axis frame, which was determined from the ODS system described in Chapter 6 was then introduced as a separate step.

7.3.3 Solution Selection

A feature of quadratic equations is the satisfaction of two solutions, although only one of these solutions is physically possible in the context of calculated suspension displacement. This was typically determined by inspection (Blundell and Harty, 2004), so a strategy for replicating an accurate inspection was required.

The eventual strategy employed was to determine the magnitude of the vector between the initial coordinates of the system and each of the two solutions after movement was determined using the simple formulation in Equation 34 shown for initial position IP and final position FP, with coordinates x, y and z.

$$\text{Magnitude} = \sqrt{(FPx - IPx)^2 + (FPy - IPy)^2 + (FPz - IPz)^2} \qquad \text{Equation 34}$$

The smallest magnitude of deflection was selected as the correct solution. The method was tested and in all cases of varying levels of deflection it was found that the correct solution could be identified, with one of the solutions always being at least an order of magnitude greater.

7.3.4 Validation of Kinematic Solver

The results produced by the kinematic solution approach were validated against a commercially available suspension kinematics calculation package, Handford Suspension Geometry V3.66 (Handford). Both kinematic solvers processed the CMM suspension joints (the collection of which was described in Chapter 5) with a 30mm vertical wheel displacement or bump. The results for the outboard joint locations matched well. As examples, the results for the front left upper wishbone outboard joint (fluwbo) are presented in Figures 139, 140 and 141.

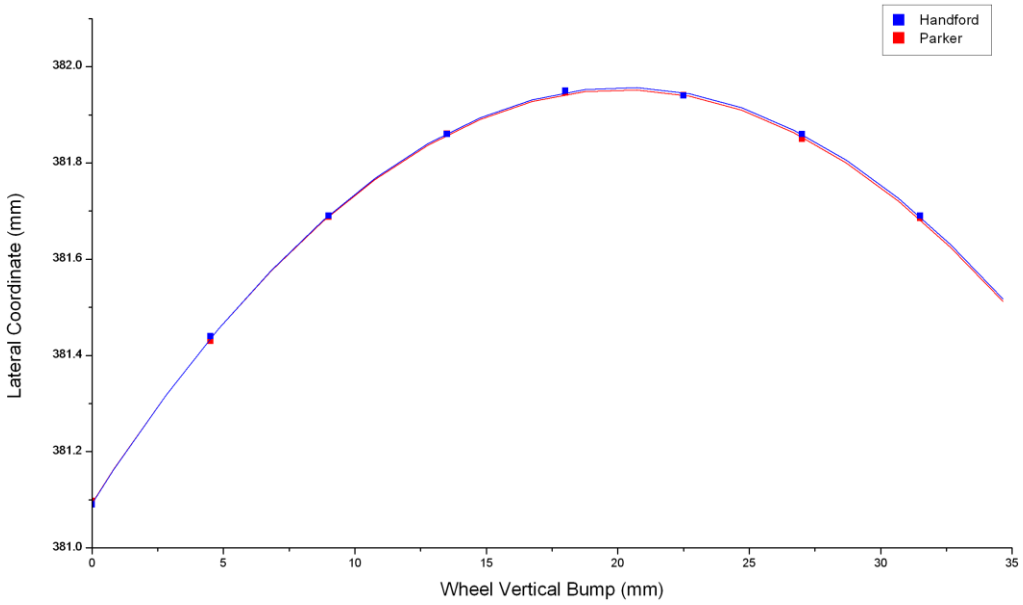

Figure 139 – Lateral coordinate of the fluwbo against wheel vertical bump during a suspension analysis comparison test.

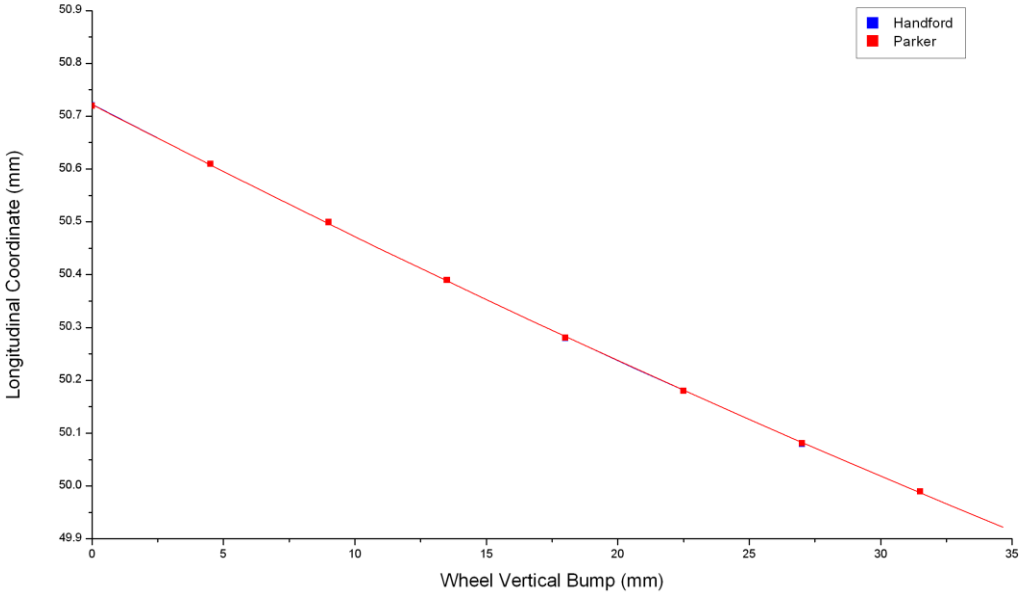

Figure 140 – Longitudinal coordinate of the fluwbo against wheel vertical bump during a suspension analysis comparison test.

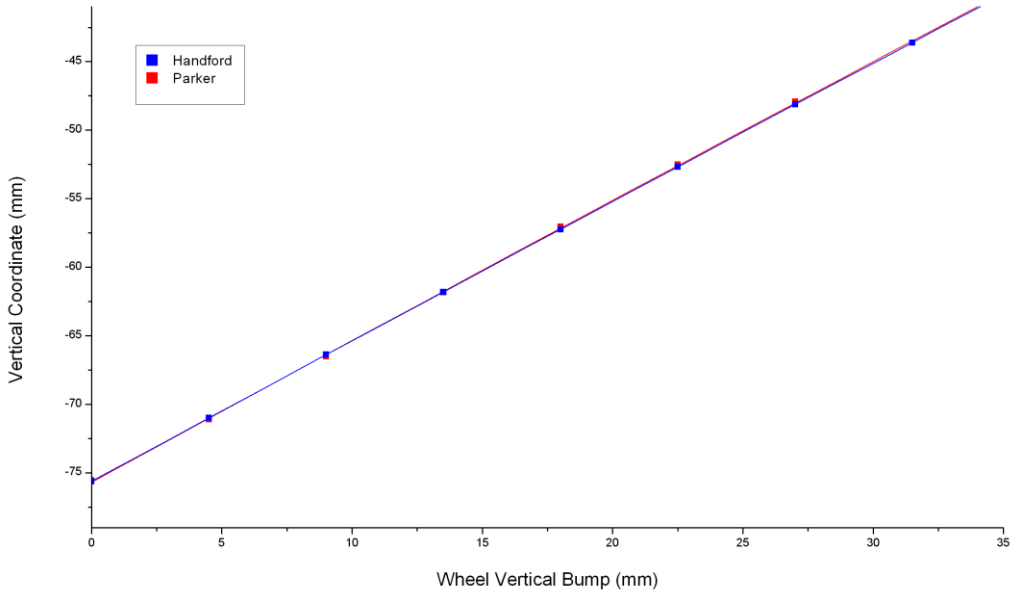

Figure 141 – Vertical coordinate of the fluwbo against wheel vertical bump during a suspension analysis comparison test.

7.4 RH2BP Solution Procedure

The procedure for the kinematic solution of the kinematics of the RH2BP, in terms of the coordinates used to solve the range of unknown points is described below, whereas the mathematics of the solution themselves were discussed in the preceding section. The following description separates front and rear suspensions and uses the left hand side for both examples. However, the right hand solution routine is solved in exactly the same manner. Since both front and rear suspensions are independent (i.e. left and right wheels do not have a mechanical link) the coordinates contributing to the solution of each side belong exclusively to that side also, with the exception of the steering rack measurement, which is recorded on the left hand side but affects both sides.

7.4.1 Front Left Suspension

In the case of the front left suspension the following points (which are also illustrated by Figure 142) need to be determined:

- Front Left Upper Wishbone Outboard Joint – fluwbo;
- Front Left Lower Wishbone Outboard Joint – fllwbo;
- Front Left Trackrod Outboard Joint – fltro;
- Front Left Damper Outboard Joint – fldo;
- Front Left Stub Axle Inboard Point – flsai;
- Front Left Stub Axle Outboard Point – flsao.

The acronyms for all these points are lower case, the convention employed to denote them as unknown at each movement of the vehicle.

The points whose location is known at each movement, namely those which are fixed to the chassis, are denoted as such by the use of an upper case acronym. These are:

- Front Left Upper Wishbone Inboard Rear Joint – FLUWBIR;
- Front Left Upper Wishbone Inboard Front Joint – FLUWBIF;
- Front Left Lower Wishbone Inboard Rear Joint – FLLWBIR;
- Front Left Lower Wishbone Inboard Front Joint – FLLWBIF;
- Front Left Damper Inboard Joint – FLDI.

One special case is the trackrod inboard joint, as this is free to move independently of the chassis by driver input to the steering. This point is therefore denoted unknown, although is determined prior to the kinematic calculation.

- Front Left Trackrod Inboard Joint – fltri.

The calculation of its position is based on a calibration constructed from the CAD model of the car and a series of calibration measurements taken from the steering rack which was described in section 5.7.2.

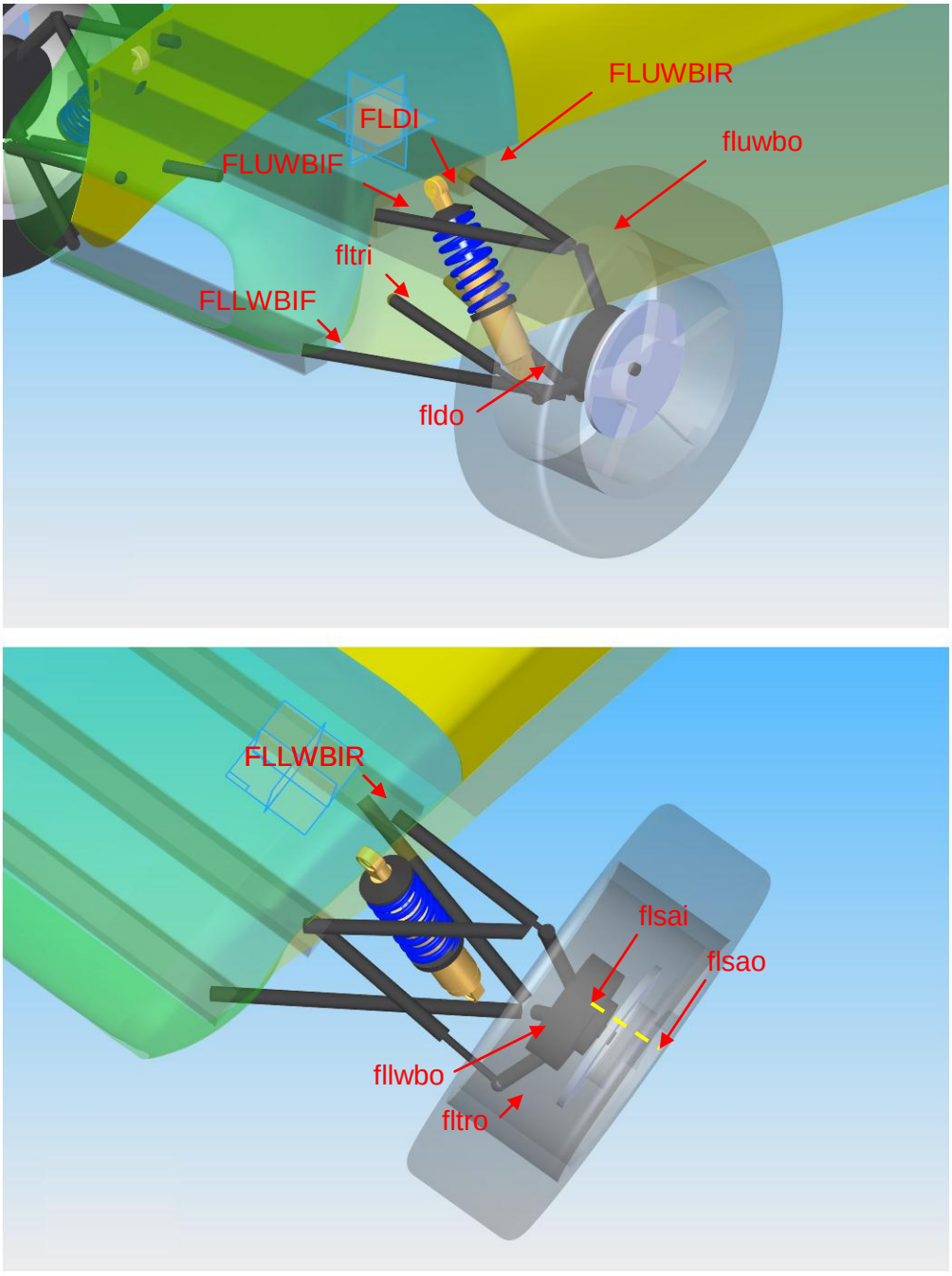

Figure 142 - Screenshots from the Solid Edge ® CAD package, illustrating the location of the coordinates involved in the calculation of the front left suspension kinematics.

A series of fixed lengths between points are also used. These are:

- Front Left Lower Wishbone Inboard Rear Joint to Front Left Damper Outboard Joint - Length_FLLWBIR_fldo;
- Front Left Lower Wishbone Inboard Front Joint to Front Left Damper Outboard Joint - Length_FLLWBIF_fldo;
- Front Left Lower Wishbone Inboard Rear Joint to Front Left Lower Wishbone Outboard Joint - Length_FLLWBIR_fllwbo;
- Front Left Lower Wishbone Inboard Front Joint to Front Lower Wishbone Outboard Joint - Length_FLLWBIF_fllwbo;
- Front Left Damper Outboard Joint to Front Left Lower Wishbone Outboard Joint - Length_fldo_fllwbo;
- Front Left Upper Wishbone Inboard Rear Joint to Front Left Upper Wishbone Outboard Joint - Length_FLUWBIR_fluwbo;
- Front Left Upper Wishbone Inboard Front Joint to Front Left Upper Wishbone Outboard Joint - Length_FLUWBIF_fluwbo;
- Front Left Lower Wishbone Outboard Joint to Front Left Upper Wishbone Outboard Joint - Length_fllwbo_fluwbo;
- Front Left Trackrod Inboard Joint to Front Left Trackrod Outboard Joint - Length_fltri_fltro;
- Front Left Lower Wishbone Outboard Point to Front Left Trackrod Outboard Joint - Length_fllwbo_fltro;
- Front Left Upper Wishbone Outboard Joint to Front Left Trackrod Outboard Joint - Length_fluwbo_fltro;
- Front Left Lower Wishbone Outboard Joint to Front Left Stub Axle Inboard Point - Length_fllwbo_flsai;
- Front Left Upper Wishbone Outboard Joint to Front Left Stub Axle Inboard Point - Length_fluwbo_flsai;
- Front Left Trackrod Outboard Joint to Front Left Stub Axle Inboard Point - Length_fltro_flsai;
- Front Left Lower Wishbone to Front Left Stub Axle Outboard - Length_fllwbo_flsao;
- Front Left Upper Wishbone to Front Left Stub Axle Outboard - Length_fluwbo_flsao;

- Front Stub Axle Inboard to Front Left Stub Axle Outboard - Length_flsai_flsao.

As with the coordinate points, there is again a special case in the damper length which varies with suspension motion. However, this length is measured with the use of a linear potentiometer, as described in section 5.6.5 and so is effectively fixed for the purposes of the kinematic calculation at each point of movement:

- Front Left Damper Inboard Joint to Front Left Damper Outboard Joint - Length_FLDI_fldo;

As was described previously, the basic principle of the kinematic solution of the unknown point involves a triangulation approach from 3 known points.

The solution of the front left suspension kinematics is illustrated by the program flow chart depicted in Figure 143, The series of individual executions of the Kinematic Solver function are shown within a for loop executing the code for each time step and calling for all four car corners (not shown). The kinematic solver function called in the routine was fully described in section 7.3.2.

Figure 143 illustrates how initially the damper length (Length_FLDI_fldo), which was previously mentioned as a special case of a known length that is not fixed, and the front left trackrod inboard joint position (fltri) are determined using predefined calibrations of the linear potentiometers measuring their movement. The six executions of the Kinematic Solver function which follow in each loop then determine the remaining unknown points. It is clear how for each execution three known points and the lengths between them and the unknown point are passed to the solver and that once a point has been determined it can then be used for the solution of subsequent points.

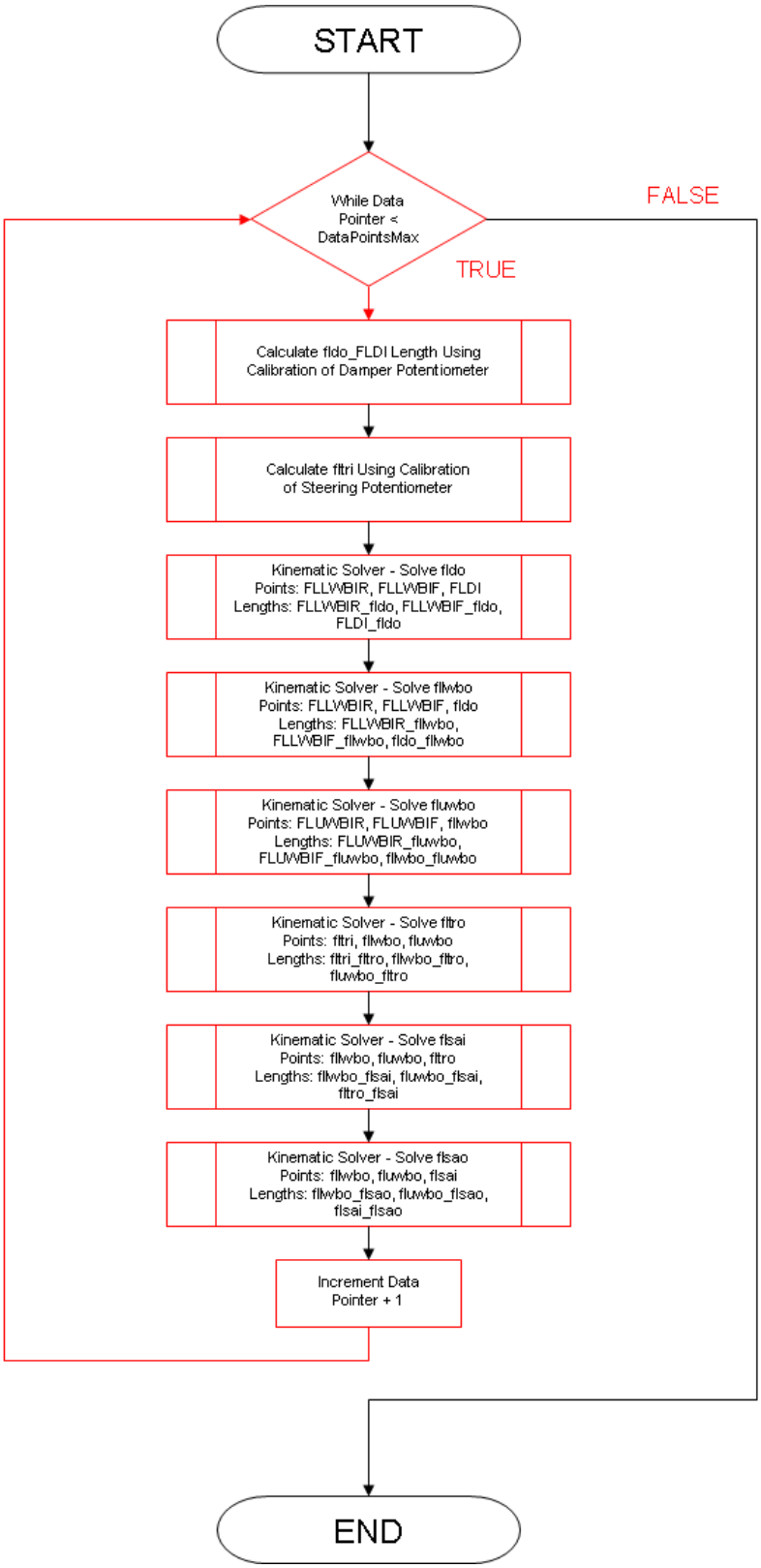

Figure 143 - Program flow chart of the front left suspension kinematic solution process.

7.4.2 Rear Left Suspension

The rear left suspension solution is greatly simplified in comparison to the front owing to the rear suspension configuration of independent trailing swing arms, reducing the unknown points to:

- Rear Left Damper Outboard Joint – rldo;
- Rear Left Stub Axle Inboard Point - rlsai;
- Rear Left Stub Axle Outboard Point – rlsao.

The simplification of the suspension system reduces the known or fixed points to just three:

- Rear Left Wishbone Inboard Joint - RLWBI;
- Rear Left Wishbone Outboard Joint – RLWBO;
- Rear Left Damper Inboard Point – RLDI.

Once again, the positions of all the coordinate points described are illustrated by the Solid Edge screen shots of the vehicle model, shown in Figure 144.

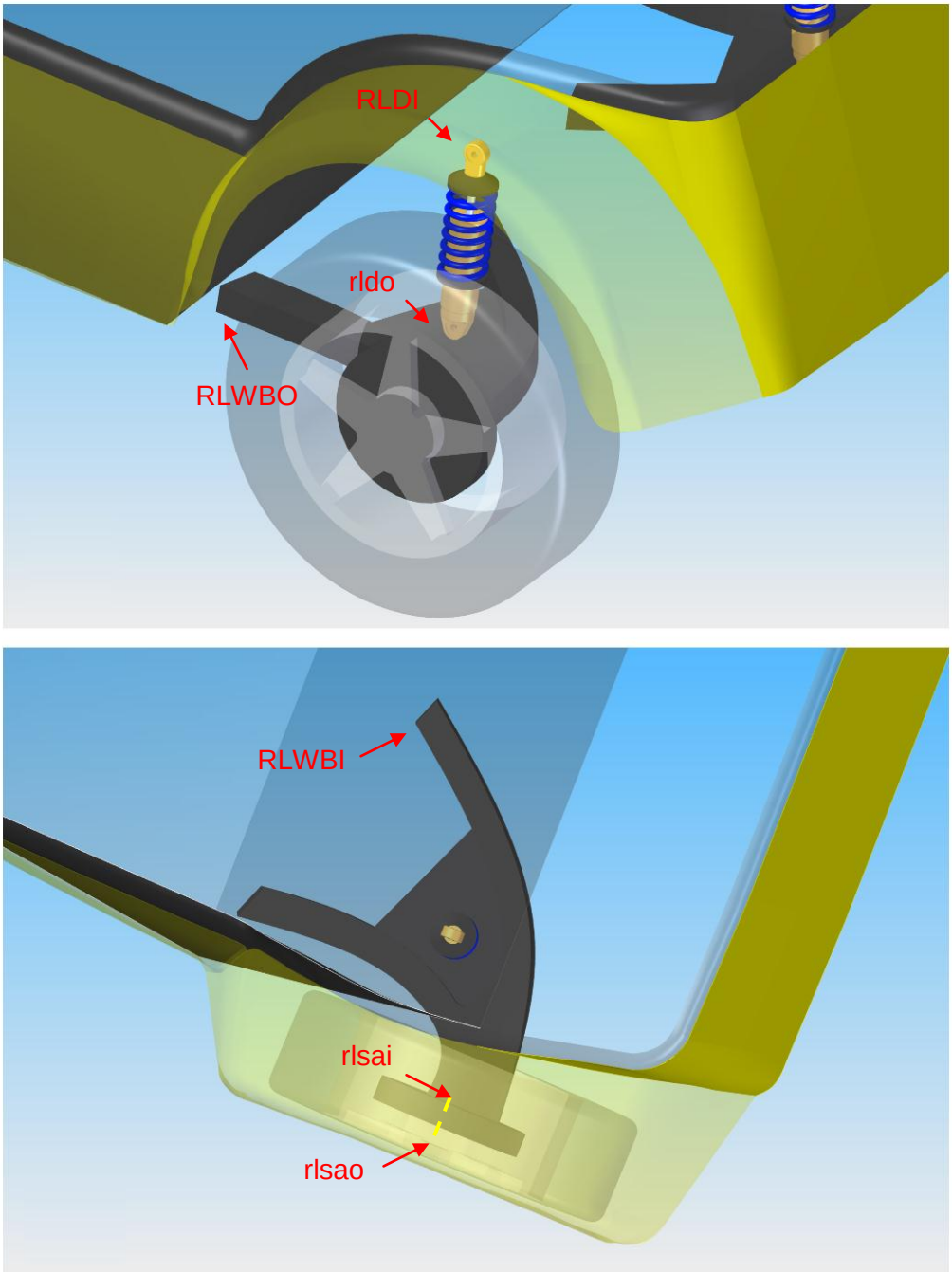

Figure 144 - Screenshots from the Solid Edge ® CAD package, illustrating the location of the coordinates involved in the calculation of the rear left suspension kinematics.

The fixed lengths between points used in the solution procedure are:

- Rear Left Wishbone Inboard Joint to Rear Left Damper Outboard Joint - Length_RLWBI_rldo;
- Rear Left Wishbone Outboard Joint to Rear Left Damper Outboard Joint - Length_RLWBO_rldo;
- Rear Left Wishbone Inboard Joint to Rear Left Stub Axle Inboard Point - Length_RLWBI_rlsai;
- Rear Left Wishbone Outboard Joint to Rear Left Stub Axle Inboard Point - Length_RLWBO_rlsai;
- Rear Left Damper Outboard Joint to Rear Left Stub Axle Inboard Point - Length_rldo_rlsai;
- Rear Left Wishbone Inboard Joint to Rear Left Stub Axle Outboard Point - Length_RLWBI_rlsao;
- Rear Left Wishbone Outboard Joint to Rear Left Stub Axle Outboard Point - Length_RLWBO_rlsao;
- Rear Left Stub Axle Inboard Point to Rear Left Stub Axle Outboard Point - Length_rlsai_rlsao;

Again the damper length is variable but is known from measurement by linear potentiometer:

- Rear Left Damper Inboard Joint to Rear Left Damper Outboard Joint - Length_RLDI_rldo;

As with the case of the front suspension, the solution procedure for the rear occurs within an incrementing for loop, controlled by a variable containing the maximum number of data points, as illustrated by Figure 145. Once again, three known points and their distance to the unknown point are passed to the solver function and once a coordinate is solved it can then be utilised in the solution of subsequent coordinates.

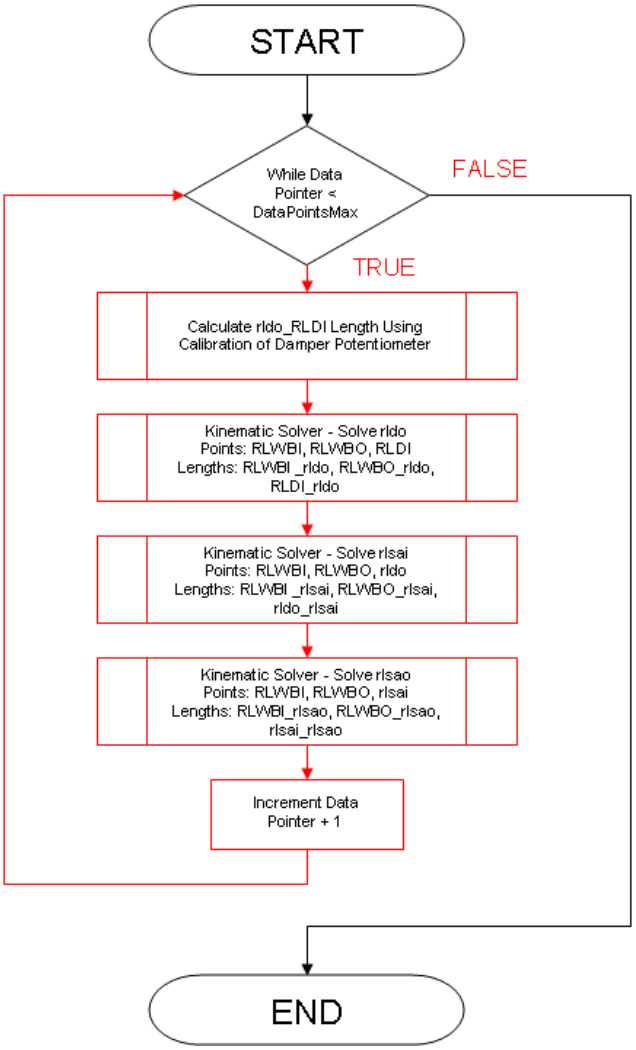

Figure 145 - Program flow chart of the kinematic solution process for the rear left suspension.

7.5 Positioning the RH2BP Model

Several key aspects to the positioning of the model on a ground plane are considered here, to fully reduce the abstraction between the recorded data and the car itself:

- A method of representing a terrain;
- A method of placing the vehicle on that terrain;
- A method of moving the vehicle model in a longitudinal and lateral sense.

The third of these was described in the previous chapter as part of the ODS development. The trajectory reconstruction method resulted in a lateral and longitudinal coordinate at each time step, measured relative to the vehicle's initial position. The representation of the terrain and model placement are described in the next section.

7.5.1 Terrain Representation

The additional complexity required for the positioning the model in an absolute sense on a representation of the circuit itself was deemed beyond the scope of this work. Methods for potentially achieving this and representing the terrain are described as further work in Chapter 9. Here however the terrain was considered flat which was a close approximation to the reality of the test area used. It was modelled using simple polygon drawing functions in OpenGL®.

The further work section describes the detail of some research actually conducted here that would allow from a more robust terrain representation and which could easily incorporate height variations to replicate real world elevation changes.

7.5.2 Vehicle Vertical Positioning

The positioning of the vehicle model at the correct height above the ground plane involved the use of the three ride height measurements made by the ODS system.

At the start of the animation, the ground height is first set to the correct location relative to the model. If Figure 146 is considered, it can be seen that this involves determining the height between the CoG location and the plane through the 3 ODS references (using the vehicle model coordinates). The height of the plane from the ground at the same location is determined using the ride height measurements from the ODS. The summation of these two heights gives the CoG vertical distance from the ground, which can then be used to determine the

vehicle model's origin height from the ground. This measurement is used to draw the ground at the correct height relative to the model origin in its initial location.

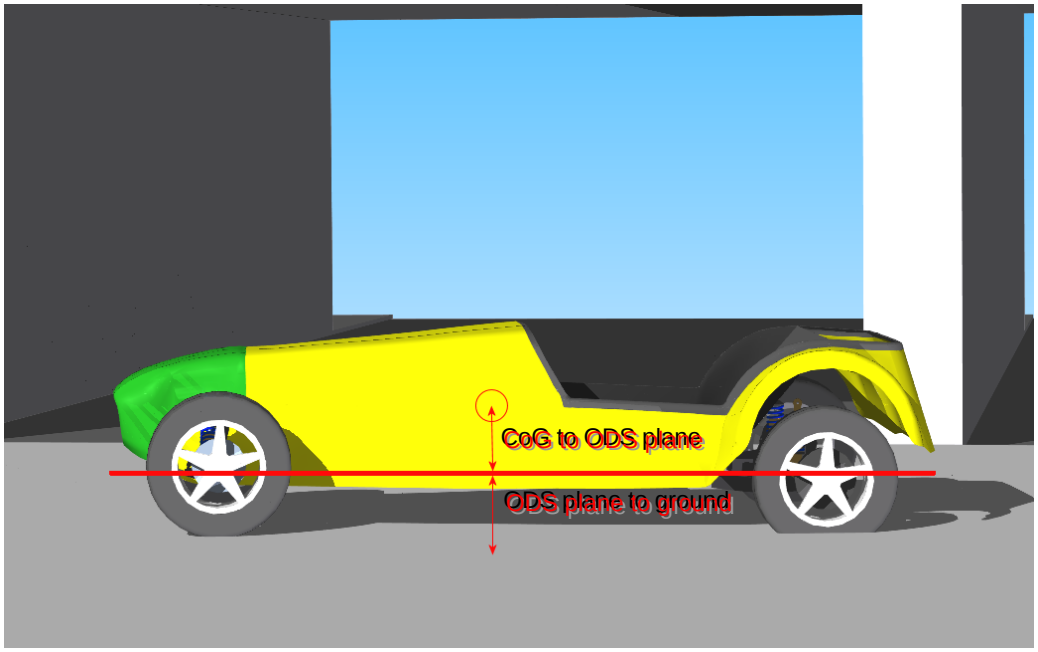

Figure 146 – Determination of the ground plane to vehicle model offset.

At subsequent time steps, the change in plane height, inferred from the three ODS measurements is used to translate all model components vertically. The ODS measurements also allow calculation of the heading, roll and pitch angles, which are applied to all component models, about the projection of the CoG onto the ODS plane during animation.

The calculation of the height to offset the ground initially and then to apply the incremental changes to the model height was made using a function derived from some of the theory surrounding 3D planes described by Ellis and Gullick (1994). Broadly this allowed three known points to define a plane, the defining equation of which could subsequently be used to determine the height of that plane at a location across it.

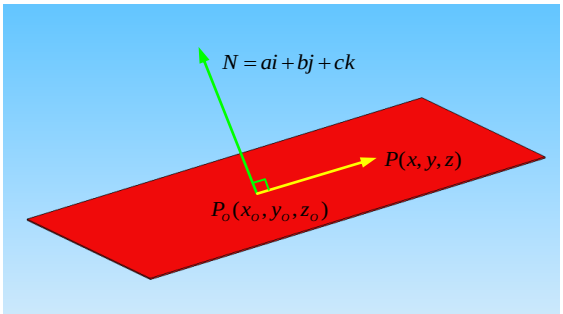

Figure 147- The formulation of a mathematical definition of a plane in 3D space (Ellis and Gullick, 1994)

If the diagram of a plane in Figure 147 is considered, $P_0 = (x_0, y_0, z_0)$ is a point on the plane and $N = ai + bj + ck$ is a nonzero normal vector. $P = (x, y, z)$ is a point lying on the plane, provided that it is perpendicular to the normal N, such that the vector

$$\overrightarrow{P_0P} = (x - x_0)i + (y - y_0)j + (z - z_0)k \qquad \text{Equation 35}$$

satisfies

$$N \cdot \overrightarrow{P_0P} = 0 \qquad \text{Equation 36}$$

Equation 36 can be expanded to give

$$a(x - x_0) + b(y - y_0) + c(z - z_0) = 0 \qquad \text{Equation 37}$$

If the left hand side is expanded and the known terms are moved to the right Equation 38 results

$$ax + by + cz = d \qquad \text{Equation 38}$$

where $d = ax_0 + by_0 + cz_0$

Determination of the coefficients a, b, c and d therefore allow the plane to be defined. Knowledge of three non-collinear points on a plane P_0, P_1 and P_2 allows this. These would be the 3 ODS measurement origins. The normal to the plane can be found by using vectors between one point and the other two, $\overrightarrow{P_0P_1}$ and $\overrightarrow{P_0P_2}$. Since both these vectors must be parallel to the plane, since all the points involved lie on the plane, the cross product of the pair will be equal to the normal to the plane; a vector perpendicular to both.

If

$$\overrightarrow{P_0P_1} = (x_1 - x_0)\mathrm{i} + (y_1 - y_0)\mathrm{j} + (z_1 - z_0)\mathrm{k} \qquad \text{Equation 39}$$

and

$$\overrightarrow{P_0P_2} = (x_2 - x_0)\mathrm{i} + (y_2 - y_0)\mathrm{j} + (z_2 - z_0)\mathrm{k} \qquad \text{Equation 40}$$

then

$$N = \overrightarrow{P_0P_1} \times \overrightarrow{P_0P_2} = \begin{vmatrix} \mathrm{i} & \mathrm{j} & \mathrm{k} \\ x_1 - x_0 & y_1 - y_0 & z_1 - z_0 \\ x_2 - x_0 & y_2 - y_0 & z_2 - z_0 \end{vmatrix} \qquad \text{Equation 41}$$

which gives

$$\begin{aligned} N = &\left[(y_1 - y_0)(z_2 - z_0) - (z_1 - z_0)(y_2 - y_0)\right]\mathrm{i} \\ &- \left[(x_1 - x_0)(z_2 - z_0) - (z_1 - z_0)(x_2 - x_0)\right]\mathrm{j} \\ &+ \left[(x_1 - x_0)(y_2 - y_0) - (y_1 - y_0)(x_2 - x_0)\right]\mathrm{k} \end{aligned} \qquad \text{Equation 42}$$

Since N is normal to the plane and P_0 lies on the plane, Equation 36 can be completed, to define the plane:

$$\begin{aligned} &\left[(y_1 - y_0)(z_2 - z_0) - (z_1 - z_0)(y_2 - y_0)\right] \times \left[x - x_0\right] \\ &- \left[(x_1 - x_0)(z_2 - z_0) - (z_1 - z_0)(x_2 - x_0)\right] \times \left[y - y_0\right] \\ &+ \left[(x_1 - x_0)(y_2 - y_0) - (y_1 - y_0)(x_2 - x_0)\right] \times \left[z - z_0\right] = 0 \end{aligned} \qquad \text{Equation 43}$$

and can be rearranged to:

$$\begin{aligned}&[(y_1-y_0)(z_2-z_0)-(z_1-z_0)(y_2-y_0)]x\\&-[(x_1-x_0)(z_2-z_0)-(z_1-z_0)(x_2-x_0)]y\\&+[(x_1-x_0)(y_2-y_0)-(y_1-y_0)(x_2-x_0)]z\\&=\\&[(y_1-y_0)(z_2-z_0)-(z_1-z_0)(y_2-y_0)]x_0\\&-[(x_1-x_0)(z_2-z_0)-(z_1-z_0)(x_2-x_0)]y_0\\&+[(x_1-x_0)(y_2-y_0)-(y_1-y_0)(x_2-x_0)]z_0\end{aligned}$$

Equation 44

The right hand side of Equation 44 is a constant for a given plane, made entirely from known points. The left hand side has 3 variables; the x, y and z coordinates of a point anywhere on the plane. Therefore for a given lateral and longitudinal coordinate, the corresponding vertical coordinate of the plane can easily be extracted from Equation 44; the method employed to determine the height changes of the vehicle model described previously.

The approach of positioning the chassis from the ODS measurement of its height from the ground and the subsequent incorporation of the wheel motion from the recorded damper and steering displacement sensors effectively replicates the effect of tyre compliance or a tyre coming out of contact with the ground, without the need for tyre simulation. This, however, is based on the assumption of no compliance in the chassis and suspension members which, in reality, will introduce an additional component of deflection.

7.6 Implementing the Animation

The implementation of the final data animation used the same fundamental approach as that described for the preliminary version in Chapter 4. The key additional requirement was the movement of suspension components from spring deflection and steering input motion and of the vehicle chassis through changes in ride height and attitude. This was achieved by combining rotations using the same quaternion approach described previously. Rotations were clearly about various different origins depending upon the component being transformed and

were determined from the calculated joint positions determined by the kinematic solver described in this chapter.

The animation involved determining the vehicle and trajectory heading from the ODS data and as such suffered similarly to the inertial trajectory approach described in Chapter 4, as a handling imbalance influenced the vehicle trajectory. The motion of the steering however did serve to give a visualisation of the handling imbalance. A potential approach to better illustrate the handling imbalance of the car is described in the further work section in Chapter 9.

7.7 Display Layout and Features

The display was to be similar to that designed for the preliminary version described in Chapter 4, again featuring a large scale view of the car to give a good reference with the surrounding terrain, a close scale view of the car to illustrate detail and a graph window.

This version included a closer view of the front suspension and also a plot of the trajectory for reference to the animated data, as illustrated in Figure 148.

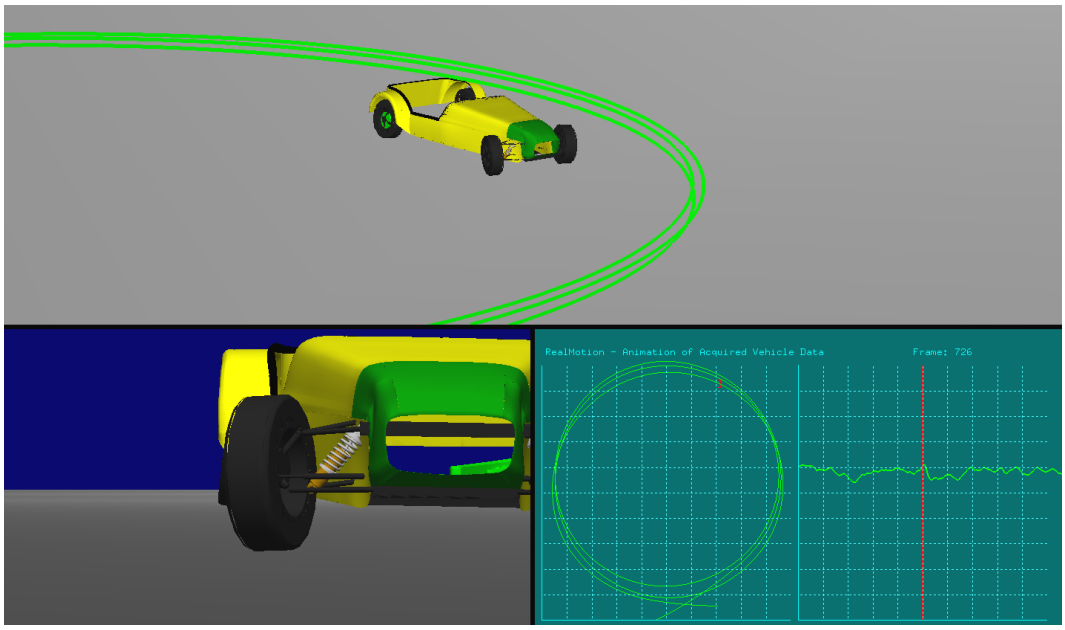

Figure 148 – The layout of the display for the final version of the data animation tool.

7.8 Closing Remarks

This chapter has described the extra complexities of developing the data animation tool to replicate suspension and body motion. This has involved calculating the motion of all components through the use of a direct kinematics solver. It has also required the development of the display to include the extra component rotations and placement of the vehicle chassis model relative to the ground, driven by the ODS height data.

The following chapter presents the final section of work conducted during this research. It details the results of tests conducted to evaluate the ODS system as well as the ability of the data animation tool to present data to the user.

Chapter 8

Testing and Results

8.1 Introduction

The testing reported in this chapter focuses on the final version of the data visualisation tool and the completed ODS system.

The testing of the ODS is considered first. Laboratory tests during the calibration of the sensor had indicated that the accuracy of height measurement was approximately 0.12mm and the ground displacement could be measured to 0.1mm assuming pixel accurate results of the autocorrelation procedure. However, the achievable accuracy of the system in operation would be reduced by a range of factors such as vibration, time between image captures and the robustness of the autocorrelation procedure to extract results from real images. Field tests would give therefore an indication of the practical accuracy of the system and its potential for further development. Additional tests are described in the Further Work section which would allow a more precise conclusion of the system's accuracy to be drawn.

Only a small volume of the total testing of the system is described in this chapter. In reality the duration of testing covered six months of work on a largely trial and error basis. This was the only realistic method for gaining an appreciation of the various issues affecting the operation of the ODS when mounted to a moving vehicle and prompted many of the design features discussed in Chapter 6.

Three tests, conducted with the ODS are described here, considering the system's ability to first measure speed in a straight-line and then subsequently displacement on a curved track; first a circular course before a more complex trajectory with turns in both directions was considered.

8.2 ODS Test1: Straight Line

The first test aimed to evaluate two key aspects of the operation of the optical sensor:

- The sensor's ability to measure speed and distance over a known track length;
- The ability of the optical sensor to record distance measurements during the event of the measured wheels locking under braking.

Previously some of the sources of error associated with the use of a Hall Effect type proximity switch for measuring wheel speed were identified. Issues with tyre growth, wear and pressure and the vehicle suspension geometry all influence the rolling circumference of the tyre and thereby the calibration of the measured rotation to a ground speed. However, the key focus of this test would be of the biggest single factor ruining a data set; that of the measured wheels locking under braking.

The test was therefore a simple straight-line test over a measured distance of 50m. The brakes were applied sharply during the run such that both front wheels locked. The test would only focus on a single optical sensor (the front) and as such was considered purely as a vehicle speed measurement instrument.

The speed readings from each of the two front wheel speed sensors are first presented alongside the front optical sensor's vector velocity and longitudinal velocity component in Figure 149. At low speeds the results from both sensors are inaccurate. The optical sensor fails to produce a displacement at a very low speed (below 6 pixels displacement), as the correlation routine does not detect a distinct shift/result. The moving point average applied to the wheelspeed data smoothes the trace produced, since the low speed means there are very few points over which to average (the number of measurement points per unit time is proportional to the speed of rotation). In practice, data at such low speeds would be of minimal importance to race car data analysis, only being relevant to the analysis of race starts.

Aside, from the low speed inaccuracies and differences, it can be seen that the trend of the results is similar for both the optical and wheel speed sensors, with the key exception of the front brakes locking, which occurs at approximately 42.7 seconds.

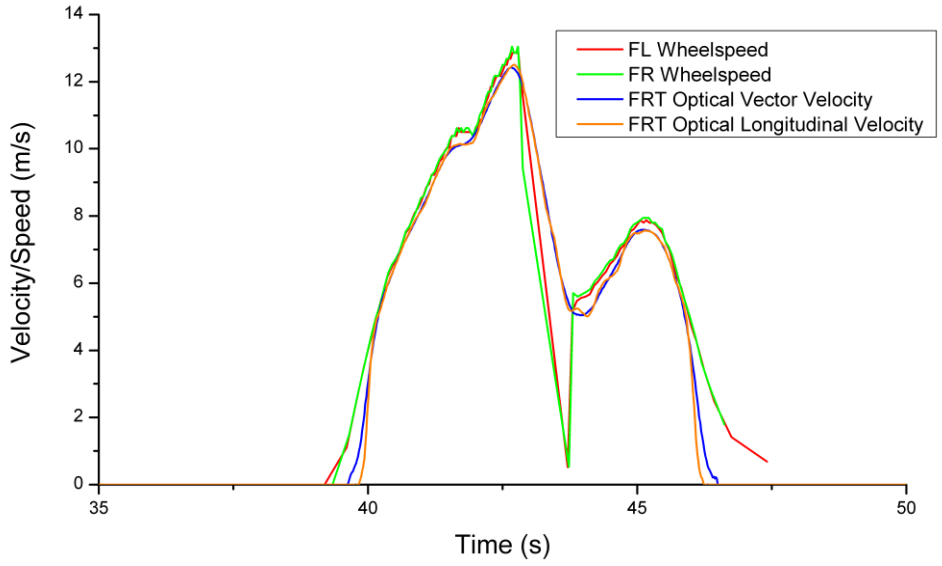

Figure 149 - Speed/Velocity Vs. Elapsed Time during the straight-line test.

The drop in the wheel speed signal caused by the wheel locking is of some use in identifying clearly the occurrence of a brake locking, although it is clear from Figure 149 that the use of the wheel speed data streams alone for analysis of the vehicle speed during this event is not viable. However, the combination of both wheel speed and optical data streams not only provides the identification of the brakes locking, but also continues to provide accurate speed measurements from the optical sensor throughout the event.

It should also be beneficial to note the detail of the optical sensor trace. In Figure 149 the optical sensor can be seen to match the wheel speed sensor in following finer detail in the vehicle's behaviour, when the throttle is lifted for a gear shift at 41.7 seconds, as illustrated in data collected and plotted in Figure 150. The acceleration of the car reduces as would be expected as is captured by both sensor approaches.

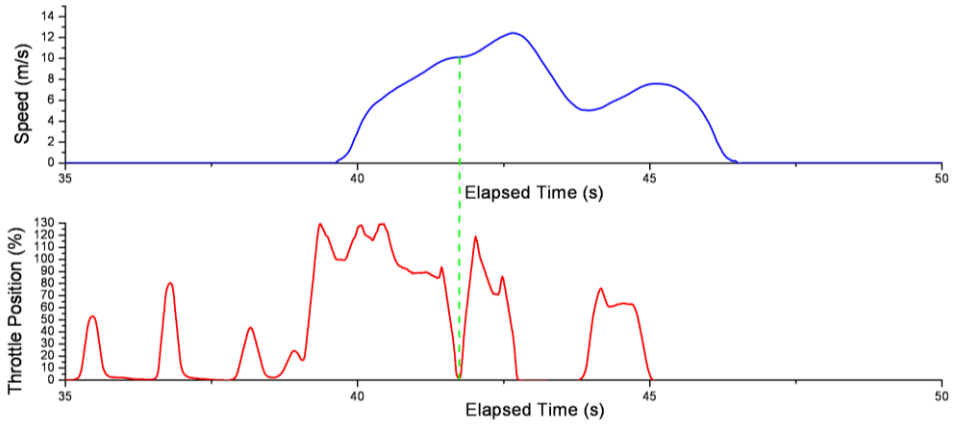

Figure 150 - Speed and Throttle Vs. Elapsed Time, collected during the straight-line test of the ODS.

The most detrimental effect of a wheel locking to motorsport data analysis is to the calculation of cumulative distance taken from the wheel speed signal. Clearly if the measured wheel speeds are to drop to 0, the cumulative distance calculation does not increase despite the vehicle still moving. This can cause alignment issues when trying to overlay data traces from two or more laps against cumulative distance, the most common way of analysing racecar data (McBeath, 2008). Figure 151 illustrates the cumulative distances from the wheel speed and optical sensors plotted against elapsed time.

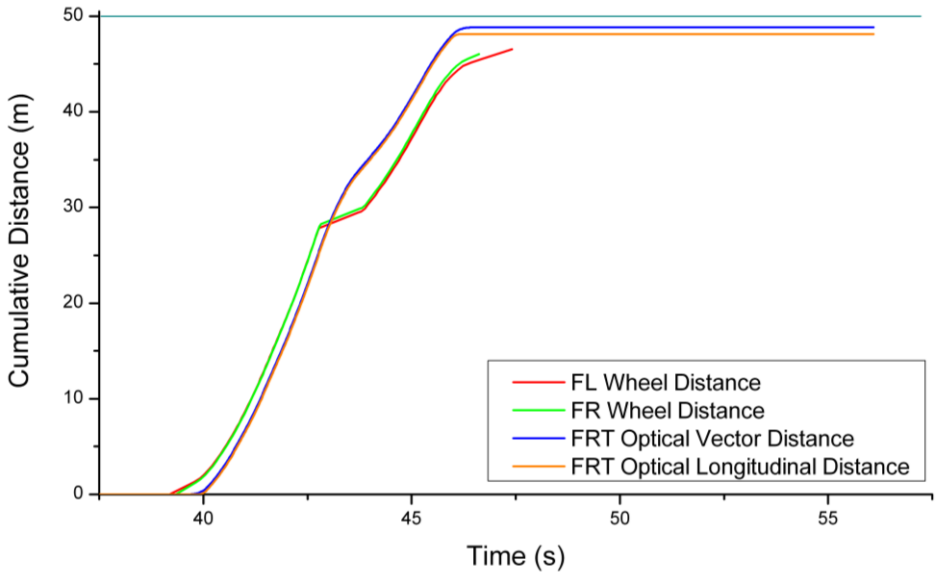

Figure 151 - Cumulative Distance Vs. Elapsed Time during the straight-line test.

The effect of the wheel lockup can clearly be seen, causing a sharper change in gradient of the distance trace in the case of the wheel speed signals. It is also clear that the total distance calculated by the wheel speed sensors is affected. The optical sensors measure around 48.8m, a small difference from the 50m physical measurement due to the optical system not being able to produce results at low speeds because of insufficient pixel shift in the images. However, the wheel speed distance calculations result in a total distance of 46.6m due to the brake locking. This is despite the apparent smoothing effect at low speeds, described previously, which serves to increase the speed measured and hence falsely increase the distance covered. It would also appear that they generally overestimate slightly from the higher speeds illustrated in Figure 149. This is likely to be due to errors in the rolling radius caused by tyre compression and the camber of the wheel resulting in a practical rolling circumference less than the calibration value, which had been measured from a tyre removed from the car.

8.3 ODS Test 2: Circle Test

The second test of the optical sensor was intended to begin the evaluation of the 3 sensor ODS for reconstructing vehicle trajectory. It was decided that the most sensible starting point for this evaluation was to test the system over a circular course at approximately constant speed. This would:

- Simplify the complexity of the reconstruction by only involving one direction of turn and minimal fluctuation in the displacements encountered at each sample point;
- Provide a course which could be easily measured to determine the accuracy of the trajectory reconstruction.

A circular course was measured and marked with cones at an inside radius of 8m and an outside radius of 12m. Figure 152 illustrates the throttle and steering patterns recorded during the test, with the car circulating clockwise, i.e. steering right. It can be seen that the vehicle is held at a roughly constant steering angle whilst negotiating the course and is balanced with fluctuations of the throttle

application. One would expect the trajectory to therefore be close to circular and as the car tracked the inside cones, albeit a small distance away from them, the measured radius from the front centrally mounted optical sensor to be approximately 9 to 10m.

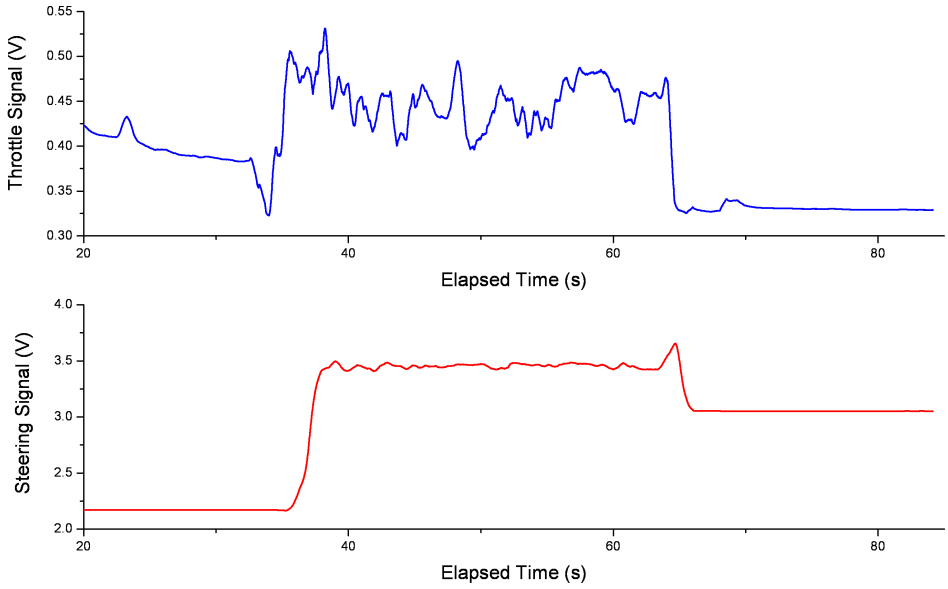

Figure 152 - Throttle and steering traces recorded with the with the data acquisition system during the circle test.

The lateral and longitudinal velocity data recorded from the optical displacement sensors is presented in Figure 153. The sensor array has produced the results that would be expected of the test, which can be fully explained by consideration of the diagram in Figure 154. All six velocity components show stable levels throughout the test which together with the driver control traces of Figure 152 corroborate the observers' views of the test, which form the basis of the previous description; the car maintained a roughly constant speed and rate of heading change. If the longitudinal velocity components are considered separately first, they show a different speed for each sensor. With Figure 154 in mind this can be explained as each sensor tracking a slightly different radius of curvature. The RL sensor on the outside of the car sees the largest curve so records the highest longitudinal velocity. The RR sensor sees the slowest velocity by the same reasoning, whilst the centrally mounted FRT sensor will see a longitudinal velocity approximately the average to the RL and RR, as shown in Figure 153.

The case of the lateral velocities is slightly more complex. Once again the RL velocity is greater than the RR as it tracks a larger radius. The directions of the front and rear lateral velocities are different however. This is because the velocities are relative to the car's initial heading; the car rotates such as illustrated in Figure 154 (a), with the car rotating about its centre of gravity in the same sense as the direction of the corner, i.e. clockwise in this case. In the initial frame as illustrated in the diagram, the front moves to the right, whilst the rear moves to the left to achieve the rotation. The magnitude of the front lateral displacement is greater owing to the front being steered, so effectively being on a tighter turning radius than the rear. Using the technique described in section 6.14 the movement is then translated into a world coordinate frame to allow plotting of the trajectory, as shown in Figure 154 (b).

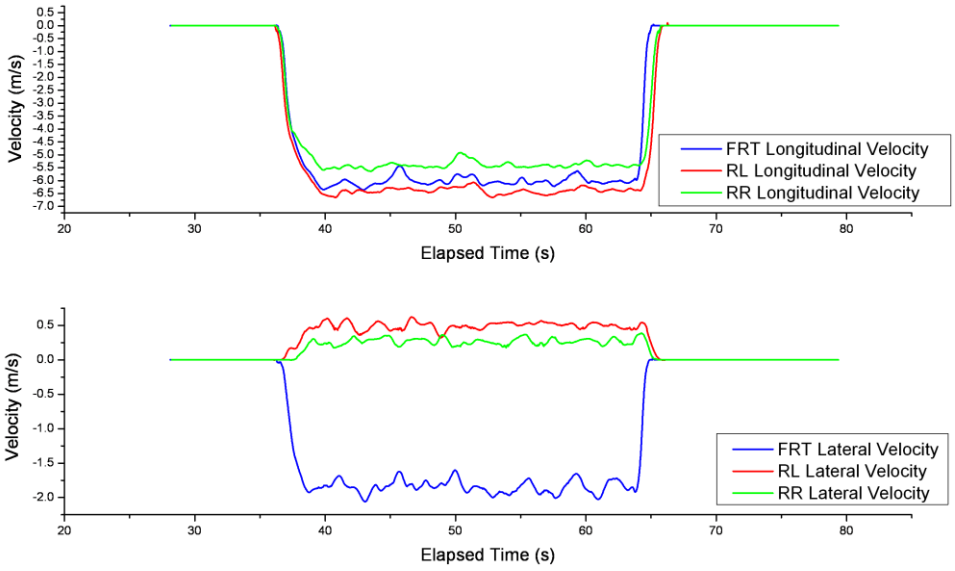

Figure 153 - Longitudinal and Lateral Velocity Vs. Elapsed Time for the three optical displacement sensors during the circle test.

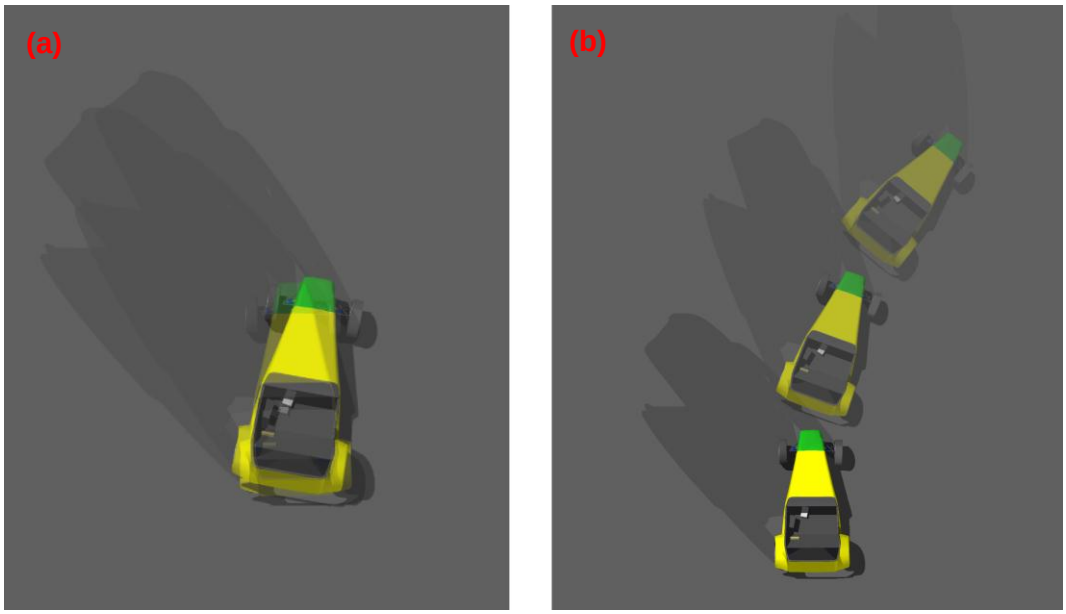

Figure 154 – The rotation of the car as it turns.

Consideration should now be given to Figure 155, which depicts trajectory reconstructions from the optical displacement data and from 1Hz GPS data collected from the u-blox EVK-5 with a positional accuracy of 2.5m (u-blox, 2008).

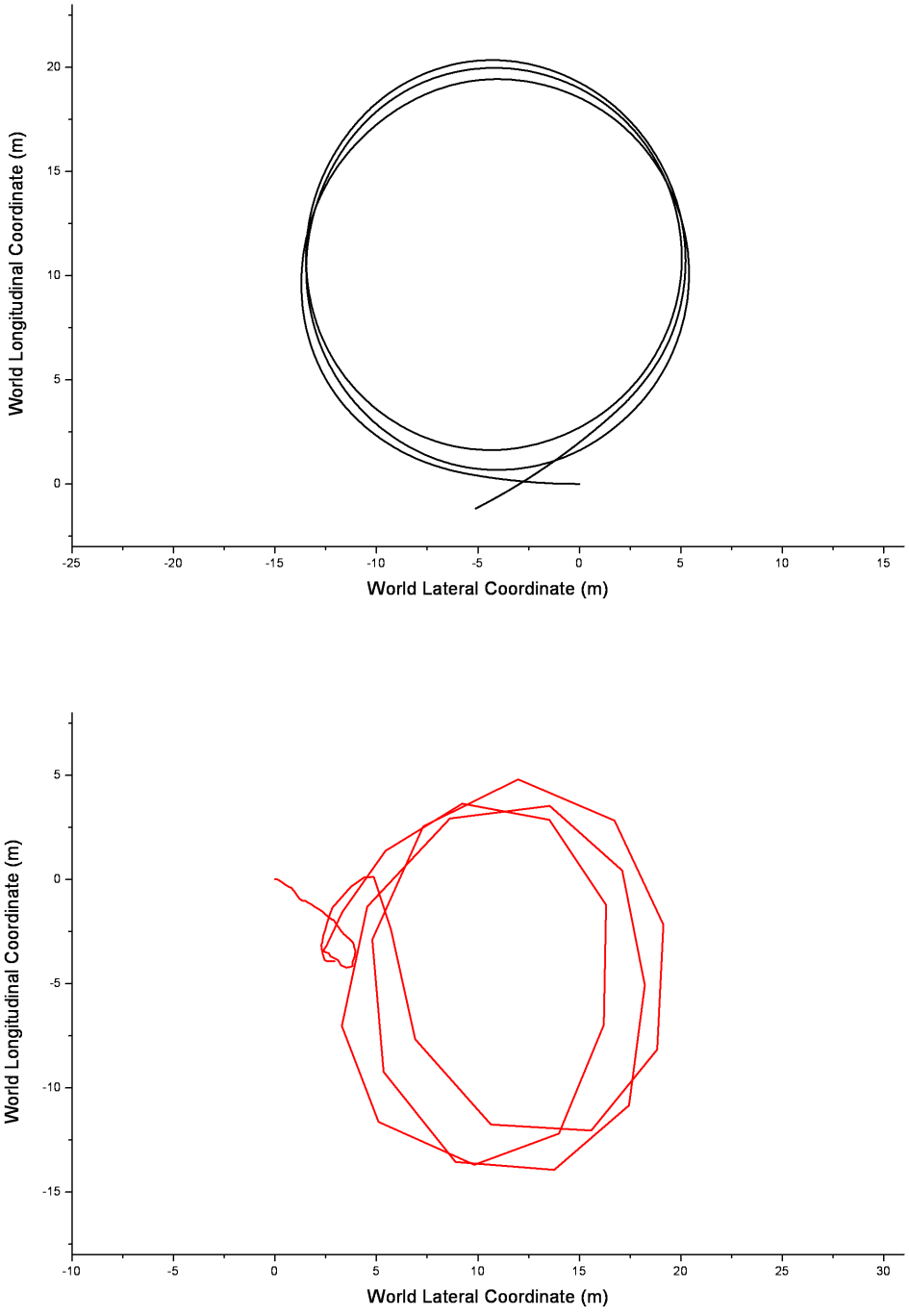

Figure 155 - The optical and GPS trajectory reconstructions of the circle test.

It is clear that the GPS data, sampled at 1Hz is of poor accuracy with the trajectory appearing slightly elliptical, with a radius of approximately 7.5m parallel to the vertical axis and 6m parallel to the horizontal axis, neither of which are

close to the predicted 9.5m. A standard racing system would typically log GPS data at 5Hz (McBeath, 2008) but the evidence of the test here suggests that there would still be a considerable difference from actual path tracked.

The optical trajectory approximation has produced encouraging results, with the three recorded laps of the circle closely matching, as was observed during the test. Measurement of the data also reveals an approximate calculated trajectory radius of 9.5m, which agrees well with the expected radius based on physical measurement.

The encouraging results obtained during this test prompted the application of the same routine to the processing of data collected from a larger more complex circuit, described in the following section.

8.4 Test 3: Circuit Test

The comparison of two or more laps of data produced by different drivers or by different configurations of vehicle setup is arguably one of the most important uses of acquired data in motorsport. It provides the most rapid method of measuring performance against a benchmark and of directing rapid changes to the car setup or to the driver's approach in order to achieve the quickest possible lap time during a track session.

The evaluation of the optical sensor's ability to approximate vehicle trajectory for comparison was made using a short circuit laid out in a facility within the University following the approximate path illustrated in the satellite photograph in Figure 156. In order that the trajectory reconstruction of several key race track features could be tested, the course was arranged such that it provided straights leading into corners of two different radii (Turns 1 and 2) and also provided a so called "change of direction" or a compound corner, whereby a right hand (Turn 1) corner lead directly into a left hand corner (Turn 2) with no intermediate straight section.

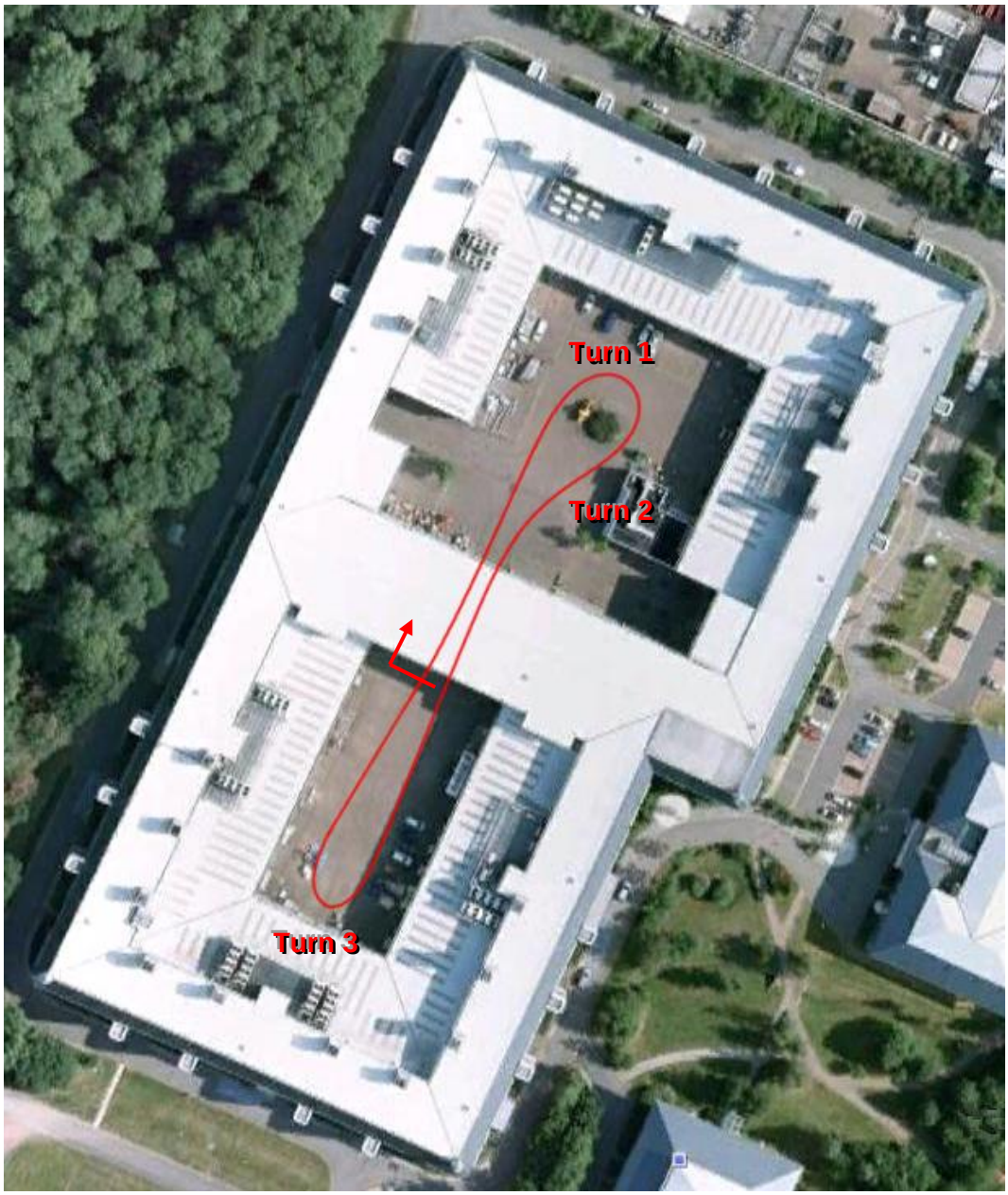

Figure 156 - Satellite Image of Holywell Park, Loughborough showing the circuit used for evaluation of lap trajectory reconstruction (google Maps, 2010b).

Initially data is considered from two individual laps 1 and 2, the uncorrected inertial and optical trajectory approximations of which are plotted in Figure 157. An initial cursory appraisal of these plots raises several clear points:

- None of the trajectory approximations join to form a complete circuit;
- The inertial approximation appears to calculate a greater lap distance in both cases;

- All trajectories show the same circuit features, although there are distinct differences in the heading of the trajectory at different points.

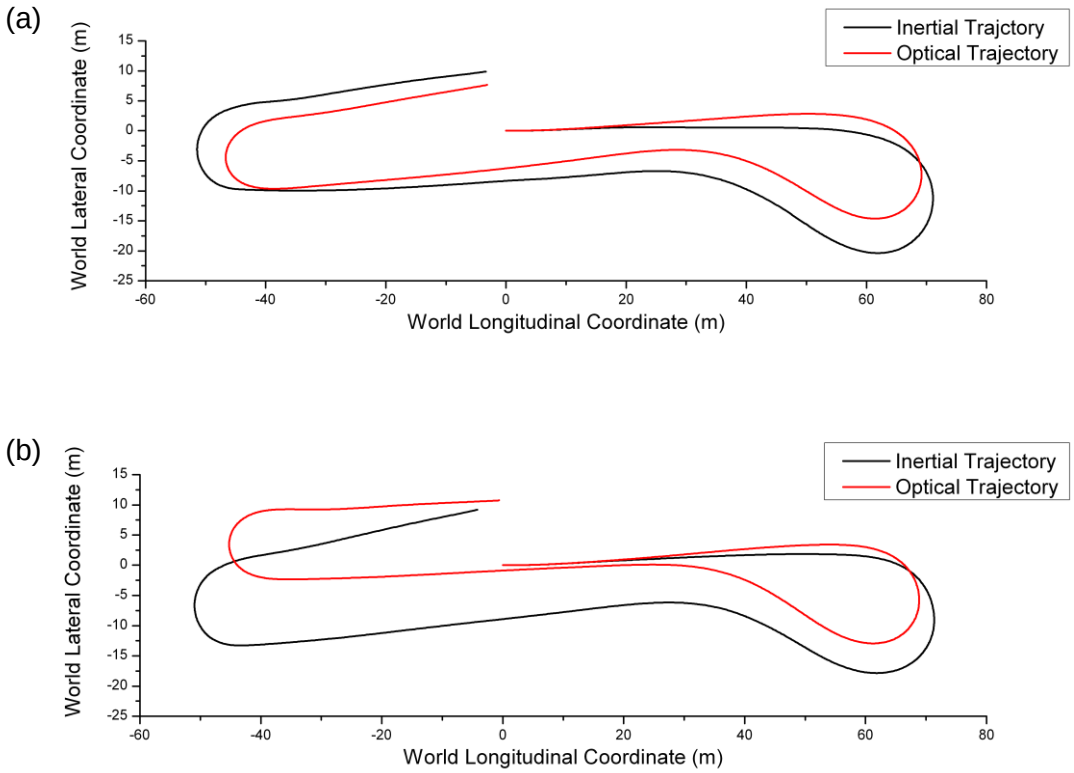

Figure 157 - The reconstructed trajectories produced by the widely used inertial approximation method and by the optical approximation method developed in this work. (a) shows Lap 1 and (b) shows Lap 2.

The mismatch of the inertial trajectory approximation start and finish was well documented in the work of Casanova *et al*. (2001) and was described in the development of the inertial trajectory approximation in section 4.5. Casanova *et al*. presented a two stage method to match the circuit ends whereby an attempt is made to correct the data by apportioning a fraction of the start and finish heading angle error as a correction to every other data point. The difference in the coordinates of the start and finish points is then corrected by stretching the data until they meet. The changes and potential errors that can be introduced by this approach are described later.

The reasons behind the mismatch error in the inertial case are again well documented by Casanova *et al*, particularly succinctly in their description of an

alternative correction method whereby a constant offset, time proportional integration drift and gain or scaling correction are all applied to the lateral acceleration data. The first and third of these corrections address setting of the accelerometer, the first shifting its zero reading and the third scaling its signal to account for poor calibration. The second compensates for integration errors accumulating from the noisy acceleration data around the lap.

As was described in Chapter 6, the omission of topographical information during the trajectory reconstruction will also introduce a mismatch error of its own, although this would be negligible in the tests performed here.

It is evident that the optical trajectory approximation also suffers an accumulation of errors from its relative construction method, the noisy nature of the optical data and the simplification of the vehicle model used to approximate the trajectory. The short length of the track itself perhaps masks some of the key differences between the error accumulation in both the optical and inertial case, however there are a number of key features of the data which suggest some differences in the errors themselves and allow additional conclusions to be derived.

There are two key features of the trajectory around the lap which suggest a more accurate approximation by the optical approach. The first of these is the leftward heading of the car prior to turn 1, a typical approach to a right hand corner, by using the available track to the left to reduce the angle of the right hand turn to the apex. This approach to the corner is confirmed by the plot of left and right wheel speeds taken from lap 2 (Figure 158). Both speed traces overlay well during the initial braking for turns 1 and 2 prior to turning in and on the straight section at the end of the lap, indicating good calibration and setting of tyre pressures. The deviation between the two traces indicates the turning of the car, as the two wheels must assume different speeds to prevent sliding, the higher speed being assumed by the outside wheel. At the very start of the plotted data the right hand trace is greater than the left prior to braking, indicating a gentle curving of the vehicle to the left. Perhaps more explicitly, this feature is also apparent in the steering data presented later in Figure 159. This gentle turn is detected by the optical approach but not the inertial, owing to the threshold which must be applied to the accelerometer data.

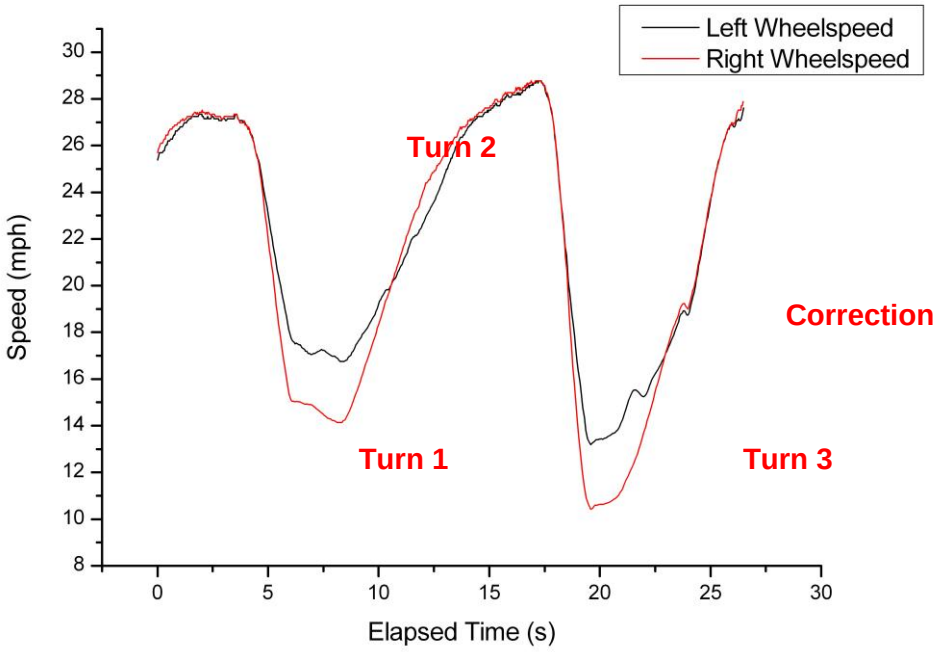

Figure 158 - Right and left wheel speed data from lap 2.

A second feature of note is the distance between the straights linking turns 3 and 1 and turns 2 and 3. These both take the car through a section of the test area which narrows to go through pillars supporting a section of first floor offices. At this point, the test area width reduced to 7.5m. Consideration once more of Figure 157 indicates that the optical trajectory data calculates a separation exceeding this distance of 7.5m, whereas the optical approach calculates 4.5 and 1m separations. From inspection, the difference in the separation in the two optical trajectory approximations appears to be due solely to a small underestimate of the heading change at turn 3 on lap 2.

Another key feature of the trajectory results which applies to both the optical and inertial approaches is the deviation of the circuit trajectory exiting turn 3. Consideration once more of Figure 157 illustrates the trajectory turning left shortly after turn 3, thus heading away from what would seem the correct heading direction towards the start point. However, analysis of several plots of recorded data indicate that the left hand correction is in fact realistic. The steering trace plotted against distance in Figure 159, with vehicle speed as a reference (taken as the faster wheel speed as is standard practice) shows the left hand deviation

in the data, shown by the steering voltage dropping below the green line indicating straight ahead at approximately 230m. The correction to the left is also noticeable in the wheel speed traces of Figure 158 at approximately 24 seconds.

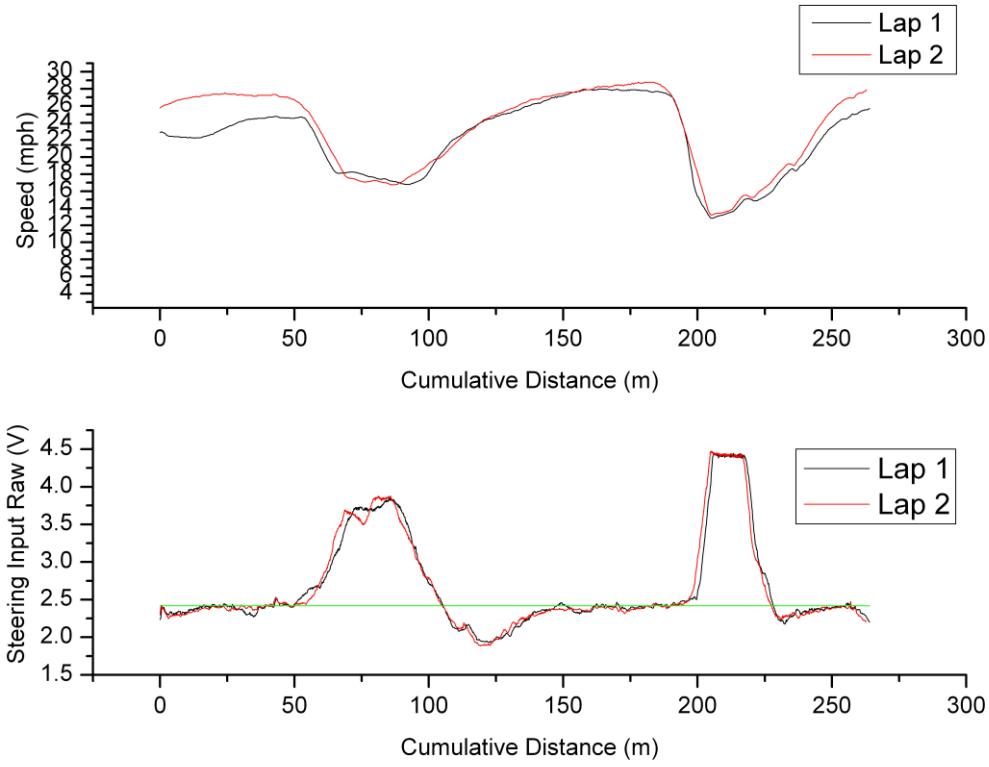

Figure 159 - Speed and steering data from Laps 1 and 2.

The fact that the left hand deviation following the exit of turn 3 is seemingly an accurate depiction indicates that the angle of heading change in turn 3 is under approximated. If the constant radius profile of turn 3 in the optical trajectory of lap 1 in Figure 157 is considered for example, one could envisage the circuit trajectory looking more appropriate if the angle through which the car turned in turn 3 was extended round such that the total cumulative heading rotation at that point slightly exceeds 360º. An illustration of this is given in the modified trajectory shown in Figure 160. The point of the left hand correction now occurs at a lower lateral coordinate and with the trajectory heading below the lateral coordinate of the start point, the left hand correction in this case duly brings the trajectory back towards the start point.

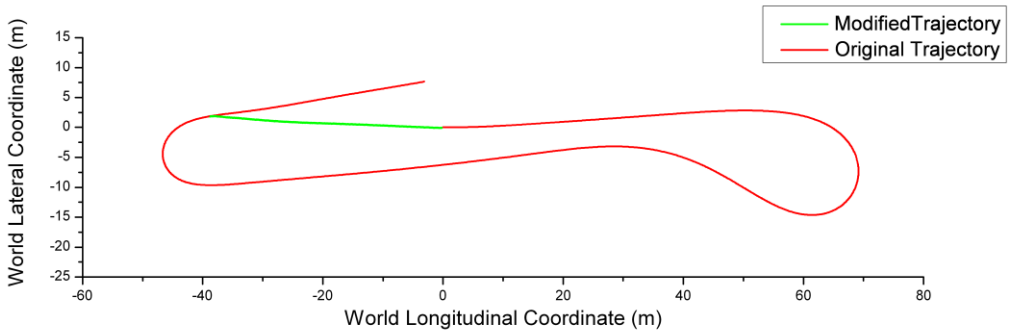

Figure 160 - Modified image of the optical trajectory approximation of lap 1.

It appears that both methods of trajectory approximation have suffered from the slow nature of the corner. It would seem that the low lateral acceleration as the steering is reduced manifests itself after filtering and thresholding as a straight trajectory too soon in the exit phase of the corner. For the same reasons the low lateral velocity caused by the steering being reduced causes errors in the correlation processing of the ODS. A minimum separation is required to detect a displacement in each axis; typically this was empirically found to be approximately 6 pixels. If it was less than this, the result was a purely longitudinal displacement or an erroneous result. The way erroneous results were handled involved interpolating the last complete result and so also produced as straight trajectory; the phenomenon observed in Figure 150. A method of preventing this issue in the case of the ODS if implemented in a commercial system is described in the further work section.

These somewhat subjective appraisals of the trajectory reconstruction are now complemented by consideration of physical measurements taken from the circuit. For this analysis, all laps in the data set are considered, with the exception of lap 4 in the case of total circuit length, as it is incomplete due to the need to move the start line marker during post processing.

Measurements were made using a surveyor's wheel, rolled around the circuit to measure an approximate average lap distance of 246m, taking into consideration potential differences in line. Comparisons are drawn with the distances approximated by each reconstruction method, illustrated in Table 11. These results indicate the optical trajectory providing a more accurate approximation of

the circuit covered, with their average under 1m from the average measured distance. However, without more comprehensive testing and measurement of the line followed, it would be difficult to conclude this definitively.

The results of the table however do illustrate well the effect of the front brakes locking, which creates an error in the inertial trajectory reconstruction. Lap 3 included the front brakes locking into turn 3, which caused an approximate 8m shortening of the calculated lap distance, compared to the approximation of the complete circuit trajectories of laps 1 and 2. The common strategy of selecting the faster of the two wheel speed signals to represent the vehicle speed at all times to reduce the errors caused by a locked wheel is also applied to the results here. It can be seen to calculate a lap distance approximately 6.5m longer than the average speed reconstructions of laps 1 and 2, which suffer no wheel locking, so can be considered more accurate. The difference is caused by the outside wheel speed being selected as the vehicle speed on turns. Meanwhile the optical trajectory approximation has calculated a similar lap length for lap 3, being only slightly longer, as one might duly expect since the car overshoots its turn in point for turn 3.

Table 11 - Driving line lap distances calculated by wheel speed and optical methods.

	Inertial Trajectory (Average Wheel speed)	Inertial Trajectory (Fastest Wheel speed)	Optical Trajectory
Lap 1	257.41m	264.00m	246.84m
Lap 2	256.95m	262.79m	245.76m
Lap 3	248.81m	254.72m	247.68m
Average of Laps 1 -3	254.39m	260.50m	246.76m
Lap 4	233.07m	239.25m	231.77m

As well as considering the overall circuit length, an attempt was made to compare the reconstruction of other key features of the track. Firstly the surveyor's wheel was used once again to measure the radii of Turns 1 and 3. These are presented in Table 12, along with the average of the reconstructed trajectories.

Table 12 - Measured and approximated radii of Turns 1 and 2.

	Measured Radius	Inertial Radius	Optical Radius
Turn 1	8.6m	9.99m	8.38m
Turn 3	5.5m	6.8m	5.69m

Table 12 shows that the optical trajectory reconstruction was close to approximating the radii measured at both corners, whilst the inertial reconstruction over-estimated somewhat in both cases.

The final key circuit feature used to evaluate the accuracy of the trajectory reconstructions was the track section going underneath an area of raised first floor offices, which can be seen close to the start line in Figure 156. At this point the approach to Turn 1 and the exit from Turn 2 come close to each other and it was in fact observed that the two lines almost overlapped on occasions. The physical road width was measured here to be 7.5m and the average separation of the optical and inertial reconstructions was as shown in Table 13. It is clear that the optical reconstruction in its raw form presented here, has more properly reproduced this track feature, with the inertial reconstruction in fact being physically impossible.

Table 13 - The physical road width and trajectory separation at the converging section underneath the first floor offices.

Measured Maximum Track width	Average Inertial Trajectory Separation	Average Optical Trajectory Separation
7.5m	7.87m	2.11m

A final consideration give to the data collected was to a comparison of the raw trajectories for the complete set of laps. The optical trajectories, plotted in shades of green in Figure 161 appear to suggest a more repeatable calculation by the optical method. When considered alongside the illustration of the more accurate reproduction of the correct circuit length, corner radii and other circuit

traits it would appear the optical data gives a better starting point for a stretching algorithm such as that applied to the inertial data. In the same light it could also be suggested that it would form a better input to a Kalman filter technique, which is suggested in the next chapter.

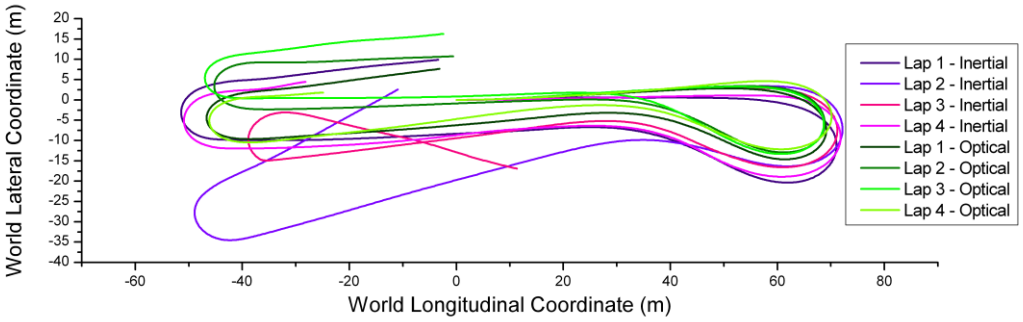

Figure 161 - Comparison of circuit trajectories for all four laps, using both the inertial and optical trajectory calculation routines.

8.5 Overall Appraisal of Visualisation Tool

This sections presents images taken from both the circle test and lap comparison tests of the visualisation software utilising ODS data.

8.5.1 Circle Test

The circle test was the first trial of the ODS system's ability to reconstruct a vehicle trajectory. It also provided the first data set for testing the final version of the graphical display application, the results of which are illustrated by the screenshots in Figure 162. These give an illustration of the software's visual impression of suspension motion and vehicle attitude which can be clearly seen through the series of screenshots. The view in this example was at a fixed point, panning to target the car, due to the relatively small size of the track used.

As is also apparent from the screenshots in Figure 162, the test of the visualisation application was performed with only a single continuous segment of data, to allow the simplest development of the suspension and vehicle attitude animation.

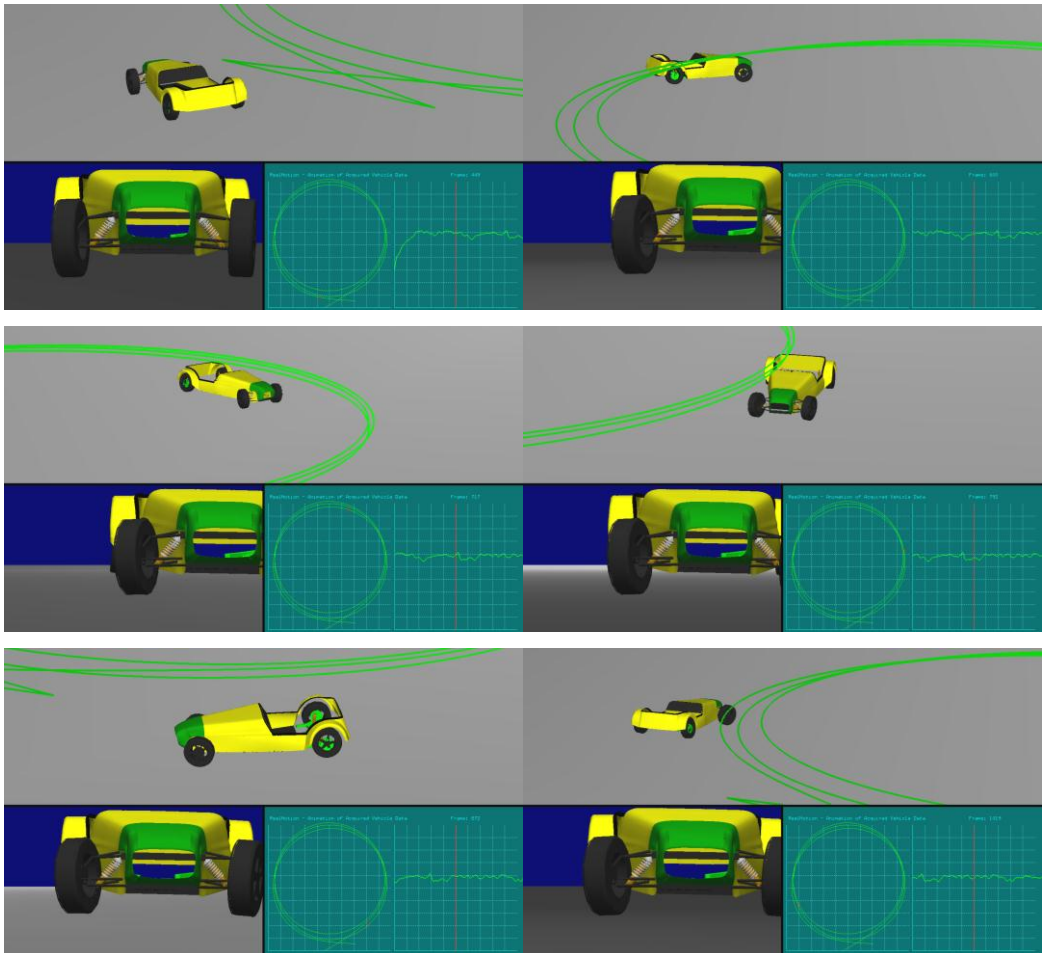

Figure 162 – Screenshots of the visual display application driven by data collected from the circle test.

8.5.2 Circuit Test

The circuit test was used partly to test the ODS ability to measure a more complex vehicle displacement than that of the circle test, but also to compare two laps of data of the same course via the graphical display.

The following screenshots illustrate key points from the comparison of two laps of data. Figure 163 illustrates the comparison of line and car speed into Turn 1 of the circuit. The comparison is fairly distinct as there is a relatively large proportional difference in speed between the two laps as can be seen in the speed graphs illustrated in the right of each screenshot. The impression of driver line and the comparison which can be drawn between the two laps is evident, with a much closer proximity between lines in comparison to the preliminary tests in Chapter 4. The close proximity of the lines around the lap start is illustrated in screen a), whilst b) and c) show the movement of the steering as well as the position visualisation.

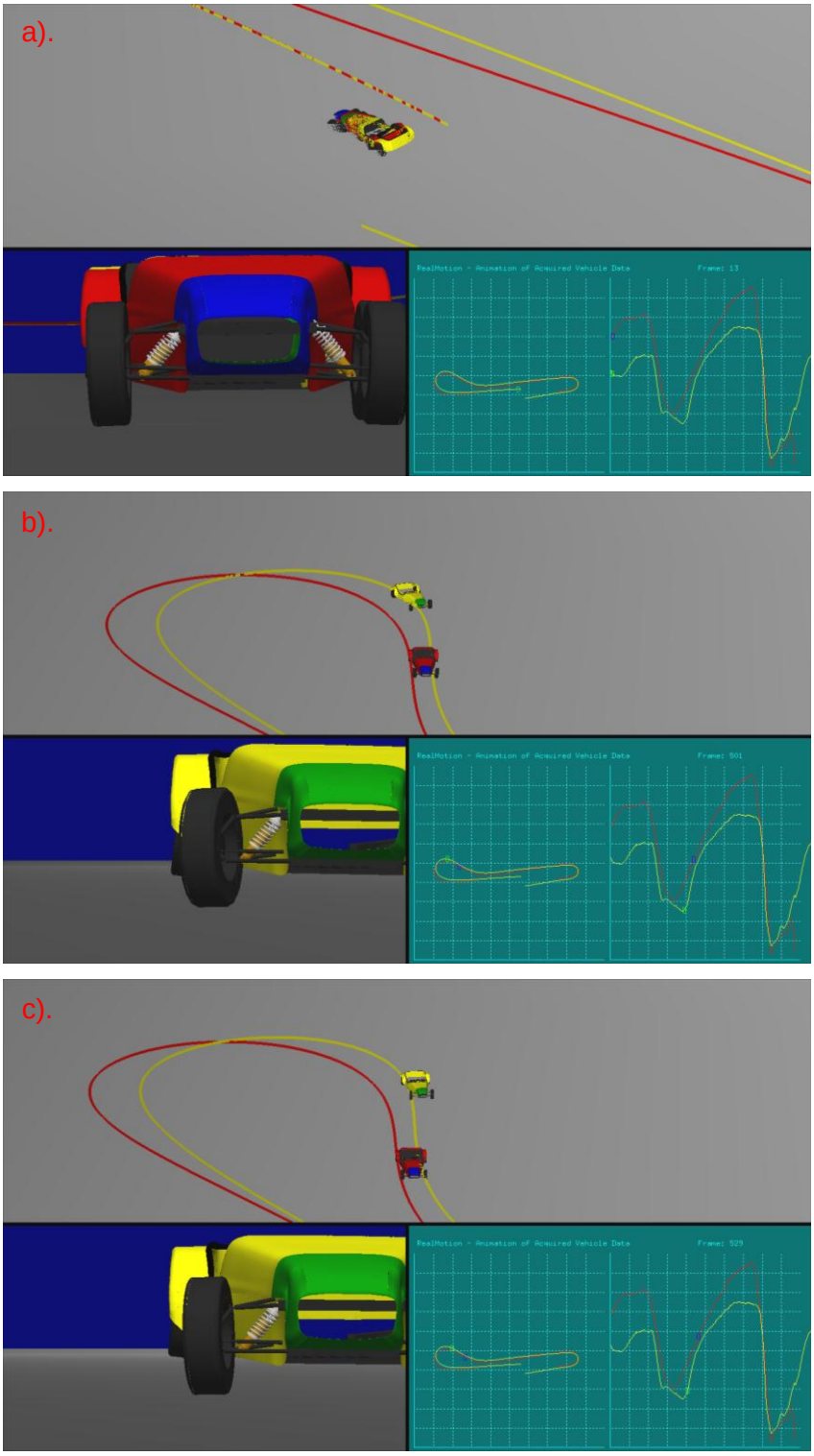

Figure 163 – Screenshots illustrating the visualisation created by the overlaying of two laps of data.

Figure 164 illustrates suspension and steering movement through Turns 2 and 3. The steering change between the left and the right hand components is clearly evident between a) and b). The suspension motion can also be seen by the position of the front right damper body and also by the raising of the rear right wheel as the vehicle weight is transferred during the transition from the right to left hand turn.

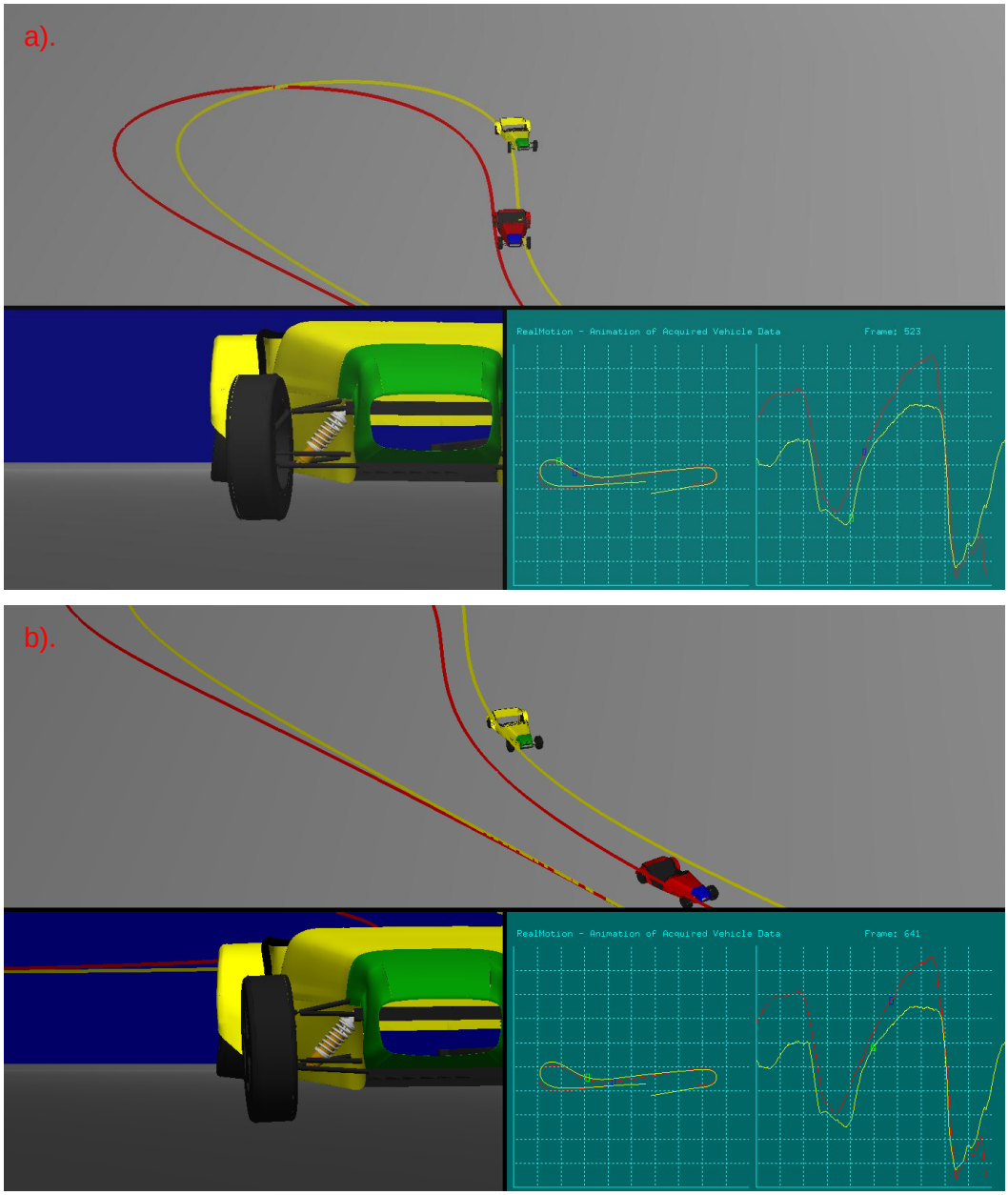

Figure 164 – Screenshots illustrating the suspension displacement recreated in the animation.

Figure 165 shows a series of screenshots depicting the entry, duration and exit of Turn 3. These are intended to mainly illustrate the overall visual impression of the software, by showing the movement of the car through the frame, the application and subsequent removal of steering lock through the corner and the suspension motion associated with the weight transfer of the car.

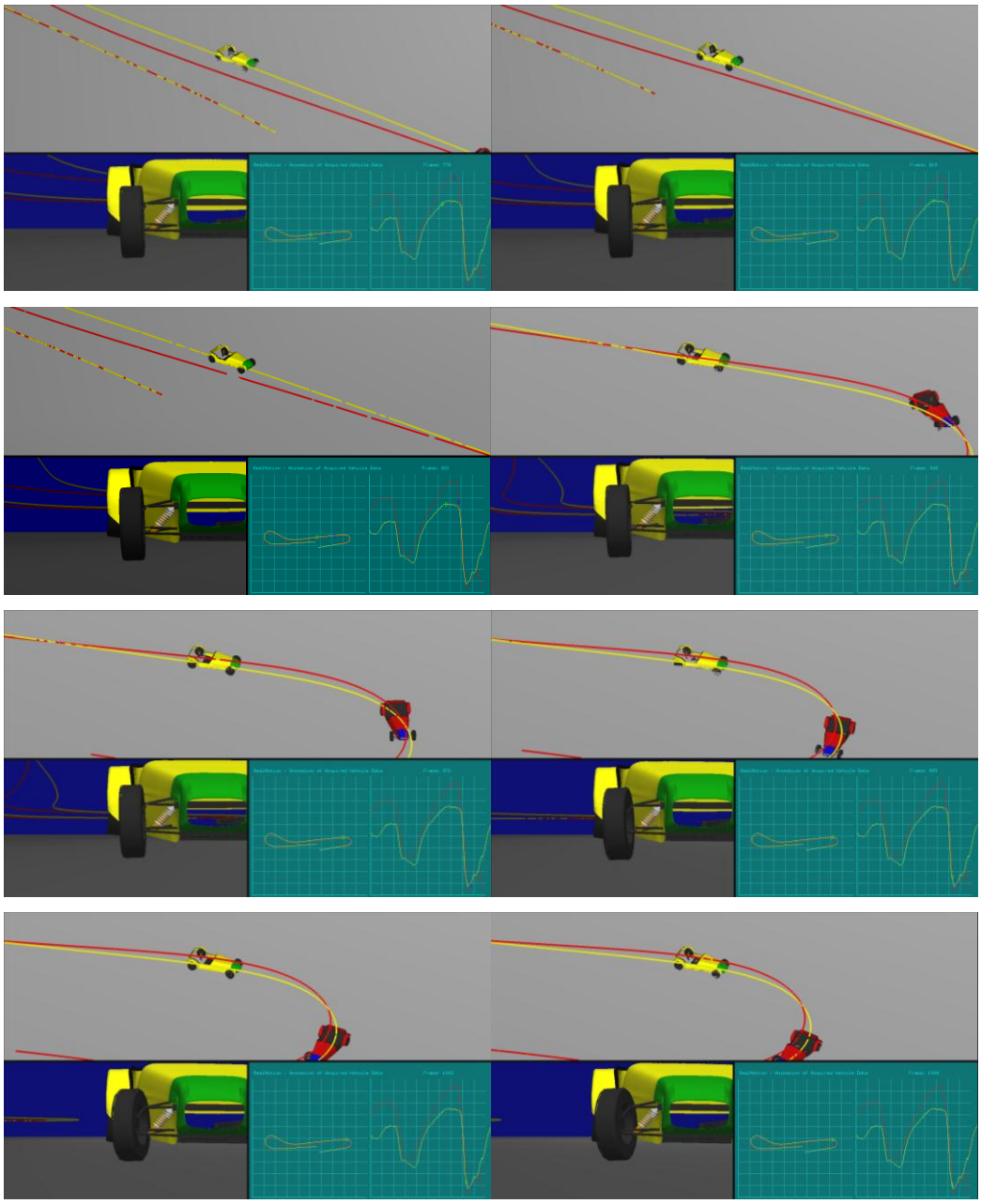

Figure 165a – Series of screenshots depicting the car negotiating Turn 3.

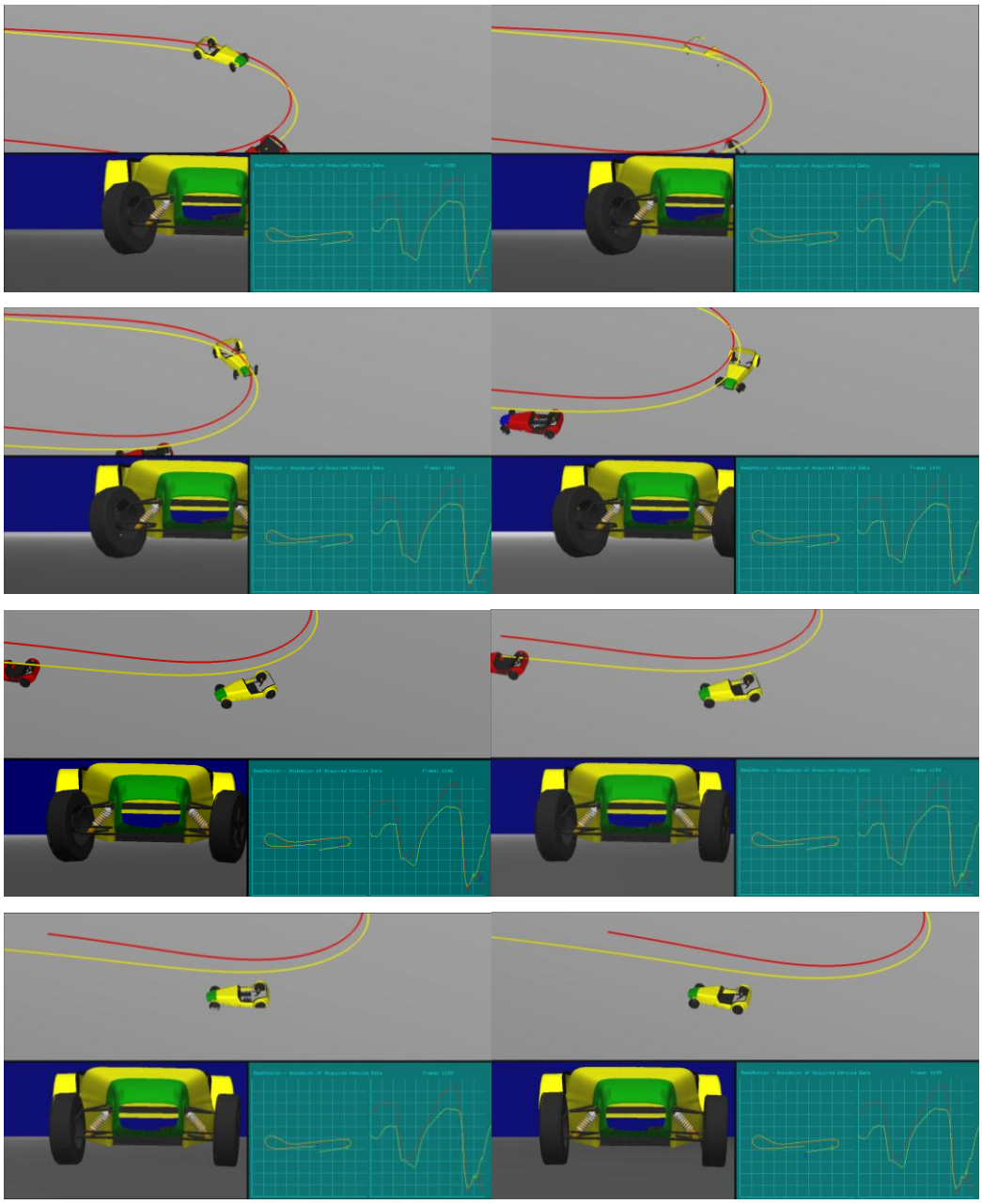

Figure 165b – Series of screen shots depicting the car negotiating Turn 3.

The following screenshots (Figure 166) illustrate in more detail the visual impression of the vehicle motion afforded by the application. Figure 166a shows the car heading in a straight-line, with body level and suspension compression equal the each side. Figure 166b shows the car negotiating a right hand corner, which is clear from the animated steering angle. As one would expect the car rolls to the left and the left suspension compresses as weight is transferred from the right hand side of the car.

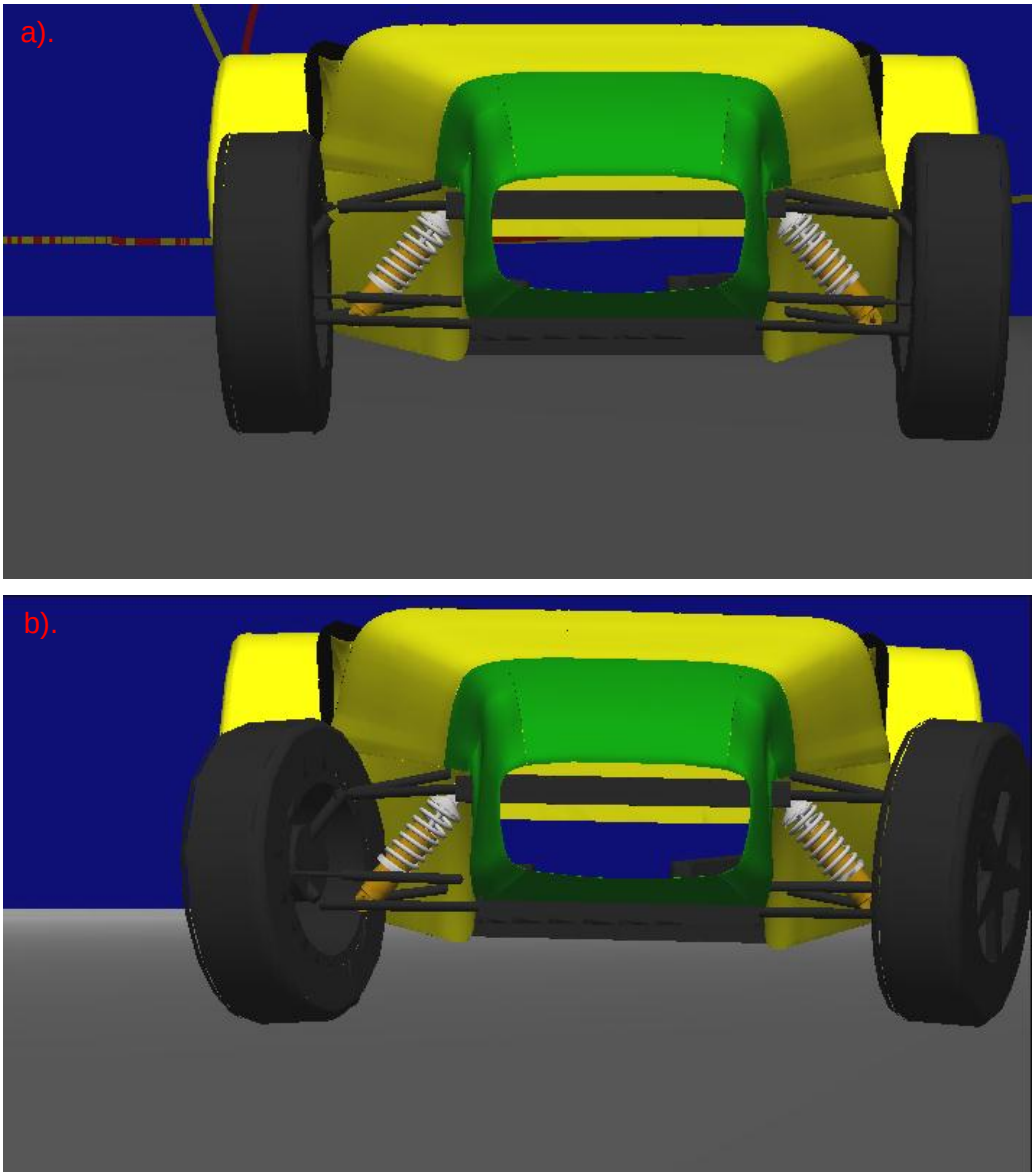

Figure 166 - The graphical visualisation of the steering and suspension motion.

The data display employed for the lap version of the data animation was of a trajectory map and plotted data display, as illustrated in Figure 167. This highlighted the position around the lap of each car during the animation. Plotted data could easily be referred to the animation or map position during playback.

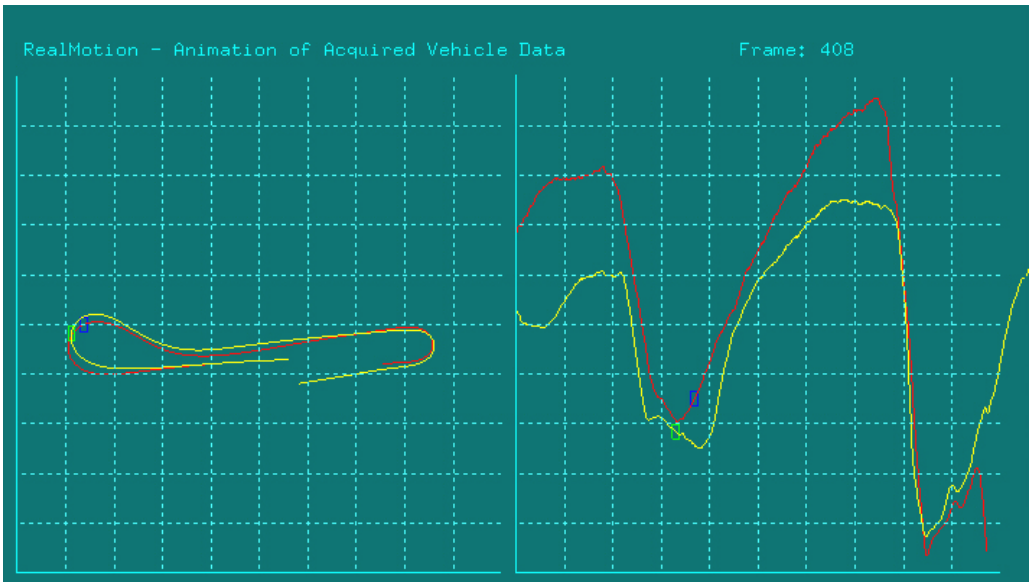

Figure 167 – The data display employed in the lap comparison version of the data animation tool.

Chapter 9

Conclusions and Further Work

9.1 Research Summary

The research presented in this thesis has studied the use of acquired data in motorsport to analyse driver and vehicle performance. The survey of literature surrounding the use of data acquisition in motorsport and of current commercially available software resulted in the following conclusions:

- The primary approaches for analysing acquired data have not developed considerably and are fundamentally based around graph plotting methods;
- A number of factors affect the proper use of acquired data at the race circuit. The increasingly restricted time available to a team to test, budgetary restrictions which result in smaller team sizes and the proliferation of data acquisition hardware available to increasingly smaller and lower level teams means that there is a growing scenario whereby acquired data is not used to its full potential.

As a direct consequence of these conclusions, it was determined that there is a growing potential and opportunity to develop a solution which will enhance the use of acquired data. The objective of the research therefore became to prove the principle of solutions to the growing issues surrounding the use of acquired data at the race circuit.

An all encompassing software approach providing tools to aid visualisation and user assimilation and for organising acquired data was conceived, with this work focussing on the user assimilation aspect. This also drove the investigation of an approach for accurately reconstructing a vehicle's trajectory; current methods were identified to be impractical for motorsport and/or of insufficient accuracy to allow accurate comparisons, most notably GPS based approaches. The research consequently branched into two distinct sections; the proof of concept of a data animation tool and the development and proof of the concept of an optical image correlation based vehicle displacement sensor, the ODS.

A data animation application was implemented in VC++ using OpenGL® which animated models reconstructed from technical drawings in the preliminary version and a combination of CMM and photogrammetric measurements in the final development. Animation was driven by data recorded in the first case from a WSbR car and in the second example by data collected from a test vehicle prepared and instrumented within this research.

The ODS system, created concurrently with the final version of the animation application was achieved by the integration of a range of imaging hardware and controlled by code developed in VC++. The system was tested in its own right using the test vehicle and its trajectory reconstruction was also integrated with the final version of the data animation.

9.2 Outcomes

In proving the principles outlined in this research, a broad range of work has been undertaken. Consequently there have been a significant number of milestones or outcomes which are worth summarising thus:

1. The work developed a data animation application able to accept data from a standard set of speed, accelerometer and suspension displacement sensors and capable of recreating the motion of a vehicle during a recorded lap. The literature indicated that this was not achieved in any other software application;
2. A kinematic suspension solver was coded, which could accept initial conditions of damper length from recorded data collected from the circuit and solve the kinematic suspension joint locations and component angles in real time;
3. A new vehicle displacement measurement approach was trialled. This involved development an optical sensor (ODS) measuring the three axis displacement of a reference point relative to the ground and in a coordinate frame fixed to the vehicle;

4. The ODS produced a vehicle ground displacement measurement using an image analysis technique not previously employed for multiple axis vehicle displacement or speed measurement and achieving a sample rate of 50Hz;
5. The theoretical ground displacement measurement resolution of the ODS was approximately 0.1mm (variable with height sensor height from ground). This offered the potential for exceeding the best vehicle displacement measurement found in the literature, of 1.5mm;
6. A vehicle height from ground measurement method was developed, with a theoretical accuracy of 0.12mm when recreating a height measurement made at an accuracy of 0.3mm;
7. Three ODS units were arranged as a system to measure vehicle displacement and attitude by an approach not previously employed elsewhere;
8. Using the three ODS system and a VC++ algorithm, a circuit trajectory was reconstructed by an approach not previously employed elsewhere;
9. The trajectory reconstruction technique itself appeared to offer a more repeatable and accurate raw trajectory approximation when compared to the universal approach of inertial reconstruction from recorded lateral acceleration and speed data;
10. The ODS system represented an approach to trajectory reconstruction and vehicle displacement measurement which would be more readily implementable under the unique demands of a motor racing environment. This is when compared alongside the most accurate GPS derived solutions, including the use of carrier phase measurement and augmentation techniques;
11. Finally the work answered the two key research aims, by proving the principle of a new display approach and of a vehicle displacement measurement technique, showing both to be worthy of further investigation. The combination of the two techniques allowed for data visualisation not previously possible, positioning the car accurately and recreating its motion in real time. The results described within this thesis and personal experience of motorsport engineering suggest this this would aid the user's understanding of a recorded data file.

9.3 Conclusions

The proof of principle of a visualisation application for aiding user assimilation of recorded racecar data and of a new displacement measurement technique have led to the development of a combined approach which has potential for improving the use of acquired data in motorsport. This broad conclusion can be divided into the following major conclusions:

1. The visualisation application has improved the presentation of racecar data beyond the use of graph based methods alone. This has included the display of gains and losses in time between two laps of data. In addition, differences in trajectory and the dynamic behaviour of the vehicle were shown to be better illustrated than by graph based analysis alone;
2. The visualisation application has been shown to handle real race car data collected under competitive conditions. The fundamental data utilised has proved the application to be applicable to all levels of motorsport as it relied solely on universally measured parameters;
3. The visualisation application has been shown to benefit from additional levels of displacement measurement, i.e. the use of the ODS for more accurate vehicle trajectory approximation. This ultimately offered the user a better comparison and visualisation of the actual events recorded in the data;
4. The ODS was shown to be theoretically capable of measuring vehicle displacement to an accuracy/resolution of 0.1mm based on a single pixel equivalent distance. This has therefore proven a system which could potentially attain a better positional accuracy than currently available methods, most notably GPS;
5. The ODS was shown to accurately measure vehicle velocity up to $12.5 m.s^{-1}$ (approximately 28mph);
6. The successful collection of speed and displacement data has proven a system which is impervious to its surroundings unlike GPS, not

affected by tyre deflection, unlike wheel speed based methods and which can potentially be made at a low cost;

7. The configuration of three ODS to form a plane approximation through the car was shown as a viable means of approximating vehicle trajectory. The system was also shown to correctly solve directional ambiguity by the trajectory reconstruction of turn manoeuvres;
8. The comparison of the ODS alongside the universal lateral acceleration and wheel speed derived trajectory calculation proved that it could better recreate a representative circuit trajectory.

9.4 Further Work

The first key area of further work should ideally focus on the system developed as a result of this research and expand the test program it was subject to. This would include a more controlled approach allowing the practical system accuracy to be determined. This could include rig based tests traversing the ODS across a surface as well as also testing the ODS's ability to recreate controlled trajectory features, such as turns of known radius, perhaps measured from video capture of the test manoeuvres. This would allow a more definitive conclusion of the system accuracy as well as the causes of the reconstruction issues encountered at turn 3 in the lap test to be drawn.

This work has aimed to prove the principle and approach employed in providing a sensor technology and software data processing application which will aid the user's understanding of data acquired from a racing car and also provide a potentially more accurate reconstruction of vehicle location. Much of the remaining further work should predominantly focus on making these approaches fully robust and commercially viable.

The hardware and coding approaches employed aimed to best replicate a full standalone hardware controlled solution. A logical stepwise progression of this would be to utilise a programmable automation controller (PAC) as an interim step, such as the National Instruments CompactRIO device. This would be an

interim step between the computer control employed here and a full bespoke hardware controller, but would potentially allow testing on a race car itself and would give a clearer indication the viability of packaging the solution within the confines of a race car.

A programmable controller or bespoke hardware controller would also allow optimisation of the data collected. The pixel shift was dependent on the speed of the vehicle, as the light pulse gap is fixed. This meant that a fixed size of correlation window had to be used and the limits of the pixel shift were prescribed. However, with a suitable design of hardware control, it is possible that this could be greatly refined to improve the correlation time as well as the capture performance of the system:

- Through use of a wheel speed sensor as an on the fly (OTF) check measure, the expected pixel displacement could be determined and used to control the shift limits correlated over by the analysis routine;
- If a fixed level of charge could be guaranteed from the light controlling device, the time separation could also be varied from the OTF wheel speed measurement. This could potentially help solve issues such as the identified errors caused in the slow turn 3 of the lap comparison test, by increasing the time separation of the light pulses so that the doubly exposed features were better separated.

The ODS units themselves require some refinement, notably with regard to lighting. The strobe controllers would ideally be replaced by a unit integrated with a system controller, perhaps outputting current on a single channel so all cameras could be synchronised. The size to which this unit could be refined is unclear but it would seem not inconceivable that it could be significantly reduced from the size of the current strobe controller units. The controller could also accept a dc input to enable it to be powered by a battery.

The size of the LED illumination itself could potentially be reduced, either as a bespoke design or by using a more compact OTS light source as an alternative interim step.

A fourth sensor mounted close to the car's CoG would also offer additional detail in the motion and trajectory reconstruction. This would allow the separation of the vehicle heading and attitude, thus illustrating sliding. An approximation of the trajectory movement would be made from the CoG mounted sensor, whilst the existing arrangement of 3 sensors in the triangular pattern used in this work would allow for the car attitude to be derived. Handling imbalances are currently only detectable from a study of the steering angle and car heading, which can make them hard to identify.

The trajectory output created by the ODS system in this work, although incorporating filtering of the data channels used, essentially produced a raw trajectory data. This is in comparison to the common-place inertial technique for example, whereby data is heavily manipulated after the initial trajectory calculation. Literature also indicated that GPS data alone was insufficient to produce an accurate trajectory reconstruction (Segers, 2008) and would commonly be used as part of a Kalman filter technique with inertial data, as described previously in section 2.3.2. A typical Kalman filter arrangement for inertial navigation could be adapted as in Figure 168 with the ODS trajectory measure replacing the GPS, which would practically be accurate to around 1m. This diagram illustrates the approach of a typical GPS and INS Kalman filter approach (Oxford Technical Solutions, 2009), with GPS positional data replaced by the ODS data.

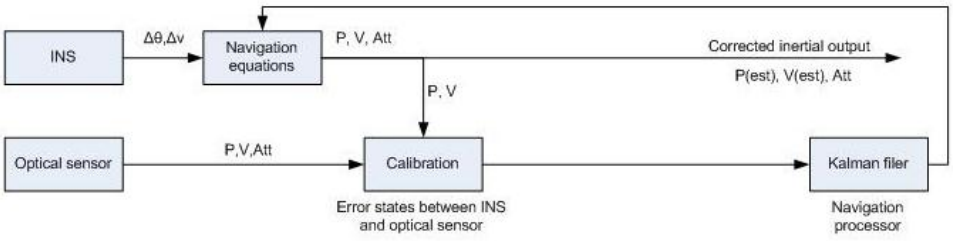

Figure 168 – Adapted GPS/INS Kalman filter navigation system approach, with the GPS input replaced by the ODS data.

The reader will have identified a key issue with regard to the ODS trajectory reconstruction in comparison to the one derived from GPS data is the relative

coordinate frame featured as opposed to the absolute coordinate measurement of GPS. A potential low cost method for addressing this issue is described by Figure 169.

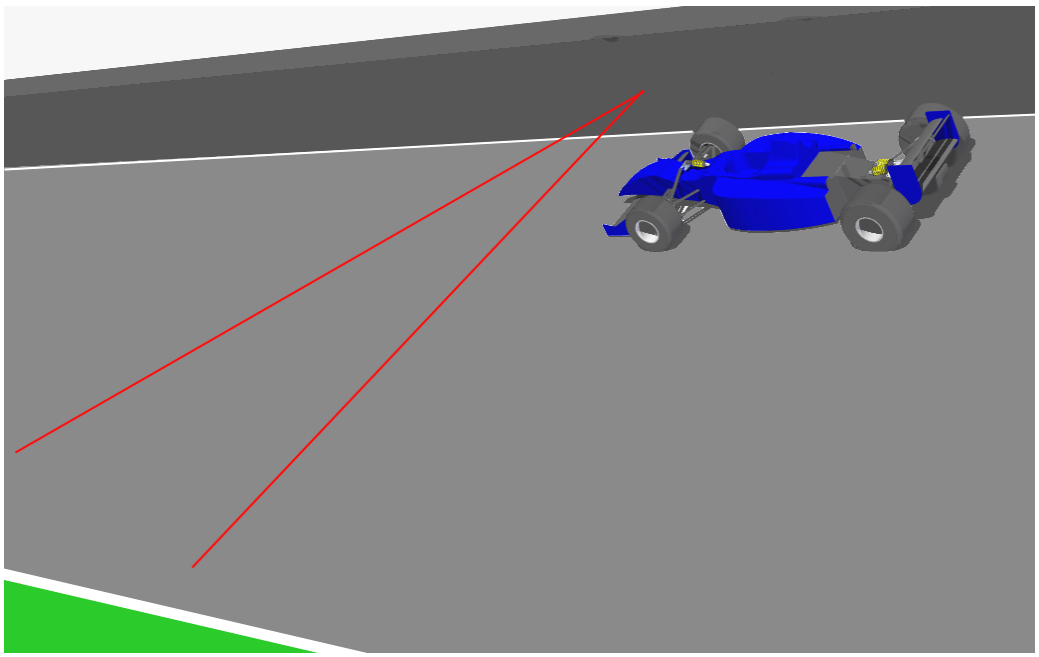

Figure 169 – A two timing beam arrangement to allow determination of lateral position across the circuit start/finish line.

A universal approach to time stamping the beginning of each lap of data at the race circuit is through the used of an infrared or microwave frequency beacon (Segers, 2008; McBeath, 2002). This involves a transmitter at the circuit side which creates a timing beam, the passing of which is identified by a receiver on the car.

The diagram in Figure 169 describes the use of two separate infrared timing transmitters which would each operate on a different frequency. Two receivers would be used on the car to identify the passing of each beam. The diagram illustrates how one is angled relative to the other. If this angle is carefully configured and known, the position across the circuit can be seen to be potentially inferred by the time separation of each beam passing and the vehicle speed through this period. As the beams are angled, the time separation for a given speed will increase with distance away from the transmitters. If the world location of a reference point on the start line is known, the location of the car at

the lap start can be determined. This would allow for a positional measurement comparable to GPS, which would then enable animated model to be positioned on a terrain topological reconstruction.

References

2D Datarecording. 2004. *Analyzer User Manual.* Karlsruhe, Germany: 2D Datatrecording.

Accuity. 2005. *AccuRange 200™ Laser Displacement Sensor.* [User Manual] Portland, OR, USA: Accuity.

Active Sensors. 2008. *CLS1320 Series Linear Potentiometer Datasheet.* Christchurch, Dorset, UK.

AiM Sports. 2003. *Race Studio 2 Analysis User Manual.* Corydon, CA, USA: AiM Sports LLC.

All About Circuits.com. 2000. *Potentiometer as Voltage Divider.* (Online) URL: http://www.allaboutcircuits.com/vol_6/chpt_3/6.html Accessed 27th May 2005.

Analog Devices. 2006. *ADXL330.* [Technical data sheet] Norwood, MA, USA.

Anandarajah, K. 2005. *Inherent Errors in Time-resolved Digital Particle Image Velocimetry.* (Ph.D. Thesis) Loughborough University, Loughborough, UK.

Anandarajah, K., Hargrave, G.K. and Halliwell, N.A. 2004. *Time-resolved Digital Particle Image Velocimetry (DPIV): Error reduction from normalisation by signal strength (NSS).* International Conference on Advanced Optical Diagnostics in Fluids, Solids and Combustion. Tokyo, Japan, 2004.

Anderson, J.A. 1995. *An Introduction to Neural Networks.* Cambridge, MA, USA: Massachusetts Institute of Technology.

Baker, M.J. 2010. *EuclideanSpace - Building a 3D World.* [Website tutorials] URL: http://www.euclideanspace.com

Barnes, D. *et al*. 2000. *Motorsports Sensor Technology.* SAE Paper 2000-01-3566.

Bishop, C.M. 1995. *Neural Networks for Pattern Recognition.* Oxford, UK: Oxford University Press.

Bitar, S., Probst, J.S. and Garsehlis, I.J. 2000. *Development of a Magnetoelastic Torque Sensor for Formula 1 and CHAMP Car Applications.* SAE Paper 2000-01-0085.

Blundell, M.V. and Harty, D. 2004. *The Multibody Systems Approach to Vehicle Dynamics.* Oxford, Oxfordshire, UK: Elsevier.

Bolduc, C. and Jackson, W. 1999. *3D Animation of Recorded Flight Data.* International Symposium on Transportation Recorders, 3-5 May 1999.

Boothroyd, G., Dewhurst, P. and Knight, W.A. 1994. *Product Design for Manufacture and Assembly.* New York, NY, USA: Marcel Dekker, Inc..

Bosch Motorsport. 2004a. *LapSim: Data Analysis, Vehicle Identification and Setup Optimisation*. [Product Specification Sheet] Markgröningen, Germany: Bosch Motorsport.

Bosch Motorsport. 2004b. *LapSim: Data Analysis, Vehicle Identification and Set-up Optimisation*. [User Manual] Markgröningen, Germany: Bosch Motorsport.

Bray. M. 2006. *Review of Computer Energy Consumption and Potential Savings.* [White Paper] Dragon Systems Software Limited.

Bunkhall, S. 2001. *Candid Camera.* International Journal: Racecar Engineering, Vol. 11, No. 10, pp 42 – 44.

Burgess, M.J., *et al*. 2004. A Tool for Rapid Vehicle Suspension Design. SAE Motorsport Engineering Conference, Dearborn, Michigan, USA , 30th November - 2nd December, 2004. SAE Paper 2004-01-3543.

Casanova, D., Sharp, R.S. and Symonds, P. 2001. *Construction of Race Circuit Geometry from On-car Measurements.* Proceeding of the Institution of Mechanical Engineers Part D, Vol 215.

CEFA. 2010. *Flight Animation Software.* [Online]. URL: http://www.cefa-aviation.com/flight_data_animation.htm

Chalko, T.J. 2009. *Estimating Accuracy of GPS Doppler Speed Measurement using Speed Dilution of Precision (SDOP) Parameter.* [Online] Nu Journal of Discovery. URL: http://nujournal.net/SDOP.pdf.

Chalko, T.J. 2007. High Accuracy Speed Measurement Using GPS (Global Positioning System). [Online] Nu Journal of Discovery. URL: http://nujournal.net/HighAccuracySpeed.pdf

Clarke, C. 2004. *High Performance.* International Journal: Racecar Engineering, Vol. 14, No. 11, pp 46- 52.

Clarke, C. 2005. *Chassis Analysis.* International Journal: Racecar Engineering, Vol. 15, No. 2, pp 44 – 50.

Compaq Computer Corporation *et al*. 2000. *Universal Serial Bus Specification: Revision 2.0.* [Industry Specification]

Competition Data Systems. 2005b. Informer. [Promotional literature]. Williamsville, NY, USA: Competition Data Systems Inc..

Corbrion, C. *et al*. 2001. A *Broad Beam Doppler Speed Sensor for Automotive Applications.* Sensor Review, Vol. 21, No. 1, pp 28 -32.

Corrsys-Datron. 2004. *The Physical Operating Principle of Correvit® Non-Contact Optical Sensors.* [Information sheet] Wetzlar, Germany: Corrsys-Datron Sensorsysteme GmbH.

Corrsys-Datron. 2009a. *The Art of the Speed.* Wetzlar, Germany: Corrsys-Datron Sensorsysteme GmbH.

Corrsys-Datron. 2009b. *Correvit® LF-II P User Manual.* Wetzlar, Germany: Corrsys-Datron Sensorsysteme GmbH.

Corrsys-Datron. 2009c. *Correvit® SF-II P User Manual.* Wetzlar, Germany: Corrsys-Datron Sensorsysteme GmbH.

Corrsys-Datron. 2009d. *Correvit® S-HR User Manual.* Wetzlar, Germany: Corrsys-Datron Sensorsysteme GmbH.

Corrsys-Datron. 2009e. *Correvit® L-350 Aqua User Manual.* Wetzlar, Germany: Corrsys-Datron Sensorsysteme GmbH.

Corrsys-Datron. 2010. *Correvit® S-350 Racing User Manual.* Wetzlar, Germany: Corrsys-Datron Sensorsysteme GmbH.

Croft, A., Davison, R. and Hargreaves, M. 1996. *Engineering Mathematics: A Foundation for Electronic, Electrical and Systems Engineers.* 2nd Edition. Harlow, Essex, England: Addison-Wesley.

Dallara. 2004. *Dallara T05.* [Technical drawings] Parma, Italy, Dallara Automobili.

DATAS. 2005. Corporate Website. [Online] URL: http://www.datas-ltd.com Accessed December 2004 – January 2005.

DICKEY-john. 2010. *DICKEY-john Corporation Corporate Website.* [Online] URL: www.dickey-john.eu . Accessed January 2010.

Ditchi, T. *et al*. 2002. *On Board Doppler Sensor for Absolute Speed Measurement in Automotive Applications.* SAE Paper 2002-01-1071

Dixon, J.C. 1996. *Tires, Suspension and Handling.* 2nd Edition. Warrendale, PA, USA: Society of Automotive Engineers.

Doogue, M. and Walsh, M. 1998. *The Design of a Track Map Based Data Acquisition System for the Dartmouth Formula Racing Team.* Springfield, MA, USA: Analog Devices, Inc..

Drivedata. 2004. Product Information Sheet. UK: Drivedata (UK) Ltd..

Eos Systems. 2004. *PhotoModeler® 5 Pro.* 30th Edition. [User manual] Vancouver, BC, Canada: Eos Systems, Inc.

European Space Agency. 2004. *EGNOS: The European Geostationary Overlay Service.* [Information sheet] Noordwijk, Netherlands.

Fairfax, M. 2001. *3DS Loader and Viewer.* (Website for distribution of freeware graphics loader). URL: http://www.torquepowered.com /community/resources/view/506 Accessed July 2006.

Fay, R.J. and Scott, J.D. 1999. *New Dimensions in Rollover Analysis.* International Congress and Exposition, Detroit, Michigan. SAE Paper 1999-01-0448.

Fey, W. R. 1993. *Data Power: Using Racecar Data Acquisition.* Memphis, TN, USA: Towery Publishing.

Fey, W. R. 2005. *Discussion on future trends in motorsport data analysis.* [Email] (Personal Communication, January 19th 2005).

Formula One Administration. 2010. *Formula 1 Official Website.* [Online] URL: http://www.formula1.com/inside_f1/understanding_the_sport/5295.html Accessed January 2010.

Giarratano, J.C. and Riley, G. 1998. *Expert Systems: Principles and Programming.* 3rd Edition. Boston, MA, USA: PWS Publishing.

GMH Engineering. 2010. *GMH Engineering Corporate Website*. [Online] URL: www.gmheng.com Accessed January, 2010.

Gonzales, R. and Wintz, P. 1987. *Digital Image Processing.* New York, NY, USA: Addison-Wesley.

google maps. 2010a. *Satellite image of Donington Park race circuit, Leicestershire.* [Online] URL: http://maps.google.co.uk/maps?hl=en&ie=UTF8&ll= 52.830397,-1.375244&spn=0.00713,0.022681&t=h&z=16

google maps. 2010b. *Satellite image of Holywell Park, Loughborough, Leicestershire.* [Online] URL: http://maps.google.co.uk/maps?hl= en&ie=UTF8&ll=52.759077,-1.24727&spn=0.001792,0.00567&t=h&z=18

Gough, S. and Huggett, D. 1998. *The Age of the Strain Gauge.* International Journal: Racecar Engineering, Vol. 8, No. 8.

Grant, I. 1997. *Particle Image Velocimetry: A Review.* Proceedings of the Institution of Mechanical Engineers, Part C: Journal of Mechanical Engineering Science, Vol. 211, No. 1.

Grewal, M.S. and Andrews, A.P. 2001. *Kalman Filtering: Theory and Practice Using MATLAB.* 2nd Edition. New York, NY, USA: John Wiley & Sons.

Grewal, M.S., Weill, L.R. and Andrews, A.P. 2007. *Global Positioning Systems, Inertial Navigation and Integration.* 2nd Edition. Hoboken, New Jersey: John Wiley & Sons.

Halliday, D. and Grider, K. 1998. *The Grip Evaluation and Measurement Device.* SAE Paper 98MSV-56.

Halliday, D. 1997. *Gem of a Tool.* International Journal: Racecar Engineering, Vol. 7, No. 8, pp 28 – 31.

Hammond, S. 2005. Personal communication with Steve Hammond, Electrical Workshop, Wolfson School of Mechanical and Manufacturing Engineering, Loughborough University, on the operation of wheel speed sensors. [Verbal communication]. October 2005.

Haney, P. 2001. Jim Hall Interview. [Online] Inside Racing Technology, URL: http://www.insideracingtechnology.com/jimhall.htm

Haney, P. and Braun, J. 1995. *Inside Racing Technology: Discussions of Racing Technical Topics.* Redwood City, CA, USA: TV Motorsports.

Haney, P. 2000. *A Little Knowledge….* International Journal: Racecar Engineering, Vol. 10, No.7, pp 20 – 24.

Harris, P. 2006. *Ride Height Simulation Software.* [Online] URL: http://www.linpotsim.com Accessed April 2006.

Hegazy, S., Rahnejat, H. and Hussain, K. 2000. *Multi-Body Dynamics in Full-Vehicle Handling Analysis under Transient Manoeuvre.* Vehicle System Dynamics, Vol., No.1., pp. 1 - 24.

How, J. Pohlman, N. and Park, C-W. 2002. *GPS Estimation Algorithms for Precise Velocity, Slip and Race-track Position Measurements.* SAE Paper 2002-01-3336.

Howard, K. 2002. *Handles Messiah.* International Journal: Racecar Engineering, Vol 12, No. 8, pp 48 – 50.

Imou, K. *et al*. 2001. *Ultrasonic Doppler Sensor for Measuring Vehicle Speed in Forward and Reverse Motions Including Low Speed Motions.* CIGR Ejournal, Vol. 3, No. 18

Jackson, P. 1999. *Introduction to Expert Systems.* Harlow, Essex, UK: Addison Wesley.

Kaehler, S.D. 2004. *FUZZY LOGIC - AN INTRODUCTION. Encoder: The Online Newsletter of the Seattle Robotics Society.* [Online] URL: http://www.seattlerobotics.org/encoder/mar98/fuz/fl_part1.html#INTRODUCTION Accessed 29th November 2004.

Kerr, D. 2005. *Introduction to Digital Image Processing.* Loughborough University Lecture Notes.

Kim, D. Y. and Slaughter, D.C. 2008. *Image-based Real-time Displacement Measurement System.* Biosystems Engineering, Vol 101, pp 388 – 395.

Kistler Instruments. 2003. *RoaDyn™ - a Tool for Rim and Chassis Development*. [Corporate Information Brochure] Winterthur, Switzerland. Kistler Instrumente AG.

Kleinhempel, W. 1993. *Automobile Doppler Speedometer.* IEEE- IEE Vehicle Navigation & Information Systems Conference, Ottawa – VNIS '93.

Kleinhempel, W. Bergmann, D. and Stammler, W. 1992. *Speed measure of vehicles with on-board Doppler radar.* Proceedings of Radar 92, Brighton, 1992, pp. 284–287.

Kowalczyk, H. 2002. *Damper Tuning with the use of a Seven Post Shaker Rig.* SAE Paper 2002-01-0804.

Laser Components. 2003. *Application Note: Non-Contact Laser Distance Measurement.* Chelmsford, Essex, UK: Laser Components (UK) Ltd..

Law, E.H. 2004. *Personal Communication on the Subject of Expert Systems Research at Clemson University.* [Email] Tuesday 30th November, 2004.

Lotus Engineering. 2004. *Lotus Suspension Software – SHARK.* [Sales brochure] Hethel, Norfolk, UK: Lotus Engineering Ltd.

Martin, B.T. and Law, E.H. 2002. *Development of an Expert System for Race Car Driver & Chassis Diagnostics.* SAE Paper 2002-01-1574.

Martz, P. 2006. *OpenGL® Distilled.* Boston, MA, USA: Pearson Education, Inc.

McBeath, S. 2002. *Competition Car Data Logging: A Practical Handbook.* Yeovil, Somerset, England: Haynes Publishing.

McBeath, S. 2008. *Competition Car Data Logging: A Practical Handbook .* 2nd Edition. Yeovil, Somerset, England: Haynes Publishing.

Mechanical Simulation Corporation. 2004a. *CarSim Quick Start Guide: Version 6.* Ann Arbor, MI, USA: Mechanical Simulation Corporation.

Mechanical Simulation Corporation. 2004b. *CarSim Version 6 Real Time.* [Product Overview Information Sheet] Ann Arbor, MI, USA: Mechanical Simulation Corporation.

Meriam, J.L. and Kraig, L.G. 1998. *Engineering Mechanics: Dynamics.* 4th Edition. New York, NY, USA: John Wiley & Sons.

Mikhail, E. M., Bethel, J. S. and McGlone, J. C. 2001. *Introduction to Modern Photogrammetry.* New York, NY, USA: John Wiley & Sons Inc.

Milliken, W.F. and Milliken, D.L. 1995a. *Race Car Vehicle Dynamics.* Warrendale, PA, USA: Society of Automotive Engineers.

Milliken, W.F. and Milliken, D.L. 1995b. *"g-g" Diagram.* [Book excerpt] Race Car Vehicle Dynamics, Chpt 9, pp 345 – 366. Warrendale, PA, USA: Society of Automotive Engineers.

Milliken, W.F., Milliken, D.L. and Best, A. 1995. *Dampers (Shock Absorbers).* [Book excerpt] Race Car Vehicle Dynamics, Chpt 22, pp 781 – 831. Warrendale, PA, USA: Society of Automotive Engineers.

Mitchell, W.C. 1998. *A Method for Data Alignment.* SAE Paper 983087.

Mitchell, W.C. 2004. *WinGeo3 User Guide.* Mooresville, NC, USA: William C. Mitchell Software.

Mitchell, W.C. 2005a. *Debrief3 User Guide.* Mooresville, NC, USA: William C. Mitchell Software.

Mitchell, W.C. 2005b. *William C. Mitchell Software*. [Corporate Website] URL: http://www.mitchellsoftware.com Accessed 18th January 2005.

Moloney, J., Coffey, S. and Perez, A. 1998. *Racing Applications for Digital Motion Analysis.* SAE Paper 983086.

MoTeC. 2002. *MoTeC Interpreter User Manual.* Croydon, South Victoria, Australia: MoTeC Pty Ltd..

MSC Software. 2003. *ADAMS/Car Quickstart Guide.* Santa Ana, CA, USA: MSC Software Corporation.

Munson, B.R., Young, D.F. and Okiishi, T.H. 1998. *Fundamentals of Fluid Mechanics.* Third Edition. New York, NY, USA: John Wiley and Sons.

Murphy, C. 2000. *Simulation Made Simple.* International Journal: Racecar Engineering. International Journal: Racecar Engineering, Vol. 10, No. 2, pp 25 - 28.

Murphy, C. 2003. *Spa for the Course.* International Journal: Racecar Engineering. International Journal: Racecar Engineering, Vol. 13, No. 10, pp 34 - 40.

National Instruments. 2009. *NI USB-6211.* [Technical data sheet] Austin, TX, USA: National Instruments Inc.

Ng, T.W. 2003. *The Optical Mouse as a Two-Dimensional Displacement Sensor.* Sensors and Actuators, Vol. 107, pp 21 – 25.

Nikravesh, P.E. 1988. *Computer-Aided Analysis of Mechanical Systems.* Englewood Cliffs, NJ, USA: Prentice-Hall.

Oatley, G.C. and Ewart, B.W. 2003. *Crime Analysis Software: 'Pins in Maps', clustering and Bayes net prediction.* Expert Systems with Applications, Vol. 25, pp 569 – 588.

Omnistar. 2010. *Worldwide Differential Positioning Service.* [Website] URL: www.omnistar.com

Ottake, S., Onoda, M. and Nagase, K. 1998. *Automotive High Pressure Sensor.* SAE Paper 980271.

Oxford Technical Solutions. 2002. *RT3000 Inertial and GPS Measurement System: Report from Silverstone F1 Test.* [White paper] Upper Heyford, Oxfordshire, UK: Oxford Technical Solutions Ltd.

Oxford Technical Solutions. 2009. *RT User Manual.* Upper Heyford, Oxfordshire, UK: Oxford Technical Solutions Ltd.

Pacejka, H.B. 2002. *Tyre and Vehicle Dynamics.* Oxford, Oxfordshire, England: Butterworth-Heinemann.

Pain, S. 2008. *When Pioneering Photography Filled the Theatres.* New Scientist, No. 2642, February 9th 2008.

Papegay, Y.A., Merlet J-P. and Dnaey, D. 2005. *Exact Kinematics Analysis of Car's Suspension Mechanisms Using Symbolic Computation and Interval Analysis.* Mechanism and Machine Theory, Vol. 40, No. 4, pp 395 – 413.

Parker, M.C. 2004a. An *Investigation of Methods for Enhancing the Display and Use of Acquired Vehicle Data for Motorsport Applications: Supplementary Folder.* [Mechanical Engineering BEng Individual Project report] Loughborough University.

Parker, M.C. 2004b. An *Investigation of Methods for Enhancing the Display and Use of Acquired Vehicle Data for Motorsport Applications: Final Report.* [Mechanical Engineering BEng Individual Project report] Loughborough University.

Parker, M.C. 2004c. *An Investigation of Methods for Enhancing the Display and Use of Acquired Vehicle Data for Motorsport Applications: Interim Progress Report.* [Mechanical Engineering BEng Individual Project report] Loughborough University.

Patrick Motorsports. 2010. Corporate Website. [Online] URL: http://www.patrickmotorsports.com/img/services/Motec-Console-108k.jpg

Performance Trends. 2002. Suspension *Analyzer V1.1 for Windows User Manual.* Livonia, MI, USA: Performance Trends Inc..

Performance Trends. 2005. *Corporate Website.* [Online] URL: http://www.performancetrends.com Accessed 17th January 2005.

Persson, N. *et al*. 2001. *Low Tire Pressure warning system Using Sensor Fusion.* SAE Paper 2001-01-3337.

Pi Research. 1997. *Inertial Sensors Application Note.* Cottenham, Cambridgeshire, UK: Pi Group Limited.

Pi Research. 1998a. *Aerodynamic Application Note.* Cottenham, Cambridgeshire, UK: Pi Group Limited.

Pi Research. 1998b. Pi *Analysis Version 6 PC Software Guide*. 1998 Edition. Cottenham, Cambridgeshire, UK: Pi Group Limited.

Pi Research. 2000. *Pi VIDS (Video Indexed Data System) User Guide.* Cottenham, Cambridgeshire, UK: Pi Group Limited.

Pi Research. 2001. *Pi Sim: Version 4 User Guide*. Cottenham, Cambridgeshire, UK: Pi Group Limited.

Pi Research. 2004a. Pi *Toolbox User Guide: Version 3.1.* Cottenham, Cambridgeshire, UK: Pi Group Limited.

Pi Research. 2004b. *Pi Club Expert Analysis User Guide.* Cottenham, Cambridgeshire, UK: Pi Group Limited.

Pi Research. 2005. *Corporate Website.* [Online] URL: http://www.piresearch.co.uk Accessed March – April 2005.

Purnell, A.J. 1998. *Innovative Computer Technology in Professional Motorsports.* SAE Paper 983089.

Race Technology. 2005. *2005 Product Catalogue.* Strelley, Nottinghamshire, England: Race Technology Ltd.

Rahnejat, H. 1998. *Multi-body Dynamics: Vehicles, machines and Mechanisms.* Bury St Edmunds, UK: Professional Engineering Publishing.

Ramsay, D.C. 1996. *Principles of Engineering Instrumentation.* Oxford, UK: Butterworth Heinemann.

Randle, S. 2004. *Parameterised Vehicle Handling Modelling.* Auto Technology Magazine, 2004, No. 3.

Renault Sport Technologies. 2006. *World Series by Renault: Formula Renault 3.5 2006 Technical Regulations.* Les Ulis Courtaboeuf Cédex, France: Renault Sport Technologies.

Replogle, D.L. 1994. A Model Driven Approach to Racecar Data Acquisition. SAE Paper 942483.

Rezaei, S. and Sengputa, R. 2005. *Kalman Filter Based Integration of DGPS and Vehicle Sensors for Localization.* IEEE transactions on control systems technology. Vol. 15, No. 6, pp. 1080-1088.

Rezaei, S. and Sengputa, R. 2007*. Kalman Filter-Based Integration of DGPS and Vehicle Sensors for Localization.* IEEE Transactions of Control Systems Technology, Vol. 15, No. 6, pp 1080 – 1088.

Rowley, W. 2004. *Introduction to Race Car Engineering: The Basics of Vehicle Dynamics.* Warren Rowley Motorsports and Rowley Race Dynamics.

Sakai, I *et al*. 1992. *Optical Speed-over-ground Sensors for On-board Vehicle Speed Measurement.* IEE Colloquium on Automotive Sensors, 1992.

Sakai, I. *et al*. 1995. *Optical Spatial Filter Sensor for Ground Speed.* Optical Review, Vol. 2, No. 1, pp 65 – 67.

Schatz, O. 2003. *Yaw-Rate Sensors.* Sensors for Automotive Technology, Chpt. 7.2, pp. 297 – 313. Weinheim, Germany: Wiley-VCH.

Segers, J. 2008. *Analysis Techniques for Racecar Data Acquisition.* Warrendale, PA, USA: SAE International.

Shreiner, D. *et al*. 2008. *OpenGL® Programming Guide: The Official Guide to Learning OpenGL®, Version 2.1.* 6th Ed. Boston, MA: Pearson Education Inc.

SimAuthor. 2010. FlightViz™ *Flight Visualisation Software: Debrief.* [Corporate sales brochure] Boulder, CO, USA.

Stone, M. L. & Kranzler, G. A. 1992. Image-based Ground Velocity Measurement. Transactions of the ASABE 35, Vol 5, pp. 1729–1735.

Strout, R. 1998. *The "Real World" – The Human Interface in Optimizing Racing Suspension Dynamics.* SAE Paper 983074.

Sugasawa, F. *et al*. 1985. *Electronically Controlled Shock Absorber System Used as a Road Sensor Which Utilizes Super Sonic Waves.* SAE Paper 851652.

Teledyne. 2010. *Vision, Flight Animation System.* [Sales brochure] El Segundo, CA, USA: Teledyne Technologies.

Templeman, G. 2008. The *Competition Car Data Logging Manual.* Dorchester, UK: Veloce Publishing Ltd.

The MathWorks, Inc. 1996. *Applications of Fuzzy Logic in Control Design.* Natick, MA, USA: The MathWorks, Inc..

Tremblay, C. 2004. *Mathematics for Game Developers.* Boston, MA, USA: Thomson Course Technology.

Trimble. 2008. Trimble *GPS Tutorial.* [Online] Trimble Navigation Limited: http://www.trimble.com/gps/TutorialRequest.aspx Accessed February 2010.

u-blox. 2007. *u-center GPS Evaluation Software.* [User guide] Thawil, Swizterland, u-blox AG.

u-blox. 2008. *LEA-5.* [Datasheet] Thawil, Swizterland, u-blox AG.

United States of America Department of Defense. 2008. *Global Positioning System Standard Positioning Service Performance Standard.* Washington DC, USA. [Online] URL: http://pnt.gov/public/docs/2008/spsps2008.pdf.

Vaduri, S. and Law, E.H. 2000. *Development of an Expert System for the Analysis of Track Test Data.* SAE Paper 2000-01-1628.

van Rutten, C. 2003a. *Accessible Simulations.* Racetech Magazine, December 2003.

van Rutten, C. 2003b. *Black Magic.* International Journal; Racecar Engineering, Vol. 13, No 4, pp 50-56.

Vishay Spectrol. 2002. *Model 971 Rotary Position Sensor.* [Technical data sheet]: Vishay Spectrol.

Wallentowitz, H., Köhn, P., and Holdmann, P. 1999. *Dynamic Properties of Tyres – Testing and Simulation.* SAE Paper 1999-01-0790.

Wallin, C., Gustavsson, L. and Donovan, M. 2002. *Engine Monitoring of a Formula 1 Racing Car Based on Direct Torque Measurement.* SAE Paper 2002-01-0196.

Westbrook, M. H. and Turner, J.D. 1994. *Automotive Sensors.* Bristol, Somerset, England: Institute of Physics Publishing.

Wikipedia. 2010. *Gimbal Lock.*
Online, URL: http://en.wikipedia.org/wiki/Gimbal_lock. Accessed October 2010.

Williams, S. 2004. *Reducing Product Development Time Using Design Based Suspension Analysis.* 3rd International Symposium on Multi-Body Dynamics: Monitoring and Simulation Techniques, Loughborough, England, 12th – 13th July 2004.

Wright, P. 1997. *Testing Times.* International Journal: Racecar Engineering, Vol. 7, No. 1, pp 36 - 39.

Wright, P. 1999. *Test Pilots.* International Journal: Racecar Engineering, Vol. 9, No. 1, pp 18 - 20.

Wright, P. 2001. *Shake Down.* International Journal: Racecar Engineering, Vol. 11, No.1, pp 26 - 32.

Yang, Y., Sharpe, R. T. and Hatch, R. R. 2002. *A Fast Ambiguity Resolution Technique for RTK Embedded Within a GPS Receiver.* [White paper] Torrance, CA, USA: NavCom Technology, Inc.

Yokomori, I. and Suzuki, Y. 2003. *Pressure Sensors.* Sensors for Automotive Technology, Chpt. 7.3, pp. 314 – 332.Weinheim, Germany: Wiley-VCH.

Young, M. J. 1998. *Mastering™ Visual C++ 6.* Alameda, CA, USA: SYBEX, Inc.

Yukawa, J. *et al*. 1998. Angular Rate Sensor for Dynamic Chassis Control. SAE Paper 980269.

Zhang, J. *et al*. 2006. *On the Relativistic Doppler Effect for Precise Velocity Determination Using GPS.* Proceedings of The International Symposium on GNSS/GPS, Sydney, Australia, 6–8 December 2004.